

**Maleation of Polypropylene and EPDM Through Reactive
Extrusion Using the Alder Ene Reaction**

By

Michael Richard Thompson

**A Thesis
presented to the University of Waterloo
in fulfilment of the
thesis requirement for the degree of
Doctor of Philosophy
in
Chemical Engineering**

Waterloo, Ontario, Canada, 1998

© Michael Richard Thompson, 1998



National Library
of Canada

Acquisitions and
Bibliographic Services

395 Wellington Street
Ottawa ON K1A 0N4
Canada

Bibliothèque nationale
du Canada

Acquisitions et
services bibliographiques

395, rue Wellington
Ottawa ON K1A 0N4
Canada

Your file *Votre référence*

Our file *Notre référence*

The author has granted a non-exclusive licence allowing the National Library of Canada to reproduce, loan, distribute or sell copies of this thesis in microform, paper or electronic formats.

The author retains ownership of the copyright in this thesis. Neither the thesis nor substantial extracts from it may be printed or otherwise reproduced without the author's permission.

L'auteur a accordé une licence non exclusive permettant à la Bibliothèque nationale du Canada de reproduire, prêter, distribuer ou vendre des copies de cette thèse sous la forme de microfiche/film, de reproduction sur papier ou sur format électronique.

L'auteur conserve la propriété du droit d'auteur qui protège cette thèse. Ni la thèse ni des extraits substantiels de celle-ci ne doivent être imprimés ou autrement reproduits sans son autorisation.

0-612-30654-2

The University of Waterloo requires the signatures of all persons using or photocopying this thesis. Please sign below, and give address and date.

ABSTRACT

An investigation into the site-specific functionalization of several polymers within a co-rotating intermeshing twin screw extruder was initiated. The Alder Ene reaction between maleic anhydride and the inherent double bond of polypropylene and EPDM, was chosen for the high temperature environment of the extruder to accomplish the desired reaction. In order to improve the incorporation of maleic anhydride into the polymer, several Lewis acids were employed as catalysts in the reaction. The high temperature application of Lewis acid into the reaction was a unique contribution of this thesis. The primary Lewis acid examined in this work was stannous chloride dihydrate, along with aluminum chloride and ruthenium chloride hydrate. The reactions were carried out in a round bottom flask, a batch reactor, a batch mixer, a single screw extruder and a co-rotating intermeshing twin screw extruder. Characterization of the maleated products by FT-IR, ¹H NMR, DSC, and GPC was used to differentiate between site-specific attachment and free radical grafting of the functionality. Polyisobutylene was used to carry out preliminary studies on the high temperature application of Lewis acids in the Alder Ene reaction. A low molecular weight polypropylene wax (Polypol-19) was chosen as a model material to study the kinetics of the reaction and identify reaction parameters useful for reaction optimization purposes. The preparation of a vinylidene-rich polypropylene for the reaction in the extruder, via β -scission has been shown to be an effective route, with thermal degradation favoured over peroxide-initiated degradation due to the reduced presence of carbonyl functionalities in the polymer. Both methods of degradation have been shown to produce greater than one site of unsaturation per chain, demonstrating their advantage over commercial polymerization for producing an

effective *ene* species in this work. Finally, EPDM was examined as a material with a high vinyl content useful for the reaction, that was also highly viscous making it more suited for reactive extrusion.

The degree of functionalization was determined by infrared analysis, though an alternative method, explored with EPDM, also showed a direct correlation between the level of maleation and the mechanical properties of an ionic network formed by neutralizing the maleated rubber. Temperature and maleic anhydride concentration were found to be the most significant factors for this Alder Ene reaction. Increased temperature and maleic anhydride reactant concentration were found to improve the extent of reaction. Significant isomerization and maleic anhydride homopolymerization side reactions have been observed in the batch reactor, beyond 230°C, indicating the presence of an optimal limit though this is likely to differ in the extruder.

The Lewis acid, which was employed as a solid or mixed in phase with molten maleic anhydride, improved succinyl anhydride incorporation with reduced acid concentration. Among the Lewis acids examined, aluminum chloride gave rise to the greatest improvement of succinyl anhydride incorporation, at least into the rubber. Ruthenium chloride was found to improve the extent of reaction in Polypol-19, degraded polypropylene and EPDM. Employing the Lewis acid in phase with the reactant (maleic anhydride) was shown to lead to higher conversion. Based on an observed “induction period” in the conversion-time plots, the formation of the Lewis acid-anhydride enophile for the reaction was relatively slow with respect to the duration of the reaction. However, when the acid was employed as a solid creating a heterogeneous reaction (omitting the limited solubility of maleic anhydride within the examined polymers), the rate of formation of the acid-anhydride enophile was probably

too low to observe an induction period. Unlike the homogeneous catalyst system, the applicability of second order kinetics to the heterogeneous catalyzed system provides immediate evidence of this phenomenon. In general, even in the absence of catalyst, the application of a second-order kinetic model to the measured succinyl anhydride results, was not valid over the entire temperature range studied due to side reactions, particularly vinylidene isomerization and homo-polymerization of maleic anhydride. The rheological results from the maleated EPDM series offered interesting results. In the absence of a Lewis acid catalyst in the reaction, the elasticity of the rubber increased with increasing degree of succinyl functionalization. Likely, these polar groups were introducing intermolecular bonds with sufficient strength to produce rheological behaviour similar to cross-linking.

ACKNOWLEDGMENTS

My most sincere thanks goes to my supervisors, Drs Costas Tzoganakis and Garry Rempel. I have such a great respect for these two men and appreciate the support and advice both have given.

A gigantic team effort is always involved in experimental work and for assistance on my thesis, I wish to express my appreciation to those individuals I sought out for either their expertise or resources. Thanks to the students of the polymer processing group, whose friendship and assistance made this thesis truly enjoyable. I wish to single out Gifford Shearer and Hauke Malz, good friends whom I could always seek out for their help. Thanks to the technicians in the Department of Chemical Engineering for putting up with my relentless exploitation of their skills. I would also like to extend my appreciation to the technicians and research assistants in the Department of Chemistry for their assistance with running the NMR spectrometer and oscillating parallel plate rheometer.

With respect to donated materials, thanks goes to Elf AtoChem, Crowley Chemicals, Montell Canada, and Uniroyal Chemicals (particularly J. Wefer for his assistance with EPDM modification). For financial support, my thanks to the Natural Science and Engineering Research Council, and the MMO, formerly known as the Ontario Centre of Material Research.

Finally, I want to thank my wife, Shari, for whom I have dedicated this thesis. I can't imagine this work meaning much without you.



Eureka!
Archimedes, "The Master"
Possibly the greatest Engineer and Mathematician in history.

This thesis is
dedicated to my wife, Shari

TABLE OF CONTENTS

	Page
Abstract	iv
Acknowledgments	vii
Table of Contents	ix
List of Tables	xiv
List of Figures	xvi
Nomenclature	xxii
CHAPTER 1. INTRODUCTION AND OBJECTIVES	1
1.1. Introduction	1
1.2. Reactive Extrusion	2
1.3. Functionalization of Polypropylene and EPDM	3
1.4. Free Radical vs. Alder Ene Grafting Reactions	4
1.5. Research Objectives	5
CHAPTER 2. LITERATURE REVIEW	7
2.1. Introduction	7
2.2. Structure of Free Radical Grafted Maleic Anhydride	9
2.3. Poly(Maleic Anhydride) and Decarboxylation	11
2.4. Free Radical Grafting Mechanism	15
2.5. Alder Ene Reaction (Site-Specific Functionalization)	18
2.5.1. Mechanism and Parameters of the Alder Ene Reaction	24
2.5.1.1. Lewis Acids in the Alder Ene Reaction	26
2.5.1.2. Inhibitors in the Alder Ene Reaction	32
2.5.1.3. Kinetics of the Alder Ene Reaction	33
2.6. Determination of End Group Functionality	35
2.6.1. Block and Graft Copolymerization	36
2.6.2. ¹ H and ¹³ C NMR	37
2.6.3. FT-IR Spectroscopy	39
2.6.4. Transition Temperatures	42
2.6.5. Rheological Properties	44

CHAPTER 3. METHODS OF VINYLIDENE GENERATION IN POLYPROPYLENE	46
3.1. Introduction	46
3.2. Commercial Ziegler-Natta Polypropylene	46
3.3. Vis-Breaking of Polypropylene	48
3.3.1. Peroxide-Induced β -Scission	50
3.3.2. Oxidation	53
3.3.3. Thermal Degradation	56
3.4. Experimental	58
3.4.1. Material	58
3.4.2. Procedures	59
3.4.2.1. Peroxide Induced Degradation	59
3.4.2.2. Thermal /Thermo-Oxidative Degradation	59
3.4.3. Analysis	60
3.5. Results and Discussion	62
3.5.1. NMR Analysis of Degraded Polypropylene	62
3.5.2. FT-IR Analysis	66
3.5.3. Molecular Weight Distribution	71
3.6. Concluding Remarks	76
CHAPTER 4. EXPERIMENTAL	78
4.1. Materials	78
4.1.1. Low Molecular Weight Polyisobutylene	78
4.1.2. Low Molecular Weight Amorphous Polypropylene	78
4.1.3. High Molecular Weight Polypropylene	79
4.1.4. Ethylene-Propylene-Diene Terpolymer	79
4.1.5. Reagents and Solvent	80
4.2. Equipment and Procedures	81
4.2.1. Bench-Top Round Bottom Flask Reactor	81
4.2.2. Parr 300 mL High Pressure Autoclave	81
4.2.3. Haake Rheomix 3000 Batch Mixer	85
4.2.4. Haake Rheomex 252 Single Screw Extruder	86
4.2.4.1. Ethylene-Propylene-Diene Terpolymer	87
4.2.4.2. Polypropylene Degradation	90
4.2.5. Leistritz LSM 30.34 Twin Screw Extruder	92
4.2.5.1. Polypropylene	95
4.2.5.2. Ethylene-Propylene-Diene Terpolymer	97
4.3. Characterization	99
4.3.1. Colorimetric Acid-Base Titration	99
4.3.2. Dilution Viscometry	102
4.3.3. FT-IR Method	102
4.3.3.1. Polyisobutylene	102
4.3.3.2. Polypol-19	105

4.3.3.3. Polypropylene	107
4.3.3.4. Ethylene-Propylene-Diene Terpolymer	110
4.3.4. Differential Scanning Calorimetry	111
4.3.4.1. Polypol-19	111
4.3.4.2. Polypropylene	112
4.3.4.3. Ethylene-Propylene-Diene Terpolymer	112
4.3.5. ¹³ C NMR Analysis	113
4.3.6. ¹ H NMR Analysis	114
4.3.7. Molecular Weight Distribution	115
4.3.8. Kinetic Rate Constant Calculations	115
4.3.9. Ionic Cross-linking of Maleated EPDM	116
4.3.10. Dynamic Mechanical Analysis	117
CHAPTER 5. PRELIMINARY EXAMINATION OF LEWIS ACIDS IN POLYISOBUTYLENE	118
5.1. Introduction	118
5.1.1. Alder Ene Product	119
5.2. Examining the Effects of Various Lewis Acids	122
5.2.1. Stannic Chloride	122
5.2.2. Titanium Chloride	126
5.2.3. Aluminum Chloride	127
5.3. Presence of Hydroquinone in the Catalyzed Reaction	128
5.4. Method of Addition	130
5.5. Concluding Remarks	133
CHAPTER 6. MALEATION OF LOW MOLECULAR WEIGHT POLYPROPYLENE VIA THE ALDER ENE REACTION: CHARACTERIZATION AND PARAMETRIC STUDY	135
6.1. Introduction	135
6.2. Characterization of Succinyl Terminated Polypropylene	137
6.2.1. FTIR Analysis	138
6.2.2. Intrinsic Viscosity	143
6.2.3. NMR Analysis	144
6.3. Comparing Methods of Succinyl Anhydride Measurement	147
6.4. Effect of Free Radical Inhibitor	151
6.5. Reaction Parameters	155
6.5.1. Effect of Temperature and Maleic Anhydride Reaction Parameters	155
6.5.2. Effect of Catalyst Concentration	161
6.5.3. Isomerization	170
6.6. Hierarchical Design for Error Analysis of the IR Method	172

6.7. Kinetics of the Alder Ene Reaction	173
6.8. Stannous Chloride vs. Ruthenium Chloride	179
6.9. Concluding Remarks	180
CHAPTER 7. MALEATION OF POLYPROPYLENE THROUGH REACTIVE EXTRUSION VIA THE ALDER ENE REACTION	182
7.1. Introduction	182
7.2. Result and Discussion	185
7.2.1. Characterization of Maleated Polypropylene	187
7.2.1.1. Molecular Weight Distribution	187
7.2.1.2. Infrared Analysis	191
7.2.1.3. NMR Analysis	192
7.2.2. Thermal Transition Properties	194
7.2.3. Effect of Reaction Parameters	197
7.2.4. Effect of Screw Speed and Feed Rate	201
7.2.5. Comparing Estimated to Measured SAh Content	202
7.2.6. Ruthenium chloride vs. Stannous chloride	206
7.3. Concluding Remarks	207
CHAPTER 8. MALEATION OF ETHYLENE-PROPYLENE-DIENE TERPOLYMER THROUGH REACTIVE EXTRUSION VIA THE ALDER ENE REACTION	208
8.1. Introduction	208
8.2. Characterization of Maleated EPDM	209
8.2.1. Molecular weight distribution data	211
8.2.2. Infrared Analysis	215
8.2.3. NMR Characterization	217
8.3. Experiments in the Batch Mixer	221
8.4. Examining Extrusion Operating Parameters	224
8.5. Effect of Screw Speed in the Twin Screw Extruder	230
8.6. Effect of Temperature and Maleic Anhydride Concentration	231
8.7. Effect of Lewis Acids	234
8.8. Comparing Estimated to Measured SAh Content	236
8.9. Glass Transition Temperature	240
8.10. Neutralization of maleated EPDM	241
8.11. Dynamic Mechanical Analysis	245

8.12. Concluding Remarks	254
CHAPTER 9. CONCLUSIONS AND RECOMMENDATIONS	256
9.1. Conclusions	256
9.2. Recommendations	259
CHAPTER 10. REFERENCES	262
Appendix I: Maleated Polyisobutylene	275
Appendix II: Conversion data from the maleation of Polypol-19	281
Appendix III: Maleated Polypol-19	286

LIST OF TABLES

	Page
Table 2.1. Types of chemical reactions classified in reactive extrusion (Brown, 1992)	8
Table 3.1. Chain transfer mechanisms in metallocene polymerization	47
Table 3.2. Four possible vinyl end groups resulting from degradation of PP	61
Table 3.3. Vinylidene concentration and molecular weight results for thermally degraded polypropylene	68
Table 4.1. Diene monomers used in ethylene-propylene-diene terpolymer	79
Table 4.2. List of reactants and composition	89
Table 4.3. Relationship of barrel temperature with resulting vinylidene concentration	91
Table 4.4. Molecular weight averages of degraded polypropylene	92
Table 4.5. Acid-base properties of maleic anhydride and thymol blue	100
Table 4.6. Operating conditions for carbon-13 NMR	113
Table 5.1. Chemical properties of the selected Lewis acid species	119
Table 5.2. Effect of temperature and catalyst concentration on SAh content	124
Table 5.3. Effect of additives on the Alder Ene reaction	130
Table 6.1. Characteristic IR wavenumbers (cm^{-1}) in several samples compared to Polypol-19	139
Table 6.2. Evaluation of two terminally anhydride functionalized polypropylenes.	148
Table 6.3. Inhibitor species in the Alder Ene reaction	154
Table 6.4. Results of the hierarchical analysis	172
Table 6.5. Estimated activation energies for different catalyst concentrations	178
Table 7.1. Experimental set 1: Examining reaction parameters	183
Table 7.2. Experimental set 2: Mixing performance	184
Table 7.3. Experimental set 3: Studying important reaction factors for non-linearity	185
Table 7.4. Results of the hierarchical analysis	200
Table 8.1. Experimental conditions for screw configuration 3	209
Table 8.2. Experimental parameters for screw configuration 4	210
Table 8.3. Comparison of Nordel and Royalene EPDM with two Lewis acids.	223

Table 8.4. Varying factor levels for maleic anhydride and Lewis acid concentration	225
Table 8.5. Repeated runs showing the vinyl effect on SAh incorporation	234

LIST OF FIGURES

	Page
Figure 2.1. Postulated homopolymer segment structures in poly(maleic anhydride)	13
Figure 2.2. Free radical mechanism for grafting maleic anhydride onto polypropylene (Adapted from N. G. Gaylord and M. K. Mishra, <i>J. Polym. Sci.: Polym. Lett. Ed.</i> , 21, 23 (1983))	17
Figure 2.3. Terminal environment of polyisobutylene	19
Figure 2.4. Vinyl isomeric structures in the Ene product	20
Figure 2.5. End-capped polyethersulfone grafted to EPDM via the Diels-Alder reaction	22
Figure 2.6. Reaction mechanism for the Alder Ene reaction	24
Figure 2.7. Reaction scheme of a Lewis acid with the maleic anhydride to form an intermediate adduct to act as a stronger enophile in the Ene reaction.	27
Figure 2.8. Mechanism for maleic anhydride attachment to a phenyl-based molecule (Adapted from Kurbanova et al., <i>J. Appl. Polym. Sci.</i> , 59, 235 (1996))	29
Figure 2.9. Stabilization mechanisms of Denisov (1991) and Klemchuk and Gande (1988)	34
Figure 2.10. Succinyl structure of maleic anhydride grafted polypropylene	38
Figure 3.1. Degradation of polypropylene by chain scission	49
Figure 3.2. Decomposition pathway of a dialkyl peroxide	52
Figure 3.3. Hydrogen abstraction from the backbone of a polypropylene chain by a primary radical.	52
Figure 3.4. Thermo-oxidation pathways for polypropylene	55
Figure 3.5. Three chain end structures for degraded polypropylene with ¹³ C chemical shift values calculated according to Lindeman and Adams (1971) and Dorman et al. (1971)	61
Figure 3.6. ¹³ C NMR spectrum in the backbone region of degraded polypropylene	63
Figure 3.7. ¹³ C NMR spectrum in the backbone region for virgin polypropylene	63
Figure 3.8. ¹³ C NMR spectrum in the region of conjugated structures for degraded polypropylene	65
Figure 3.9. ¹³ C NMR spectrum in the region of conjugated structures for virgin polypropylene	65
Figure 3.10. ¹ H NMR spectrum of degraded polypropylene	66
Figure 3.11. FT-IR spectra of a series of degraded polypropylenes corresponding to varying barrel temperatures [unlabeled spectra below 370/10 are 380/20 (highest), 380/30, 370/20, and 370/30 (lowest)]	67
Figure 3.12. FT-IR spectra of a series of degraded polypropylenes corresponding to varying peroxide levels [unlabeled spectra below 0.5 wt % are 0.2 wt % (highest), 0.1, 0.05, 0.02, and 0.01 wt % (lowest)]	68

Figure 3.13. Vinylidene group content as a function of peroxide concentrations	69
Figure 3.14. FT-IR spectra of thermal- and peroxide-degraded polypropylene, examining the carbonyl groups included in the polymer due to the method of chain scission.	70
Figure 3.15. Change in the number-average molecular weight of degraded polypropylene due to random scission for increasing concentrations of peroxide	71
Figure 3.16. Molecular weight distributions for virgin polypropylene and degraded polymer via the two methods.	73
Figure 3.17. Comparison of the vinylidene concentration in degraded polypropylene samples with theoretical vinylidene concentrations for chains with one (dotted line) or two (solid line) terminal vinyls per chain.	74
Figure 3.18. Theoretical vinylidene growth versus experimental measured vinylidene content in degraded polypropylene.	76
Figure 4.1. Photos of the autoclave reactor for the Alder Ene reaction	83
Figure 4.2. Schematic diagram of the Parr reactor	84
Figure 4.3. Sample torque plots for EPDM in a Haake Rheomix 3000	86
Figure 4.4. Screw design for the Haake Rheomex 252 single screw extruder	87
Figure 4.5. Picture of the single screw extruder setup for maleation of EPDM	88
Figure 4.6. Photo of the twin screw extruder setup	94
Figure 4.7. Two screw configurations used in a Leistritz co-rotating twin screw extruder. The kneading elements are denoted by KS with the stagger angle of 60° unless the block was designated as neutral (N). Reversing elements are denoted with a L suffix.	96
Figure 4.8. Screw configurations: 3) extensive mixing, high torque at the kneading block and comb elements, and 4) conveying with low mixing potential, low torque.	97
Figure 4.9. Correlation between FT-IR relative absorbance at 1784 cm ⁻¹ and the concentration of succinyl anhydride bound in polyisobutylene.	104
Figure 4.10. Correlation between FT-IR relative absorbance at 1792 cm ⁻¹ and the concentration of succinyl anhydride bound onto low molecular weight polypropylene.	106
Figure 4.11. Correlation between FT-IR relative absorbance at 888 cm ⁻¹ and the concentration of vinylidene in KF6100 polypropylene.	107
Figure 4.12. Correlation between FT-IR relative absorbance at 1792 cm ⁻¹ and the concentration of succinyl anhydride bound onto KF6100 polypropylene.	109
Figure 5.1. FT-IR spectra of Glissopal 1000 (polyisobutylene) compared to the succinyl terminated Ene product	120
Figure 5.2. Proposed ring opening in the presence of a Lewis acid.	123

Figure 5.3. FT-IR spectra of a series of maleated polyisobutylenes produced by varying the temperature and catalyst concentration in the reaction (peak wavenumber included).	125
Figure 5.4. Comparing the anhydride absorbance peak in the region of carbonyl stretching vibrations	128
Figure 5.5. FT-IR spectra of two maleated polyisobutylenes in the region of the anhydride absorbance, comparing the effect of the method of enophile formation.	131
Figure 6.1. Isomeric structures of succinyl terminated polypropylene: (I) Exo double bond; (II) endo double bond.	138
Figure 6.2. FTIR spectra comparing the virgin polypropylene and Ene product in the region of the vinylidene.	140
Figure 6.3. FTIR spectra comparing the virgin polypropylene and end product in the carbonyl region.	141
Figure 6.4. FTIR spectra examining poly(maleic anhydride) in the carbonyl region.	142
Figure 6.5. ¹ H solution NMR spectrum of a) Polypol-19 and b) succinyl terminated polypropylene.	144
Figure 6.6. ¹³ C solution NMR spectrum of succinyl terminated polypropylene.	146
Figure 6.7. Evaluating the correlation between FT-IR and acid-base titrimetry as methods of measuring the concentration of the terminal functionality (standard deviation error bars)	149
Figure 6.8. Comparing trends among FT-IR, ¹ H NMR and T _g measurements of succinyl terminated polypropylene	150
Figure 6.9. FT-IR Spectra of a catalyzed Alder Ene product (solid line) reacted in the presence of hydroquinone with virgin Polypol-19 (dashed line) included for reference.	152
Figure 6.10. Effect of TEMPO concentration in the Alder Ene reaction on the anhydride and vinylidene content in polypropylene product (standard deviation error bars).	153
Figure 6.11. Conversion profiles as a function of temperature and maleic anhydride concentration in reactions with no catalyst present.	156
Figure 6.12. Effect of temperature in the Alder Ene reaction for reactions using 8 mole eq. maleic anhydride and 0.5 % mole eq. SnCl ₂ ·2H ₂ O.	158
Figure 6.13. Relative succinyl anhydride absorbance values of 0.5 mol % SnCl ₂ heterogeneous system using Polypol-19 after a 5 min. reaction, indicated on two response surfaces including a constant MAh concentration line for determination of the activation energy	159
Figure 6.14. Effect of maleic anhydride concentration used in the catalyzed Alder Ene reaction (0.5 % mole eq. SnCl ₂ ·2H ₂ O) at 220°C and 240°C.	160
Figure 6.15. Effect of Lewis acid concentration on the conversion (FT-IR with standard deviation error bars) in the Alder Ene Product (region of optimal anhydride incorporation has been expanded).	162
Figure 6.16. Conversion based on titrated succinyl anhydride group in the Alder Ene product with respect to the Lewis acid concentration (standard deviation error bars).	163

Figure 6.17. Effect of Lewis acid concentration on the glass transition temperature of the Alder Ene product.	165
Figure 6.18. Varying the SnCl ₂ ·2H ₂ O concentration for reactions using 2.7 mole eq. maleic anhydride at 240°.	166
Figure 6.19. The effect of SnCl ₂ ·2H ₂ O concentration at 220°C for the reaction using 2.7 mole eq. maleic anhydride.	167
Figure 6.20. Effect of temperature and SnCl ₂ ·2H ₂ O concentration in the reaction conversion at 2.7 mole eq. maleic anhydride.	169
Figure 6.21. Relative succinyl anhydride absorbance values of 2.8 mol-eq MAh homogeneous system using Polypol after a 5 min reaction	170
Figure 6.22. Variance in the relative vinylidene infrared absorbance due to isomerization as it is affected by temperature and catalyst concentration (no maleic anhydride present in reactions using 0.05 % and 0.5 % mole eq. SnCl ₂ ·2H ₂ O).	171
Figure 6.23. FT-IR monitored reaction with increasing succinyl concentration in minute increments (lowest peak at 1792 cm ⁻¹ corresponds to 1 minute elapsed, 2, 3, 4, highest peak at 5 minutes).	174
Figure 6.24. Best linear fit to FTIR measurements assuming second-order reaction kinetics.	175
Figure 6.25. Second-order rate constants for the catalyzed Alder Ene reaction (95% confidence interval error bars). Determined from titration data (circles) and FT-IR data (squares).	176
Figure 6.26. Plot of second-order kinetic rate constants versus temperature for four catalyst concentrations in the reaction of maleic anhydride with the vinylidene of polypropylene.	177
Figure 7.1. Effect of maleic anhydride concentration on the MWD of the maleated polypropylenes.	187
Figure 7.2. Differences in the MWD between two maleated polypropylenes (41 and 47G) and their hexadecylamine grafted counterparts (41 and 47E). Sample 55E was a highly maleated polypropylene sample grafted with hexadecylamine, used for comparison.	189
Figure 7.3. Effect of processing conditions on the MWD of the maleated polypropylenes.	190
Figure 7.4. Carbonyl region of the FT-IR spectra for several maleated polypropylenes produced in the presence of either stannous chloride (9 and 12G) or ruthenium chloride (37 and 38G).	191
Figure 7.5. ¹ H NMR spectra of a maleated sample (42G) and its hexadecylamine grafted product (42E) in the region of 0-6 ppm for the upper two plots, with the alkyl region (0-3 ppm) of 42E expanded in the lower view.	193
Figure 7.6. DSC crystallization thermograms of select samples from series G and E.	196
Figure 7.7. Crystallization transition properties (T _c and ΔH _c) for the maleated polypropylenes (G series) and their hexadecyl chain extended products (E series).	197
Figure 7.8. Crystal melting endotherms for several maleated and hexadecylamine grafted products.	198
Figure 7.9. Comparing the kinetic-estimated conversion with the conversion values derived from FT-IR measurements (deviation bars for conversions within a ±5°C range).	204

Figure 7.10. Effect of several reaction and operating parameters on the difference observed between measured and estimated conversion, given as percent error	205
Figure 8.1. Changes in the molecular weight distribution of EPDM resulting from chain scission (due to processing) and fractionation (due to purification).	212
Figure 8.2. Molecular weight distributions of maleated EPDMs via the catalyzed Alder Ene reaction at 210-230°C with unmodified EPDM included for comparison.	213
Figure 8.3. Molecular weight distributions of maleated EPDMs via both catalyzed and uncatalyzed Alder Ene reactions at 270°C with unmodified EPDM included for comparison.	214
Figure 8.4. Infrared spectra of maleated and virgin EPDM in the carbonyl (1600-1900 cm ⁻¹) and fingerprint (900-800 cm ⁻¹) regions.	216
Figure 8.5. ¹³ C NMR spectrum of maleated EPDM (Sample 43F) in the backbone region	218
Figure 8.6. ¹³ C NMR spectrum of maleated EPDM (sample 43F) in the unsaturated region (edge of the trichlorobenzene peak seen at right-hand side of figure)	218
Figure 8.7. ¹ H NMR spectrum of EPDM with overlapping spectra scaled to show the succinyl anhydride and double bond resonances of several maleated samples. Top-to-bottom: (43F) Lewis acid catalyzed, extruded product; (58F) highly maleated Alder Ene solution product; (59) peroxide-induced maleated EPDM; (EPDM) virgin EPDM	219
Figure 8.8. Two proposed structures of a succinyl anhydride EPDM adduct resulting from a concerted mechanism involving either allylic hydrogen A or B.	221
Figure 8.9. Torque plots of the maleation experiments for Royalene and Nordel EPDM.	223
Figure 8.10. Comparison of viscosity between ground extrudates from several experiments with their solvent purified samples (ppt) for evidence of cross-linking.	227
Figure 8.11. Comparing the viscosity curves of the maleated EPDM/PP samples (ppt) along with the virgin blend (ppt) to identify any occurrence of scission	228
Figure 8.12. Effect of temperature and maleic anhydride concentration on the molecular weight distribution through scission that occurred during uncatalyzed maleation of EPDM.	233
Figure 8.13. Changes in the molecular weight distribution of maleated EPDMs within the stannous chloride dihydrate series, grouped according to Lewis acid concentration.	235
Figure 8.14. Correlation between the FT-IR measured succinyl anhydride (SAh) content and the predicted SAh content estimated from kinetic data in Chapter 6 for the first set of experiments in the twin screw extruder (deviation bars for conversions within a ±5°C range).	238
Figure 8.15. Correlation between the FT-IR measured succinyl anhydride (SAh) content and the predicted SAh content estimated from kinetic data in Chapter 6 for the second set of experiments in the twin screw extruder (deviation bars for conversions within a ±5°C range).	239
Figure 8.16. Glass transition temperature measured for samples 30-56F from the twin screw extruder	241

Figure 8.17. Relative torque plots of virgin EPDM and three maleated EPDMs versus neutralization time, using the steady-state torque within the range $t=300$ to $t=0$, as a baseline.	242
Figure 8.18. Relative torque calculated at $t=300$ s from a model fitted to the Rheocord data.	243
Figure 8.19. Relaxation moduli and complex viscosity of virgin EPDM at 230°C.	245
Figure 8.20. Cole-Cole plot of virgin EPDM and processed EPDM (p-EPDM) examining the effects of processing and purification of the rubber.	246
Figure 8.21. Cole-Cole plot (logarithmic scale) of the maleated EPDM sample produced at 230°C from Table 8.2 in the absence of catalyst.	248
Figure 8.22. Cole-Cole plot (logarithmic scale) of the maleated EPDM sample produced at 230°C from Table 8.2 in the presence of a Lewis acid.	249
Figure 8.23. FT-IR spectra of EPDM samples to determine the presence of poly(maleic anhydride)	252
Figure 8.24. Apparent viscosity curves for two EPDMs grafted with poly(maleic anhydride) compared to the virgin resin.	253
Figure 9.1. Structure and select properties of m-isopropenyl- α - α -dimethylbenzyl isocyanate (taken from R. W. Dexter et al., J. Coat. Technol., 58, 43 (1986))	260

NOMENCLATURE

Abbreviations

ABS	Acrylonitrile Butadiene Styrene Terpolymer
CP/MAS	Cross-Polarization/Magic Angle Spinning
DMF	Dimethylformamide
DSC	Differential Scanning Calorimetry
ENB	5-Ethylidene-2-Norbornene
EPDM	Ethylene Propylene Diene Terpolymer Rubber
EPR	Ethylene Propylene Copolymer Rubber
ESR	Electron Spin Resonance
FT	Fourier Transform
GPC	Gel Permeation Chromatography
HALS	Hindered Amine Light Stabilizer
HD	1,4-Hexadiene
HDI	Hexamethylene Diisocyanate
HOMO	Highest Occupied Molecular Orbital
HPLC	High Pressure Liquid Chromatography
IR	Infrared
LUMO	Lower Unoccupied Molecular Orbital
MAh	Maleic Anhydride
MAO	Methylalumoxane
MFI	Melt Flow Index
m-TMI	m-Isopropenyl- α - α -Dimethylbenzyl Isocyanate
MO	Molecular Orbital
MWD	Molecular Weight Distribution
NMR	Nuclear Magnetic Resonance Spectroscopy
PDI	Polydispersity Index
PEO	Poly(ethylene oxide)
pMAH	Poly (Maleic Anhydride)
PO	Polyolefin
PP	Polypropylene
SAh	Succinyl Anhydride
TEMPO	2,2,6,6-Tetramethylpiperidinyl-1-Oxy Free Radical
TMS	Trimethylsilane
UV	Ultraviolet

Symbols

γ_0	Initial Strain
$\dot{\gamma}$	Shear Rate (s^{-1})
$\dot{\gamma}_0$	Initial Shear Rate (s^{-1})

σ	Shear Stress (Pa)
σ_0	Initial Shear Stress (Pa)
δ	Phase Angle (degrees)
γ	Strain
η	Viscosity (Pa-s)
Θ	Maleic Anhydride-to-Vinylidene Mole Ratio
ρ	Density (g/mL)
ω	Frequency (Hz)
ω_c	Cross-over Frequency
A	Pre-Exponential Arrhenius Coefficient (s ⁻¹)
$A_{\text{wavenumber}}$	Absorbance
C	Concentration (mol/g or mol/L)
ΔE	Energy Difference (J)
ΔH_c	Crystal Cooling Enthalpy
ΔH_m	Crystal Melting Enthalpy
E_a	Activation Energy (J)
FW	Formula Weight (g/mol)
G'	Storage Shear Modulus (Pa)
G''	Loss Shear Modulus (Pa)
G_c	Cross-over Modulus (Pa)
I	Intensity
k	Kinetic Rate Constant (L/mol s)
L/D	Length-to-Diameter Ratio
M	Mass (g)
\dot{M}	Mass Flow Rate (g/min)
M_N	Number Averaged Molecular Weight
M_w	Weight Averaged Molecular Weight
N	Screw Speed (rpm)
t	Time (s)
t_0	Minimum Residence Time (s)
\bar{t}	Mean or Average Residence Time
T	Temperature (Kelvin or deg. Celcius)
T_c	Crystallization Temperature
T_g	Glass Transition Temperature
T_m	Crystal Melting Temperature
V	Volume (mL)
X	Conversion

CHAPTER 1. INTRODUCTION AND OBJECTIVES

1.1. INTRODUCTION

Many of the ethylene and propylene homopolymers and copolymers used in everyday consumer products, are characterized as materials with good mechanical and thermal properties, easy processibility, low cost and chemical inertness (Duca and Moore, 1996). These properties lend themselves well to the manufacture of bottles, packaging, fibres and tapes, to name just a few applications. However, due to the chemical inertness of this family of thermoplastics, they are not very useful in engineering applications such as the automotive and aerospace industries. Among the polyolefin family, polypropylene has been receiving intense interest by researchers because of its growth potential in commercial applications. Manufacturers of polypropylene, like Montell, insist the future of the automotive industry will see their product replacing currently used engineering thermoplastics (Mapleston, 1995). To broaden their application spectrum, polypropylene properties need to be modified via conventional co-polymerization processes with polar monomers or via reactive extrusion routes. A recent review of functional modification of polypropylene was given by Xu and Lin (1994).

Ethylene-propylene-diene polymer (EPDM), a terpolymer of the same family as polypropylene, exhibits the same chemical inertness yet on account of its elasticity, has significant penetration into the automotive market. Used in tires, weather sealant, hoses, belts, electrical sheaths and as engine mounts (Mark et al., 1986), the applications of EPDM in the automotive industry are quite extensive. However, to further promote the growth of

EPDM within the automotive sector and other specialty industries, the properties of the rubber must be extended through blends and composites to impart greater tensile strength and thermal and environmental stability. To achieve this blending of properties, EPDM needs functionalities incorporated into the chain beyond the usual unsaturation to compatibilize with other engineering resins such as polyamides and polyesters. Enhanced functionalities in EPDM may also improve coupling with fillers and reinforcing agents like glass fibres.

Ultimately, the long-term growth of these materials, requires polymer modification to broaden their distribution within the market.

1.2. REACTIVE EXTRUSION

The medium of contemporary organic chemistry is generally low viscosity solvents; an environment where reactants may experience chaotic mixing and high diffusivity. Operating conditions surrounding these classical reactions generally encompass subzero to moderate temperatures ($\sim 100^{\circ}\text{C}$) with reaction times ranging from minutes to days. These conditions appear ideal when compared to the limitations which reactive extrusion imposes. In reactive extrusion, the diffusion of reagents to the necessary sites of reactivity is comparatively slow due to the highly viscous state of a polymer melt which acts as the medium of the reaction. Dispersion of reactants in the extruder is limited to linear mixing (i.e. no flow re-orientation) unless a twin-screw geometry can be utilized. Reaction times are limited by the residence time distribution of the process, typically ranging from seconds to minutes in duration. Finally, purification procedures in the extruder are confined to the removal of volatile components exclusively. Still, reactive extrusion is a fast-developing field, for its low capital cost and ability to handle highly viscous materials in bulk reactions,

relieving companies of the costly recovery and environmental expenses of using solvents. The modularity of the extruder design makes it possible to design a reactor with appropriate mixing functionality at different stages of a reaction and thereby alter the residence time of the material. At each stage, reactive agents may be introduced or volatile products/by-products may be removed (Tzoganakis, 1989). A commonly employed modification reaction using reactive extrusion, is free radical maleation.

1.3. FUNCTIONALIZATION OF POLYPROPYLENE AND EPDM

Maleated polypropylenes, such as DuPont's commercially-available FUSABOND™, are produced to introduce the properties of adhesion and paintability as well as improved thermal stability, tensile strength, elongation and hardness (Trivedi and Culbertson, 1982) in the polymer. With polar groups introduced, the polymer is often used to compatibilize polypropylene with engineering resins such as polyamide for impact modification (Bidaux et al., 1996; Duvall et al., 1994; Lin et al., 1995) and liquid crystal polymers for improved tensile strength (Datta and Baird, 1995). Ethylene-propylene-diene terpolymer (EPDM) is another commonly maleated material. The functionalization of EPDM rubber has led to the formation of thermoplastic elastomer (Caywood, 1975; Datta et al., 1996ab; Dean, 1993; Dean, 1994; Siadat et al., 1980), provided replacement engineering resins with improved heat resistance and weatherability compared to ABS copolymer (Park et al., 1994) and acted as an impact modifier when EPDM must exhibit varying levels of compatibility in resins such as polyamides and polyesters (Gaylord, 1989), polypropylene (Van Gisbergen et al., 1991), acetal copolymer (Xie et al., 1997), polyphenylene oxide/polystyrene (Golba and Seeger, 1987) and silicone (Konar et al., 1994).

Other grafted comonomers onto polypropylene include acrylic acid (Rao et al., 1996), methacrylic acid (Nowak and Jones, 1965), glycidyl methacrylate and styrene/hydroxyethyl acrylate (Togo et al., 1990), 2-isopropenyl-2-oxazoline (Liu and Baker, 1994), and fumaric and itaconic acid (Ide and Sasaki, 1977; Yazdani-Pedram et al., 1996). For EPDM, the variety of grafted functionalities include styrene (Shung and Hu, 1996), dibutyl maleate (Greco et al., 1987), methyl methacrylate and 2-vinylnaphthalene (Park et al., 1994), acetyl sulfate (Siadat et al., 1980), pyrrole (Zoppi and De Paoli, 1996) and 2-(dimethylamino)ethyl methacrylate (Immirzi et al., 1987). All these polymers of grafted functionality have an important role in the “reactive” compatibilization of blends and are produced using similar grafting mechanisms.

1.4. FREE RADICAL VS. ALDER ENE GRAFTING REACTIONS

Depending on the nature of the process, grafted comonomer and homopolymeric species of the comonomer are either statistically distributed along the polymer backbone via free radical reactions or at specific sites via the Alder Ene reaction. Maleic anhydride is a logical choice for these reactions which are performed at high temperatures due to its reluctance to homopolymerize caused by the steric and polar properties of this 1,2-disubstituted species. Maleic anhydride is introduced at a reactive double bond via the Alder Ene reaction, but the comonomer content incorporated is limited to the number of original sites of unsaturation in the polymer. The content of maleic anhydride grafted by free radicals onto polypropylene is typically below 10 wt %, though typically greater in EPDM possibly due to improved solubility of the comonomer. The low concentration observed in free

radical functionalization is due to simultaneous grafting and less desirable side reactions, such as β -scission, branching, and cross-linking.

1.5. RESEARCH OBJECTIVES

The work described in this thesis investigated the application of site-specific chemistry for the reactive modification of a polypropylene homopolymer (at a terminal vinylidene) and an EPDM (at the hindered double bond of the ethylidene norbornene monomer). The motivation towards this goal was to functionalize these polymers without altering their molecular weight distributions through cross-linking or chain scission, which is characteristic of the free radical grafting method. In order to reduce the notably long reaction time inherent to the Alder Ene reaction for use in a twin screw extruder, it was necessary to study the novel application of Lewis acids as catalysts in this high temperature environment. Several Lewis acids were examined in this work, though the majority of experiments employed stannous chloride dihydrate. The reaction incorporated maleic anhydride into a polymer with a reactive double bond to produce a succinyl anhydride moiety. The work proceeded in three stages according to the objectives: i) determine the feasibility for the reactions and provide evidence of site specific functionalization, ii) optimize the processing conditions of the reaction via kinetic modelling and screw design, and iii) examine the usefulness of Lewis acids as catalyst at high temperatures.

This thesis is comprised of nine chapters including this introduction. The first four chapters are essential in establishing a detailed understanding of the Alder Ene reaction and those reactions which would interfere with either the polymer chain distribution or the nature of the attached anhydride species. Chapter 3 examines the process of generating vinylidene-

terminated polypropylene through chain scission. Two methods of degradation were studied with the goal of maximizing the terminal vinylidene group while minimizing oxidative functional groups which compete for the chain end. Four materials were investigated for the Alder Ene reaction: polyisobutylene, amorphous polypropylene wax, degraded isotactic polypropylene and EPDM; each of them comprised a chapter in this thesis, numbered 5 through 8 respectively. Chapter 5 was a preliminary study on polyisobutylene, of several classically employed Lewis acids. Chapter 6 characterized the structure of a maleated polypropylene wax with a terminal succinyl anhydride moiety produced within a batch reactor and in the absence of oxygen. This chapter distinguished the difference between a maleated polymer produced via the Alder Ene reaction and a free radical grafted product. Reaction parameters were examined with the intended goal of maximizing the terminal functionality. This included a kinetic study to confirm the catalytic nature of a Lewis acid in the reaction. Chapters 7 and 8 scaled the Alder Ene reaction up to the twin screw extruder through the use of higher molecular weight polymers. Reactive extrusion of polypropylene allowed an examination of mixing within the extruder though higher molecular weight chains imply fewer reactive sites for a terminal functionality like vinylidene. EPDM provided a high vinyl content in exchange for a highly viscoelastic material which constrained the mixing efficiency of the extruder.

CHAPTER 2. LITERATURE REVIEW

2.1. INTRODUCTION

Several comprehensive reviews on reactive processing exist (Tzoganakis, 1989; Xanthos, 1992; Burlett and Lindt, 1993; Schulz and Turner, 1982; Lambla, 1994) which examine the aspects of chemistry and mass-transport phenomenon during a reaction. A review by Burlett and Lindt (1993) outlined the general criteria for selecting chemical mechanisms to be used in any reactive processing environment. A chemistry which can be conducted in reactive processing equipment must, i) involve reactants which are soluble in the polymer matrix, ii) not involve reaction temperatures which will degrade the polymer, iii) be sufficiently reactive to proceed within the limited residence time of the extruder, iv) involve reactants which can be handled by the processing equipment, and v) produce by-products that are easily removed (if present at all). Brown (1992) categorized the types of chemical reactions into the six groups seen in Table 2.1. Among olefinic homopolymers and copolymers such as polyethylene, polypropylene and ethylene-propylene copolymer, the relatively low polarity of these species limits the methods of modification essentially to oxidation and photochemical degradation (Lambla, 1994), to which this family of polymers is particularly sensitive. Henceforth, the latter three categories in Table 2.1 have been the primary focus of researchers, as a means of extending the usefulness of this class of polymers. Polymer modification of propylene-based polymers began with free radical chain scission for producing resins with "controlled rheology" (Tzoganakis et al., 1988a,b,c; Suwanda et al., 1988; Kowalski, 1971) to improve processability. Comonomer grafting to

Table 2.1. Types of chemical reactions classified in reactive extrusion (Brown, 1992)

Type of Reaction	Description
Inter-chain Copolymer Formation	Formation of random, block, or graft copolymers through either ionic or covalent bonds.
Bulk Polymerization	Synthesis of polymer from monomers, pre-polymers, or a mixture
Functionalization/Functional Group Modification	Controlling chemical and physical properties of a polymer by rearrangement of functional side groups along the polymer chain.
Graft Reaction	Reaction of polymer and monomer to form grafted polymer or copolymer
Controlled Degradation	Scission of polymer chains to produce controlled rheology products or monomer.
Coupling/Cross-linking Reactions	Reactions increasing the molecular weight and/or viscosity of a polymer by use of reactive agents to produce branching, cross-linking, or end-linking.

polypropylene was, as stated by Kowalski (1992), a logical development of the radical chemistry for controlled rheology polypropylene. Maleation is the most intensely studied comonomer for grafting to polyolefins (PO). Extensive investigation into the mechanism for grafting maleic anhydride (MAh) onto polypropylene has been presented in recent years. However, the grafting site and structure of the functionality on the polymer chain is still a subject of contention (Gaylord and Mishra, 1983; Gabara and Porejko, 1967ab; De Roover et al., 1995; Rengarajan et al., 1995; Flat and Lambla, 1995; Borsig et al., 1995; Ho et al., 1993). Included in this embroiled subject of anhydride structure is the contentious suggestion of polymeric and oligomeric maleic anhydride growth, despite the reaction occurring above its ceiling temperature. Free radical grafting of functional groups onto polypropylene has a deleterious effect on the molecular weight of the polymer, decreasing the

chain length through β -scission (Gaylord and Mishra, 1983; Borsig et al., 1995; Coutinho and Ferreira, 1994).

As discussed in Chapter 1, site-specific reactions are a means of reducing the occurrence of side-reactions such as chain scission and homopolymerization. However, often analytical methods have difficulties in discerning the structure of the bound functionality at low concentrations such as those terminally attached to a polypropylene chain. Thus, understanding the mechanisms of free radical grafting and homopolymerization are important so that they may be negated as possible explanations for the presence of the attached functional group.

The rest of this chapter shall discuss literature results and theories on free radical grafting, homopolymerization, the Alder Ene reaction and side reactions which may occur simultaneously with the Alder Ene reaction. Despite the high ethylene content in ethylene-propylene-diene terpolymer (EPDM), it appears that the propylene segment is most susceptible to free radical reactions including chain scission and functional group grafting. Rheological measurements of free radical maleated ethylene-propylene rubber (Wu and Su, 1991) disclosed simultaneous reactions of crosslinking and chain scission, though β -scission dominated. Therefore, the proposed mechanisms detailed below are equally applicable to EPDM although the theme of the discussion shall focus on polypropylene.

2.2. STRUCTURE OF FREE RADICAL GRAFTED MALEIC ANHYDRIDE

Gaylord and Mishra (1983) proposed that maleation occurred at a tertiary radical along a polypropylene backbone, grafting either a single maleic anhydride (MAh) species or a polymeric anhydride chain grown from a maleic anhydride excimer (a free radical dimer

produced by excitation of MAh due to rapid decomposition of an initiator). De Roover et al. (1995) argued that the attached maleic anhydride and succinic anhydride species were located at the end of the polypropylene chain as a poly(maleic anhydride) segment. Rengarajan et al. (1995) contradicted this hypothesis through analysis by CP/MAS ^{13}C NMR, based on which they concluded that maleic anhydride reacted with a tertiary radical on the polypropylene backbone. Rengarajan et al. (1995) also proposed that the generated succinyl radical now attached to the methine carbon of polypropylene could lead to a cross-linkage through the anhydride species. Flat and Lambla (1995) substantiated the claims of Rengarajan et al. (1995) by using bromomaleic anhydride to graft to polypropylene. They observed negligible change in the viscosity of the system and a product which was completely amorphous. The weakly bound bromine atom of the anhydride was thought to homolytically cleave upon comonomer grafting, preventing the occurrence of the anticipated cross-linkage due to the moderately stabilized succinic anhydride radical. Borsig et al. (1995) also found indications of cross-linking through the anhydride group at low maleic anhydride reactant concentrations. Gaylord et al. (1987) dismissed the possibility of cross-linking occurring through appended maleic anhydride radicals, stating that the formation of cross-links was simply due to the less favoured abstraction of hydrogen from a backbone methylene carbon. In ethylene-propylene copolymer (EPR), the site of anhydride attachment was dependent on the comonomer sequence (Heinen et al., 1996). In random EPR, the anhydride was detected through ^{13}C NMR to be located at both methylene and methine carbons, however, in alternating EPR, methylene sequences greater than three carbons long were required for maleic anhydride to graft to the methylene units along the backbone. Heinen et al. (1996)

detected single succinyl anhydride groups attached to both polypropylene and EPR, however, only short maleic anhydride oligomers were observed in the polyethylenes tested.

Therefore, the majority of research work appears to indicate that the grafted anhydride group exists as a single unit on the polymer chain, though possibly acting as a coupling agent at low maleic anhydride reactant concentrations. The difficulty appears in conclusively identifying the presence of poly(maleic anhydride). As discussed in section 2.3, the structure of the homopolymer is so varied that identification may be complicated.

2.3. POLY(MALEIC ANHYDRIDE) AND DECARBOXYLATION

In a treatise on the homopolymerization of maleic anhydride, Trivedi and Culbertson (1982) stated that until the early 1960s, maleic anhydride was thought to be incapable of homopolymerization. Several methods including γ - and UV-radiation, electrolysis and organic peroxide initiation, were discovered subsequent to 1961 to overcome the reluctance of maleic anhydride towards polymerization (Trivedi and Culbertson, 1982). However, any investigation of poly(maleic anhydride) must consider decarboxylation of the cyclic anhydride, in spite of generally held conceptions that the reaction does not occur. It is presumably due to decarboxylation being overlooked that identification of polymeric and oligomeric maleic anhydride chains during grafting reactions onto a polymer, are typically missed. While neglected within the polymer grafting literature, the presence of decarboxylation has been observed by numerous researchers (Ordelt, 1973; R. Bacskai, 1976; Braun et al., 1969; Bhadani and Prasad, 1976; Zweifel and Völker, 1973) during the homopolymerization of maleic anhydride.

The polymerization of maleic anhydride in the presence of dibenzoyl peroxide did not show the Tromsdorff-Norrish gel effect and tended to exhibit a high rate of chain-transfer to monomer and initiator (Joshi, 1962). Joshi (1962) attributed the chain-transfer reaction to two labile hydrogens in maleic anhydride. Due to the strong chain-transfer character of the reaction, molecular weights of the species tend to be quite low, typically below 1000 g/mol. The structure of the polymer was thought to consist of cyclopentanone, succinyl anhydride, and conjugated ketoolefin units (Zweifel and Völker, 1973) which are shown in Figure 2.1. Braun et al. (1976) observed the evolution of carbon dioxide during benzoyl peroxide-initiated polymerization and based on proton NMR characterization described the repeat units of the polymer as a cyclopentanone structure. Decarboxylation was thought to occur simultaneously with polymerization. Bhadani and Prasad (1977) studied cathodic polymerization of maleic anhydride using N-methylpyridinium iodide as an effective electrolyte. The dark brown electrochemical product was found by IR to be similar to pyridine-initiated poly(maleic anhydride); both methods generated carbon dioxide during the reaction. Initiation via pyridinyl free radicals was ruled out due to the presence of benzoquinone (a free radical trapping agent) in the medium. Bhadani and Prasad (1977) suggested that the polymerization, like pyridine-initiated reactions, followed an anionic mechanism. Zweifel and Völker (1973) employed triphenyl and tributyl phosphine initiators to grow polymers consisting of primarily cyclopentanone units or conjugated ketoolefinic units, respectively. Infra-red, NMR and mass spectroscopy were utilized to confirm the structure of the different polymers and it was postulated that CO₂ was generated during base-initiated anionic polymer chain growth as a side reaction from the development of conjugated ketoolefinic units. Bacskai (1976) disputed the earlier proposed poly(maleic anhydride)

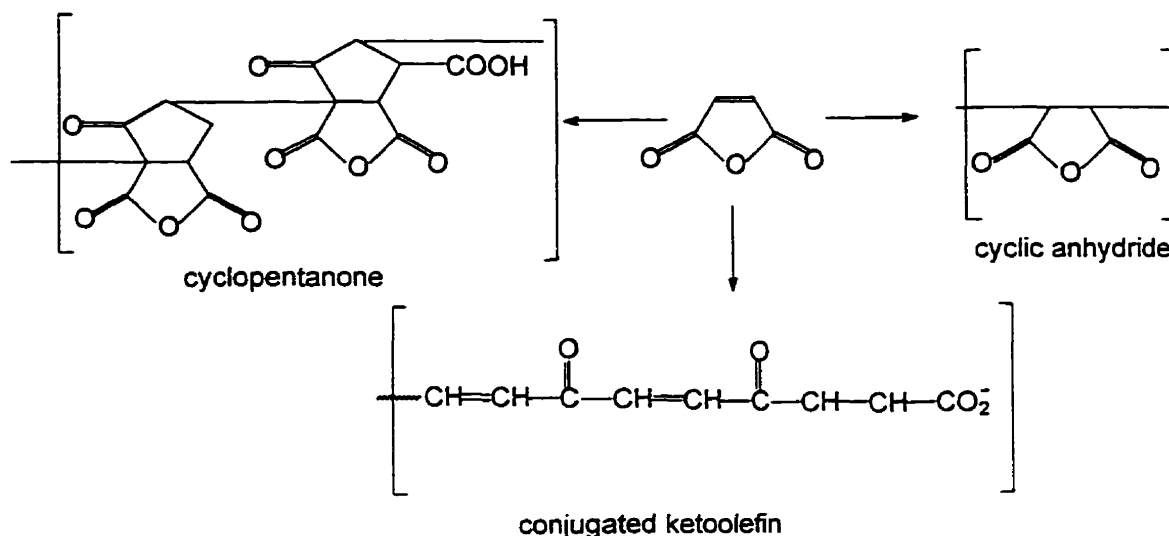


Figure 2.1. Postulated homopolymer segment structures in poly(maleic anhydride)

structures, namely the cyclopentanone (adjacent succinyl anhydride rearrangement) and ketoolefin (anhydride ring-opening) repeat units found in benzoyl peroxide-initiated and pyridine-initiated reactions respectively. Bacskai (1976) found that benzoyl peroxide-initiated polymer evolved only ~5 mol % CO_2 (based on maleic anhydride) during reaction and was characterized as possessing the appropriate cyclic anhydride repeat unit. Base-initiated (pyridine, triphenylphosphine or tributylphosphine) polymers exhibited significant decarboxylation (up to 60 mol % CO_2 based on maleic anhydride) with anhydride and cyclopentanone groups in the chain backbone as observed by NMR. The overall mechanism for homopolymerization appears to be quite complicated and it is clear from the contradictory findings of the aforementioned studies, that the actual nature of maleic anhydride homopolymerization is not understood.

Carbon dioxide being evolved during polymerization of maleic anhydride has been assumed by the previous authors, to be a part of the mechanism and not due to the preformed

product. Tate (1967) found that maleic and itaconic anhydride polymers decarboxylate in a consistent manner during heating and hydrolysis. Evolution of 0.30 moles CO_2 per mole itaconic acid and 0.15 moles CO_2 per mole maleic acid was generated from tested polymers. Tate (1967) observed that alternating copolymer of ethylene and maleic anhydride generated no CO_2 , and neither did the MAh monomer, leading to the conclusion that diads or triads were required for decarboxylation and structural rearrangement of the polymer. The theory of Tate (1967) could be used as an indicator of homopolymeric grafts of maleic anhydride on the polypropylene, since the anhydride concentration would be perceived as decreasing with time during heating. However, it should be mentioned that the conflicting ideas on maleic anhydride rearrangement and homopolymerization should be used as a cautionary note to not reading too much into this interpretation of decarboxylation.

Physically, the polymer product has been described, varying in appearance from a creamy white powder (Sharabash and Guile, 1976) to a black-brown solid (Bhadani and Prasad, 1977; Bacskai, 1976). Infrared analysis of the polymer (Sharabash and Guile, 1976; Joshi, 1962; Zweifel and Volker, 1973) will be discussed in section 2.6.3. Proton NMR (Bacskai, 1976) showed a broad band at 4.1 ppm which was assigned to the CH polymer backbone corresponding to the cyclic anhydride structure. Carboxylic acid groups if present, usually due to hydrolysis, were observed by proton NMR at 13.7 ppm. Unfortunately, NMR peak assignments were limited in the literature for a polymer that has been found to possess a very complex and varied structure.

2.4. FREE RADICAL GRAFTING MECHANISM

The mechanism for free radical grafting of maleic anhydride has been shown to be similar for both polypropylene and ethylene-propylene-diene terpolymer. It was proposed that a peroxy radical abstracts a labile hydrogen from the backbone of the polymer (Gaylord and Mehta, 1982; Gaylord and Mishra, 1983; Gaylord et al., 1987), generally considered at the tertiary carbon, although Greco et al. (1989) felt that the secondary hydrogen fit the observed results more appropriately for EPDM. Borsig et al. (1995) and Ho et al. (1993) had similar theories for polypropylene based on the notion that the reactivity of a tertiary hydrogen compared to a secondary hydrogen was 6:1, yet the abundance of secondary hydrogens to tertiary hydrogens improved the odds such that a secondary hydrogen abstraction would occur significantly. The double bond of the diene of EPDM has been found to not participate in the radical reactions (Sheng and Hu, 1996; Coutinho and Ferreira, 1994). With the presence of maleic anhydride, excimers and homopolymeric species, numerous addition reactions may occur at a macroradical site yielding a succinyl anhydride radical (Russell and Kelusky, 1988; Gaylord et al., 1987) or graft copolymer (Gaylord and Mishra, 1983). With the high chain transfer efficiency of the monomer and its tendency to form excimers, the radical grafting efficiency (ratio of grafted maleic anhydride to peroxy radicals) is always significantly higher than unity (Wu and Su, 1991; Oostenbrink and Gaymans, 1992; Coutinho and Ferreira, 1996; Greco et al., 1989; Borsig et al., 1995) and this efficiency value increases with temperature and decreases with increasing peroxide and maleic anhydride reactant concentrations as a result of excimer quenching. Despite the ceiling temperature for maleic anhydride at 150°C (Kellou and Jenner, 1976), Gaylord et al.

(1987) observed homopolymerization of maleic anhydride above 150°C in the presence of peroxide undergoing rapid decomposition. The generation of maleic anhydride excimers has been thought to account for the undesirable ionic coupling/electron transfer between maleic anhydride units resulting in homopolymeric MAh growth (Gaylord and Mishra, 1982). Hydrogen abstraction by the succinyl radical, excimer, or growing poly(maleic anhydride) chain, have all been attributed to scission and cross-linking reactions which degraded the olefin chains. Figure 2.2 presents the variety of reactions (with the exception of chain degradation or cross-linking) which are thought to occur during free radical maleation of polypropylene.

Scission and cross-linking during maleation have been investigated by several research groups (Wu and Su, 1991; Gaylord et al., 1987; Xie et al., 1997; Ho et al., 1993; Borsig et al., 1995), in an attempt to minimize such side-reactions. Polypropylene appears to exclusively degrade via β -scission during maleation. In EPDM, scission was found to dominate based on rheological measurements (Wu and Su, 1991), with cross-linking occurring only at high peroxide concentration. The presence of maleic anhydride appeared to increase both scission and cross-linking, when present. It has been proposed that cross-linking occurred before the scission reaction during the reactive functionalization of EPDM.

While scission and cross-linking degradative mechanisms can not be avoided, additive species such as DMF and stearamide have been found to interfere/quench excimers (Wu and Su, 1992; Gaylord et al., 1987; Gaylord and Mishra, 1983). These side-reactions are aside from thermo-mechanical and oxidative degradation which arise from processing (Kolbert et al., 1996; Baranwal, 1968) bearing predominantly β -scission. However, Kolbert

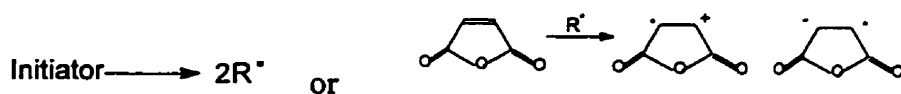
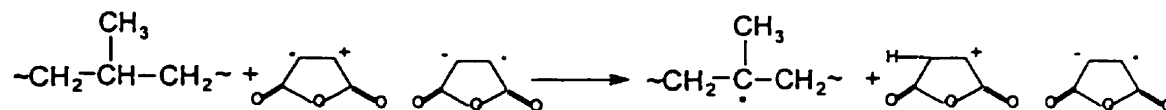
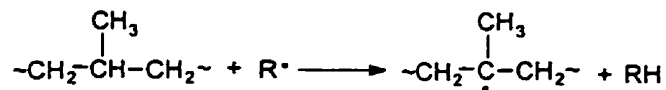
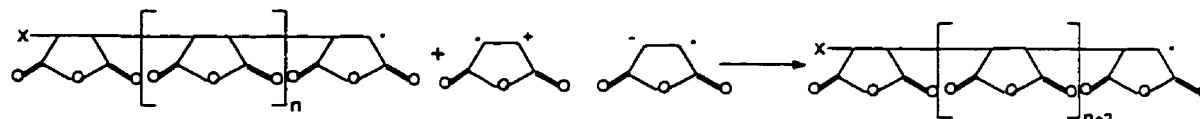
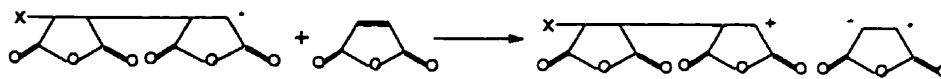
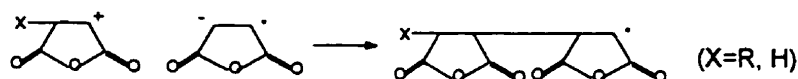
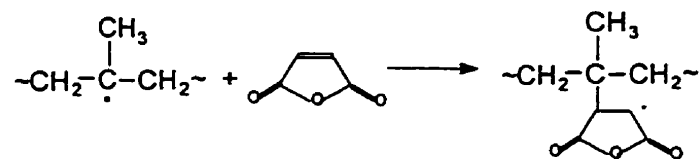
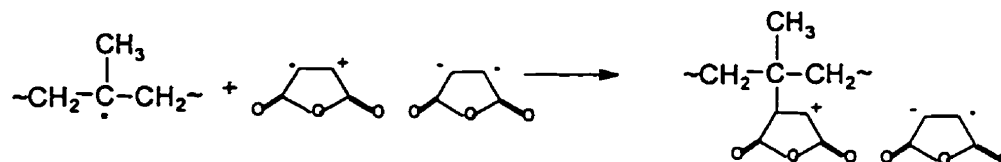
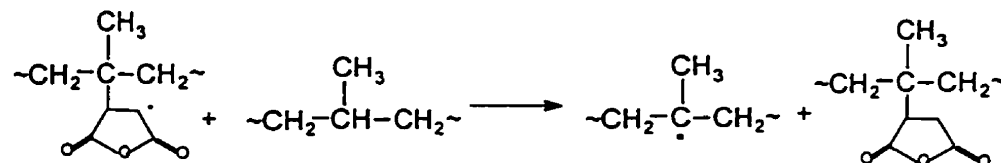
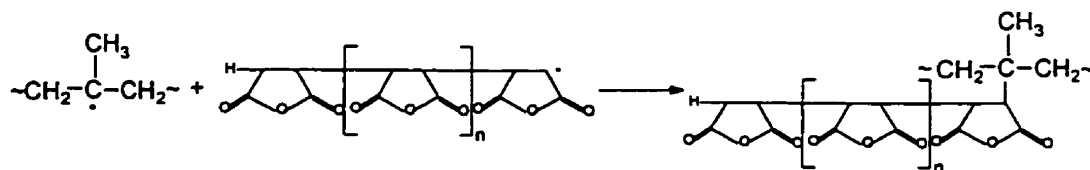
Initiation:**Hydrogen Abstraction:****Propagation:****Chain-Transfer:****Termination by Combination:**

Figure 2.2. Free radical mechanism for grafting maleic anhydride onto polypropylene (Adapted from N. G. Gaylord and M. K. Mishra, *J. Polym. Sci.: Polym. Lett. Ed.*, 21, 23 (1983))

et al. (1996) identified the occurrence of branching through the diene of EPDM at high temperatures.

2.5. ALDER ENE REACTION (SITE-SPECIFIC FUNCTIONALIZATION)

To reduce the occurrence of polymer degradation, several studies have examined chemical mechanisms that would produce “site-specific” functionalization. In polypropylene, the only prevalent reactive site for reactions not involving free radical chemistry is its terminal vinylidene group. Studies to date on the terminal functionalization of polypropylene have typically been performed in solution. A majority of the example chemical mechanisms producing terminally functionalized polypropylene begin with low molecular weight polymer, either degraded or synthesized to a degree of polymerization where sufficient vinylidenes are present, typically $\overline{M}_n < 5000$ g/mol. The chemistries explored include hydroboration, hydroalumination, epoxidation, silylation, maleation via Alder Ene addition, chlorination, and oxymercuration-demercuration (Mülhaupt et al., 1991; Nemes et al., 1992; Thompson et al., 1998ab; Shioni et al., 1992ab, 1993; McGee, 1994; Sawaguchi and Meno, 1996a). The functional groups generated as a result of these reactions include anhydride, silane, thiol, epoxide, borane and its hydroxyl derivative, and carboxylic acid species. Among the chemical mechanisms listed, the Alder Ene reaction is best suited to the field of reactive extrusion. Researchers functionalizing ethylene-propylene-diene terpolymer have also begun to utilize the Alder Ene reaction and even the Diels-Alder reaction, as a means of modification that reduces the possible occurrence of chain degradation as well as cross-linking. In the case of EPDM, site-specific functionalization has been more heavily pursued in commercial ventures than polypropylene as observed by the number of patents on

record. What follows is a review of the Alder Ene reaction for the different polymers studied in this thesis.

Two research groups, Tessier and Maréchal (1984ab, 1990) and Walch and Gaymans (1994) have discussed NMR (both proton and carbon-13), FT-IR and titration results for an Alder Ene reaction between maleic anhydride and polyisobutylene. The environment of the terminal vinyl group in polyisobutylene (shown in Figure 2.3) has a similar structure to that of polypropylene. Therefore, many of the parameters affecting the reaction using polyisobutylene may be extended to polypropylene.

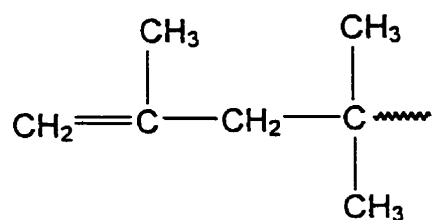


Figure 2.3. Terminal environment of polyisobutylene

The series of papers by Tessier and Maréchal (1984ab, 1990) studied the Ene reaction between monochelic and telechelic vinylidene terminated polyisobutylene (derived from α -chlorooligoisobutylene) and maleic anhydride. Extensive ^{13}C and ^1H NMR analysis identified the proper peak assignments for the vinyl isomers and the succinyl anhydride group. It was found that from the two allylic hydrogens in the *ene* reactant (vinylidene group), both conceivable products (shown in Figure 2.4) were formed with the ratio of the pendant vinyl structure (I) to the internal vinyl (II) being present as approximately 60% to 35%. The remaining 5% of the original vinylidene was isomerized to an internal vinyl prior to coordinating with a maleic anhydride species and did not react. Preliminary experiments

performed with a model material, 2,4,4-trimethyl-1-pentene identified a disuccinyl anhydride functionality as approximately 4 % of the product yield (Tessier and Maréchal, 1984a) which was not observed in any of the polymeric samples. The secondary Alder Ene reaction was

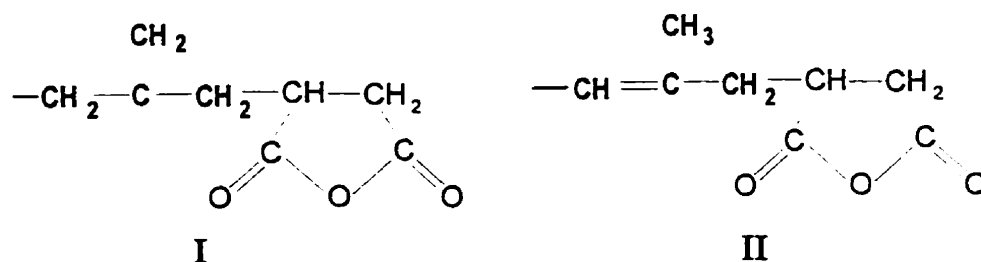


Figure 2.4. Vinyl isomeric structures in the Ene product

made possible by the pendant vinylidene present in the product, though steric hindrance from the polymer essentially inhibited the reaction.

Walch and Gaymans (1994) continued on the work of Tessier working with monochelic and telechelic vinylidene terminated polyisobutylene with a number-average molecular weight of 1800-2300 g/mol (calculated from vapour pressure osmometry). They found that Ene reactions in the bulk produced higher conversions (83 %) than those performed in solution (57 %) with the polymer appearing yellowish to light brown in colour. The darkening of the polymer was attributed to poly(maleic anhydride). Of particular interest with respect to the work in this thesis was their study of a reaction in the presence of a Lewis acid catalyst, though under mild conditions (41°C, 16 h). Two Lewis acids were compared, finding TiCl_4 to be suitable for the reaction system (67 % conversion), while AlCl_3 gave disappointing results (14 % conversion).

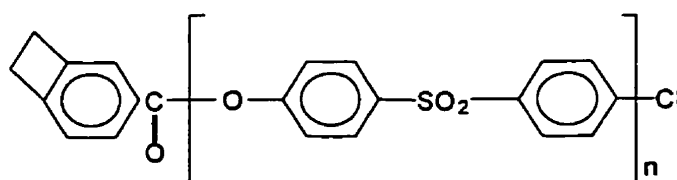
Several terminally functionalized metallocene polypropylenes ($\overline{M}_N = 880$ g/mol, PDI 2.3) were produced by Mülhaupt et al. (1991) with maleic anhydride, silane, thiol, epoxide,

borane and its hydroxyl derivative, and carboxylic acid moieties. To produce an anhydride-terminated polypropylene, the Ene mechanism was studied by reacting the wax and maleic anhydride in a resin kettle for 4 h at 225°C. The authors obtained an 87 % conversion for their reaction in the melt, based on the anhydride functionality which was measured by IR and ¹H NMR spectroscopy. Kotlar and Borve (1995) used a polypropylene with 1.7 wt % unsaturation for covalent attachment to a phenol-formaldehyde resin via the Ene reaction. No mention of the molecular weight of the polypropylene was given, though the degree of unsaturation would indicate a value of $\overline{M}_N \leq 2500$ g/mol. A high molecular weight polypropylene was added to improve the processability of the reactants, allowing the reaction to proceed in a 25 mm Clextral BC21 co-rotating twin screw extruder with an average reaction time of 2.5 minutes. Similar to Coran and Patel (1983), a Lewis acid activator was used (SnCl₂•2H₂O) to convert the methylol group of the phenol-formaldehyde resin into a suitable enophile, where subsequent attachment of the reactant species to polypropylene was achieved by the Alder Ene reaction. An optimal methylol content in the polymer corresponded to a reaction system employing the minimum concentration of catalyst and vinyls and the maximum concentration of the methylol reactant studied.

The patent literature is more replete with examples of Alder Ene reactions (peroxide-free grafting) particularly for ethylene-propylene terpolymers which shall be discussed in Chapter 8. Two patents concerning the Ene reaction for low molecular weight polyolefin wax should be mentioned (Schaufelberger, 1963; Sirinyan et al.,1994). Schaufelberger (1963) used high molecular weight polyethylene, that was subsequently cracked at 425-600°C to generate a wax with a molecular weight of 1000-5000 g/mol. The wax was reacted

with maleic anhydride at 180-250°C. Sirinyan et al. (1994) used semi-crystalline polypropylene wax (1000-8000 g/mol) to react with 4-5 wt % maleic anhydride in xylene at 140°C for 4 h to produce a binder for coating plastic substrates. Polypropylene wax with higher molecular weight (i.e. $\overline{M}_N = 6500$ compared to $\overline{M}_N = 4300$ g/mol) was found to show marginal improvement in the anhydride incorporation, a finding similar to Kotlar and Borve (1995) with respect to the effect of a reduced concentration of vinyls on the reaction.

Recently, both patent and journal literature has shown an increased interest in exploring alternative methods of functionalizing EPDM which do not involve free radical reactions, for example the Diels-Alder and Alder Ene mechanisms. These efforts have been initiated to reduce the degree of scission and cross-linking that occur during high temperature modification. Diels-Alder reactions to attach 1,2-dihydro-4-chloroformylbenzocyclobutene end-capped polymers (one of these structures is shown in Figure 2.5) onto EPDM were performed in a Brabender batch mixer at temperatures of 250-280°C (Dean, 1994; Dean, 1993). The structure formed by the reaction gave an aromatic ring adduct, which ensured its irreversibility due to the arising resonance stability. Dean observed exclusive grafting with an absence of polymer degradation and non-grafted homopolymerization. Jiang and Hamed (1997) reacted fullerene (C_{60}) with the hindered double bond of ethylidene norbornene in



1,2-dihydro-4-chloroformylcyclobutyl-polyethersulfone

Figure 2.5. End-capped polyethersulfone grafted to EPDM via the Diels-Alder reaction

EPDM at 105°C by cycloaddition. The product exhibited an interpenetrating network with a cross-link density of 2.5 mole/m³ as measured by equilibrium swell data in benzene. An experimental control of EPDM without fullerene did not exhibit reversible deformation and completely dissolved in benzene proving that the fullerene participated in the formation of gel.

Reactions involving the Alder Ene mechanism have occurred primarily in the patent literature for EPDM (Caywood, 1977; Roncetti and Banzi, 1992; Coran, 1987; Hammer and Sinclair, 1994; Sweeney et al., 1971). However, a few authors have produced Alder Ene products within studies investigating peroxide-catalyzed functionalization simply as a measure of maleation at the lowest possible peroxide concentration (Oostenbrink and Gaymans, 1992; Wu and Su, 1991). The two most in-depth investigations of the Alder Ene reaction for the maleation of EPDM were Caywood (1977) and Roncetti and Banzi (1992). Caywood (1977) examined the process of incorporating maleic anhydride into EPDM via the Alder ene reaction, to generate a polymer capable of forming ionic cross-links in the presence of a weak base such as zinc or magnesium oxide. EPDM rubbers containing either 1,4-hexadiene (6.6 wt %) or 5-ethylidene-2-norbornene (4.4 wt %) were examined with respect to their ability to incorporate maleic anhydride in the absence of covalent crosslinking. The reaction was carried out in a Werner-Pfleider twin screw extruder, along with a hot press and a roll mill. Attached succinyl anhydride content between 2-4 wt % was measured for product modified using the Alder ene reaction with less than 5 % gel observed. For comparison, 4.8 wt % Lupersol 101 dialkyl peroxide was used, incorporating only 1.5 wt % maleic anhydride into the EPDM product with 70 % gel observed. Roncetti and Banzi (1992) studied the

maleation of EPDM rubber (3.5 % 5-ethylidene-2-norbornene or 1.2 % butadiene monomer) via the Alder Ene reaction at 270°C in a Brabender PLE 651 plastograph. The reference is unique in the use of catalysts within the Alder Ene reaction for EPDM rubber and therefore is discussed in depth in section 2.5.1.1.

2.5.1. Mechanism and Parameters of the Alder Ene Reaction

This versatile and simple reaction provides a unique opportunity to functionalize polyolefins at their sites of unsaturation under operating conditions which would otherwise exclude other attempts to modify the polymer. Similar in mechanism to the Diels-Alder reaction, the Alder “Ene” Reaction involves the addition of two unsaturated species (Figure 2.6). The Alder Ene reaction is an “indirect addition” involving electron interaction between

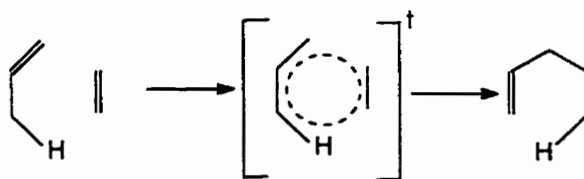


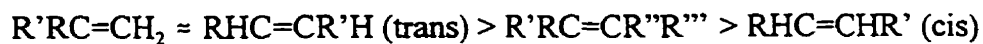
Figure 2.6. Reaction mechanism for the Alder Ene reaction

the highest occupied molecular orbital (HOMO) energy state of the *ene* (an unsaturated species with an allylic hydrogen available) and the lowest occupied molecular orbital (LUMO) energy state of the *enophile* (an unsaturated species with neighbouring electron-withdrawing groups). A discussion of molecular orbital (MO) theory is beyond the scope of this work, however, the reader should recognize that the energy states mentioned refer to the π -system and that the ΔE term presented later refers to the energy difference in quantum states between the two reacting species. The reaction, sometimes referred to as a pericyclic

reaction, has a 6-centre transition intermediate due to its concerted mechanism (Figure 2.6). The product shows the *enophile* attached to the *ene* with the formation of a new π -bond. For some species different possible isomeric products may arise, as is the case with polypropylene which will be discussed towards the end of this section. The π -bond of a carbonyl group may also act as an *enophile* in the reaction, but carbon double bonds will react almost exclusively if present.

The intermolecular reaction generally requires high temperatures (200-600°C; Hoffmann, 1969). An optimum temperature exists for the Ene reaction, after which the retro-Ene reaction dominates (thermal reversion; review by Ripoll and Vallée, 1993). Reaction times in the literature are in the order of hours to days for high conversions. The reaction time is dependent on the acidity and basicity of the *ene* and *enophile* respectively, and the reaction conditions mentioned previously. The reaction rate is enhanced by a reduction in ΔE between the appropriate HOMO and LUMO states for the two reacting species. Generally, electron-donating substituents will raise the energy of both HOMO and LUMO states of an individual molecule. Electron-withdrawing substituents tend to lower the energy of both HOMO and LUMO states of an individual molecule (Smith, 1994). Through examination of the literature, one finds that the electron-donating substituents of the vinylidene group in polypropylene provides a highly reactive *ene* for the reaction. Albisetti et al. (1956) have found that 1,1-disubstituted *enes* (i.e. $RR'C=CH_2$) give higher yields in reactions with *enophiles* containing various nitrile and carbonyl groups, than linear or non-terminal vinyls. Snider et al. (1979) concurred with the claim of Albisetti et al. (1956), stating that the Ene reaction occurs preferentially to unsaturated species containing at least one disubstituted site.

Unlike disubstituted vinyls which exclusively yield the Alder Ene product, mono-substituted olefins produce a mixture of Ene and [2+2] cycloaddition products. Trivedi and Culbertson (1982) ranked the reactivity of the substituted olefins as:



The ΔE of the reaction system may be further reduced through the presence of a Lewis acid (Smith, 1994). The Lewis acid co-ordinates with the *enophile*, lowering its LUMO energy state (increasing the basicity of the reactant). The acid behaves as a catalyst allowing the Ene reaction to proceed faster and at lower temperatures (Snider, 1974, 1979), thus, avoiding the retro-Ene reaction. Stronger Lewis acids provide greater enhancement to the reaction (Smith, 1994). Reviews on the Alder Ene reaction are given by Hoffmann (1969), Oppolzer (1984) and Trivedi and Culbertson (1982).

2.5.1.1. Lewis Acids in the Alder Ene Reaction

A Lewis acid is an electrophilic centre capable of accepting an electron pair. In the case of metal salts acting as 'neutral' Lewis acids, the metal atom is electron-deficient possibly enhanced by the covalent attachment of ligands (i.e. groups or atoms attached to the metal). Lewis acids can normally be described in the form of MX_n , where X is a ligand generally a halogen atom, an amine or other organic functionality, and n is the normal valency of the metal M (Smith, 1994). Neutral Lewis acids react with Lewis bases to form an adduct ($MX^- B^+$). The strength of the acid is dependent on the electrophilic nature of the central atom and the electron affinity of the ligands. Group IVA atoms, which include tin, form MX_4 Lewis acid species which have only weak acidic properties (Smith, 1994). Our

Lewis acid, $\text{SnCl}_2 \cdot 2\text{H}_2\text{O}$, was chosen for its mild acidic nature, though the aquo ligands are thought to have been replaced by DMF when that solvent was present.

The mechanism for the catalyzed Ene reaction has largely been neglected in the literature, with only a few intermediate structures proposed regarding the involvement of the Lewis acid. Those intermediate species were hypothesized from structural analysis of the Ene product, and not as a result of direct analysis. Kurbanova et al. (1996) suggested a scheme for Lewis acid co-ordination with maleic anhydride, which is shown in Figure 2.7 modified to account for the polarity of the system as described by Snider et al. (1979). The metal catalyst co-ordinates with the anhydride functionality of maleic anhydride due to its greater basicity towards the Lewis acid than the electron-rich propylene vinylidene. The driving force for the extraction of the Lewis acid with respect to the succinyl anhydride moiety attached to polypropylene and hence defining the catalytic nature of the species, is also basicity. The basicity of maleic anhydride must exceed that of the Ene product (succinyl-terminated polypropylene) in order for the Lewis acid to withdraw from the product anhydride. In the event of the end product complexing more strongly to the catalyst, higher quantities of the Lewis acid would be required (Snider et al., 1979).

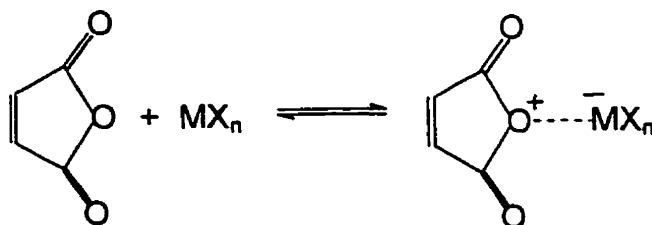


Figure 2.7. Reaction scheme of a Lewis acid with the maleic anhydride to form an intermediate adduct to act as a stronger enophile in the Ene reaction.

Isomerization has been observed by Snider et al. (1979) in cyclic and acyclic low molecular weight species during catalyzed Ene reactions. The rearrangement of the vinyl was attributed to the generation of hydrogen chloride from the Lewis acid. The hydrogen chloride reduces the vinyl according to Markovnikov's rule, placing the chlorine atom at the more substituted carbon of the double bond. The elimination reaction (dehydrochlorination) will generate a new vinyl. However, there are now three hydrogens on the β -carbons adjacent to the carbon attached to the chlorine; two of those hydrogens would lead to a new vinylidene, while the other hydrogen will generate an internal vinyl. Thermal dehydrochlorination has been used to generate vinylidene in polyisobutylene (Walsh and Gaymans, 1994; Tessier and Maréchal, 1984ab, 1990) at high temperatures. At the processing temperatures of the extruder (greater than those used by Snider), thermally-induced isomerization is another possible mechanism for vinyl rearrangement.

Although the possibility of a Lewis acid carbonyl-ene reaction tends to be less favoured, reactions with the carbonyl versus the vinyl of an enophile must be considered. Lewis acid-promoted carbonyl-ene reactions are typically recognized as an ionic rather than concerted mechanism with a dipolar Friedel-Crafts intermediate (Achmatowicz and Bialecka-Florjanczyk, 1996). The *ene* vinyl coordinates with the carbonyl carbon yielding either a hydroxyl or oxo-cyclic species such as a lactone (IR absorbance $\sim 1780\text{ cm}^{-1}$).

Results presented by Kurbanova et al. (1996) on the cationic functionalization of polystyrene with maleic anhydride via Lewis acids, have demonstrated the susceptibility of phenyl rings to reaction with these catalysts (proposed mechanism for the reaction given in Figure 2.8). Other work (Tsuchida et al., 1972) supported the findings of Kurbanova et al.

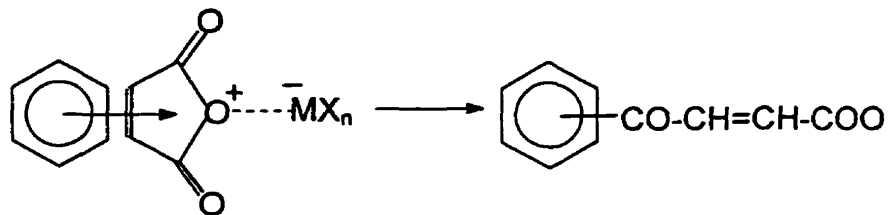


Figure 2.8. Mechanism for maleic anhydride attachment to a phenyl-based molecule (Adapted from Kurbanova et al., *J. Appl. Polym. Sci.*, 59, 235 (1996))

(1996). Due to the common presence of phenyl rings in free radical inhibitors, conventional chemical products may not be useful for this work (discussed in Chapters 5-6). Less orthodox chemical species may be necessary to initiate the Ene reaction in the absence of undesirable free radical side-reactions.

The efficiency of a Lewis acid employed as a catalyst for the Ene reaction is reactant-specific. For example, Prashad et al. (1989) examined the Lewis acid-catalyzed Ene reaction of formaldehyde with 1,3-diarylcyclopentene. In their investigation, they found that ZnCl_2 and Me_3Al yielded no product, while AlCl_3 and EtAlCl_2 in conjunction with ZnCl_2 yielded the product at low efficiency. The best catalyst examined was diethyl aluminum chloride giving 61% yield. Oppolzer (1984) documented this selectivity in catalysis efficiency for several reactions using a range of Lewis acids. The Lewis acids investigated include ZnCl_2 , SnCl_4 , $\text{BF}_3 \cdot \text{OEt}_2$, Et_2AlCl , TiCl_4 , $\text{TiCl}_2(\text{OiPr})_2$, Me_2AlCl , and AlCl_3 . The stoichiometric ratio of Lewis acid to *enophile* generally ranged from 0.2 to 1. This treatise was the most extensive found in the literature on the catalytic effect of Lewis acids. Trivedi and Culbertson (1982) added to this compilation several Brønsted acids, namely HCl , HBr , phosphoric acid and phosphinic acid from their review of Ene reactions using maleic

anhydride. Mikami et al. (1988) demonstrated the diastereocontrol of different Lewis acids in the Ene reaction. The threo or erythro selectivity of their synthesized steroid resulted from the use of SnCl_4 or $\text{Me}_n\text{AlL}_{3-n}$, respectively. Snider et al. (1979) found that AlCl_3 was an effective catalyst for thermal Ene reactions, however, isomerization and hydrochlorination of the *ene* species and of the reaction product were observed. It was reported that EtAlCl_2 gave products in high yield without the presence of chlorine contamination or isomerization, possibly due to its ability as a HCl scavenger.

Other catalysts which exhibit merit in pericyclic reactions are ruthenium and rhodium chloride, two species examined by du Pont in 1965 (Alderson et al., 1965; R. Cramer, 1965). A paper by Trost et al. (1995) recognized the reaction of alkenyl to alkynyl species via ruthenium catalyst ($\text{CpRu}(\text{COD})\text{Cl}$, cyclopentenyl-cyclooctadienyl ruthenium chloride) as an intermolecular formal Alder Ene reaction. Chloride hydrates of ruthenium and rhodium in the presence of alcohol were investigated by Alderson et al. (1965) in reactions involving olefins with diolefins such as ethylene with butadiene to produce 1,4-hexadiene, under moderate temperatures of 30-150°C. It was found that the major product was a straight chain diene without side- or chain-reactions observed. This behaviour was also noted by dimerization of ethylene, propylene, methyl acrylate and butadiene species to the exclusion of higher molecular weight species (Alderson et al., 1965). Ruthenium chloride is a milder catalyst usually requiring temperatures as high as 200°C compared to 120°C for rhodium chloride in the Ene reaction. The presence of an alcohol or acetone was found to promote high catalytic activity regardless of the actual quantity of these species. Even small quantities of water (ca. 0.5 part H_2O per part catalyst) could be tolerated by the hydrated

catalysts. If no alcohol or acetone was present, Alderson et al. (1965) found that conversions were only one-third of those obtained with the solvents. These transition metal chlorides were co-ordinating with the *enophile* vinyl enhancing its reactivity. This phenomenon is opposite to the previously mentioned Lewis acid species which withdraw electrons from the active oxygen of the enophile, removing electrons from the species to increase its susceptibility to attack (Cramer, 1968).

Interest in ruthenium chloride to catalyze the Ene reaction commercially has only been noted in one reference, US Patent 5,153,270 assigned to Ausimont S. r. l., Italy. The authors, Roncetti and Banzi (1992) incorporated succinyl anhydride into ethylene-propylene-diene terpolymer (EPDM) containing either 1.2 % butadiene or 3.5 % ethylidene norbornene as the diene monomer. The reaction was carried out at 270°C in a Brabender PLE 651 plastograph. Powdered maleic anhydride (1-2 wt %) and solid catalyst (RhCl_3 , RuCl_n , RhBr_3 and $\text{Rh}(\text{NO}_3)_3$) at a concentration of 0-0.1 wt % were added once the elastomer had softened, for a reaction time of five minutes. Catalyst concentrations of 0.05 and 0.1 wt % with the lower level of maleic anhydride present was favoured for anhydride incorporation, ~99 % conversion was achieved. Anhydride content in the uncatalyzed product was found to be only 31–44 %. Rhodium halide catalysts were the most efficient at 99 % and 98 % conversion for the chloride and bromide species, $\text{Rh}(\text{NO}_3)_3$ gave 67 % conversion and ruthenium chloride yielded 69 % conversion. Conversion values were calculated from FT-IR and acid titration data. While these results are promising with regards to this thesis, the data is held with some degree of skepticism since the reaction was determined to take less than 1 minute for the conditions outlined. The similarities between the patent of Roncetti and Banzi

(1992) and what was intended for this work suggested the value of this reference and is the primary reason for the expressed interest in ruthenium chloride in this thesis (rhodium species are too expensive to be considered). Within this thesis, further experimentation with ruthenium chloride for the maleation of EPDM will hopefully reveal a more in-depth understanding of the reaction that was preliminarily investigated by Roncetti and Banzi (1992).

2.5.1.2. Inhibitors in the Alder Ene Reaction

Due to the processing temperatures required for the Ene reaction to proceed at a reasonable rate, free radical mechanisms are possible competitive reactions. Pinazzi et al. (1963) studied the incorporation of maleic anhydride onto polyisoprene at 180-240°C for evidence of the reaction mechanism proceeding via the thermal Ene reaction opposed to a free radical reaction. NMR analysis of the product showed vinyl isomerization which the presence of thiophenol, a highly efficient radical acceptor, did not affect. However, the inhibitor considerably hindered the maleation of polyisoprene using a free radical initiator. It was concluded that the prevention of free radical formation was important to exclude undesirable byproducts in Ene reactions. Trivedi and Culbertson (1982) suggested hydroquinone and t-butylcatechol as radical inhibitors in Ene reactions using maleic anhydride as the *enophile* to produce various alkenylsuccinic anhydrides. Irwin and Selwitz (1968) studied the effect of different inhibitors in thermal Ene functionalization with maleic anhydride. Phenothiazine was found to give higher reaction efficiency with respect to maleic anhydride and produce the lowest weight fraction of poly(maleic anhydride) compared to hydroquinone or 2,2'-di(p-hydroxyphenyl) propane. An alternative inhibitor not discussed in

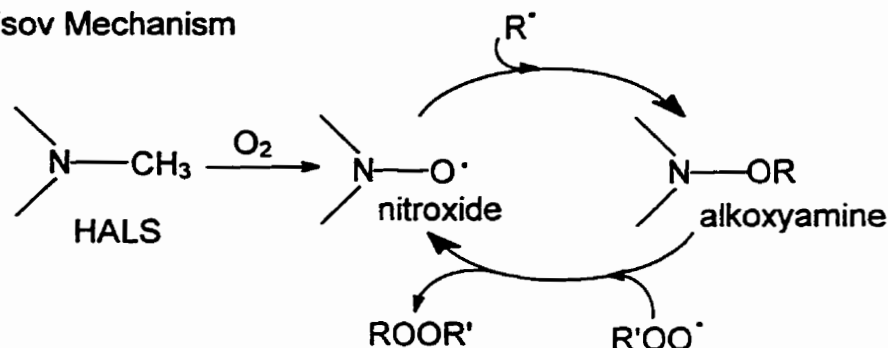
the literature for the Alder Ene reaction was a species which has been shown to act as a radical trapping agent, namely 2,2,6,6-tetramethylpiperidinyl-1-oxy (TEMPO) (Moad et al., 1981). TEMPO is an nitroxyl intermediate from the HALS (hindered amine light stabilizer) family. HALS species are discussed in polymer processing literature providing UV stabilization without interfering with other additives such as antioxidants (Gray, 1991; Step, 1994). Moad et al. (1981) found that alkyl and phenyl radicals, may be trapped by the stable free radical nitroxide, forming alkoxyamines. The extent of this trapping reaction is a function of the nitroxide and reactant concentrations. More recent theories on HALS stabilization are found in the papers of Gray (1991), Ekman et al. (1995) and Step et al. (1994). Derivatives of HALS produce stable nitroxyl radicals via oxidation which subsequently may react with alkyl radicals forming an alkoxyamine. The active nitroxyl radical is regenerated by oxidation induced by a peroxy radical. The cyclic "non-sacrificial" nature of the mechanism is the strength in this type of stabilization (Gray, 1991). The cyclic stabilization mechanisms of Denisov (1991) and Klemchuk and Gande (1988) are shown in Figure 2.9.

Clearly, these stabilizers and nitroxyl species in general, are most effective in the presence of oxygen based on the stabilization mechanism. From solution studies, the rate of scavenging alkyl radicals was found to be very high, 10^7 - 10^9 $M^{-1} s^{-1}$, while peroxy radicals are known to be considerably lower in concentration (Step et al., 1994).

2.5.1.3. Kinetics of the Alder Ene Reaction

The kinetics of the Alder Ene reaction using maleic anhydride as the enophile has been found to be described by a second-order expression; first-order with respect to the *ene*

Denisov Mechanism



Klemchuk and Gande

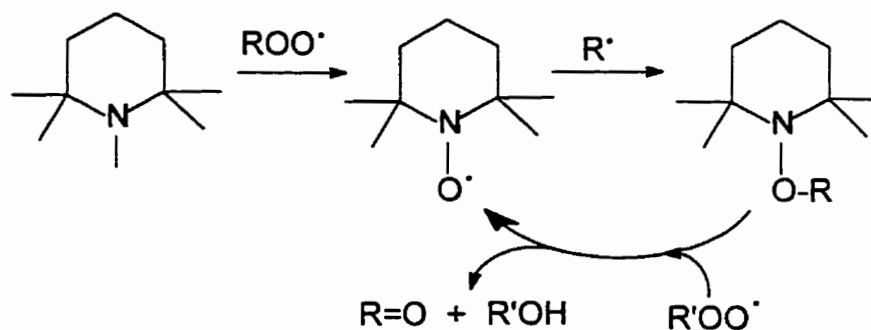


Figure 2.9. Stabilization mechanisms of Denisov (1991) and Klemchuk and Gande (1988)

and *enophile* respectively (Rondestvedt and Wark, 1955; Benn et al., 1977). The kinetic nature of the reaction has only been studied in the literature for small molecules. Rondestvedt and Wark (1955) initially examined and dismissed the possibility of the Ene reaction possessing a radical chain mechanism. They proceeded to confirm the second-order nature of an Ene adduct formed between allylbenzene and maleic anhydride, based on measurements of extracted maleic anhydride. The activation energy for the Arrhenius equation was determined to be 84 KJ/mol over a temperature range of 127-153°C. No significant change in the results of Rondestvedt and Wark (1955) was observed for reactions performed in the presence or in the absence of a free radical inhibitor. An extensive kinetic

investigation of alkenes initiated by Benn et al. (1977) examined numerous effects including alkyl chain length, free radical inhibitors and degree of substitution at the vinyl group. The activation energy was found to be 90 KJ/mol for all alk-1-enes covering n-propyl to n-nonyl species and 75.5 KJ/mol for cis-dec-5-ene and 77.1 KJ/mol for trans-dec-5-ene over a temperature range of 127-180°C. These results are in contradiction to the theory of a concerted mechanism which should favour a cis-addition (Hoffmann, 1969), yet still confirm other aspects of the reaction with the reduction of the activation energy for an increased degree of substitution due to the greater electron density situated at the π -bond. Similar to Rondestvedt and Wark (1955), an inhibitor did not affect the rate of reaction.

2.6. DETERMINATION OF END GROUP FUNCTIONALITY

Due to the low concentration of the site-specific functional groups in the polymer, detection of the functionality and evidence of its covalent attachment are difficult. From telechelic/monochelic synthesis literature (low molecular weight polymers $\overline{M}_N = 1000$ -10,000 g/mol with both end groups of a linear chain functionalized), the common approach to determine functionality of the polymer is ^1H and ^{13}C NMR, molecular weight distribution by GPC, and acid-base titration (Walch and Gaymans, 1994; Xu et al., 1995; Hashimoto et al., 1995; Chasmawala and Chung, 1995). This problem of functional group detection is complicated by the properties of our two polymers, i.e. EPDM and polypropylene, in particular their lack of solubility in most solvents except at elevated temperatures, their susceptibility to thermal degradation, and the crystallinity of polypropylene. For example, evidence by solution nuclear magnetic resonance spectroscopy of the terminal functionality in our polymer is typically inconclusive since the signal intensity is found only slightly above

the noise of the instrument and signal detection is complicated by the inhomogeneity of the polymer sample being analyzed. Rengarajan et al. (1990) were unable to detect the maleic anhydride carbonyl signal of polypropylene-g-maleic anhydride in solution ^{13}C NMR (75 MHz). However, analysis in the solid state using CP/MAS NMR showed the anticipated chemical shifts just above the noise of the spectrum. Unfortunately, most classical methods of chemical structural analysis are uninformative with regards to this project, leaving sparse information to derive conclusions. The most promising methods shall be mentioned for the analysis of the anhydride and unsaturation functionalities.

2.6.1. Block and Graft Copolymerization

This technique is not seen as an analytical method for detecting terminal functionality, but it is capable of “amplifying” the presence of the trace functional groups. By covalently attaching to other functionalized polymers, new properties are added to the polymer which may be more easily detected by any one of the following methods of analysis. This method of functional group determination was employed by Mauler et al. (1995) in a HO-telechelic liquid rubber. The key factor is to choose a polymer which will react with the functionalized sample and exhibit different properties (i.e. spectroscopy, thermal and rheological) which are not obscured by the principal polymer. Chasmawala and Chung (1995) synthesized a block copolymer of polycaprolactone-block-polyisobutylene to gain better insight into the efficiency of their reaction producing a telechelic polyisobutylene. Using GPC and ^1H NMR, they were able to determine the extent of metathesis degradation in their synthesis route.

2.6.2. ^1H and ^{13}C NMR

Shiono and Soga (1992) in their analysis of a metallocene polypropylene (derived from a $\text{Et}[\text{H}_4\text{Ind}]_2\text{ZrCl}_2/\text{MAO}$ catalyst) showed that backbone proton chemical shifts were between 1-2 ppm with the vinylidene resonance occurring at 4.8 ppm [$\text{CH}_2=$]. At high resolution (i.e. 500 MHz), they observed the vinylidene as a doublet and were just able to detect a 2-butenyl group at 5.5 ppm [$-\text{CH}=\text{CH}-$]. Sawaguchi et al. (1995) observed similar resonances within a highly cracked polypropylene, with a doublet for the vinylidene at 4.83 and 4.77 ppm. They also observed a small broad resonance at 5.44 ppm possibly corresponding to either a terminal or internal vinyl. According to Tessier and Maréchal (1984b), the internal vinyl arising from an Ene synthesis at the vinylidene group occurs at 5.14 ppm [$(\text{CH}_3)_2\text{C}=\text{CH}^*$]. Carbon resonances were observed (Shiono and Soga, 1992; Busfield and Hanna, 1991; Nemes et al., 1992; Sawaguchi et al., 1995) between 14-48 ppm for the polypropylene backbone with the vinylidene carbons shown at 148 ppm [$=\text{C}^*(\text{CH}_3)-$] and 112 ppm [$\text{C}^*\text{H}_2=$]. For the internal vinyl, the given peaks at 127.9 ppm [$(\text{CH}_3)_2\text{C}^*=$] and 135.4 ppm [$=\text{CH}-$] were determined by Tessier and Maréchal (1984b). The observed chemical shifts correspond closely with the calculated values using the Lindeman-Adams (1971) and Dorman (1971) correlations. The two NMR resonances for the $\text{R}_2=\text{CH}-$ proton of 5-ethylidene-2-norbornene (ENB) in EPDM were observed at 5.1 and 5.3 ppm (Chiantore et al., 1994; Tanaka et al., 1975). The backbone structure of EPDM was best discussed by Lee et al. (1996) using ^{13}C NMR. The only reference found for NMR analysis of maleic anhydride incorporated into EPDM was Heinen et al. (1996), who used a ^{13}C -enriched anhydride species for ^{13}C NMR analysis. They found single succinyl anhydride rings

attached at the tertiary sites within polypropylene sequences ($\delta=34$ ppm methylene; $\delta=48.2$ and 49.8 ppm, methine) and attached at the secondary sites ($\delta=31.1$ methylene and 44.3 ppm methine).

Maleic anhydride functionalized polypropylene (tertiary grafted) was characterized by Tang et al. (1994) using ^{13}C NMR. The succinyl anhydride functionality gave the following carbon shifts: 62.6 ppm [a], 172.9 ppm [b], 169.7 ppm [c] and 32.7 [d, calculated]. Figure 2.10 shows the carbons of the succinyl anhydride structure as they appear, covalently attached, to the polypropylene. Since different carbon environments can affect the chemical shifts of carbons up to 12 bonds away from the carbon of interest, the chemical shifts of the anhydride will differ slightly at the terminal site of polypropylene. Tessier and Maréchal (1990) characterized succinic anhydride terminally bound via an Ene reaction with a vinylidene in a similar electron environment to the proposed polypropylene system. Proton peak assignments indicated that the terminal succinic anhydride possessed a complex splitting pattern between $2\text{--}3$ ppm with a separate broad peak at 3.3 ppm. ^1H and ^{13}C spectra for the reaction of an anhydride and amine were included in the work of Tessier and Marechal (1984b), however, due to the complex splitting patterns, the peak assignments

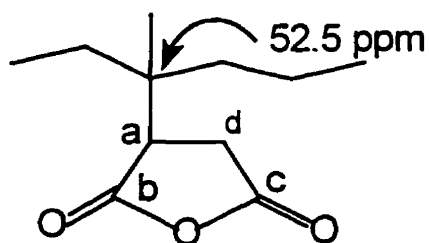


Figure 2.10. Succinyl structure of maleic anhydride grafted polypropylene

were not given in this section. Russell and Kelusky (1988) examined the proton spectra of several maleated alkyl species including n-eicosane (secondary bound anhydride) and dodecane (terminal bound anhydride). The methine and two methylene protons of dodecylsuccinic anhydride were assigned to 3.30, 3.20 and 2.83 ppm while the same groups were found at 3.42, 3.01, and 2.77 respectively, in n-eicosane. They also analyzed poly(maleic anhydride) and found a broad group of resonance centred at 4.5 ppm, which they used to determine that the majority of their grafted anhydride species were single units.

2.6.3. FT-IR Spectroscopy

This is probably the most widely used spectroscopic method to observe qualitatively and to a lesser extent quantitatively, the extent of functionalization in polymers. The higher sensitivity of FT-IR (estimated at 0.1 group per 1000 carbon atoms; Cudby, 1965) compared to NMR will distinguish this method as a valuable tool in structural analysis for this work. Unfortunately, the vibrational modes of the polypropylene backbone (characterized by Liang and Pearson, 1960) interfere or completely obscure many absorbance regions of the analyzed wavelengths (mid-IR, 500-4000 cm^{-1}). Many researchers place the vinylidene fingerprint absorbance in the region of 830 cm^{-1} . However, Haslam et al. (1972), de Kock and Hol (1964) and Lomente (1962) contradict this value, stating the shoulder at 888 cm^{-1} is the true vinylidene functionality. Indeed the peak height at 888 cm^{-1} has been observed in a study of polypropylene degradation to increase with increasing peroxide concentration (Thompson et al., 1997). In this thesis, the vinylidene will be characterized by the 888 cm^{-1} peak. A second absorbance at 1650 cm^{-1} is also observed in polypropylene corresponding to the vinylidene. The vinyl of ENB in EPDM has been identified (Coutinho and Ferreira, 1994a) at 1680-1630

cm^{-1} (C=C stretching) and $960\text{-}900\text{ cm}^{-1}$ (=C-H out-of-plane deformation), though Tosi et al. (1972) stated that the characteristic peaks resided at 1686 cm^{-1} and 806 cm^{-1} and Levine and Haines (1970) identified the unsaturation bands at 1700 cm^{-1} and 806 cm^{-1} . Levine and Haines (1970) went on to state that the out-of-plane deformation band at 806 cm^{-1} was unsuitable for analysis due to interference from propylene units.

An excellent reference for molecular characterization of maleic anhydride grafted polypropylene by FT-IR was given by De Roover et al. (1995). The carbonyl absorbance wavenumbers of model compounds relevant to the grafting of maleic anhydride are: citraconic anhydride, 1780 cm^{-1} ; 2,3-dimethylmaleic anhydride, 1770 cm^{-1} ; n-octadecylsuccinic anhydride, 1792 cm^{-1} ; poly(maleic anhydride), 1784 cm^{-1} ; and maleic anhydride, 1780 cm^{-1} . Bands at 1780 cm^{-1} and 1865 cm^{-1} were used to confirm terminal attachment by Mülhaupt et al. (1991) and Tang et al. (1994) monitored the relative absorbance of A_{1780}/A_{841} to quantify maleic anhydride content grafted to polypropylene. Rengarajan et al. (1990) used the peaks at 1790 cm^{-1} and 1865 cm^{-1} to confirm tertiary succinic anhydride attachment. Walch and Gaymans (1994) who terminally attached maleic anhydride onto polyisobutylene [similar environment at the end of the chain to that of polypropylene] observed the succinic anhydride group at 1790 cm^{-1} , 1855 cm^{-1} , and 715 cm^{-1} . There is no conclusive band assignment among these authors for maleic anhydride attachment even for those species in very similar electron environments.

Again in maleated EPDM, the identification of the asymmetrical stretching band for the carbonyl groups in the attached succinyl group varied among authors. Coutinho and Ferreira (1994b) observed that band in maleated EPDM by diffuse reflectance FT-IR at 1780 cm^{-1} , Datta et al. (1996a) stated the band resided at 1777 cm^{-1} and still Immirzi et al. (1987)

quoted the band at 1786 cm^{-1} . Both Coutinho and Ferreira (1994b) and Oostenbrink and Gaymans (1992) produced calibration curves, though the latter curve was based on the absorbance ratio of 1785 cm^{-1} to 715 cm^{-1} , an internal reference which Coutinho and Ferreira (1994b) found to be questionable due to its dependence on the nature of the chain backbone. Coutinho and Ferreira (1994b) found a higher covariance coefficient with 1465 cm^{-1} for an internal reference.

In a study on the homopolymerization of maleic anhydride, Joshi (1962) compared the IR spectrum of the monomer species and the resulting polymer. Characteristic bands of the 5-member cyclic anhydride species (1848 cm^{-1} / 1790 cm^{-1} for the C=O stretch and 1240 cm^{-1} for the C-O-C stretch) were found also in the polymer albeit slightly shifted in frequency. Sharabash and Guile (1976) found similar vibrations between both monomer and polymer for the carbonyl stretching vibrations at 1780 cm^{-1} and 1859 cm^{-1} . However, peaks for the polymer are noticeably broader. Other bands due to conjugation (1600 cm^{-1} , C=O-) and bands associated with the unsaturation (895 cm^{-1} and 840 cm^{-1} for the CH out-of-plane bend; 695 cm^{-1} for the -CH=CH) were not observed by Joshi (1962) in the polymer. The carbonyl vibrations of the cyclopentanone unit (1770 and 1725 cm^{-1}) and the ketoolefin unit (1695 cm^{-1}) were identified by Zweifel and Volker (1973) for poly(maleic anhydride) segments.

Reactions of anhydrides with amines have been characterized by several authors (Song and Baker, 1992; Maréchal et al., 1995; Tessier and Maréchal, 1984b). Imides absorb at 1711 cm^{-1} and 1772 cm^{-1} . Amides are observed at 1530 cm^{-1} (NH), 1620 cm^{-1} (tertiary amide, C=O) and 1645 cm^{-1} (secondary amide, C=O). Shiono et al. (1993) determined the molar extinction coefficients for the secondary amide peak at 1645 cm^{-1} and the methyl peak

at 1165 cm^{-1} which they used as an internal reference. Primary amines absorb at 3300 cm^{-1} while the carbonyl group of carboxylic acids occurs at $\sim 1700\text{ cm}^{-1}$ with the hydroxyl group of the acid present at 940 cm^{-1} and 3100 cm^{-1} . Polar interactions between the anhydride and tertiary amine appear at 1740 cm^{-1} while the carboxylate anion of the acid is seen at 1400 cm^{-1} and 1550 cm^{-1} .

2.6.4. Transition Temperatures

Glass transition temperature (T_g) represents the first measurable change in the specific volume of the polymer sample upon heating from the glassy state. The T_g is affected by substituents which increase the stiffness of the polymer (inter-chain cohesion), e.g. polar groups (Dealy and Wissbrun, 1990). According to Dealy (1990), even trace quantities of solvents adhering to the polymer can appreciably lower the glass transition temperature which may be interpreted in a broader sense to suggest that even low scale changes to or around the polymer, can be detected. Due to the high crystallinity of polypropylene, its amorphous polymer fraction is difficult to observe and, therefore, dynamic mechanical analysis would be desirable for greatest sensitivity. However, Shiono et al. (1993) produced a secondary butyl amine monochelic functionality on a metallocene polypropylene ($\overline{M}_N = 3500\text{ g/mol}$) which they characterized by DSC. They found both the heat of fusion and crystalline melt temperature were unaffected by the terminal group. However, the glass transition temperature did increase slightly. The glass transition temperature was found by Greco et al. (1987) to increase with the degree of maleic anhydride grafted onto EPDM. Greco et al. (1987) attributed the increased rigidity of the rubber to the increase in polarity contributed by the functional groups. Van Krevelen (1976) has proposed correlations based

on structural groups to estimate the glass transition temperature. According to his work, the structural group contributions and any polar interactions are additive based on weight fraction. Therefore, it is possible that the terminal functionality may be detected by its influence on T_g . However, the change will most likely be difficult to distinguish from instrumental noise.

Aside from the glass transition temperature, the melting temperature and its relation to the crystalline content of the polymer can be used to characterize copolymers formed by derivatization of the terminally functionalized polypropylene. Song and Baker (1992) used DSC thermograms above the polymer T_g , to characterize the influence of diamine cross-linking via anhydride and carboxylic acid functionalized polymers on the crystallinity of that polymer. The onset of an exothermic deviation in the DSC thermogram was considered to be due to degradation of the polymer, and therefore this method could also compare the thermal stability of the initial and modified polymers. Looking at other polymers, Tang et al. (1994) prepared a graft copolymer from polypropylene-g-maleic anhydride and PEO and observed that the increasing ester content decreased the crystalline behaviour of the polypropylene. The crystalline behaviour was measured by T_m , ΔH_m , T_c , and ΔH_c using DSC cooling studies and it was found to decrease as the amorphous character of the PEO groups in the copolymer increased. According to van Krevelen (1976), with an increasing aliphatic side chain length, the crystal melting temperature decreases until the number of $-(CH_2)_n-$ units approaches five and then the temperature increases. Unfortunately, van Krevelen (1976) did not develop correlations for graft copolymer, particularly when the grafted chain structure radically differs from the polymer backbone. However, the melting temperature

and its relation to the crystalline content of the polymer could be used to assist in characterization of the terminal functionality indirectly through the use of block and graft copolymer formation, though the measurement for the terminally functionalized polymer alone is uninformative as already stated above in reference to Shiono et al. (1993).

2.6.5. Rheological Properties

Rheological measurement of maleated EPDM is a highly informative technique in distinguishing the site of functionalization. The loss and storage moduli, G'' and G' values are measures of the response of the material to small amplitude oscillations (deformation). The phase angle, δ , is a measure of the lag between shear stress and applied shear strain observed in the sample. If we assume a small sinusoidal oscillation of frequency, ω , then the modulus (which is typically related to viscoelastic behaviour) can be defined by this series of equations.

$$\text{Stimulus (Strain)} \quad \gamma = \gamma_o \sin(\omega t) \quad (2.1)$$

$$\dot{\gamma} = \gamma_o \omega \cos(\omega t) \quad (2.2)$$

$$\text{Response (Stress)} \quad \sigma = \sigma_o \sin(\omega t + \delta) \quad (2.3)$$

$$\text{Linear Relaxation Modulus} \quad G = \frac{\sigma_o}{\gamma_o} \cos \delta + i \frac{\sigma_o}{\gamma_o} \sin \delta = G' + iG'' \quad (2.4)$$

$$\text{loss tangent} \quad \tan \delta = \frac{G''}{G'} \quad (2.5)$$

For small frequency experiments, it is the strain amplitude which dictates departure from linear viscoelastic theory. Therefore, since the above equations rely on the linear behaviour

of the polymer, the strain of the experiment should be constant for the frequency range of the dynamic mechanical analysis.

According to Dealy and Wissbrun(1990), a relaxation modulus curve can be used to infer changes in polymer chains. Lower frequencies correspond to large molecular motions and the storage modulus reflects the entanglement density of these chains. The storage modulus at higher frequencies solely reflects shorter chain mobility since larger molecular motions are constrained by the imposed shear. Within this region, only segmental motion among the higher molecular weight fraction of the polymer distribution contributes to the storage modulus. Ho et al. (1993) observed a decrease and then increase with maleic anhydride concentration in polypropylene for G' at low frequencies. Clearly, chain scission was occurring at low MAh concentrations. Ethylene-propylene-diene terpolymer maleated by the Alder Ene reaction in a Haake Rheomix 600 mixer (Wu and Su, 1991) demonstrated lower entanglement density (shorter chains) than the original EPDM rubber. This conclusion was derived on the basis of lower storage modulus values in the lower frequency region based on dynamic mechanical analysis in a parallel plate fixture.

CHAPTER 3. METHODS OF VINYLIDENE GENERATION IN POLYPROPYLENE

3.1. INTRODUCTION

The degradation of polypropylene is a superior method to commercial polymerization processes towards the generation of a vinylidene-terminated polymer, since the former method is capable of yielding functionalities close to 2.0 (i.e. both chain ends functionalized) unlike the latter which is limited to 1.0. Subsequently in Chapter 7, degraded polypropylene shall be used as the source of a vinylidene-rich *ene* species in the Alder Ene reaction. This chapter reports on several different methods by which the vinylidene functionality can be generated, examining Ziegler-Natta polymerization, as well as thermal, peroxide-initiated and thermo-oxidative degradation.

3.2. COMMERCIAL ZIEGLER-NATTA POLYPROPYLENE

Confining ourselves to the current literature, this section will focus on metallocene Ziegler-Natta chemistry although classical Ti/Al catalysts undergo similar pathways to generate the desired terminal vinylidene (typically in lower concentration). Commercially, polypropylenes synthesized by classical Ziegler-Natta processes have negligible terminal vinylidene groups due to the undesirable nature of this functionality with respect to the traditional end-product applications (e.g. film, bottles, packaging, etc.) Good melt strength tends to be another important consideration for polypropylene customers, requiring long polymer chains which diminish the concentration of any terminal functionalities. For these reasons, limited commercial sources of polypropylene were available for this work.

Metallocene catalysis has recently become an attractive alternative to classical Ti/Al polymerization, overlooked in the past by a large portion of the polymer community due to its low activity. The discovery of the synergistic combination of methylalumoxane (MAO) with metallocenes, produced polymerization activities useful for polymer production. The single-site nature of the catalyst under appropriate conditions (Chien and Tsai, 1993), ensured that the polydispersity of the molecular weight distribution of the product polymer approached 2.0 (a Flory most probable distribution) via termination by chain-transfer (Huang, 1995). Chain growth can be terminated by one of several chain transfer reactions. Excluding chain transfer to solvent and other minor chain transfer reactions, there are four chain transfer mechanisms prevalent in the polymerization of α -olefins (Huang, 1995). Table 3.1 provides a description of those chain transfer mechanisms along with a description of the

Table 3.1. Chain transfer mechanisms in metallocene polymerization

Chain Transfer Mechanism	Description	End Group Formation / New Active Centre (Zr-*)
β -Hydrogen Elimination	metal centre abstracts a hydrogen at the β -C of the polymer chain.	Vinylidene terminated polypropylene / Zr - H (gives n-propyl end group)
Chain Transfer to Monomer	β -H elimination and olefin insertion to metal centre.	Vinylidene terminated polypropylene / Zr-CH ₂ -CH ₂ -CH ₃ (gives n-propyl end group)
Chain Transfer to MAO	Exchange methyl group of MAO with growing polymer chain at metal centre.	Aluminum terminated polypropylene / Zr-CH ₃ (gives isopropyl end group)
β -CH ₃ Elimination	Metal centre abstracts a CH ₃ group at the β -C of the polymer chain	allyl terminated polypropylene / Zr-CH ₃ (gives isopropyl end group)

end group and the new active centre formed. Many of the commonly employed metallocenes in homogeneous Ziegler-Natta polymerization such as $\text{Et}(\text{H}_4\text{Ind})_2\text{ZrCl}_2$, lead to chain transfer via β -elimination and to some degree chain transfer to monomer (Shiono and Soga, 1992b; Huang, 1995). Both chain transfer mechanisms lead to polypropylenes with a vinylidene chain end. The benefit of these materials compared to degraded polymers, would be the lack of oxidation functionalities which may arise in the presence of oxygen.

3.3. VIS-BREAKING OF POLYPROPYLENE

The mechanism of β -scission for polypropylene is common among the different methods of degradation, however, the manner of initiation differs. For those degradation methods involving an oxidation agent (i.e. peroxide or oxygen), β -scission must first begin with the formation of a macroradical via hydrogen abstraction. This intermediate radical on the polypropylene chain (shown in Figure 3.1) has been found to favour the tertiary position at a ratio of 1:10:50 for primary:secondary:tertiary (Borsig et al., 1995). The tertiary radical is stabilized by hyper-conjugation which consequently weakens the adjacent bonds (lowers their dissociation energy) along the alkyl chain. Energetically, the formed tertiary radical is favoured over a secondary or primary site, although, steric hindrance from the side group produces sufficient instability to cause rapid β -scission. It is generally assumed in the literature that the generated macroradical, R' , is not energetic enough to abstract a backbone hydrogen. According to the proposed mechanisms shown in Figure 3.1 for a free radical-initiated β -scission, the homolytic cleavage of the original chain results in two shorter chains, one of which is thought to possess a terminal vinylidene due to termination by disproportionation (Rado, 1962; Suwanda et al., 1988, Tzoganakis et al., 1988; Triacca et al.,

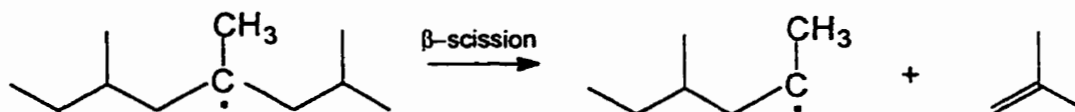


Figure 3.1. Degradation of polypropylene by chain scission

1993; Sawaguchi et al., 1995). The extent of degradation can be measured using the degree of scission (u),

$$u = \frac{1}{r_N} - \frac{1}{r_{N_0}} \quad (3.1)$$

where r_N and r_{N_0} are the chain length of the polymer at time t and $t=0$ respectively. The degree of scission is the number of β -scissions occurring per repeat unit.

The probability of scission for any chain in the MWD, is proportional to the length of that chain. Longer chains have a higher probability of degradation, resulting in the removal of the high molecular weight tail of the distribution. At the beginning of the degradation reaction, the higher order moments of the MWD decrease dramatically until eventually the rate of change levels off as the degree of scission increases further. With longer chains broken and shorter chains more prevalent, the degree of scission must now change significantly to further change the MWD. A critical chain length exists, such that no further cleavage of the molecule will occur (Florea, 1993). The molecular weight distribution narrows as the degree of scission increases, tending towards the most probable distribution (a random distribution with a polydispersity of 2.0). If the initial MWD was the most probable distribution, then only the molecular weight averages decrease, while the polydispersity remains at 2.0.

Four sources of chain degradation may occur during polymer processing to cleave the polypropylene chain. Intensive mechanical shearing and thermal degradation ($T > 300^{\circ}\text{C}$) involve destruction of covalent bonds of the chain without the intermediate tertiary radical (unless intra- or inter-molecular transfer occurs; Grassie and Leeming, 1975). These two degradation mechanisms do not introduce oxidation functionalities (i.e. carbonyl-based groups) onto the polymer chain. At the processing temperature of polypropylene, oxidation via oxygen (atmospheric, injected into the process system, or absorbed into the polymer) is often referred to as thermo-oxidative degradation, feasibly producing low concentrations (depending on the precautions employed to minimize the presence of oxygen) of functionalized polypropylene aside from the vinylidene group (Adams, 1970; Hinsken et al., 1991; Adams and Goodrich, 1970). These functionalities, which shall be discussed in section 3.3.2, are located at the chain end and, therefore, are in direct competition with the vinylidene group. Finally, organic peroxide-initiated degradation is generally found to be a clean source of degradation with negligible carbonyl-based functional groups introduced, provided that oxidation via oxygen can be prevented. The following sections shall discuss these individual degradation reactions, with the exception of mechanical degradation which is the only non-random mechanism, preferring to cleave in the chain centre. It is rarely significant under extrusion conditions.

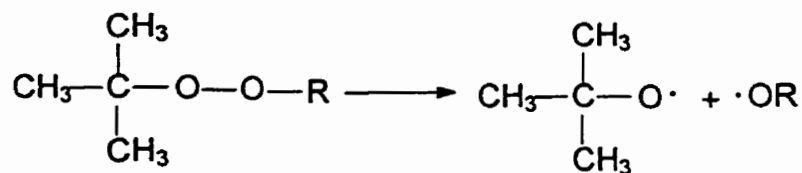
3.3.1. Peroxide-Induced β -Scission

Dorn (1985) discussed the generation of free radicals from organic peroxides. The peroxide decomposes by first-order kinetics (Harpell and Walrod, 1971) with the rate constants, k_d , expressed by an Arrhenius equation. The rate of decomposition of a peroxide

has been determined to be dependent on the reaction medium. For 2,5-dimethyl-2,5-di(*t*-butyl-peroxy) hexane, Harpell and Walrod (1971) found that the half-life of the initiator at 163°C was 3.5 minutes in benzene, yet 17.0 minutes in low density polyethylene (LDPE) (measured in an oscillating disk rheometer). The “cage” recombination reaction became increasingly significant with increasing viscosity. It was found that the activation energy remained constant, independent of the reaction medium, indicating that the pre-exponential constant in the Arrhenius equation quoted by suppliers are generally 3-5 times too high for reactions carried out in the melt. A review by Kowalski (1992) presented further sources which confirmed the findings of Harpell and Walrod (1971).

Peroxides exhibit two possible decomposition steps, the secondary reaction is limited to high temperatures and mediums of low reactivity (Dorn, 1985). In the case of dialkyl peroxides, which are favoured in reactive processing due to their long decomposition half-life at typical extrusion temperatures, the two steps of decomposition are shown in Figure 3.2. The *t*-butyloxy radical (primary decomposition product) is sufficiently reactive to abstract a hydrogen from the backbone of the polymer chain (Figure 3.3). However, the methyl radical (secondary decomposition product) is more energetic due to the instability of the species (bond dissociation energy for $\text{CH}_3\text{-H}$ is 104 kcal/mol compared to *tert*- $\text{C}_4\text{H}_9\text{O-H}$ which is 103 kcal/mol). In this work, it was important that the secondary reaction predominates since the chemical species of acetone and methane which remain after hydrogen abstraction, will not hydrolyze the maleic anhydride nor kill the catalyst as would the *t*-butanol generated as a primary decomposition product. However, at high concentrations of peroxide, the acetone concentration may be sufficient to react with the macro-radical, producing a carbonyl functionality in the product (particularly if devolatilization operations are inadequate to

Primary Decomposition Reaction



Secondary Decomposition Reaction

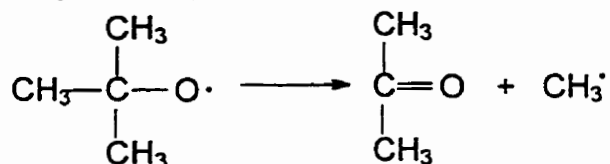


Figure 3.2. Decomposition pathway of a dialkyl peroxide

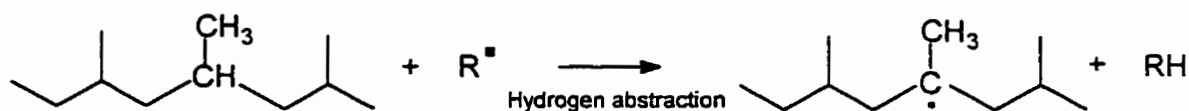


Figure 3.3. Hydrogen abstraction from the backbone of a polypropylene chain by a primary radical.

reduce volatile concentration). At high peroxide concentrations, processing temperatures must be kept high to prevent undesirable cross-linking from occurring (Rado, 1962).

The energetic nature of the peroxide is important with respect to the rate of hydrogen abstraction. The energy required to cleave the hydrogen-carbon bond is too high to normally occur without a “bond-making” reaction occurring simultaneously in the transition state (Harpell and Walrod, 1973; Pryor, 1966). The rate of hydrogen abstraction will be improved

by the low R-H bond strength of the polymer and the strength of the bond formed in the hydrogen transfer. Pryor (1966) stated that the rate of hydrogen abstraction has been shown for aliphatic hydrocarbons to be primary < secondary < tertiary, while for the attacking radical to be: $t\text{-BuO}\cdot < \text{CH}_3\cdot$. Gray et al. (1971), used gas-phase kinetics to determine the relative rates of hydrogen abstraction by a methyl radical from a methyl (CH_3), methylene (CH_2), and methine (CH) group, to be 1:6:25.

Organic peroxide initiated β -scission of polypropylene has been studied by numerous authors (Ebner and White, 1993; Dorn, 1985; Hudec and Obdrzalek, 1980), primarily examining the effects of the process operating conditions and peroxide level on the molecular weight distribution of the degraded polymer, with the intent of controlling its molecular weight properties (high MFI, low die swell). Several researchers approached the process of controlled degradation via kinetic modeling (Tzoganakis et al., 1988a,b,c; Suwanda et al., 1988; Pabedinskas et al., 1994; Triacca et al., 1993; Ryu et al., 1992; Rado, 1962). Other researchers have taken an interest in “on-line” (measurements done in a side-stream) or “in-line” (measurements done in the main process stream) rheometric measurements for feedback process control (Curry et al., 1988; Dreiblatt et al., 1987; Dumoulin et al., 1993; Fritz and Stohrer, 1986; Nelson et al., 1993). All these research groups considered exclusive degradation via peroxide initiator, and neglect the contributions of atmospheric oxygen and possible side-reactions produced by dialkyl peroxide decomposition.

3.3.2. Oxidation

The presence of carbonyl functionalities (i.e. methyl ketones, aldehydes and γ -lactones) in the degraded product is attributed to atmospheric oxygen (thermo-oxidation)

which imparts a yellowish appearance to the product if present in significant concentrations. Adams (1970) studied the non-volatile products of thermo-oxidative degradation for polypropylene. Based on infrared analysis and derivatization via acid and base treatments of the polypropylene functionalities, the functional groups detected in the degraded material were characterized to be γ -lactone, acetyl ester, aldehyde, hydroperoxide and peroxyacid (low temperature processing only, i.e. $<100^{\circ}\text{C}$), methyl ketone and carboxylic acid. Adams (1970) proposed an oxidation scheme providing pathways to the various functionalities observed in his study. Similar pathways were later proposed by Hinsken et al. (1991). Due to the instability of the tertiary radical, no functionalities are thought to form at the tertiary site, rather rapid β -scission resulted in all functional groups being terminally positioned. Figure 3.4 combines the pathways from the two works for the three most abundant functional groups: aldehyde, methyl ketone, and γ -lactone. Adams and Goodrich (1970) melt processed polypropylene without antioxidant stabilizer in a torque rheometer at 210°C with air injection, to produce material containing 25% vinyl groups with ketones, aldehydes and acids being present in similar proportions with respect to the total functional group concentration of the polymer. Hoff (1984) observed that anti-oxidants retarded thermo-oxidation over a processing range of $120\text{-}280^{\circ}\text{C}$ and that oxidation was dependent on the type of anti-oxidant used. However, oxidation products were always present. In addition, Harpell and Walrod (1971) found the initiator to be only 91% efficient in the presence of quinoline anti-oxidant, and that the efficiency was further lowered if quinoline was replaced by either an amine antioxidant (69%) or a phenolic antioxidant (50%).

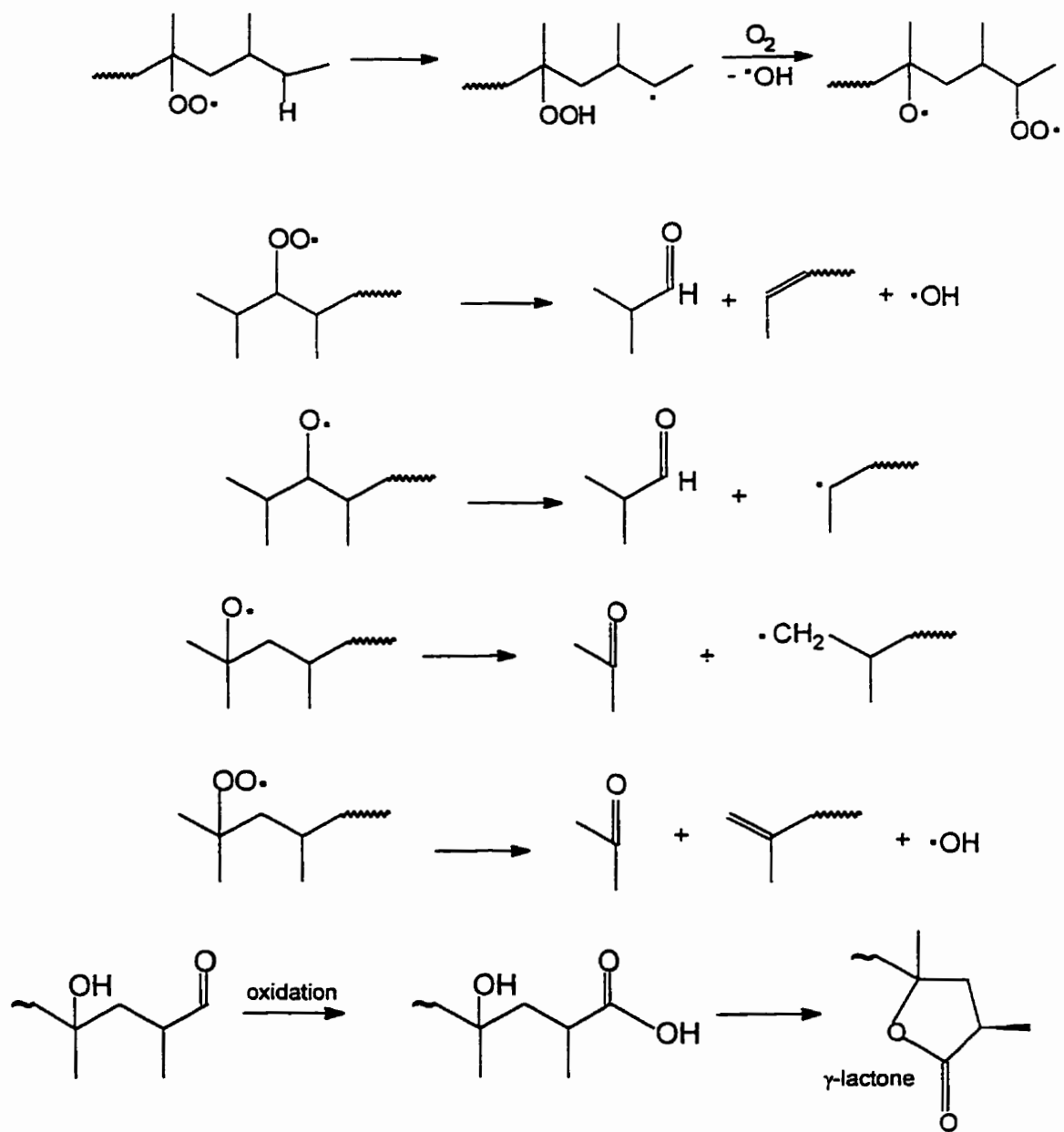


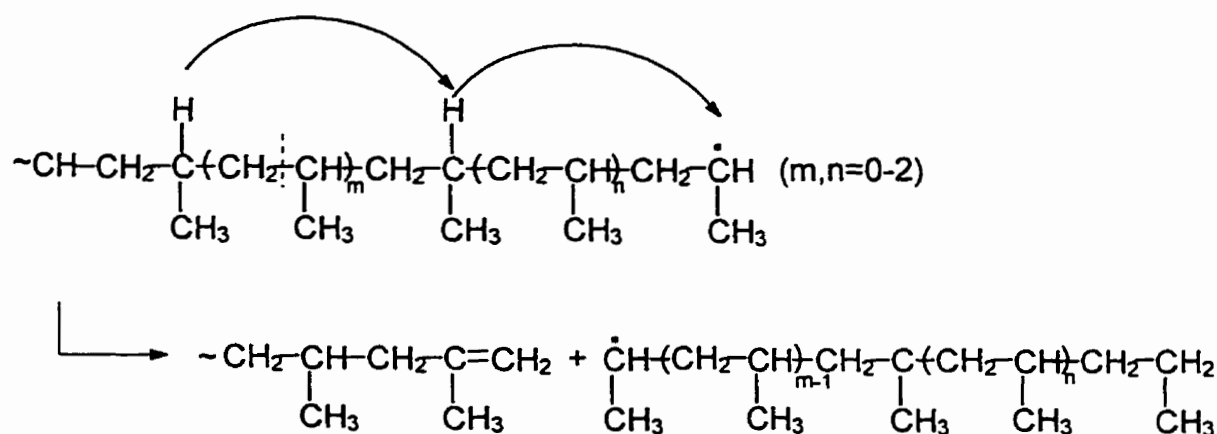
Figure 3.4. Thermo-oxidation pathways for polypropylene

3.3.3. Thermal Degradation

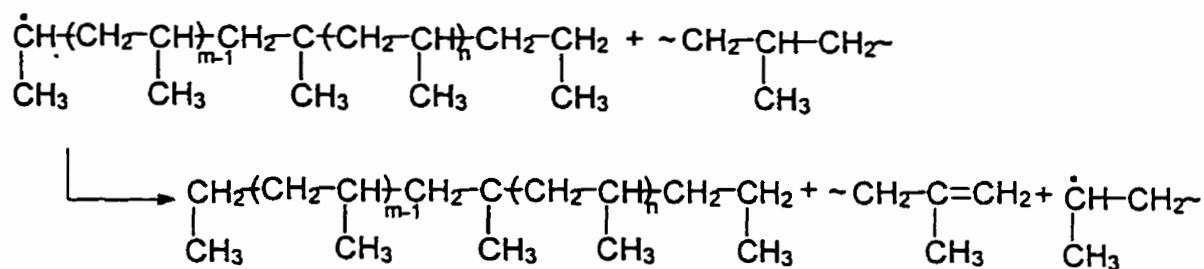
The premise of thermal degradation hinges on the idea of "weak links" incorporated within the backbone of a polymer chain during polymerization due to side-reactions and the presence of impurities. These weak-links may be peroxy groups, carbonyl groups, or structural irregularities such as head-to-head or tail-to-tail configurations. These groups are sites of radical initiation due to their lower relative stability than normal carbon-carbon links (Jellinek, 1978; Grassie and Scott, 1985). Grassie and Scott (1985) classified thermal degradation reactions into two classes, depolymerization and substituent. Unlike polystyrene, polyolefins do not depropagate to any significant extent, meaning that volatiles are generated similarly to non-volatile cleaved chains, as a result of both intra- and inter-molecular chain transfer processes.

Thermal degradation of both syndio- and iso-tactic polypropylene was studied by Sawaguchi et al. (1995, 1996) at 370°C under a nitrogen atmosphere for a duration of up to 90 minutes in a Pyrex glass tube. While they characterized the degraded polymer similarly to others using molecular weight determination, crystal melting temperature and density measurement, NMR, and FT-IR analysis, their focus was different, with the intent being on the generation of vinylidene groups for subsequent functionalization. By 60 minutes, the number-average molecular weight of the polymer had dropped to 2.1 % of the original value for polymers with isotactic stereoregularity or 3.7 % for the syndiotactic species, however, the vinylidene concentration in moles per gram polymer were identical. Based on ¹H NMR analysis, Sawaguchi and Seno (1996) found that 95 mol % of the unsaturated groups were vinylidenes, while the remaining 5 mol % were attributed to either internal or terminal vinyls.

Approximately 80 % of the degraded polymer was determined to possess two vinylidene end groups per molecule. Based on their results and analysis of the volatile components from the degradation reaction, they proposed that the mechanism of degradation was predominantly “step-wise back-biting of secondary terminal macroradical followed by β -scission” :



and “intermolecular chain transfer of secondary terminal volatile radical followed by β -scission”:



Both mechanisms were taken directly from Sawaguchi et al. (1995).

Unfortunately, thermal degradation only occurs under an inert atmosphere devoid of oxygen. Therefore, the extrusion of polypropylene at temperatures above 350°C, as was done in this thesis, combined the mechanisms of thermal and thermo-oxidative degradation. The purpose of exploring the more energy-intensive method of inducing chain scission compared to peroxide-initiated degradation, was based on reducing the number of possible

functionalities present in the product. It is possible that the lower processing temperatures employed (eg. 200-250°C) with peroxide-induced methods (as is their energy-conservative manner) favour a greater variety of thermally-allowable oxidative functionalities than at the higher temperatures proposed for the thermal/thermo-oxidative method. Since carbonyl-based functionalities are likely to interfere with Lewis acid-maleic anhydride enophile formation, reducing the variety and concentration of these groups in the polymer, would improve the extent of the Alder Ene reaction and decrease side-reactions. This aspect is addressed in Chapter 7.

3.4. EXPERIMENTAL

3.4.1. Material

The polypropylene, grade KF6100, was donated by Montell Canada. The polymer was characterized in a Kayeness Galaxy V capillary rheometer to possess a melt flow index (MFI) of 3.0 g/ 10 min (according to ASTM D1238 at 230°C under 2.16 Kg weight). The molecular weight distribution of the polymer was measured by high temperature gel permeation chromatography (GPC) [discussed in the analysis section]. The molecular weight averages for KF6100 were determined to be: $\overline{M}_N = 49,800$ g/mol, $\overline{M}_w = 528,000$ g/mol, PDI = 11. The peroxide used was Lupersol 101 (2,2-dimethyl-2,5-(*t*-butylperoxy)hexane) supplied by Elf AtoChem. The Arrhenius parameters for Lupersol 101 decomposition in dodecane, as described by the supplier, are $A = 8.73 \times 10^{15} \text{ s}^{-1}$ (pre-exponential constant) and $E_a = 38127$ cal/mol (activation energy).

3.4.2. Procedures

3.4.2.1. Peroxide Induced Degradation

Controlled-rheology polypropylene samples were produced at 200°C in a Haake Rheocord 90 fitted with a Rheomix 3000 batch mixer. Unstabilized KF6100 polypropylene powder was mixed with Lupersol 101 peroxide. The peroxide range studied varied from 0.01-2 wt %. The duration of the reaction was 5 minutes, which exceeded the 99 % lifetime of the peroxide. To reduce the contribution of oxygen in the degradation and thereby increase the vinylidene content in the final product, an effective antioxidant, Irganox 1010 (Ciba-Geigy) was blended at 0.1 wt % with the polymer. A sample of each degraded product was drawn as a thin film for IR analysis.

3.4.2.2. Thermal /Thermo-Oxidative Degradation

The polypropylene was degraded at high temperature in a Haake Rheocord 90 fitted with a Rheomex 252 single screw extruder (screw design shown in Chapter 4). The rod die which comprised zone 4 of the extruder was fitted with a 6 mm diameter nozzle, and the barrel temperature profile was set as follows, 150, 240, 370/380, and 290°C for zone 1 to zone 4 respectively, with the first zone located just downstream of the feed section. The screw speed was varied from 10-30 rpm for the two temperatures examined in zone 3 resulting in six products. A portion of the extrudate from each sample was drawn as a film for infrared analysis.

3.4.3. Analysis

The degraded product was analyzed by ^{13}C and ^1H NMR to confirm the mechanism of chain degradation. The samples were run in a Bruker AC-300E NMR spectrometer fitted with a 10 mm high temperature probe for ^{13}C NMR or a 5 mm high temperature probe for ^1H NMR. Samples prepared for ^{13}C NMR analysis were dissolved at 10 wt % in tetrachloroethylene ($\delta \sim 120$ ppm) or 1,2,4-trichlorobenzene ($\delta \sim 130$ ppm) at 117°C . Acquisition of a spectrum involved 8500 scans using a pulse delay of 18 s without a signal lock (to improve the signal-to-noise ratio) or spinning the sample (due to the inhomogeneity of the solution). Proton decoupling was achieved using the inverted gate method. Samples prepared for ^1H NMR were dissolved at 2-5 wt % in toluene- d_8 at 100°C . The spectrum acquisition involved 64 scans with a 9 s pulse delay. Characterization was made based on the peak assignments of Sawaguchi et al. (1995), Sawaguchi and Meno (1996) and Busfield and Hanna (1991) which are compiled in Table 3.2 and from calculations using the empirical correlations for ^{13}C NMR of Dorman et al. (1971) and Lindeman and Adams (1971). Figure 3.5 shows the three anticipated chain ends of degraded polypropylene with the calculated chemical shift value placed above or underneath their respective carbon. The reference used in the analysis and calculations was TMS.

The drawn films were characterized at 2 cm^{-1} resolution in a Nicolet 520 FT-IR spectrometer. A relative peak height absorbance pertaining to the vinylidene observed at 888 cm^{-1} in the FT-IR spectra, was calculated using the C-C-C bending peak at 459 cm^{-1} as an internal reference. An IR calibration curve for vinylidene concentration was generated using a low molecular weight amorphous polypropylene. The calibration equation (eqn 4.5) and a

Table 3.2. Four possible vinyl end groups resulting from degradation of PP

End Group	Partial Structure	Chemical Shifts
Vinylidene	$\begin{array}{c} \text{CH}_2=\text{C}-\text{CH}_2 \\ \\ \text{CH}_3 \end{array}$	111.6, 144.3, 22.6* 111.5, 22.5-23.8‡ 148.5 (calc) ‡
Vinylene	$\begin{array}{c} \text{CH}_3-\text{CH}=\text{CH}-\text{CH}- \\ \\ \text{CH}_3 \end{array}$	123.3‡
n-propyl	$\begin{array}{c} \text{CH}_3-\text{CH}_2-\text{CH}_2-\text{CH}- \\ \\ \text{CH}_3 \end{array}$	14.4, 20.0, 20.1, 30.5, 39.6, 40.7*
Isopropyl	$\begin{array}{c} \text{CH}_3-\text{CH}-\text{CH}_2- \\ \\ \text{CH}_3 \end{array}$	22.5-23.8, 25.7, 48.2‡
internal vinyl	$\begin{array}{c} \text{CH}_3-\text{C}=\text{CH}- \\ \\ \text{CH}_3 \end{array}$	20.6, 134.2, 140.7 (calc)*

* observed chemical shifts by Sawaguchi et al. (1995), Sawaguchi and Meno (1996).

‡ observed chemical shifts by Busfield and Hanna (1991)

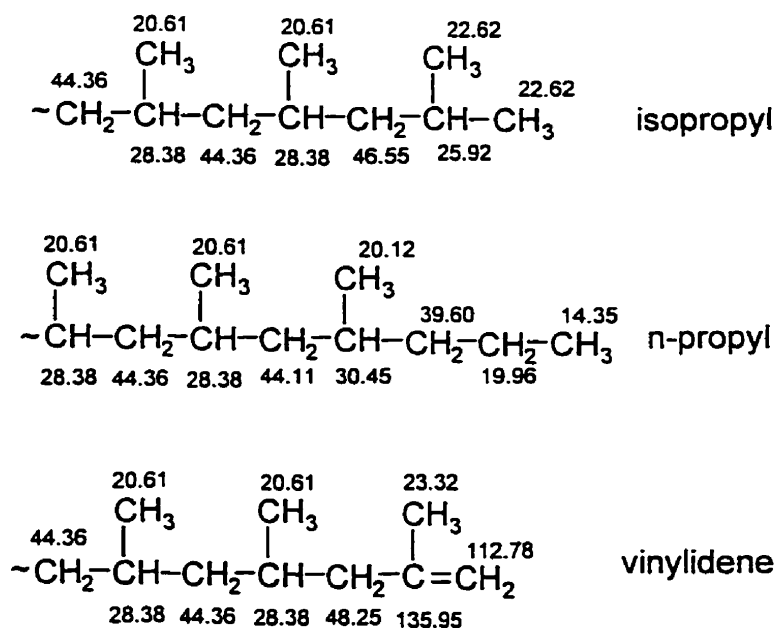


Figure 3.5. Three chain end structures for degraded polypropylene with ^{13}C chemical shift values calculated according to Lindeman and Adams (1971) and Dorman et al. (1971)

detailed description of the procedure used to generate the curve is discussed in Chapter 4. Molecular weight analysis of the polypropylene samples was done according to the procedure in section 4.3.7.

3.5. RESULTS AND DISCUSSION

Both methods of degradation examined in this chapter included thermo-oxidative degradation on account of the presence of oxygen in the extruder. For simplicity, the methods will be differentiated within the text, in terms of the primary method of degradation (thermal or peroxide), with no mention of the presence of oxidation being made henceforth.

3.5.1. NMR Analysis of Degraded Polypropylene

Figure 3.6 presents the ^{13}C NMR spectrum for 0.5 wt % Lupersol 101 degraded polypropylene in the region of 15-50 ppm. The broad peaks at 21.8, 28.8 and 46.5 ppm corresponded to the methyl, methine and methylene groups respectively whereas their respective calculated shifts resided at 20.61, 28.38 and 44.36 ppm. This comparison showed that the calculated chemical shifts based on empirical correlations, were reasonably close to the observed peaks, but varied with some degree of error. The n-propyl end group was confirmed by moderate intensity resonances at 14.4 ppm (not shown in the figure), 20.1 and 20.7 ppm, with a shoulder at 30.4 ppm. In comparison, the ^{13}C spectrum of virgin polypropylene (Figure 3.7) yielded lower intensities in the chemical shifts corresponding to n-propyl end groups (recall from Table 3.1 that n-propyl groups were feasible during polymerization due to the different chain transfer mechanisms present). The increased

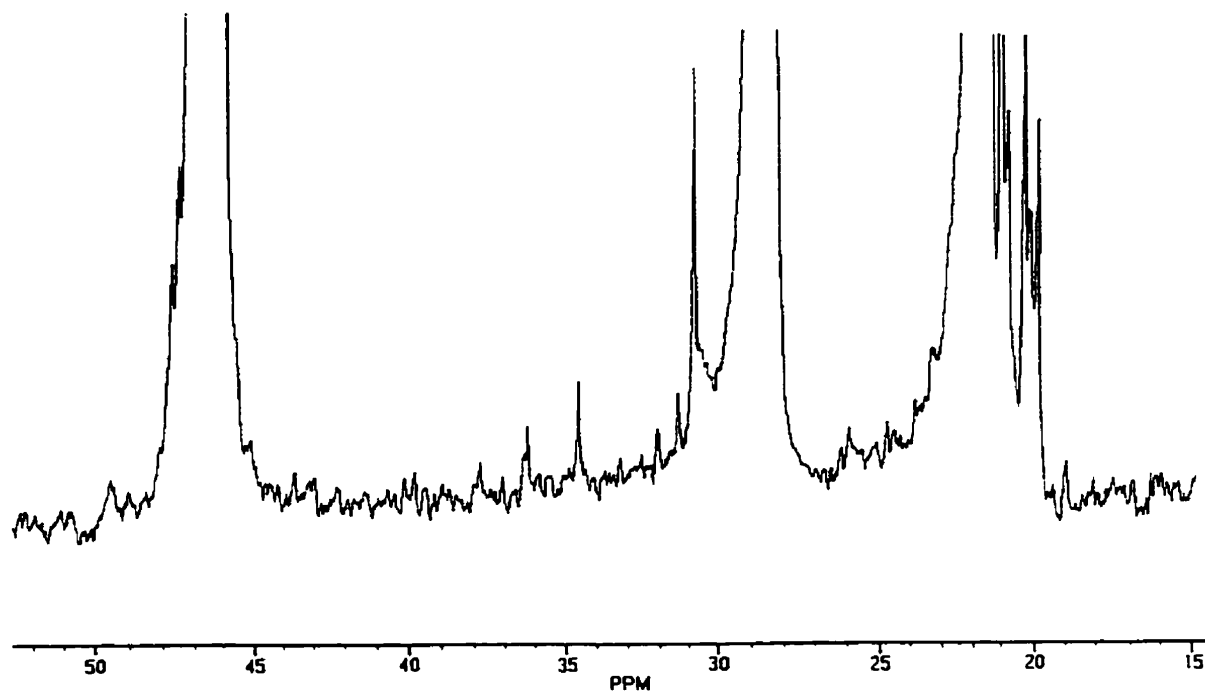


Figure 3.6. ^{13}C NMR spectrum in the backbone region of degraded polypropylene

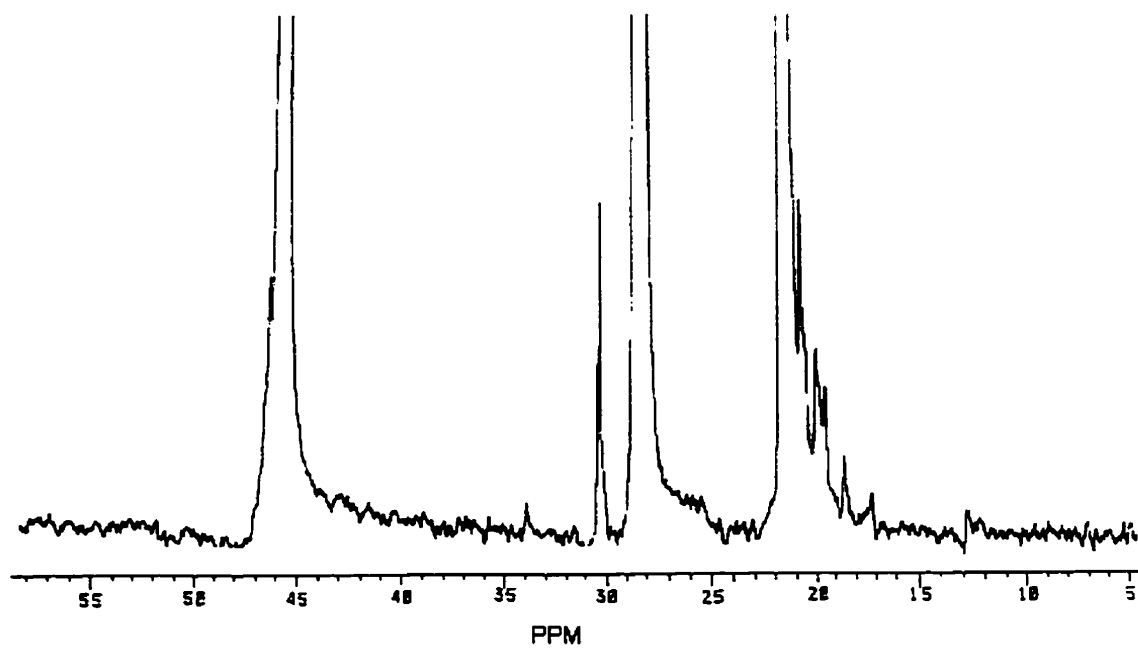
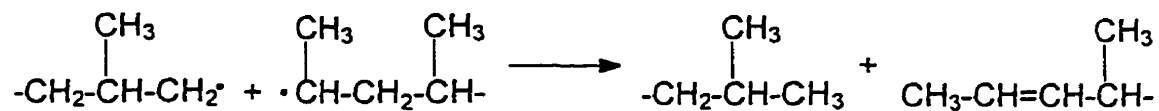


Figure 3.7. ^{13}C NMR spectrum in the backbone region for virgin polypropylene

generation of n-propyl groups was also observed in the work of Busfield and Hanna (1991). The isopropyl end group was observed at 25.7 ppm in small concentration within the degraded sample, though the 48.2 ppm chemical shift appeared only as a shoulder peak in Figure 3.6.

Figure 3.8 shows the 100-150 ppm region of the ^{13}C NMR spectrum for degraded polypropylene. The presence of vinylene within the degraded sample was not significant from the baseline noise of the instrument. Busfield and Hanna (1991) concluded that the vinylene group which could be generated via hydrogen abstraction by a macroradical (shown



above) did not occur to any significant degree. Internal vinyl groups, similar to the vinylene, were not observed to any significant extent. The two expected resonances at 149.2 and 144.92 ppm were just barely visible above base-line noise in Figure 3.8, yet they were not seen in the virgin spectrum of Figure 3.9. Comparison of these two figures (Figures 3.8 and 3.9) may be complicated due to the difference in scaling of the two spectra. The latter chemical shift was concluded to be the sought-after vinylidene peak based on Table 3.2, however, the shift at 149.2 ppm has similar intensity to 144.92 ppm and could still be a vinylidene resonance based on calculated values listed in Table 3.2. The vinylidene and n-propyl end groups were the two primary functionalities resulting from degradation in both the work of Busfield and Hanna (1991) and Sawaguchi et al. (1995), as they were observed in Figures 3.6-3.9. Though, oxidation functionalities were observed in the infrared spectrum for the degraded sample (i.e. methyl ketone, lactone and aldehyde groups primarily), they had

insufficient concentration to be resolved from the base-line by NMR spectroscopy (proton or carbon).

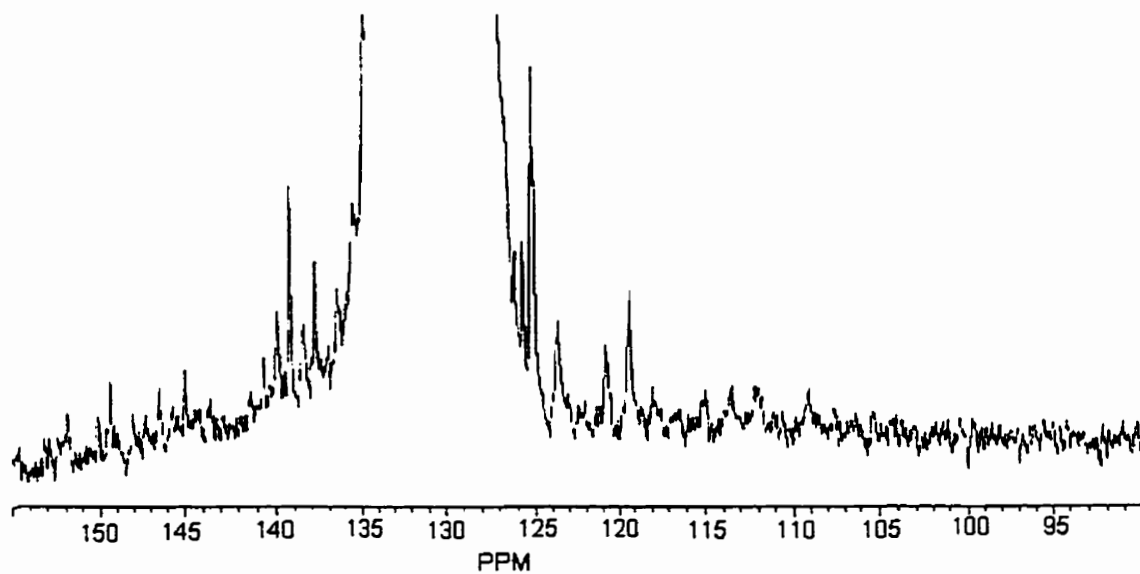


Figure 3.8. ^{13}C NMR spectrum in the region of conjugated structures for degraded polypropylene

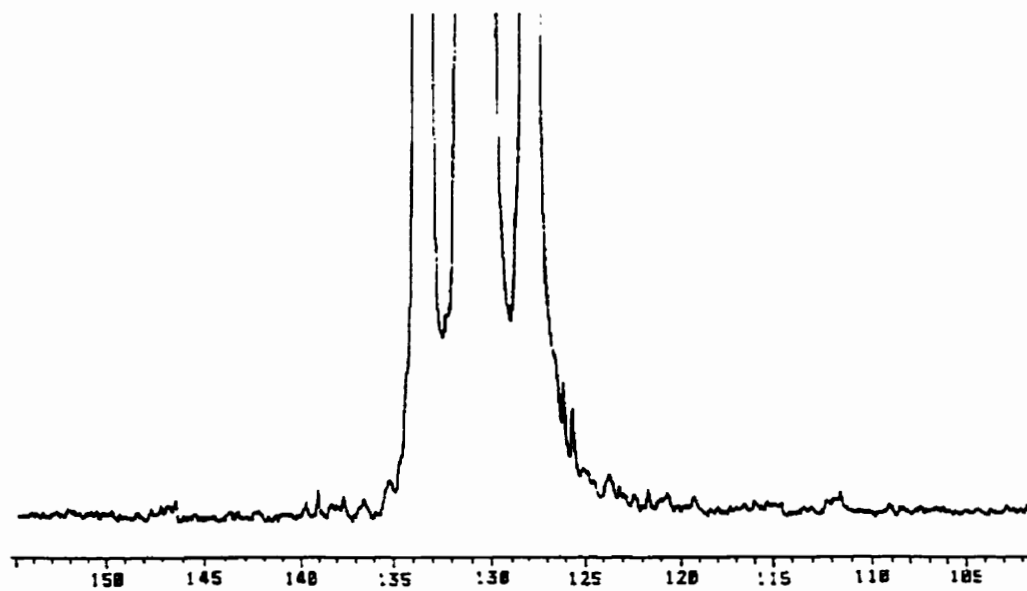


Figure 3.9. ^{13}C NMR spectrum in the region of conjugated structures for virgin polypropylene

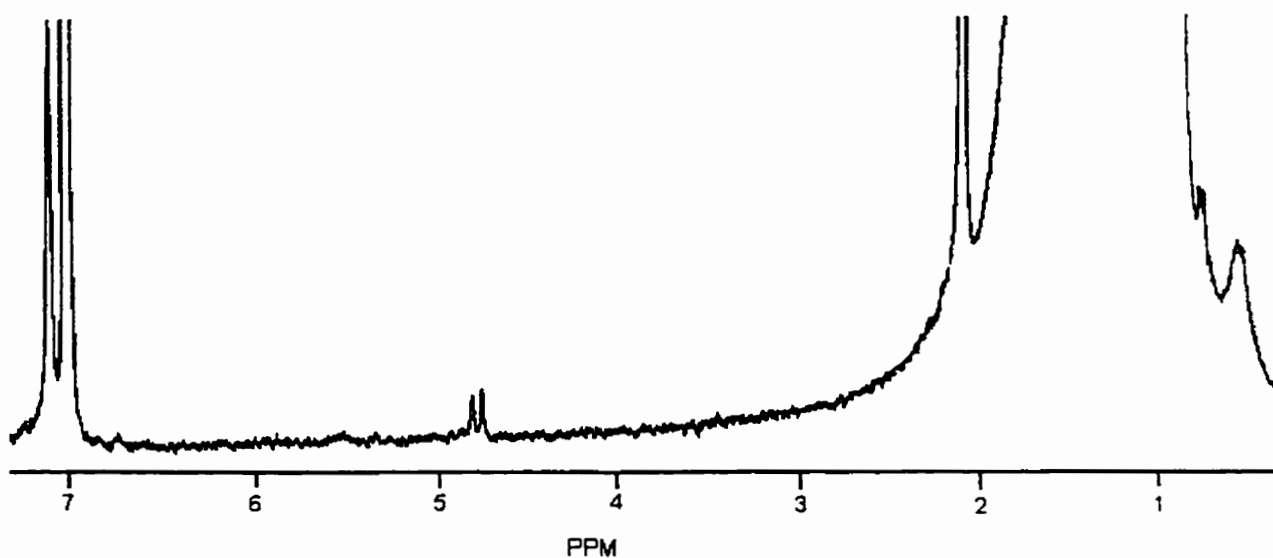


Figure 3.10. ^1H NMR spectrum of degraded polypropylene

In the ^1H NMR spectrum of the 0.5 wt % degraded polypropylene, the vinylidene appeared as a doublet at 4.81 and 4.75 ppm (shown in Figure 3.10). Sawaguchi et al. (1995) attributed the two peaks to two non-equivalent olefin protons. The backbone resonance of polypropylene (i.e. methyl, methylene and methine groups) were contained between 0.5-1.7 ppm in the spectrum. The strong resonance at 7.0 ppm was the solvent.

In general, NMR analysis was not a reliable method of characterizing the functionalities discussed in this thesis. The concentration of these groups, particularly at the chain end, were too low to accurately characterize the polymer.

3.5.2. FT-IR Analysis

Figures 3.11 and 3.12 show the FT-IR spectra of the degraded polypropylene samples in the region of the vinylidene absorbance at 888 cm^{-1} . Both figures clearly show the ability of the respective method, peroxide or thermal, to increase the concentration of vinylidene

groups in the product. A shoulder absorbance at 912 cm^{-1} was observed only in the peroxide series (Figure 3.12) which was likely an internal vinyl group. The 888 cm^{-1} peak height was observed to grow with increasing peroxide content, which is shown clearly in Figure 3.13 where the trend of relative vinylidene absorbance is plotted with increasing peroxide concentration. The nature of the absorbance curve does not indicate the onset of a plateau at the higher peroxide content in this experiment. Since two variables are changing at the same time during the thermal degradation, it was more conducive for clarity, to present the vinylidene concentration and molecular weight results in tabular form (Table 3.3). The degree of chain scission and the vinylidene concentration, are shown in Table 3.3 to increase

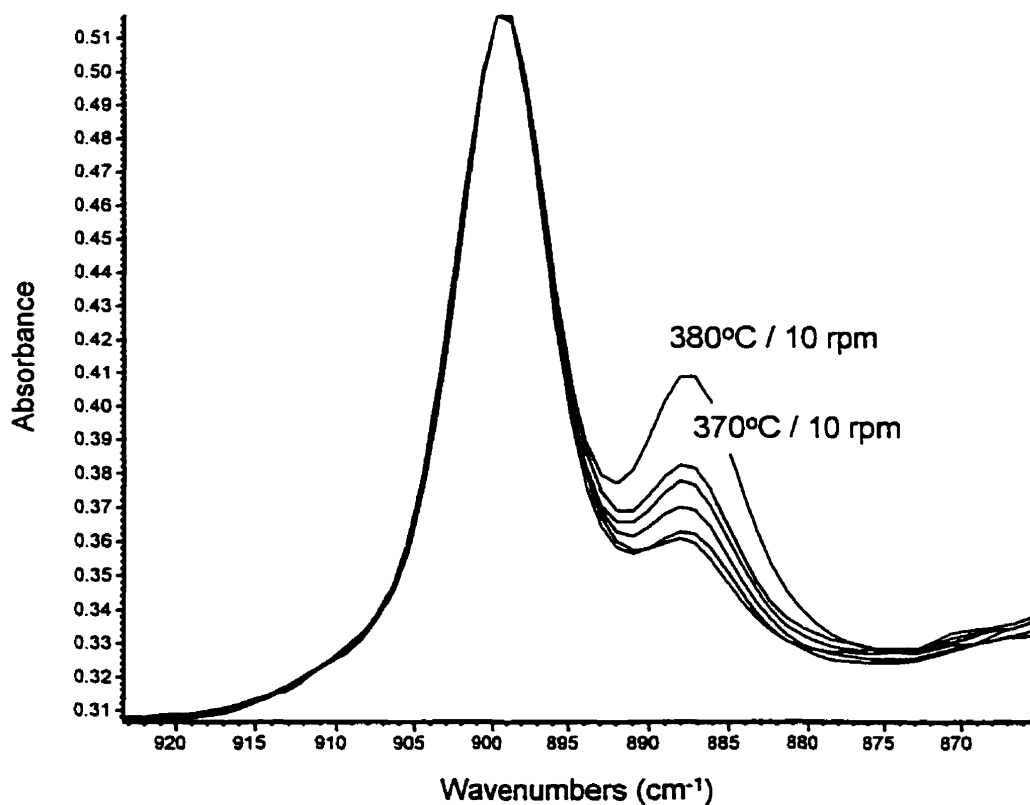


Figure 3.11. FT-IR spectra of a series of degraded polypropylenes corresponding to varying barrel temperatures [unlabeled spectra below 370/10 are 380/20 (highest), 380/30, 370/20, and 370/30 (lowest)]

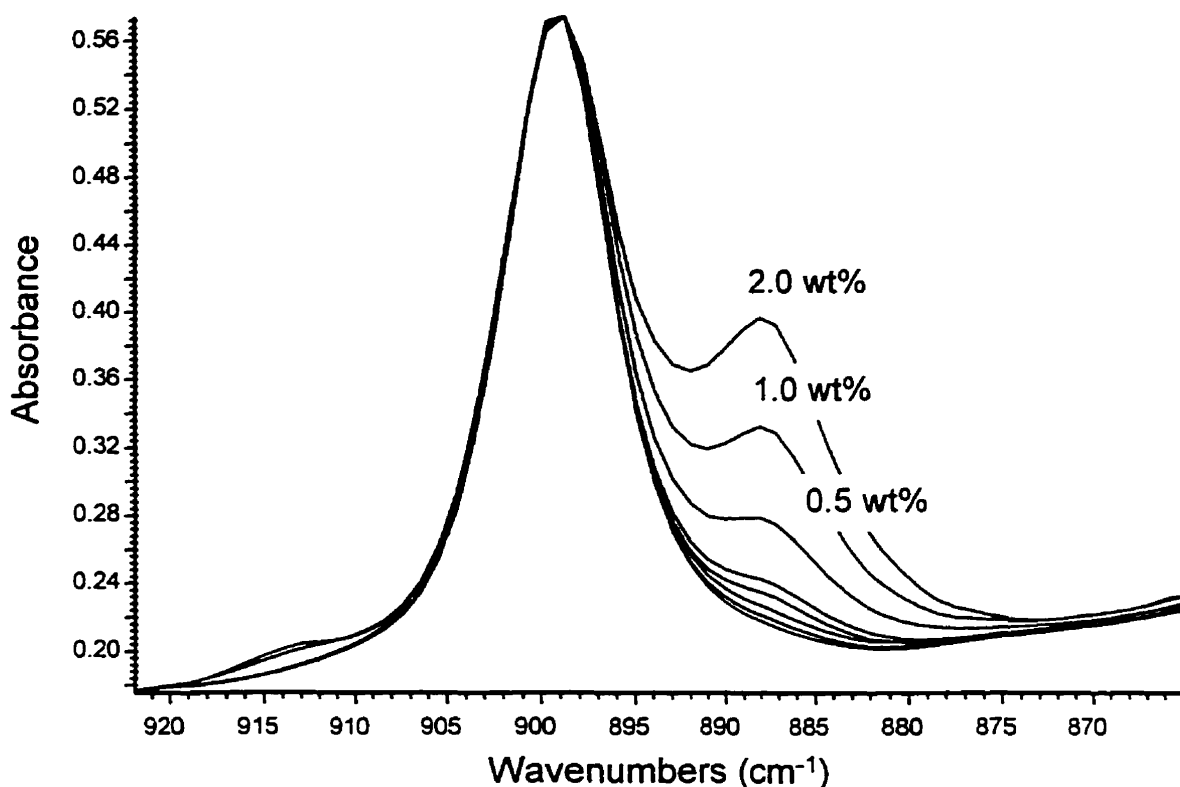


Figure 3.12. FT-IR spectra of a series of degraded polypropylenes corresponding to varying peroxide levels [unlabeled spectra below 0.5 wt % are 0.2 wt % (highest), 0.1, 0.05, 0.02, and 0.01 wt % (lowest)]

with temperature and with residence time (inversely related to screw speed). The terminal vinylidene concentration was increased in the degraded polypropylene via β -scission. This reaction relies on the ideal assumption of no oxygen being present during the high

Table 3.3. Vinylidene concentration and molecular weight results for thermally degraded polypropylene

Sample	\overline{M}_N (g/mol)	\overline{M}_w (g/mol)	Vinylidene Conc. (mol/g)
TD 370°C / 10 rpm	18670	49290	5.2×10^{-5}
TD 370°C / 20 rpm	22270	66140	4.7×10^{-5}
TD 370°C / 30 rpm	25900	79090	3.8×10^{-5}
TD 380°C / 10 rpm	17970	46220	6.1×10^{-5}
TD 380°C / 20 rpm	18600	53200	4.9×10^{-5}
TD 380°C / 30 rpm	21410	62730	4.3×10^{-5}

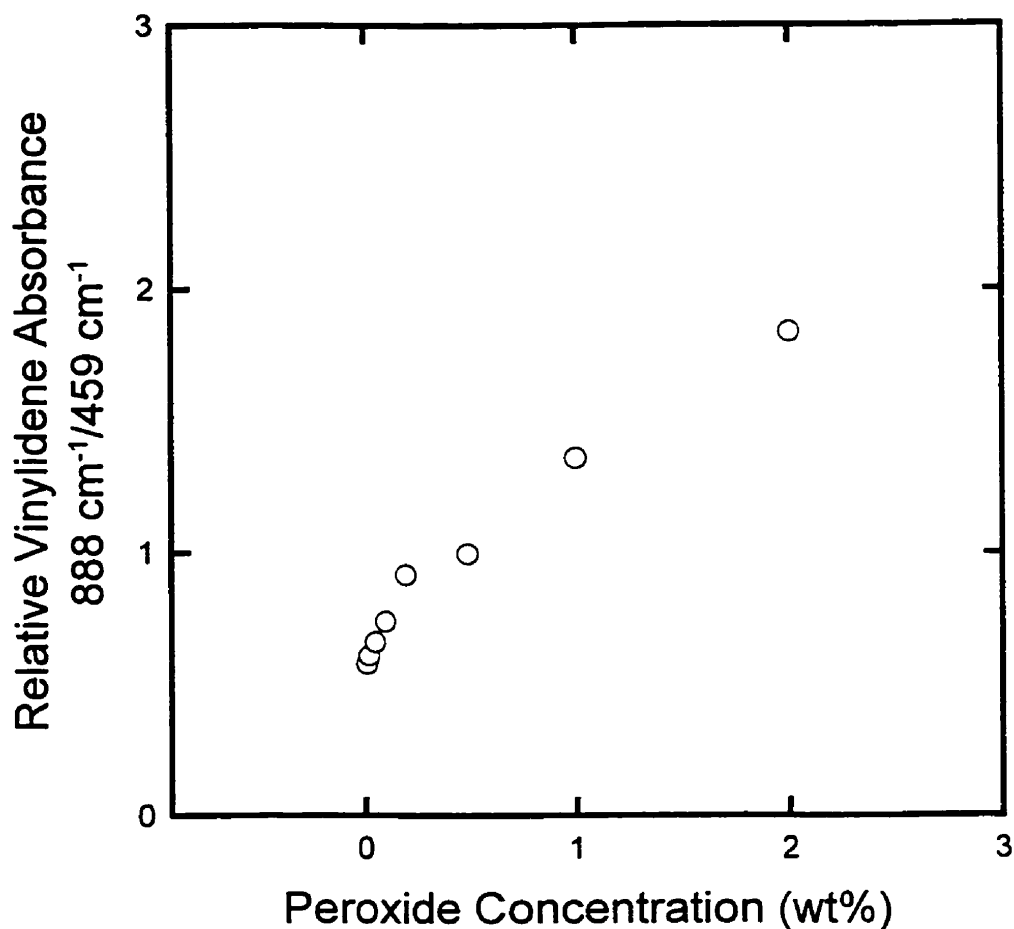


Figure 3.13. Vinylidene group content as a function of peroxide concentrations

temperature reaction, to produce oxidative functionalities including methyl esters, methyl ketones, aldehydes, carboxylic acids and lactones (Adams and Goodrich, 1970; Hinsken et al., 1991), in place of the desired unsaturation at the chain end. However, comparison of the carbonyl region of the infrared spectrum among degraded polypropylene samples from the peroxide or thermal method, shows that several oxidation functional groups (i.e. methyl ketones, aldehydes, and methyl esters) were significantly decreased at temperatures above 350°C (Figure 3.14). The strong peak at 1730 cm⁻¹ for methyl ketones along with the

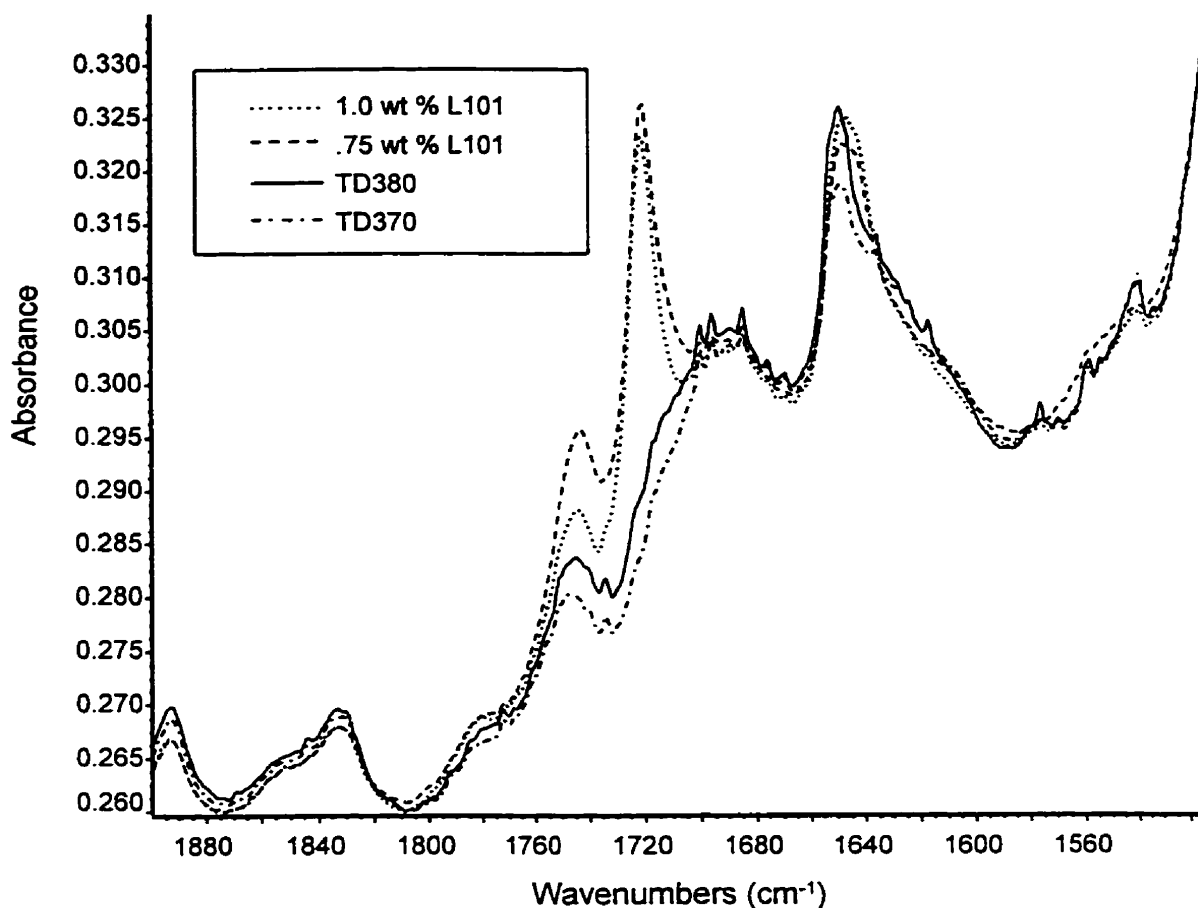


Figure 3.14. FT-IR spectra of thermal- and peroxide-degraded polypropylene, examining the carbonyl groups included in the polymer due to the method of chain scission.

shoulder vibration at 1722 cm^{-1} for aldehydes which were observed in the peroxide produced samples, had practically disappeared in the thermally degraded samples (TD370 and TD380, both produced at 20 rpm). The methyl ester peak at 1748 cm^{-1} varied between the samples, but was always lower in intensity among the thermally degraded samples.

The reduction in carbonyl functional groups should result in the vinylidene group being the dominant chain end functionality. This made thermal degradation, not peroxide-induced degradation, a more suitable method for inducing β -scission when the goal was to maximize the vinylidene group concentration. With regards to the incorporated carbonyl

groups interfering with the Lewis acid-anhydride enophile formation, both methods of degradation are examined in Chapter 7.

3.5.3. Molecular Weight Distribution

Figure 3.15 shows the number-average and weight-average molecular weights of the peroxide-degraded samples including the virgin resin. The chain length of the polypropylene

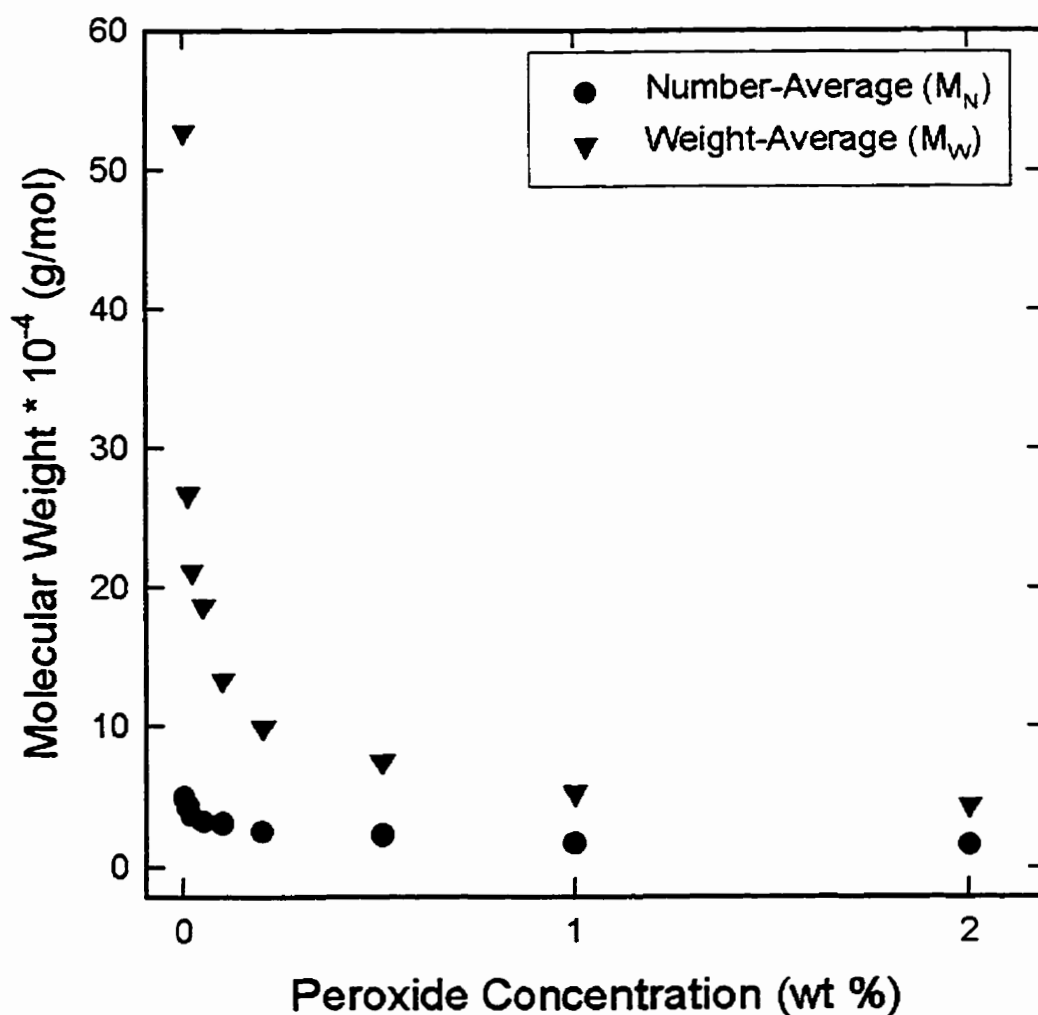


Figure 3.15. Change in the number-average molecular weight of degraded polypropylene due to random scission for increasing concentrations of peroxide

exhibited an exponential decay due to the postulated random nature of β -scission (Rado, 1962; Suwanda et al., 1988; Tzoganakis et al., 1988; Triacca et al., 1993). The number-average molecular weight in Figure 3.15 was seen to be approaching a plateau, while the more sensitive weight-average molecular weight indicates continued decrease in chain lengths as the chain distribution approaches a polydispersity of two.

The molecular weight averages for the six thermally degraded polypropylenes have already been disclosed in Table 3.3. The molecular weight of these samples, decreased with increasing temperature and decreasing screw speed. The most dramatic change in molecular weight occurred at 10 rpm for both temperatures examined, with the polydispersity indicating that the polymers were closely approaching a random (Flory) distribution. Figure 3.16 compares the shape of the molecular weight distributions for the degraded polypropylene according to the method of degradation along with the MWD of the virgin material. The MWD of the thermally degraded sample was narrower than that of the peroxide degraded product, despite the degree of scission being less. It is possible that the difference between the two distributions can be accounted to non-homogeneous dispersion of peroxide in the polymer.

The highly degraded polypropylene chains near the plateau region of Figure 3.15, and those polymers listed in Table 3.3, have no industrial relevance since the resulting polymers are tacky and lack sufficient melt strength to be useful in the majority of end-products. However, the high vinylidene content exhibited by these polymers are useful in the preparation of terminally functionalized polypropylenes with a variety of functional groups. The hypothesis of a critical chain length for free-radical degradation of polypropylene,

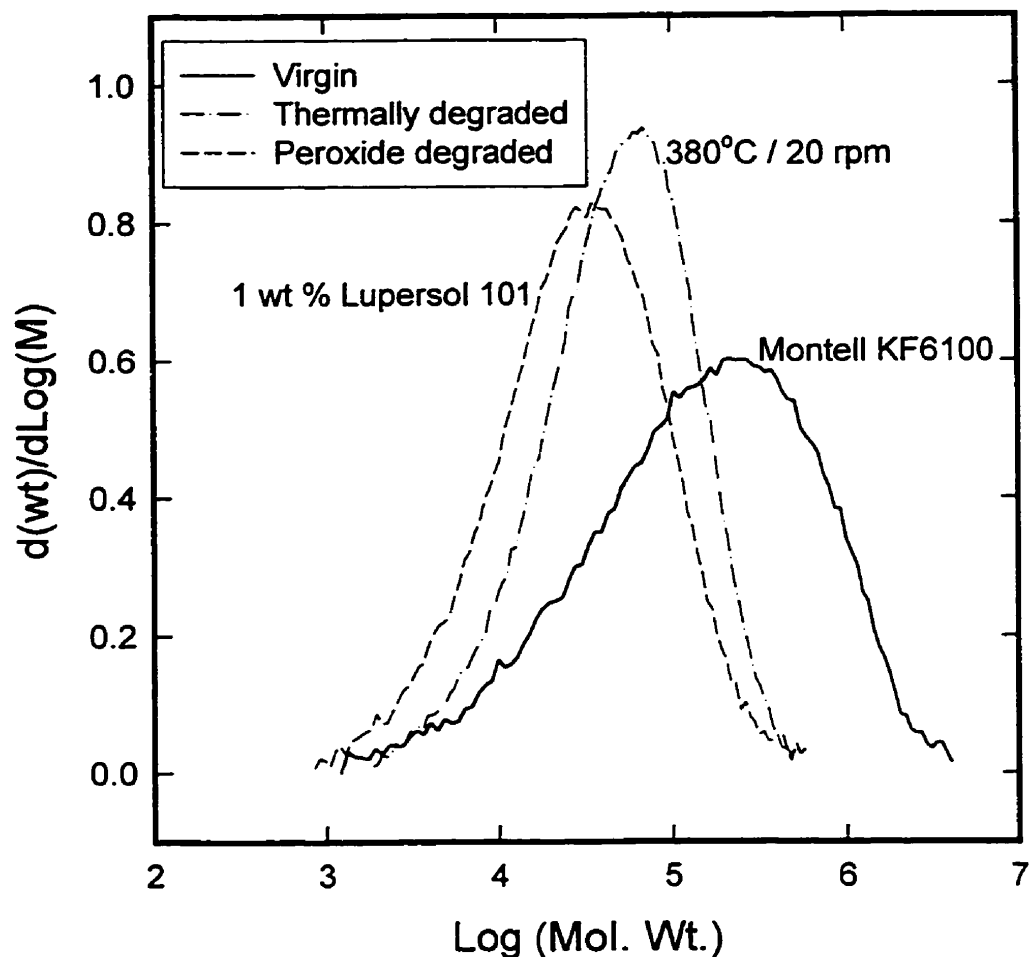


Figure 3.16. Molecular weight distributions for virgin polypropylene and degraded polymer via the two methods.

suggests that the maximum vinylidene content is likewise limited. The advantage of chain scission in producing terminal vinyls compared to Ziegler-Natta polymerization lies with the possibility of both chain ends possessing a double bond via degradation (Sawaguchi et al., 1995; Sawaguchi and Seno, 1996) provided that competing functionalities for the chain end produced by oxidation can be suppressed.

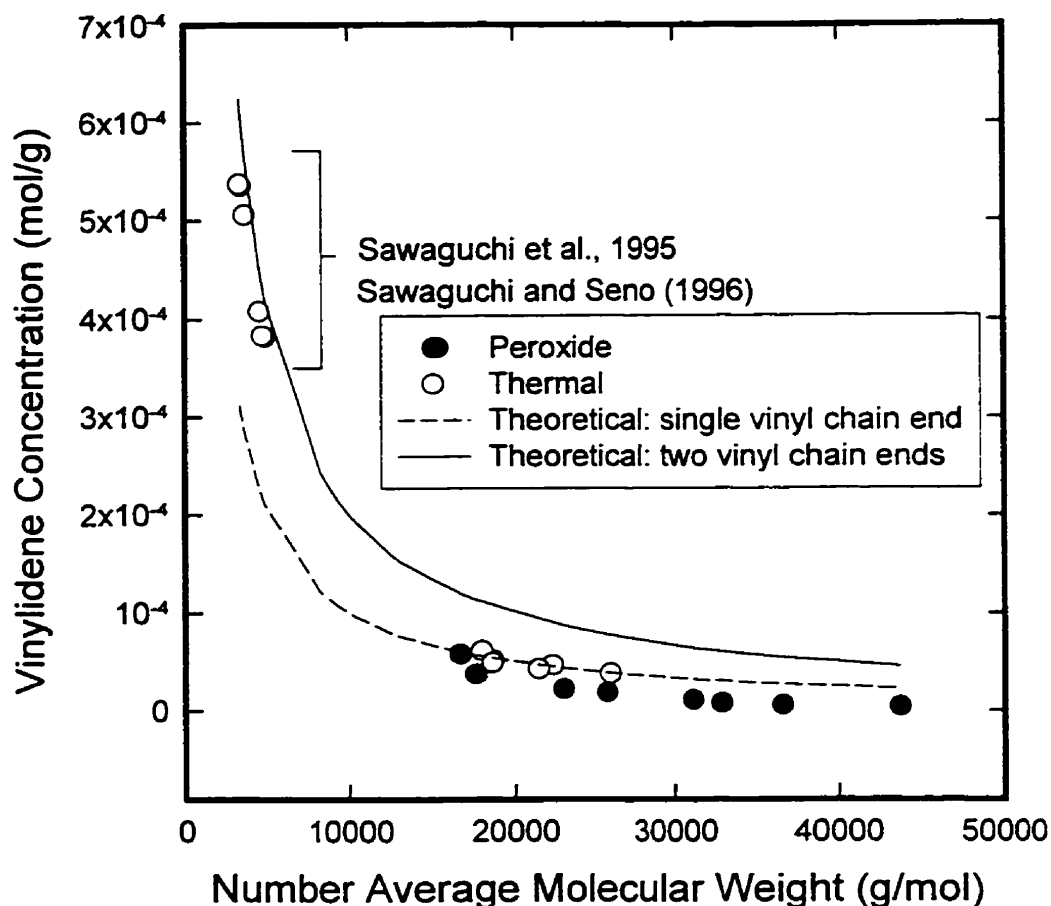


Figure 3.17. Comparison of the vinylidene concentration in degraded polypropylene samples with theoretical vinylidene concentrations for chains with one (dotted line) or two (solid line) terminal vinyls per chain.

Extensive thermal degradation has been shown (Sawaguchi et al., 1995; Sawaguchi and Seno, 1996) to obtain vinylidene functionalities close to 2.0. Figure 3.17 compares the experimental products, both peroxide and thermally degraded, plotting their vinylidene concentrations calculated from eqn (4.6) versus the number-average molecular weight. For comparison, the theoretical concentration of double bonds for chains within the range of molecular weights of interest to this work, were included in Figure 3.17 for polymers with one or two terminal vinylidenes per chain. Within the regression error for eqn (4.6), a

significant difference was observed between the peroxide degraded and thermally degraded polypropylene in Figure 3.17 with the peroxide method yielding less vinylidene groups for a corresponding number-average chain length. The vinylidene concentration of the degraded polypropylenes, both peroxide and thermally degraded, were observed to approach but never exceed the theoretically calculated concentration for one terminal vinylidene per chain. Experimental data taken from Sawaguchi et al. (1995) and Sawaguchi and Seno (1996) are plotted in Figure 3.17, indicating the trend in vinylidene growth with increased degree of scission. If the literature data can be considered reasonable values for the extrusion process despite the presence of oxygen, then the current trend in our degraded polymer suggests that further degradation of the polymer below 20,000 g/mol will begin to produce telechelic species.

The generation of vinylidene-terminated chains were shown to increase in a manner almost proportional to $1/\overline{M}_N$ in Figure 3.18. Rather at high peroxide concentrations the rate of vinyl formation is still relatively large compared to the change in \overline{M}_N . This agrees with the assumption that there is a tendency for high degrees of scission to generate telechelic polymers with two functionalized chain ends. Based on this fact, it should be possible to generate telechelic polypropylene species via polymer degradation. This figure also confirms that a greater number of vinylidene groups are produced per chain scission via thermal degradation than in the presence of peroxides. In conjunction with the infrared results, these findings indicate that the loss of vinylidene groups amongst the peroxide degraded chains can be attributed to oxidative functionalities competing successfully for the chain end.

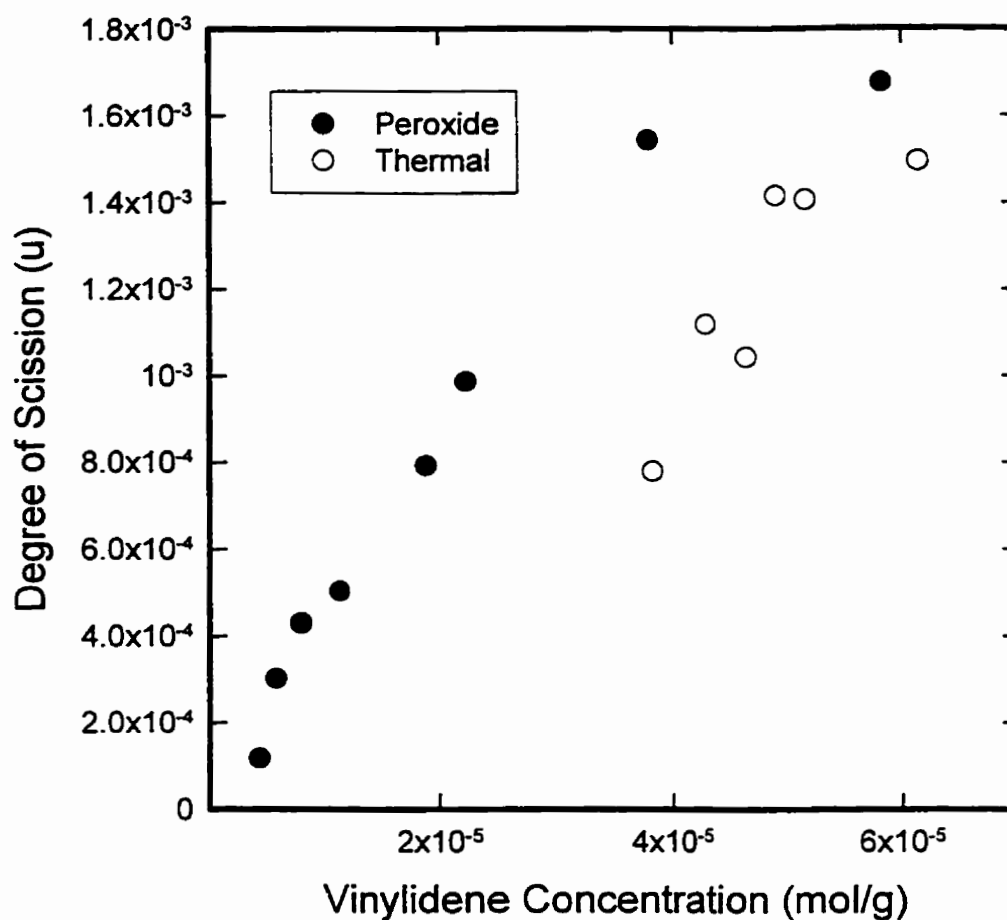


Figure 3.18. Theoretical vinylidene growth versus experimental measured vinylidene content in degraded polypropylene.

3.6. CONCLUDING REMARKS

Two methods of polypropylene degradation have been examined, thermal and peroxide induced. Both methods employed included thermo-oxidative degradation due to the presence of atmospheric oxygen in the reactions. The high temperatures used to thermally degrade the polymer chains, were found to reduce the presence of several undesirable carbonyl-based oxidation functionalities (i.e. methyl ketone, methyl ester and aldehyde

groups). Examining the ratio of the vinylidene concentration to the degree of scission, it was apparent that the thermal degradation reaction produced more chain ends with a double bond than a carbonyl functionality, compared to those material degraded using an organic peroxide. Evidence was also provided which indicated that the trend in vinylidene generation did not follow the number-average molecular weight of the polymer, but rather continued to grow unabated with increasing degree of scission. Extrapolation of this trend beyond the degrees of scission examined in this work, should lead to the production of telechelic polymers provided oxidative functionalities can be further reduced.

CHAPTER 4. EXPERIMENTAL

4.1. MATERIALS

4.1.1. Low Molecular Weight Polyisobutylene

Terminal succinyl functionalization of an aliphatic polymer had only been thoroughly characterized for polyisobutylene and with the terminal unsaturation in polyisobutylene similar in structure to that of polypropylene, the polymer was ideal as a model material for examining the effect of the different Lewis acids on the reaction system. The low molecular weight polyisobutylene chosen was Glissopal 1000 (BASF, supplied values: $\overline{M}_v = 1000$ g/mol; 85% vinylidene functionality).

4.1.2. Low Molecular Weight Amorphous Polypropylene

The choice of a model polymer for studying the maleation of polypropylene via the Alder Ene reaction, was dependent on finding a material with a high vinylidene content without extraneous functionalities which generally arise from polypropylene degradation (i.e. ketone, aldehydes, and γ -lactones). The material finally decided upon was a low molecular weight ($\overline{M}_n = 2010$ g/mol, $\overline{M}_w = 10,300$ g/mol, data supplied by the manufacturer) amorphous polypropylene (Polypol-19) donated by Crowley Chemical. According to the manufacturer, Polypol-19 contained 0.1% Topanol CA and 0.17% DLDTP or DLST (ICI) to inhibit oxidation. Two Polypol-19 batch-averaged vinylidene concentrations used were 2.5×10^{-4} mol/g and 1.8×10^{-4} mol/g, each measured by ^1H NMR analysis.

4.1.3. High Molecular Weight Polypropylene

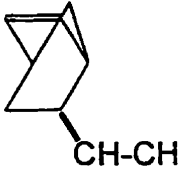
The polypropylene, grade KF6100, was donated by Montell Canada. The polymer was characterized in a Kayeness Galaxy V capillary rheometer yielding a melt flow index (MFI) of 3.0 g/ 10 min (according to ASTM D1238 at 230°C under 2.16 Kg weight). The molecular weight distribution of the polymer was measured by high temperature gel permeation chromatography [discussed in section 4.3.7]. The molecular weight averages for KF6100 were determined to be: $\overline{M}_n = 49,800$ g/mol, $\overline{M}_w = 528,000$ g/mol, PDI = 11.

4.1.4. Ethylene-Propylene-Diene Terpolymer

The ethylene-propylene-diene-monomer (EPDM) rubber examined came from two sources, each employing a different diene termonomer (structural configuration of the two dienes are shown in Table 4.1). The material containing the 5-ethylidene-2-norbornene (ENB) diene was the major focus of this work.

Royalene IM7100 ethylene-propylene-diene terpolymer (74% ethylene, 26% propylene content) containing 5 wt % 5-ethylidene-2-norbornene (ENB) was supplied by

Table 4.1. Diene monomers used in ethylene-propylene-diene terpolymer

Chemical Species	Abbreviation	Structure
5-ethylidene-2-norbornene	ENB	
1,4-hexadiene	HD	$\text{CH}_2=\text{CH}-\text{CH}_2-\text{CH}=\text{CH}-\text{CH}_3$

Uniroyal Chemical in pellet form ($\overline{M}_n=130,000$ g/mol, $\overline{M}_w=350,000$ g/mol, Mooney viscosity $ML_{1+4}=70$ at 120°C). Nordel 1040 EPDM (54% ethylene, 42% propylene) containing 4 mol % (0.01 wt %) 1,4-hexadiene as the diene termonomer was supplied by DuPont Canada in bale form ($\overline{M}_n=29,834$ g/mol, $\overline{M}_w=217,514$ g/mol).

4.1.5. Reagents and Solvents

Maleic anhydride was provided by Monsanto Chemical and Aldrich Chemical in the form of briquettes. The Lewis acids, SnCl_4 , TiCl_4 , AlCl_3 , $\text{SnCl}_2 \cdot 2\text{H}_2\text{O}$, and ruthenium chloride (commercial RuCl_3 denoted as $\text{RuCl}_n \cdot x\text{H}_2\text{O}$) were supplied by Aldrich Chemicals and used as received. Stannous chloride dihydrate, ruthenium chloride hydrate and aluminum chloride were kept in a desiccator until needed, while the other catalysts were liquids at room temperature and simply required precautions to maintain a nitrogen atmosphere. The free radical inhibitors, TEMPO (free radical 2,2,6,6-tetramethyl-1-piperidinyloxy), butylcatechol, benzoquinone and hydroquinone were also supplied by Aldrich. Magnesium oxide (MgO , supplied by Alfa-Johnson Matthey) was used as a Lewis base as suggested by Coran and Patel (1983) to suppress isomerization by neutralizing any free HCl generated by the Lewis acid. To form an elastomer via ionic cross-links between maleated EPDM chains, zinc oxide (ZnO) was used as a neutralizing agent (supplied by Fisher Scientific along with stearic acid which was used as an accelerator in the neutralization reaction). The peroxide chosen for degrading polypropylene, was Lupersol 101 (2,2-dimethyl-2,5-(t-butylperoxy)hexane) supplied by Elf AtoChem. The Arrhenius parameters for Lupersol 101 decomposition in dodecane, as described by the supplier, are

$A=8.73 \times 10^{15} \text{ s}^{-1}$ (pre-exponential constant) and $E_a=38127 \text{ cal/mol}$ (activation energy). The dimethylformamide (EM Science) was dried by distillation over 4A molecular sieve and stored with more molecular sieve to maintain its anhydrous state. All other solvents (1-octanol, 1-dodecanol, ethanol, 2-propanol, xylene, acetone, hexane and toluene) were supplied by BDH Chemicals.

4.2. EQUIPMENT AND PROCEDURES

4.2.1. Bench-Top Round Bottom Flask Reactor

Approximately 12-15 g Glissopal 1000 was charged into a 300 mL round bottom flask and the system was heated to 180-230°C. Once the viscosity of the polymer became low enough, a magnetic stir bar was introduced to agitate the system. Upon reaching the desired conditions, 1 wt% hydroquinone and 1.8 mole equivalence maleic anhydride with respect to the vinylidene content were added, generating a yellowish mixture. After 2 minutes of mixing, a chosen catalyst was added and the system was allowed to react for 5 minutes. Typically, fumes evolved from the reactor upon addition of the catalyst, which subsided after 1-2 minutes. The reaction was terminated by the addition of 1 mL distilled water which discoloured the solution. Once the water had evaporated, the product was dissolved into hexane and subsequently filtered through a coarse fritted-glass filter to remove the insoluble residue of unreacted maleic anhydride, unbound poly(maleic anhydride) and catalyst. The cleaned product was collected by evaporating the hexane and vacuum drying for 16 h at 120°C.

4.2.2. Parr 300 mL High Pressure Autoclave

A Parr 300 mL high pressure autoclave was set up for use as a resin kettle. Figure 4.1 shows photos of the reactor setup. The lines dedicated for maleic anhydride injection and polymer sampling (right side of the apparatus shown in Figure 4.1 and in the schematic in Figure 4.2) were traced using heating tape to prevent solidification. The Lewis acid, generally $\text{SnCl}_2 \cdot 2\text{H}_2\text{O}$, was massed and if added in solid form, it was ground using a mortar and pestle before placing it into a catalyst bucket which was attached to the inside of the reactor, inline with one of the inlet nitrogen feeds. If the Lewis acid was to be added with the molten maleic anhydride via a syringe, the solid catalyst was dissolved in 40 μL of an appropriate solvent prior to mixing with the other reagents.

For dissolving $\text{SnCl}_2 \cdot 2\text{H}_2\text{O}$, the chosen solvent was dried HPLC grade dimethylformamide. Dimethylformamide (DMF) was chosen for its good chemical and thermal stability below 350°C (Riddick, 1970), low volatility, high boiling point, solubility with stannous chloride and low potential for killing the catalyst. The seemingly large excess of maleic anhydride compared to the small volume of DMF present, was hoped to overcome the potential for the solvent preferentially co-ordinating with the catalyst. The precautions for purity and dryness of the solvent were designed to prevent the decomposition products of DMF, in particular dimethylamine, formaldehyde and formic acid, from reacting with the succinyl functionality. Dimethylformamide is a solvent for maleic anhydride and poly(maleic anhydride), not reacting with the anhydride (Bhadani and Prasad, 1977). Also, the presence of DMF is believed to interfere with the homopolymerization mechanism of maleic anhydride (Gaylord and Mehta, 1982) as discussed in Chapter 2. During free radical-

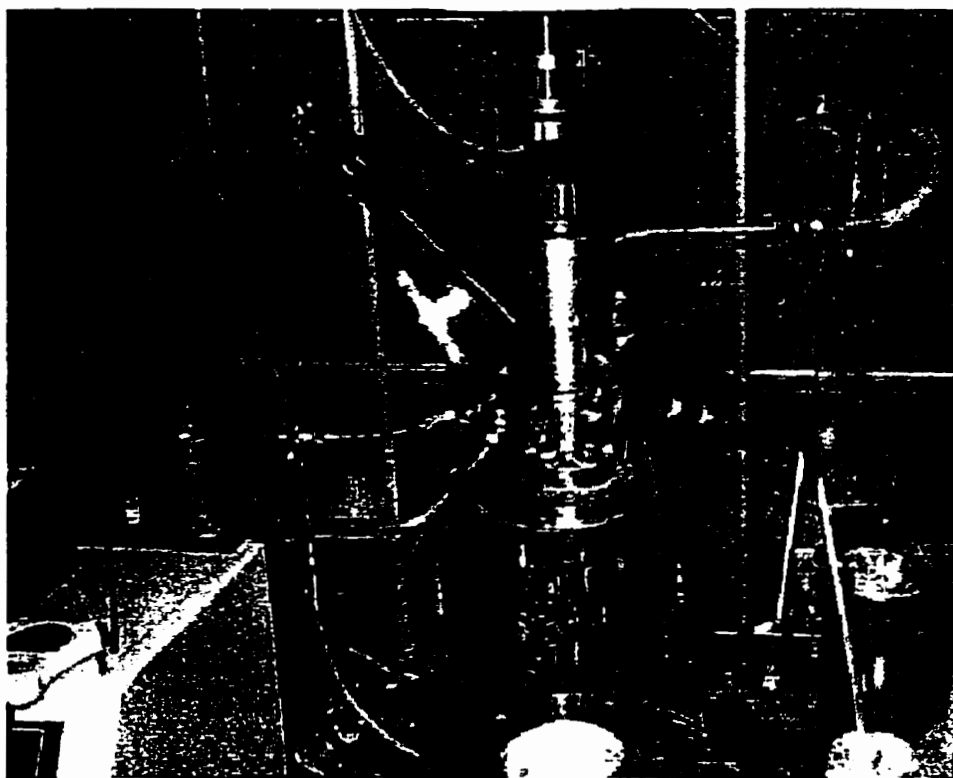


Figure 4.1. Photos of the autoclave reactor for the Alder Ene reaction

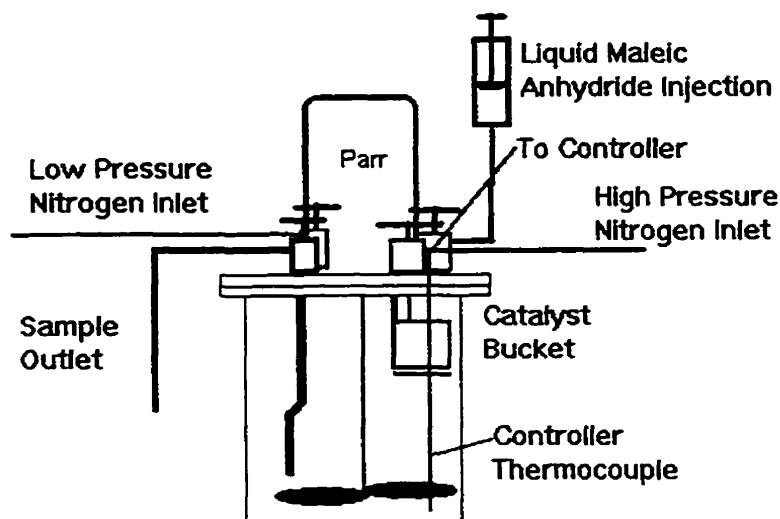


Figure 4.2. Schematic diagram of the Parr reactor

initiated grafting experiments of maleic anhydride onto low density polyethylene, Gaylord and Mehta (1982) found that 2 mol % DMF, based on maleic anhydride, decreased product cross-linking to 28 % gel while 20 mol % DMF prevented cross-linking completely.

As stated in Chapter 2, the presence of an alcohol with ruthenium chloride has been observed (Anderson et al., 1965) to promote the addition reaction. Hence, to dissolve solid ruthenium chloride hydrate, 1-dodecanol (Aldrich Chemical) was chosen to add the Lewis acid to the reaction. There was a concern over esterification of the anhydride with this solvent, which was unavoidable.

Approximately 70 g of low molecular weight polypropylene was charged into the vessel per run. The polypropylene wax (including catalyst if employed as a solid in the bucket) was heated to 230°C using a Parr 4843 controller, under a nitrogen blanket and constant agitation (300 rpm). Once thermal equilibrium was obtained, a 1 mole equivalence

of molten maleic anhydride (at 70°C, $\rho = 1.30$ g/mL according to Trivedi and Culbertson, 1982) with respect to the vinylidene content, was injected into the reactor along with TEMPO and catalyst if dissolved into a solvent. The reactor was subsequently pressurized to 0.55 MPa to reduce volatilization of the reactants at the reaction temperature and to force open the catalyst bucket (if present). Samples were extracted from the pressurized reactor at 60 s intervals, with the nitrogen flow regulated to maintain a constant system pressure. The first fraction of each polymer sample was discarded. The individual samples were immediately dissolved in 100 mL cyclohexane and then filtered using a fritted glass filter assembly. Any residual reactants were removed during filtering due to their insolubility in cyclohexane. The solvent was evaporated and the final product was dried in a vacuum oven for 16 h at 120°C. The samples were stored in a desiccator until spectroscopic measurements could be performed, to avoid hydrolysis of the anhydride.

4.2.3. Haake Rheomix 3000 Batch Mixer

Preliminary experiments for EPDM were performed in a Haake Rheocord 90 fitted with a Rheomix 3000 batch mixer. Two roller rotors were used to mix the polymer melt. The Rheocord 90 had been fitted with a torque cell rated for 200 N·m (shear pins on the mixer allowed for the maximum torque, therefore, typically shutdown alarm limits were set for 180 N·m in the software). The set of reactions done in the batch mixer, which did not include neutralization experiments, are discussed in the characterization section 4.4.9.

The batch mixer was heated and the torque cell was calibrated prior to the experiments. The EPDM elastomer was fed into the Rheomix and mixed at 60 rpm for a duration of approximately 2 minutes at which point fusion was completed (a rapid rise in

torque was produced indicating the onset of fusion, which dissipated and finally leveled off upon homogenization of the polymer melt, as shown in Figure 4.3). A mixture of maleic anhydride and Lewis acid catalyst was ground together in a mortar and added at the nip region between the two rollers (no TEMPO was used due to its high volatility and highly toxic nature). The reaction was allowed to proceed for 5 minutes with the product being collected and cooled prior to purification and analysis. These preliminary experiments were performed as listed in Table 8.3.

4.2.4. Haake Rheomex 252 Single Screw Extruder

A Haake Rheomex 252 (specially modified to possess a pressure tap 200 mm upstream of the die) was subsequently attached to the Rheocord 90. The Rheomex 252 was protected from excessive torque by fitting the extruder with a shear pin rated for 160 N·m and

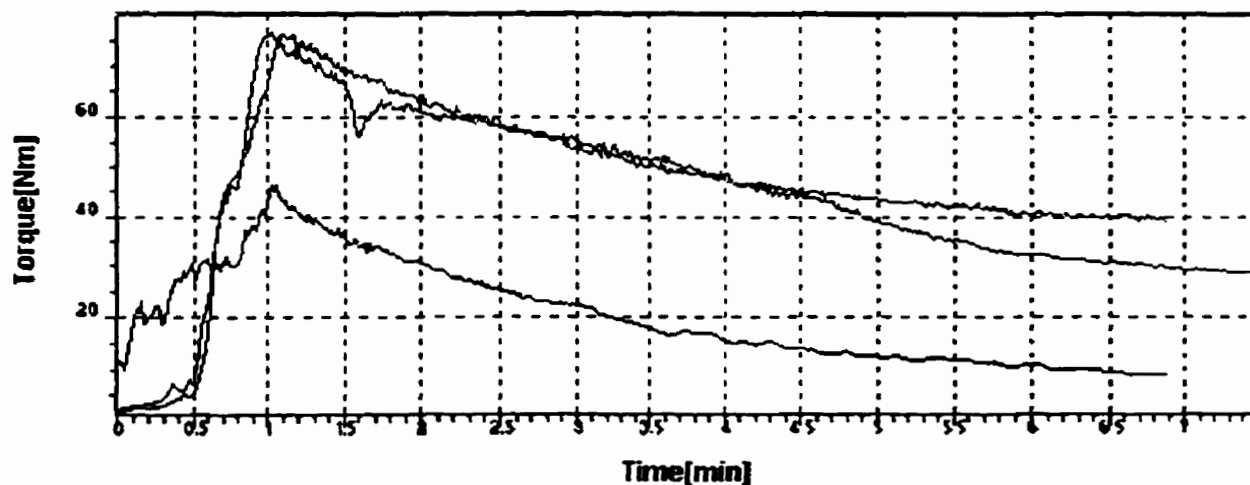


Figure 4.3. Sample torque plots for EPDM in a Haake Rheomix 3000

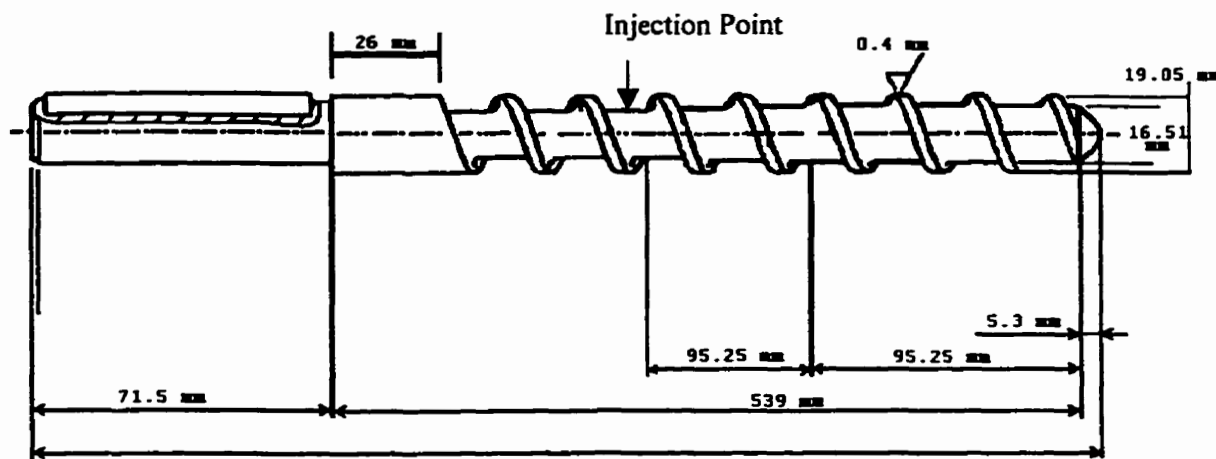


Figure 4.4 Screw design for the Haake Rheomex 252 single screw extruder

setting the software shutdown alarm to 155 N·m. All experiments were done using a rod die (at zone 4) to which various nozzles with different bore diameters (1-6 mm) could be fitted. Pellets were charged to the extruder via a vibrating (pneumatically controlled) feed hopper. The design of the screw is shown in Figure 4.4. The screw has a 3:1 compression ratio with an $L/D = 27$.

4.2.4.1. Ethylene-Propylene-Diene Terpolymer

To provide a closed system for the reaction, the single screw extruder was the next progressive step from the batch mixer for experiments involving EPDM rubber. A rod die with a 5 mm diameter nozzle fitting was attached to the extruder. The reactants were injected at the pressure tap 200 mm from the die (prior to the taper section of the screw) via a custom-made injection stem. The stem was made from a pressure tap blind which was bored out to allow 1/8" tubing be inserted the length of the stem (to prevent variation in tube diameter from that attached to the pump). The tubing was held in place via a 1/8" union welded to the

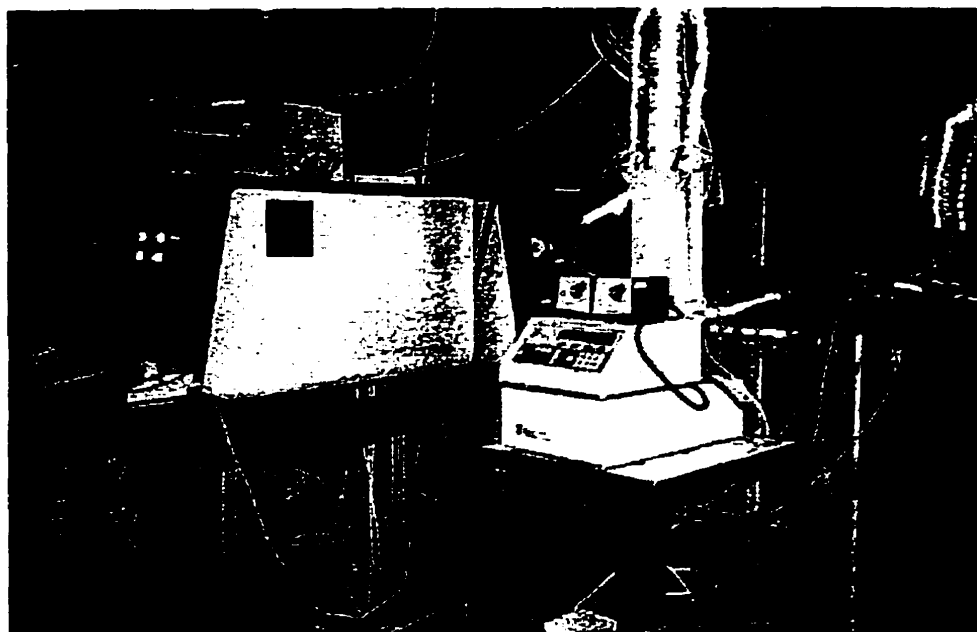


Figure 4.5. Picture of the single screw extruder setup for maleation of EPDM

blind. A high pressure syringe pump capable of holding 260 mL of liquid was used. The pump and injection lines were traced using $\frac{1}{4}$ " copper tubing that carried heated water (75.0°C) circulated by a Grant W14 (14L) water bath with a Grant ZDL controller. The tracing along with the heating tape on the valves, maintained the maleic anhydride above its melting point. The complete setup for the extruder is shown in Figure 4.5. A Dynisco PT452 (0-34.5 MPa range) pressure transducer was used to monitor the pressure at the end of the extruder, prior to the rod die. Melt temperature was monitored by a thermocouple (Haake) mounted midway along the die channel.

The extruder was heated at the following temperature profile: 130/ 180/ 230/ 230°C and the torque cell was calibrated. A 50% Royalene EPDM / 50% KF6100 polypropylene (w/w) blend of pellets was charged to the feed hopper. Pure EPDM could not be fed into the extruder because the hopper angle was insufficient for the bulk density of the rubber to

prevent bridging. Three screw speeds were chosen to provide a range in residence (and reaction) times for the functionalization experiments: 30, 50, and 70 rpm. The mass flow rate (\dot{M}) of EPDM/PP resin for each of these screw speeds (N) was measured by collecting the exiting extrudate for 1 minute and recording its mass. Several repeats for each screw speed allowed a calibration curve ($\dot{M} = 0.65146 \cdot N$ [g/min]) to be generated, valid within the aforementioned range. The standard error calculated for the slope of this curve was 0.00687.

The liquid reactants were prepared in a round bottom flask on a heating mantle (according to Table 4.2). The catalyst and TEMPO were weighed into a vial and dissolved in DMF.

Table 4.2. List of reactants and composition

Reagents	Composition
Maleic Anhydride	74.20 g
Stannous chloride	0.0170 g. (0.01% mole eq.)
DMF	140 μ L
TEMPO	0.010 g

The liquid reactants, combined with molten maleic anhydride, were drawn into the syringe pump and subsequently allowed to thermally equilibrate. The system maintained maleic anhydride above its melting point at 75°C. At this temperature, the density of molten maleic anhydride had been measured to be $\rho_{75^\circ\text{C}} = 1.28$ g/mL using a graduated vial, thereby ensuring that accurate reactant-polymer ratios were maintained during experimentation. Since the site of reactant injection lies 200 mm upstream from the onset of the die, it can be seen from the screw diagram (Figure 4.4), that the fluid shall impinge upon polymer not fully

melted (i.e. in the melting zone of the extruder). The pressure measured at the syringe pump ranged from 17-26 MPa when injected into the extruder under steady operation, opposed to 83-138 KPa when the injector exit was unimpeded. To reduce the occurrence of polymer creeping up the injector stem and ultimately obstructing the reactant flow, upon start-up the reactants began to enter the extruder prior to polymer melt/solid filling the corresponding region of the screw. It was initially feared that the syringe pump would not be sufficiently responsive to adjust to the rapid changes in pressure at the point of injection, to maintain i) the correct flow rate and ii) to provide adequate pressure to prevent the polymer from blocking the injector. Generally, with adequate precautions the pump operated without any problems.

A set of experiments (listed in Table 8.4) was run varying maleic anhydride concentration and reaction time. A separate single experiment was also run using reactants without catalyst for comparison, to produce a conventional Alder Ene product.

The products were purified by dissolving into hot xylene followed by precipitation of the polymer from solution by the introduction of a four fold excess of acetone based on volume. Residual maleic anhydride and poly(maleic anhydride) should remain in solution with acetone. The polymer was collected by filtration and washed repeatedly with acetone and finally dried for 16 h at 120°C in a vacuum oven.

4.2.4.2. Polypropylene Degradation

Both peroxide-induced and thermal/thermo-oxidative degradation methods (discussed in Chapter 3) for generating the vinylidene group were examined, to determine if the oxidation functional groups interfere with the Alder Ene reaction. Since the vinylidene group

concentration affects the extent of reaction due to the bimolecular nature of the Alder Ene mechanism, it was desirable to make the degree of unsaturation similar between the two methods. The 6 mm diameter nozzle was used in the rod die. Two vinylidene concentrations were produced from each method.

Two thermal/thermo-oxidative polypropylene batches were prepared by altering the temperature of the third barrel zone. Table 4.3 shows the barrel temperature profile and the resulting vinylidene group concentration (along with its standard deviation) determined using the infrared calibration curve (Thompson et al., 1997) described by eqn (4.6) in section 4.4.3.3. To better differentiate between the two concentrations in a factorial experiment, TD370 (i.e. Zone 3 set to 370°C) was diluted 50/50 w/w with virgin polypropylene.

Table 4.3. Relationship of barrel temperature with resulting vinylidene concentration

Samples Name		TD370	TD380
Vinylidene concentration (mol/g)		4.66×10^{-5}	4.92×10^{-5}
		$\pm 5.8 \times 10^{-6}$	$\pm 5.2 \times 10^{-6}$
Barrel Temperature	Zone 1	150°C	150°C
	Zone 2	240°C	240°C
	Zone 3	370°C	380°C
	Zone 4	290°C	290°C

Obviously, the molecular weight distribution of the two resins produced different mixing performance in the twin screw extruder during subsequent experiments using the Alder Ene reaction. However, no practical alternative was available.

For the peroxide-induced degradation product, the samples were produced in the single screw extruder at 30 rpm using a barrel profile of 140, 180, 230 and 190°C for the die.

Two dialkyl (Lupersol 101, Elf AtoChem) peroxide levels were used, 0.75 wt % and 1.0 wt %, producing average vinylidene concentrations of $4.84 \times 10^{-5} \pm 4.9 \times 10^{-6}$ mol/g (sample PD075) and $6.02 \times 10^{-5} \pm 4.3 \times 10^{-6}$ mol/g (PD100) respectively. Sample PD100 was diluted 50/50 w/w with virgin polypropylene. Table 4.4 shows the GPC results for the degraded materials (prior to any dilution).

Table 4.4. Molecular weight averages of degraded polypropylene

Sample	\overline{M}_N (g/mol)	\overline{M}_w (g/mol)	Polydispersity
TD370	22270	66140	3.0
TD380	18600	53200	2.9
PD075	19850	64900	3.3
PD100	17615	53380	3.0

4.2.5. Leistritz LSM 30.34 Twin Screw Extruder

The final level of reaction scale-up for polypropylene and EPDM was carried out in a Leistritz LSM30.34 modular twin screw extruder (screw diameter = 34 mm; L/D = 30) set up in a co-rotating screw configuration. The extruder possesses 10 heating zones not including the die. The polymer was fed into the extruder at zone 1 by a K-Tron F-1 series loss-in-weight feeder regulated by a K-Tron KDU controller. The liquid reactants were fed into the extruder at zone 4 using a syringe pump (operating under constant flow control; maximum pressure 52 MPa). The syringe body and the exit tubing were traced as discussed in section 4.2.4.1.

The Lewis acid catalyst and TEMPO were weighed into a vial and subsequently dissolved into 140 μ L of the chosen solvent. Dimethylformamide (DMF) was used to

dissolve stannous chloride, while 2-octanol was used for ruthenium chloride. The liquid reactants were prepared in a round bottom flask, starting with the heating of maleic anhydride on a heating mantle. The liquid reactants, combined with molten maleic anhydride, were drawn into the syringe pump and subsequently allowed to thermally equilibrate. The system maintained maleic anhydride above its melting point at 75°C. The equilibrium time also allowed for the slow formation of the Lewis acid-maleic anhydride adduct which was observed in previous work (Thompson et al., 1998a). Figure 4.6 shows a picture of the experimental setup.

The introduction of low viscosity liquid reactants into the polymer melt requires that the screw design provide both dispersive and distributive mixing. Based on a short article by Andersen (1997) of Werner & Pfleiderer Corp., the mixing considerations for such a reaction system will be discussed as it pertains to the screws used in this thesis. Dispersive mixing should be immediate upon introduction of the low viscosity fluid, accomplished by large kneading blocks to transmit high shear stress to the polymer system. The presence of left-handed conveying or kneading elements prior to the injection zone, create a melt seal which isolates the region where the liquid reactants are added and prevents their leakage back towards the feed zone. The high pressure generated due to the melt seal should ensure that maleic anhydride remains in its liquid state above 200°C. Kneading blocks, while beneficial for dispersive mixing, also contribute to distributive mixing due to their inherent high leakage flow (thereby increasing residence time). A typical stagger of 60 or 90° between the lobes has proven to be advantageous for both modes of mixing. To increase residence time and mixing simultaneously, neutral kneading blocks may be used, though such a zone would also increase the required screw torque. A kneading section prior to the zone of liquid

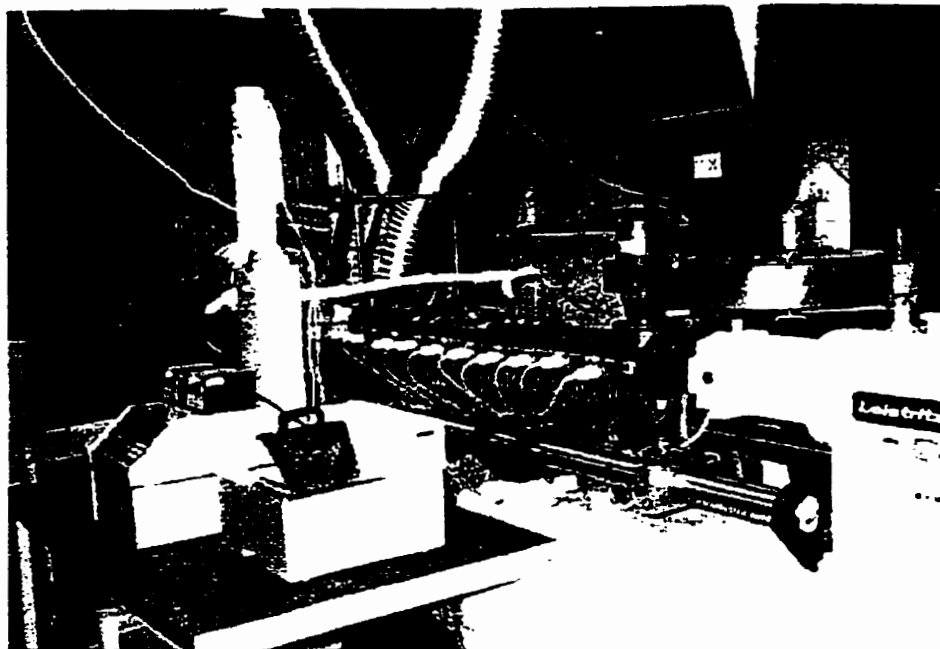


Figure 4.6. Photo of the twin screw extruder setup

introduction, homogenizes the polymer melt stream. Andersen (1997) stated that material flow upstream of a region of low viscosity additive feeding must first be mixed “to allow uniform stress input”.

Including the comb elements, three intensive mixing sections were present in the screw configurations used in this thesis (with the exception of screw configuration 4) to provide the greatest intimacy of contact between maleic anhydride and the polymer melt. Improved intimacy of the reactant was an important consideration due to the inherent immiscibility of the reactant in polypropylene or EPDM. The three mixing sections were not combined into a single section to reduce the occurrence of temperature buildup, though concerns with regards to exceeding the torque limit of the extruder were also a consideration.

No devolatilization section in the extruder was possible due to the low mass flow rate of EPDM and polypropylene melt used (to maximize the reaction time), else the polymer was found to exit preferentially at the vent section.

4.2.5.1. Polypropylene

The three sets of experiments (presented in Tables 7.1-7.3 along with the results) quote a barrel temperature which was uniformly applied to zones 4 through 10. The barrel temperature profile prior to zone 4 was set as 130/170/190°C with the die at 200°C. Temperatures were kept at 230°C and below since Thompson et al. (1998a) observed that reaction temperatures below 240°C ensured dominance of the Alder Ene mechanism with respect to side-reactions like homopolymerization of maleic anhydride or isomerization of the reactive double bond.

Two screw designs were studied (shown in Figure 4.7) which varied the degree of mixing. Measured at 210°C using a carbon black tracer, the minimum residence time for screw configuration 1 varied between 225 s (at 40 rpm, 40 g/min) to 431 s (at 20 rpm, 20 g/min). The second screw design (configuration 2 in Figure 4.7) which was used for the third experimental set (Table 7.3), attempted to increase the degree of channel fill within the intensive mixing regions. The kneading blocks in the second configuration were mostly left-handed opposed to the use of neutral kneading blocks in the first screw configuration. Therefore, the second screw design possessed a greater residence time as well as mixing for the reaction. Screw configuration 2 was used at a fixed screw speed and feed rate of 30 rpm and 30 g/min respectively, resulting in a minimum residence time of 370 s at 210°C.

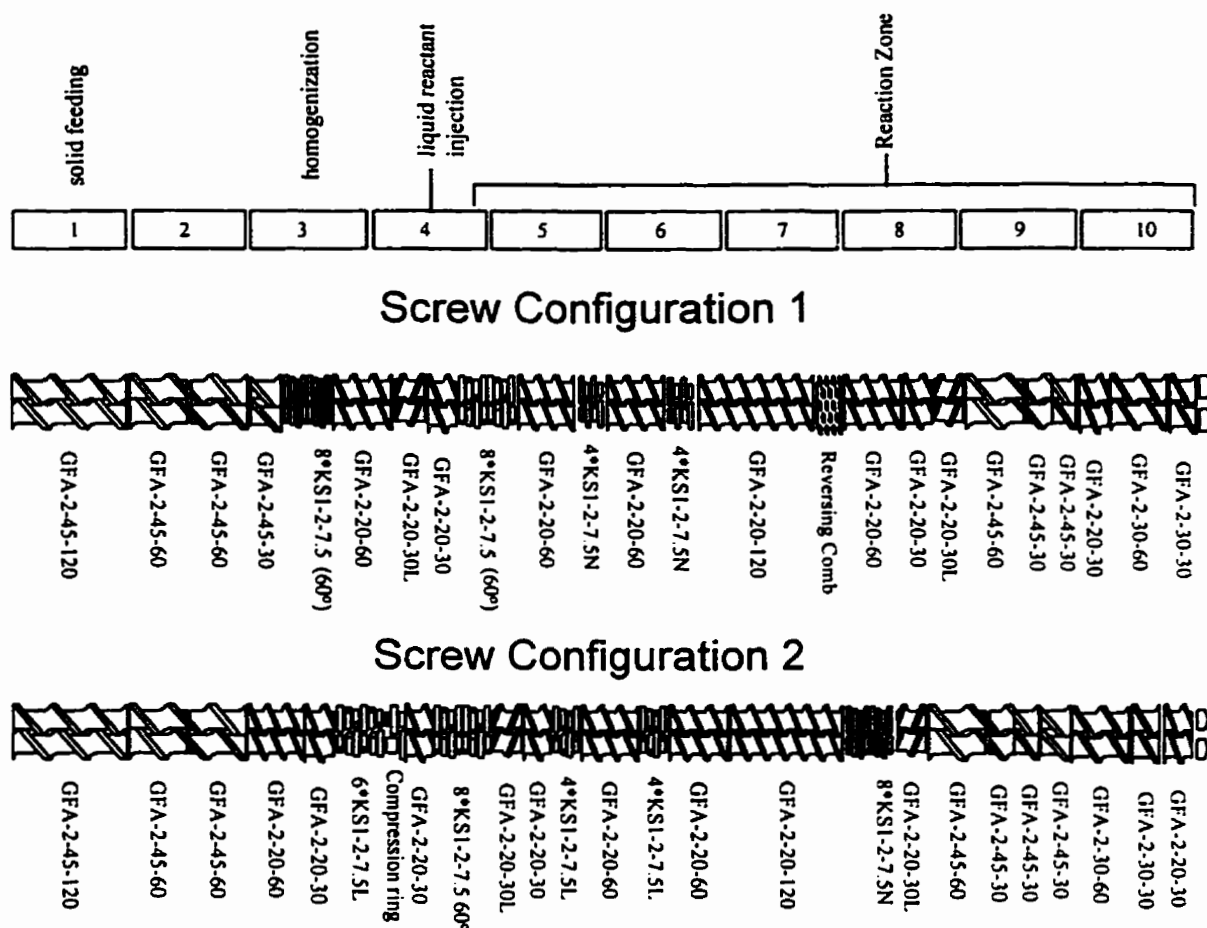
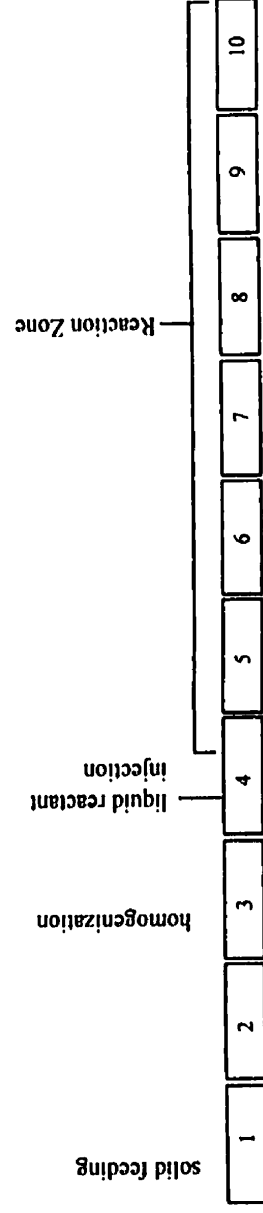


Figure 4.7. Two screw configurations used in the Leistritz co-rotating twin screw extruder. The kneading elements are denoted by KS with the stagger angle of 60° unless the block was designated as neutral (N). Reversing elements are denoted with a L suffix.

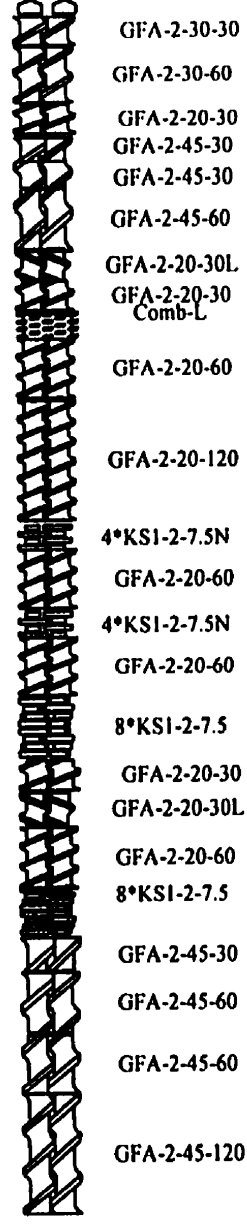
For analysis, a 3 g sample of each product was purified by dissolving into 100 mL boiling xylene followed by precipitation through the addition of an excess of acetone (400 mL) and finally filtered through a fine grade fritted-glass filter. Residual maleic anhydride and poly(maleic anhydride) remained in solution with acetone due to their high solubility. The polymer collected by filtration was washed repeatedly with acetone and finally dried for 16 h at 120°C in a vacuum oven.

4.2.5.2. Ethylene-Propylene-Diene Terpolymer

Two screw designs were studied (shown in Figure 4.8) which varied the degree of mixing. Screw configuration 3 produced extensive dispersive mixing at the kneading blocks and comb elements where the polymer was thought to fill the screw channel and would consequently result in a long residence time. However, with the extruder operating near its maximum torque limit due to the energy required to mix the rubber, the barrel temperature profile had to be set high (270°C), not allowing examination of lower temperatures which



Screw Configuration 3



Screw Configuration 4

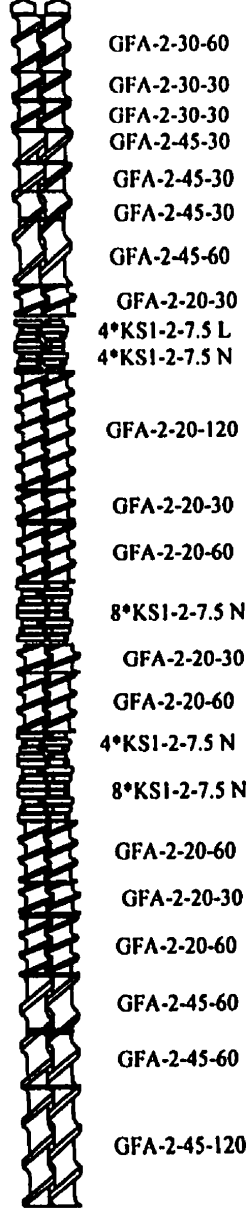


Figure 4.8. Screw configurations: 3) extensive mixing, high torque at the kneading block and comb elements, and 4) conveying with low mixing potential, low torque.

have been found previously to improve the extent of reaction (Thompson et al., 1998a). The high barrel temperature and tendency of the screw design to produce extensive viscous dissipation likely resulted in significant degradation or scorching of the EPDM rubber. Screw configuration 4, shown in Figure 4.8, had a much lower inherent mixing capacity using primarily neutral kneading blocks with only one reverse kneading section and no reverse conveying elements or combs present. The reduced mixing capacity of this screw configuration, allowed the use of moderate barrel temperature profiles and reduced the possibility of polymer degradation. However, the homogeneity of the partially miscible maleic anhydride reactant in EPDM was reduced.

Two sets of experiments (presented in Tables 8.1 and 8.2), one for each screw configuration were run varying several reaction parameters. For the first experimental set, the complete barrel temperature profile was:

Feed	2	3	4	5	6	7	8	9	10	Die
130°C	180°C	240°C	270°C	270°C	270°C	270°C	270°C	270°C	270°C	270°C

The minimum residence time measured using a carbon black tracer, ranged from approximately 350 to 450 s for screw speeds of 30 and 20 rpm respectively. For screw configuration 4, the first three zones were set to 130/150/180°C with the die at 210°C. Zones 4 through 10 were set according to the experimental design in Table 8.2. For the second experimental set, the screw speed and polymer feed rate were fixed at 50 rpm and 25 g/min respectively resulting in a minimum residence time of approximately 300 s (at 210°C).

For analysis, a 3 g sample of each product was purified by dissolving into 200 mL boiling xylene followed by precipitation through the addition of an excess of acetone (800

mL) and finally filtered through a fine grade fritted-glass filter. Residual maleic anhydride and poly(maleic anhydride) will remain in solution with acetone due to their high solubility. The polymer collected by filtration was washed repeatedly with acetone and finally dried for 16 h at 120°C in a vacuum oven.

4.3. CHARACTERIZATION

4.3.1. Colourimetric Acid-Base Titration

The colourimetric titration technique described by Gaylord and Mehta (1982) was used to determine the quantity of anhydride groups bound to the polyisobutylene, polypropylene and EPDM products. Approximately 1.3-1.6 g product was dissolved into a solution consisting of 60 mL xylene with 100 μ L H₂O added to hydrolyze the anhydride. Rondestvedt and Wark (1955) found that free maleic anhydride could be rapidly hydrolyzed while the alkyl-maleic anhydride Ene adducts were unaffected. A similar situation was observed in this work. The presence of water was confirmed to have a negligible effect on the succinyl anhydride peak based on FT-IR analysis. However, for consistency in the measurements, the addition of water was continued, although, reduced to 50 μ L. The solution was refluxed for 1 h to allow the water to evaporate prior to cooling the system. No water must remain in the system prior to cooling due to the immiscibility of water in xylene, since subsequent homogenous division of the solution into three aliquots for titration would not be possible. Once the system reached room temperature, the solution was transferred quantitatively into a 100 mL volumetric flask and topped with xylene. Due to the complete solubility of polyisobutylene and amorphous polypropylene in xylene, the titrations could be

carried out at room temperature compared to the elevated temperature proposed by Gaylord and Mehta (1982), overcoming volatility issues with the alcohol solvents used in the acid and base solutions. Degraded polypropylene and EPDM required the xylene to remain near its boiling point to remain dissolved. Fortunately, the degree of maleation in these products was too small to use titration measurements anyway. Titration of each product was repeated three times using 25 mL aliquots that were compared to a blank. The first 25 mL of solution was lost in order to properly clean the transfer pipet and beaker used for the titration. Three drops of 1% thymol blue in N,N-dimethylformamide (EM Science) and 5 mL 0.05 N standardized ethanolic KOH were added to each aliquot yielding a deep blue solution. Table 4.5. presents the acid/base properties of thymol blue and maleic anhydride. A 0.05 N standardized isopropanolic HCl solution was titrated against the remaining KOH in the system till a sharp end-point was observed with a yellow tint to the solution. In calculations, it was understood that the strong base neutralized both acid functionalities of the dicarboxylic acid which accounted for the 1/2 term in eqn (4.1). The anhydride content attached to the polymer in moles per gram polymer, can be calculated as:

$$[SAh] = \frac{0.5 \cdot C_{HCl} (V_{HCl}^b - V_{HCl}^s)}{\frac{1}{4} M_{polymer}} \quad (4.1)$$

Table 4.5. Acid-base properties of maleic anhydride and thymol blue

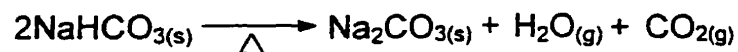
Species	$-\log_{10} K_a$	pH Transitions in aqueous solution
Maleic Anhydride [†]	1.83	~3.7
	6.07	~9.5
Thymol Blue [*]	1.65	1.2-2.8 (Red → Yellow)
	8.90	8.0-9.6 (Yellow → Blue)

[†] Trivedi and Culbertson, "*Maleic Anhydride*", Plenum Press (1982), p.7

^{*} Skoog, West and Holler, "*Fundamentals of Analytical Chemistry*" 5th ed., Saunders College Publishing (1988), p. 184

where V represents the volume of the acid added in litres, C stand for the concentration of HCl in molarity, M was the mass of the polymer in grams and b and s stand for blank and sample respectively. It should be noted that the presence of any poly(maleic anhydride) in the product would complicate analysis since only one of the two carboxyl groups are titratable in the homopolymer as observed (Restaino et al., 1956) with LiOH, NaOH, KOH, or $(\text{CH}_3)_4\text{NOH}$. This may be related to the various structural units observed in poly(maleic anhydride) (see section 2.3).

The isopropanolic 0.05 N HCl solution was standardized using Na_2CO_3 as a primary standard. The $\text{Na}_2\text{CO}_{3(s)}$ was derived from analytically pure $\text{NaHCO}_{3(s)}$ (100.2%, Mallinckrodt Inc.) via thermal decomposition for 1 h at 280°C in a furnace (eqn. below, Skoog et al., 1988).



The potentiometric neutralization of Na_2CO_3 (using an Orion 420A pH meter equipped with a Ag+/AgCl combination probe) yielded two end-points due to the dibasic nature of the species. The sharper second end-point was used to determine the concentration of the acid solution quantitatively. The ethanolic KOH solution was standardized by the newly standardized HCl solution. Both acid and base solutions had to be standardized after three days had elapsed due to concerns over carbonic acid generation via atmospheric CO_2 and solvent losses by evaporation.

4.3.2. Dilution Viscometry

The analysis was performed at 60°C using anhydrous decahydronaphthalene (supplied by Aldrich) as the solvent. A Cannon-Ubbelohde viscometer (Ever Ready Thermometer Co. Inc.) was used for the measurements, heated in a 50 L oil bath containing Dow-Corning 200 silicone fluid (350cSt grade). A Barnant Series 10 propeller and motor assembly was used to circulate the fluid and a custom-made heater/controller unit was used for temperature control. The upper section of the oil bath was divided to avoid vibration from the motor being transferred to the viscometer during the measurements. The supplied conditions provided efflux times greater than 200 s, in accordance with ASTM D2857. The efflux times for three different concentrations between 0.001-0.005 g/mL were measured for each sample product. The intrinsic viscosity was determined by extrapolating the inherent viscosity to zero concentration.

4.3.3. FT-IR Method

The films were characterized at 2 cm^{-1} resolution in a Nicolet 520 FT-IR spectrometer. A sample was scanned 20 times covering a wavenumber range from 500 to 4000 cm^{-1} . Higher numbers of scans were not found to be necessary, since no detectable differences were observed in base-line noise.

4.3.3.1. Polyisobutylene

The low viscosity of the polymer made it necessary to sandwich the samples between a pair of NaCl disks. The absorbance wavenumbers pertinent to the modification were: 890

cm⁻¹ (vinylidene), 1784 cm⁻¹ (anhydride) and 1792 cm⁻¹ (succinyl anhydride). An internal reference peak at 1390 cm⁻¹ (methyl absorbance) was used to account for variance in sample thickness between specimens. Walch and Gaymans (1994) calibrated FT-IR measurements of the anhydride absorbance centred at 1784 cm⁻¹ relative to the backbone absorbance at 1390 cm⁻¹ yielding an anhydride-isobutylene ratio value. The anhydride-isobutylene ratio for their calibration standards, were determined by ¹H NMR. The equation that Walch and Gaymans (1994) generated was,

$$\frac{[anhydride]}{[isobutylene]} = 0.024 \cdot \frac{A_{1784\text{ cm}^{-1}}}{A_{1390\text{ cm}^{-1}}} \quad (4.2)$$

Where A stands for the peak height absorbance of the corresponding subscripted wavenumber. Attempting to confirm equation (4.2), six succinyl-terminated polyisobutylene products were titrated to determine their anhydride-isobutylene ratio. Using linear regression analysis, the slope was determined to be 0.0246 ± 0.0036 (correlation constant, R²=0.86), a very close fit to the slope in eqn (4.2). The equation of Walch and Gaymans (1994) assumed a zero anhydride absorbance ratio in the virgin polymer. Unfortunately, a broad peak centred at 1780 cm⁻¹ found in Glissopal prevented a similar assumption being made for this work. If the regression analysis accounted for this discrepancy, the correlation constant was increased to R²=0.94, with the calibration curve better represented by eqn (4.3) and shown in Figure 4.9.

$$\frac{[anhydride]}{[isobutylene]} = 0.03384 \cdot \frac{A_{1784\text{ cm}^{-1}}}{A_{1390\text{ cm}^{-1}}} - 0.00394 \quad (4.3)$$

The standard errors in the slope and intercept were 0.0057 and 0.00212, respectively. Equation (4.3) was used to determine the extent of reaction taking place for the different

reaction conditions examined in chapter 5. Recall, we are primarily interested in the succinyl anhydride functionality at 1792 cm^{-1} not 1784 cm^{-1} . However, as it will be discovered in Chapter 5, the succinyl anhydride peak was usually centred at 1784 cm^{-1} with only a shoulder (if present) at 1792 cm^{-1} .

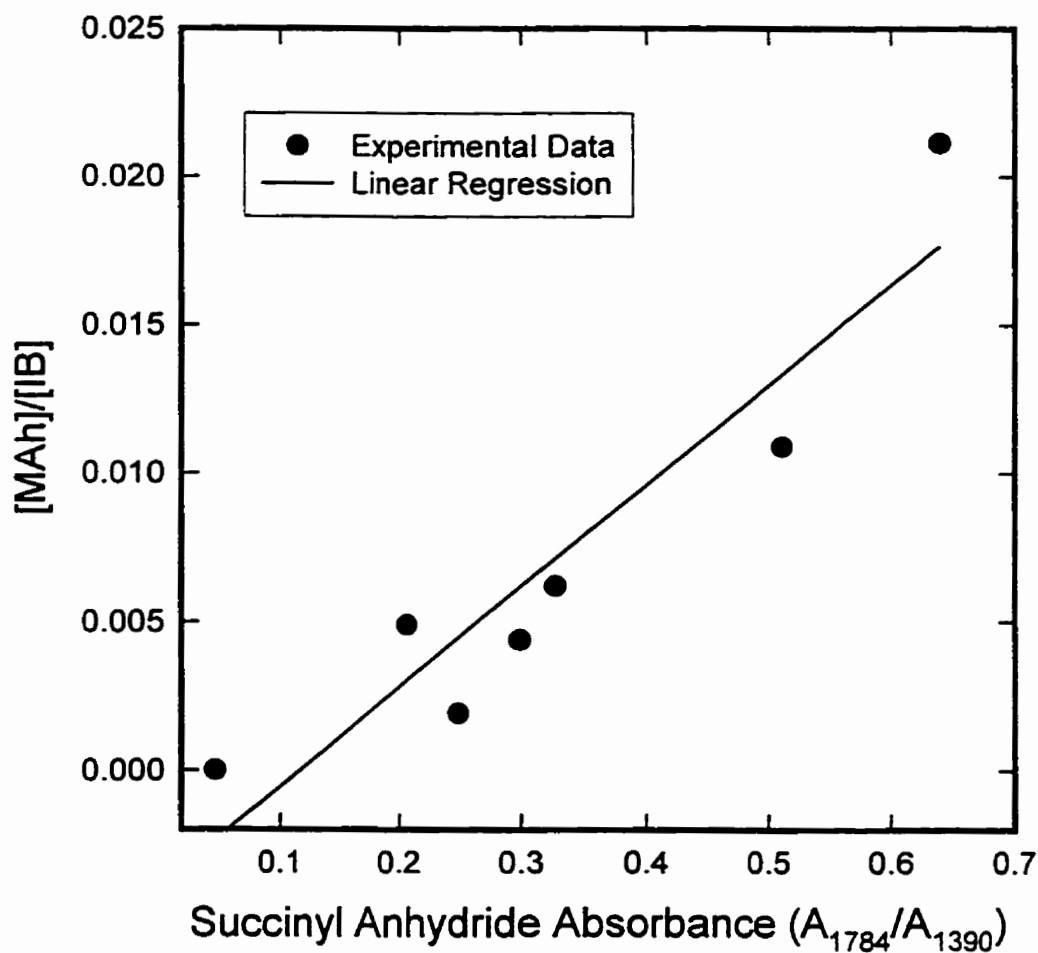


Figure 4.9. Correlation between FT-IR relative absorbance at 1784 cm^{-1} and the concentration of succinyl anhydride bound onto polyisobutylene.

4.3.3.2. Polypol-19

The waxy nature of the polymer allowed for simplified sample preparation by smearing the material on a NaCl disk. The absorbance wavenumbers pertinent to the modification were: 888 cm^{-1} (vinylidene), 1784 cm^{-1} (anhydride), 1792 cm^{-1} (succinyl anhydride), and 1865 cm^{-1} (succinyl anhydride). To determine the kinetics of the reaction, the strong succinyl anhydride peak at 1792 cm^{-1} was used along with an internal reference peak at 974 cm^{-1} , which pertained to the polymer backbone (mixed C-H absorbance). A succinyl anhydride calibration curve (shown in Figure 4.10) was generated by mixing a terminally functionalized Polypol-19 containing a high anhydride concentration ($1.439 \times 10^{-4} \pm 1.020 \times 10^{-5}$ moles anhydride per gram polymer as measured by the titration method of Gaylord and Mehta, 1982), with molten Polypol-19 at various concentrations. Linear regression of the data resulting in:

$$C_{SAh} = 5.12 \times 10^{-5} \left(\frac{A_{1792\text{cm}^{-1}}}{A_{974\text{cm}^{-1}}} - 0.027 \right) \quad (4.4)$$

where C_{SAh} is the concentration (mol anhydride/g polymer) of succinyl anhydride bound to the polymer chain and $A_{1792\text{cm}^{-1}}$ and $A_{974\text{cm}^{-1}}$ are the peak intensities of absorbances corresponding to the succinyl anhydride and internal reference respectively. Linear regression of the data had a covariance constant, $R^2 = 0.99$. The standard error in the calculated slope of the calibration curve was 5.6×10^{-7} mol/g polymer.

The calibration curve was useful in deriving kinetic data so that the activation energy for the Lewis acid catalyzed Alder Ene reaction and its uncatalyzed counterpart could be estimated. The necessity of the calibration curve, aside from its ease of use, was due to the

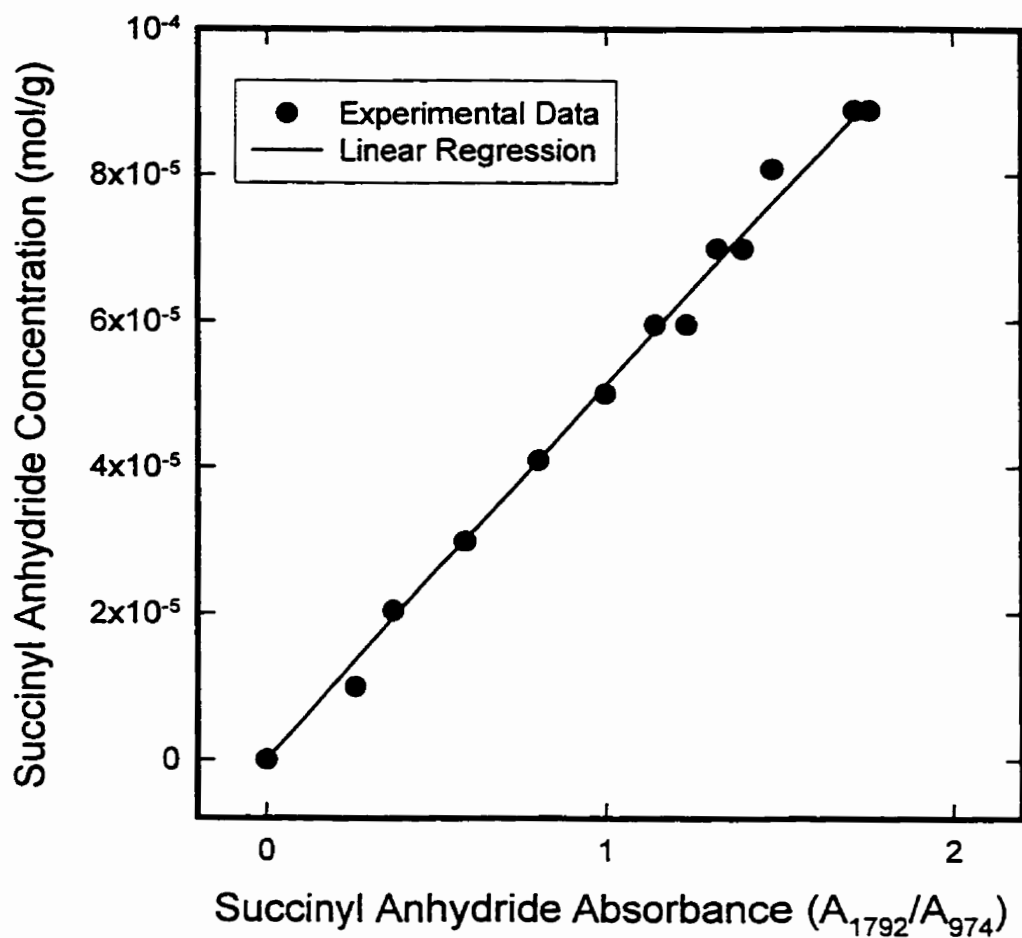


Figure 4.10. Correlation between FT-IR relative absorbance at 1792 cm^{-1} and the concentration of succinyl anhydride bound onto low molecular weight polypropylene.

concentration of anhydride incorporated into the polymer being very low, typically 1-5 mole %. In this instance, the use of acid-base titration was not very informative since the results could never be considered significant above the governing sources of error indicative of titration methods. Infrared spectroscopic methods exhibit greater sensitivity towards very low concentrations of functional groups, making this avenue of analysis quite practical.

4.3.3.3. Polypropylene

Sample films were prepared between two teflon films in a hot press at 170°C under 40 kN force for 5 minutes. The absorbance wavenumbers pertinent to the modification were: 888 cm^{-1} (vinylidene), 1784 cm^{-1} (anhydride), 1792 cm^{-1} (succinyl anhydride), and 1865 cm^{-1} (succinyl anhydride). The C-C-C bending vibration at 459 cm^{-1} was used as an internal reference. Vinylidene concentration in polypropylene was determined using a calibration curve that has been presented previously (Thompson et al., 1997) and shown in Figure 4.11.

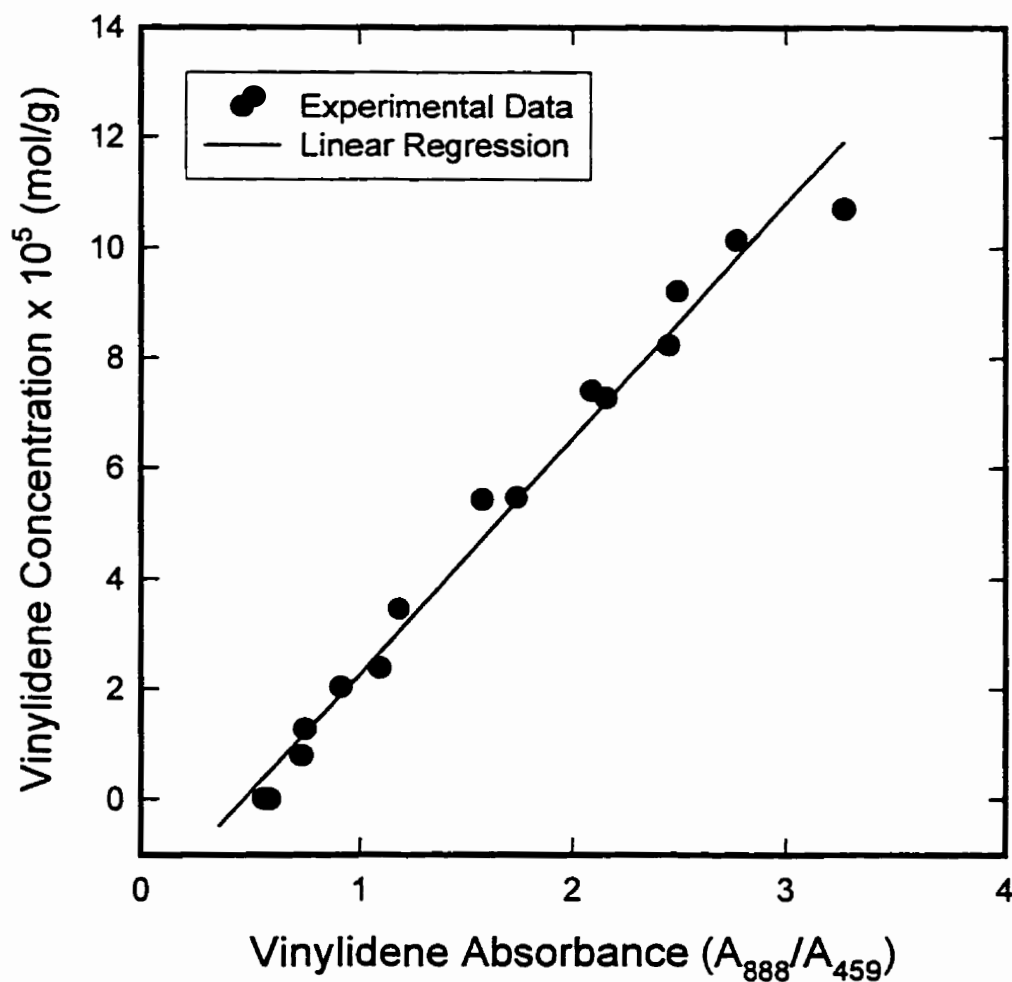


Figure 4.11. Correlation between FT-IR relative absorbance at 888 cm^{-1} and the concentration of vinylidene in KF6100 polypropylene.

Calibration samples were prepared on a single KF6100 film which had been shaped to ensure its positioning in the IR sample holder was consistent. The film of KF6100 did not possess any detectable vinylidene groups. The area of the polypropylene film exposed to the incidence beam of the spectrometer was traced out. Different vinylidene concentrations were made for IR analysis by varying the mass of Polypol-19 smeared evenly within the traced region on the film. Polypol-19 had a known vinylidene content of 2.458×10^{-4} moles per gram polymer, determined by ^1H NMR. The double bond concentration was calculated as,

$$C_{\text{vinylidene}} = \left(\frac{I_{\text{vinyl}}}{2} \right) \left(\frac{6}{I_{\text{propyl}}} \right) \frac{1}{FW_{\text{propane}}} \quad [\text{mol C=C / gr. polypropylene}] \quad (4.5)$$

Equation 4.5 relates the number of vinylidene groups (found by integrating the two characteristic vinyl peaks at 5 ppm, I_{vinyl} , which account for the two terminal protons in the molecule) to the number of propane units (found by integrating those peaks which are characteristic of the polymer backbone in the region of 0.5-1.7 ppm, I_{propyl} , which account for the six protons per repeat unit). The formula weight (FW_{propane}) of the monomeric unit transforms the vinylidene mole fraction calculated from the NMR peak intensities, into a concentration with the units of mole C=C per gram polypropylene. Once all the calibration standards were measured, the polypropylene film was cleaned of Polypol-19 and the traced area was cut out and weighed. Vinylidene group concentrations were calculated based on,

$$\frac{2.458 \times 10^{-4} M_{\text{Polypol-19}}}{M_{\text{Polypol-19}} + M_{\text{traced_PP}}} \quad (\text{mol C=C per gram polymer}) \quad \text{where } M \text{ is the mass of Polypol-19}$$

used. The correlation between the vinylidene group concentration, $C_{\text{vinylidene}}$ (mol C=C per gram polymer) and the relative IR absorbance at 888 cm^{-1} was:

$$C_{\text{vinylidene}} = 4.291 \times 10^{-5} \cdot \frac{A_{888\text{cm}^{-1}}}{A_{459\text{cm}^{-1}}} - 2.030 \times 10^{-5} \quad (4.6)$$

where A is the intensity of the absorbance band corresponding to the subscript wavenumbers.

The standard errors in the slope and intercept were 1.599×10^{-6} and 2.925×10^{-6} , respectively.

A correlation between the succinyl anhydride concentration in the product and its relative infrared absorbance at 1792 cm^{-1} was established using a highly maleated low molecular weight polypropylene wax (Polypol-19, Crowley Chemical) at different concentrations smeared onto a film of KF6100 polypropylene (shown in Figure 4.12) similar

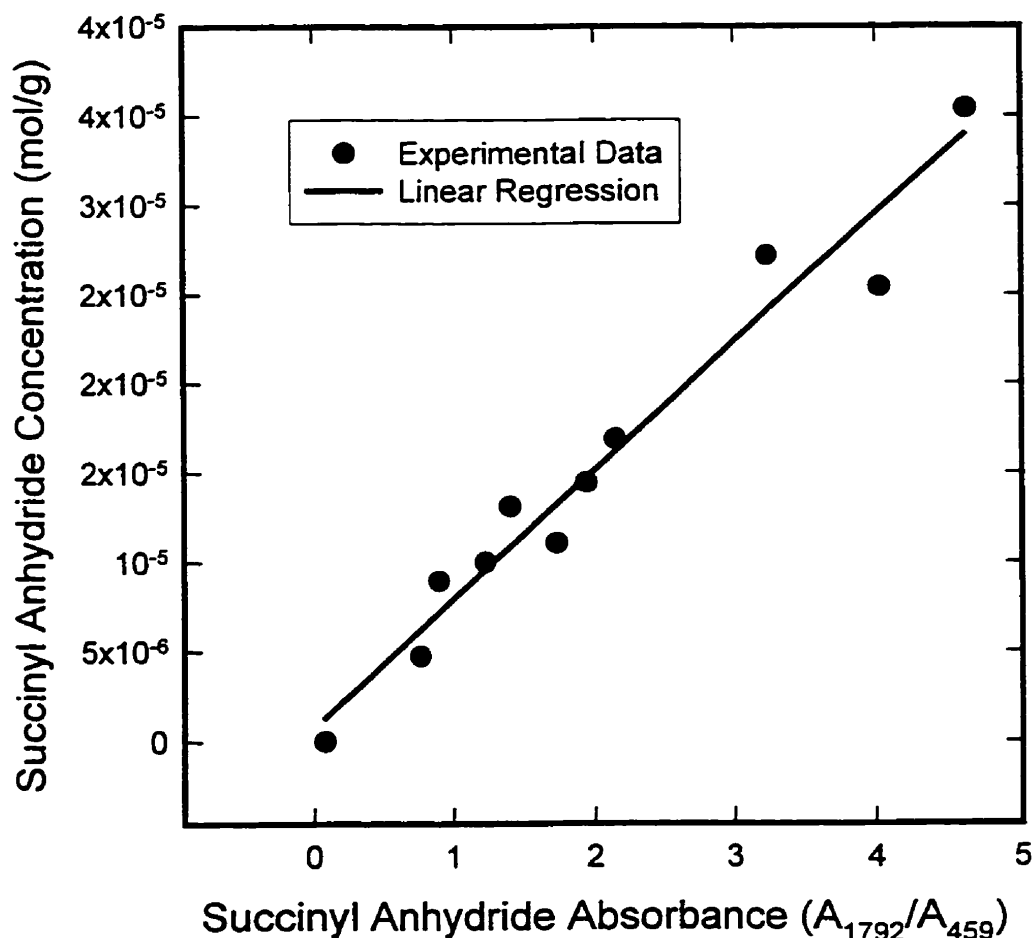


Figure 4.12. Correlation between FT-IR relative absorbance at 1792 cm^{-1} and the concentration of succinyl anhydride bound onto KF6100 polypropylene.

to the manner that the vinylidene calibration samples were prepared. The terminally functionalized Polypol-19 containing a high anhydride concentration ($1.439 \times 10^{-4} \pm 1.020 \times 10^{-5}$ moles anhydride per gram polymer as measured by the titration method of Gaylord and Mehta, 1982), was produced in bulk at 240°C for 16 h under nitrogen and in the presence of hydroquinone. The calibration curve for succinyl anhydride concentration was

$$C_{SAh} = 7.22 \times 10^{-6} \cdot \frac{A_{1792 \text{ cm}^{-1}}}{A_{459 \text{ cm}^{-1}}} + 7.21 \times 10^{-7} \quad (4.7)$$

where C_{SAh} is the concentration of attached succinyl anhydride in moles per gram polymer and A is the peak height absorbance corresponding to the subscript wavenumber. The standard errors for the slope and intercept coefficients were 5.17×10^{-7} and 1.25×10^{-6} respectively and the correlation coefficient was $R^2=0.97$.

4.3.3.4. Ethylene-Propylene-Diene Terpolymer

Sample films were prepared between two teflon films in a hot press at 150°C under a compressive force of 0.13 MN for 5 minutes. A relative peak height absorbance pertaining to the succinyl anhydride attached to the polymer that was observed at 1792 cm^{-1} in the FT-IR spectra, was calculated using the symmetrical methyl bending vibration at 1395 cm^{-1} as an internal reference. The succinyl anhydride concentration attached to EPDM was determined using a calibration curve developed based on calibration standards provided by Uniroyal Chemical. This curve is as follows:

$$C_{SAh} = 125.271 \cdot \frac{A_{1792 \text{ cm}^{-1}} - A_{1930 \text{ cm}^{-1}}}{I_{1395 \text{ cm}^{-1}}} \quad (4.8)$$

where C_{SAB} is the succinyl anhydride concentration in wt %, A is the peak absorbance at the subscript wavenumber and I is the peak area for the absorbance centred at 1395cm^{-1} .

4.3.4. Differential Scanning Calorimetry

Measurement of the thermal transitions were performed using a TA Instruments differential scanning calorimeter (DSC) 2920 cell. For each analysis, approximately 7-12 mg of sample was used for low molecular weight materials (Polypol-19), while only 3-6 mg of sample was possible for the higher molecular weight polymers. Temperature calibration was done using indium ($T_m=156.61^\circ\text{C}$) at the start of each day while base-line calibration was only necessary when the examined temperature range went below 0°C . The temperature ramp rate varied between materials and was dependent on which transition was being measured. For glass-rubber transition measurements, the ramp rate was generally larger to accentuate the change in heat capacity. The increased ramp rate had the effect of inflating the T_g , though, only by 3°C per order of magnitude change in the ramp rate (Eisenberg, 1993).

4.3.4.1. Polypol-19

A temperature sweep between -40°C to 25°C used a ramp rate of $15^\circ\text{C}/\text{min}$. Solid CO_2 was used to cool the instrument cell. To avoid variance in the measurements, no vibration could be tolerated. That meant that the cell could not have more CO_2 added once the instrument heating cycle began, which occasionally resulted in an individual run being discarded due to a complete loss of solid coolant. For reference, the virgin Polypol-19 exhibited a glass transition with an inflection point at -25.36°C . The presence of a small

peak in the thermogram centred at 17.38°C for the heat of fusion indicated that the polymer possessed a low level of crystallinity.

4.3.4.2. Polypropylene

The crystallization temperature and the heat of crystallization (T_c and ΔH_c respectively) were measured to determine the effect of the MAh functionality reacted with hexadecylamine, had on the crystallinity of the polymer. Samples were heated using a ramp rate of 10°C per minute from 30°C to 200°C. Data from the second heating/cooling cycle were collected to determine the transition temperatures. Crystal melting temperature was not used quantitatively since the transition was very broad and difficult to integrate consistently between samples due to a poor base-line.

4.3.4.3. Ethylene-Propylene-Diene Terpolymer

The glass transition temperature (T_g) of EPDM and maleated EPDM samples was measured using the TA Instruments mechanical cooling accessory (a refrigeration unit using ethylene as a coolant). Samples were cooled to -75°C and heated using a ramp rate of 20°C per minute to 150°C. Data from the second thermal sweep were collected and the temperature was determined from the inflection point of the glass transition during the heating cycle. Aside from the measured T_g , the EPDM resin showed a characteristic ethylene fusion peak at 120°C and a broad endotherm at 44°C, which Greco et al. (1987) have attributed to the packing of short ethylene sequences. The glass transition temperature has been observed to decrease in a previous study (Greco et al., 1987) in a linear manner with increasing anhydride functionality due to the increased polarity of the rubber.

4.3.5. ^{13}C NMR Analysis

Carbon-13 NMR analysis was performed on a 300 MHz Bruker AC300E instrument using inverse gated decoupling to circumvent Nuclear Overhauser Effects (NOE). The samples were prepared according to Table 4.6. Pulse width and relaxation times (listed in Table 4.6) were varied hoping to achieve magnetization equilibrium. No spin was required due to the inhomogeneity of the polymer solution; spinning would only broaden the peaks. No lock signal was required to adjust for sample homogeneity, since repetitive scanning was already required to improve the signal-to-noise ratio. The acquisition time was 0.95 s. The

Table 4.6. Operating conditions for carbon-13 NMR

Material	Tube Size (mm)	Solvent and Conc. (wt %)	Pulse Width (μs)	Relaxation Time (s)	Temp. ($^{\circ}\text{C}$)
Polypol-19	5	Benzene- d_6 , 10 wt %	10 (67°)	30	23
Polypropylene	10	TCB*, 20 wt %	4.5 (30°)	15	120
EPDM	10	TCB*, 20 wt %	4.5 (30°)	15	120

* 0.02 wt % Irganox 1010 (Ciba-Geigy Canada Ltd.) stabilized 1,2,4-trichlorobenzene (EM Science).

number of scans collected varied from 2000 for EPDM, to 4000 for polypropylene and 5000 for Polypol-19, all which were stored in a 32 K data size. The number of scans was varied according to the findings of other researchers and due to concerns with respect to damaging the probe over prolonged runs at high temperatures. The spectra spanned 0-210 ppm, anticipating anhydride related peaks in the region of 150-175 ppm. All chemical shifts were referenced to TMS. For ^{13}C studies, peak assignments for maleated polypropylene and maleated Polypol-19 were done as suggested by Busfield and Hanna (1991), Heinen et al.

(1996), and Rengarajan et al. (1990). Carbon peak assignments for EPDM were obtained from several references (Heinen et al., 1996; Kolbert et al., 1996; Lee et al., 1996; Russell and Kelusky, 1988).

4.3.6. ^1H NMR Analysis

The analysis was done on a Bruker AC-300E NMR spectrometer using TMS as the reference. The probe temperature varied from room temperature for Polypol-19 samples, to 100°C for polypropylene and EPDM samples. Each sample was prepared as a 5-10 wt% polymer solution using benzene- d_6 or hexane- d_{14} as solvents for Polypol-19, and toluene- d_8 for degraded polypropylene and EPDM samples. The signal was acquired using a 20 s relaxation delay (Kolbert et al., 1996) for a pulse width of 11.5 μs (90° flip angle). The proton spectra spanned a field of 0-15 ppm. Typically 32-64 scans were accumulated in a 16 K data size. Peak assignments for the maleated polypropylene and Polypol-19 samples were done according to Tessier and Maréchal (1984ab, 1990) and Russell and Kelusky (1988), who examined maleated species with similar structures. Proton chemical shifts for our maleated EPDM do not exist in the literature. Therefore, it was necessary to look for assistance at the work of Russell and Kelusky (1988) who examined the ^1H NMR spectra of grafted maleic anhydride in different conformations on long chain alkanes. The EPDM resonances identified as the polymer backbone came from the work of Chiantore et al. (1994).

4.3.7. Molecular Weight Distribution

The molecular weight of the polypropylene samples was measured using a Waters 150 CV+ high temperature gel permeation chromatograph (GPC) fitted with three Waters Styragel HT6E linear columns. A capillary viscometer in series with a differential refractometer was used to measure the absolute molecular weight of the polymer samples. The instrument used a mobile phase of 1,2,4-trichlorobenzene containing 0.02 wt% Irganox 1010, which was heated to 140°C. The samples were prepared at a concentration of 0.4 mg/mL for high molecular weight polymers and 0.7 mg/mL for degraded materials. The low molecular weights of the amorphous polypropylene and polyisobutylene (based on supplied data), were below the useful range of the columns and, therefore, could not be used in this instrument.

4.3.8. Kinetic Rate Constant Calculations

The simple second-order kinetic model for the autoclave batch reactor, given in equation (4.9), was used to estimate the reaction rate constant. This model is valid provided the mole ratio of the double bonds to maleic anhydride is never exactly unity. The model assumes that all measured anhydrides are attached in a single manner at the specified sites for polypropylene and EPDM. Effects of the catalyst (such as isomerization of the double bond) and any possible adsorption/desorption issues are neglected in this equation

$$kC_A t = \frac{1}{\Theta - 1} \ln \left| \frac{\Theta - X}{\Theta(1 - X)} \right|, \quad \Theta = \frac{C_{B_0}}{C_A} \quad (4.9)$$

where k is the rate constant, C_{A_0} is the initial concentration of double bonds, C_{B_0} is the initial concentration of maleic anhydride reactant and X is the reaction conversion. Conversion was measured as the ratio of the final concentration of succinyl anhydride bound onto the polymer chain over the initial concentration of reactive sites (double bonds). The possible occurrence of the retro-Ene reaction has been neglected in these calculations, and the inclusion of a free radical trapping agent is not anticipated to affect the kinetics of the reaction.

4.3.9. Ionic Cross-linking of Maleated EPDM

It was desirable to determine a correlation between some mechanical property of the maleated EPDM and its succinyl content to provide another measure to support the trends observed by infrared analysis for the effects of the reaction parameters. However, according to Oostenbrink and Gaymans (1992), the melt viscosity of maleated EPDM was unaffected by the grafted anhydride content. Rather, it was dependent on the peroxide concentration. Thus, a method was developed to correlate the anhydride content to the torque measurement in a batch mixer based on the work of Datta et al. (1996a,b) which showed that a relative torque increase resulted from the ionic cross-linking of maleated EPDM rubber. The results from this technique were independent of the extent of chain degradation yet reflected the anhydride incorporation. The energy of mixing could be measured in a torque rheometer during the neutralization of maleated EPDM using zinc oxide as a cross-linking agent and stearic acid as a reaction accelerator. Stearic acid along with water and several other organic acids have all been observed (Caywood, 1977) to accelerate the reaction through their active hydrogen which opens the anhydride ring.

The maleated EPDM was charged into a Haake Rheomix 3000 batch mixer operating at 170°C and 80 rpm. The measured torque was allowed to reach steady state over a 5 minute period. During that time the melt temperature climbed to 195°C. A mixture of 10 phr ZnO and 1 phr stearic acid was added to the rubber and, subsequently, allowed to react for another 5 minutes before the newly formed ionic thermoplastic elastomer was collected. In a method similar to Datta et al. (1996a,b), a relative torque plot, for the time period after the metal salt was added, was calculated using the steady-state torque prior to neutralization as the base-line. Formation of the ionic network was confirmed through FT-IR analysis by the disappearance of the anhydride peak at 1792 cm^{-1} and the emergence of a new peak at 1565 cm^{-1} corresponding to the carboxylate anion (Datta et al., 1996a,b). Confirmation of the interpenetrating network was observed by the insolubility of the elastomer in phenyl solvents which previously dissolved virgin EPDM and its maleated derivatives.

4.3.10. Dynamic Mechanical Analysis

Storage and loss moduli and complex viscosity of the polymer samples were measured on a Rheometrics RMS-605 Mechanical Spectrometer using a parallel plate attachment at 230°C under a nitrogen atmosphere. Sample discs (25 mm diameter and 2.3 mm thickness) were prepared in a hot press at 170°C. The samples were run in the RMS-605 over a frequency range of 0.1 to 100 rad/s under 20 % strain.

CHAPTER 5. PRELIMINARY EXAMINATION OF LEWIS ACIDS IN POLYISOBUTYLENE

5.1. INTRODUCTION

Due to existing thorough characterization studies on the maleation of polyisobutylene via the Alder Ene reaction, it was logical to begin preliminary studies with this material. The similarities in the geometry of the *ene* species of polyisobutylene (i.e. a terminal vinylidene) to that of polypropylene shall prove useful in transferring these results to maleation studies of polypropylene and EPDM in subsequent chapters. With the maleated species being well characterized by FT-IR and NMR spectroscopy (Walch and Gaymans, 1992; Tessier and Maréchal, 1984ab,1990), the difficulties in band assignment were not present, allowing one to confidently study the reaction unencumbered. Using the published works of Walch and Gaymans (1992) and Tessier and Maréchal (1984ab, 1990) as the foundation, preliminary studies into the application of Lewis acids for high temperature Alder Ene reactions were initiated. This chapter examines several of the classical Lewis acids employed as catalysts in the Alder Ene reaction. The Lewis acid species chosen are listed in Table 5.1 along with their chemical properties data.

It was the intention of this study to determine the feasibility of introducing Lewis acids into a high temperature reaction system and to identify the parameters which would promote the catalytic effect.

Table 5.1. Chemical properties of the selected Lewis acid species

Lewis Acid	Formula Weight (g/mol)	Melting Point (°C)	Boiling Point (°C)	Density (g/mL)	Compatible solvents*	Physical State (25°C)†
AlCl ₃	133.34		190	2.44	H ₂ O, al., chl., CCl ₄ , eth, bz.	Wh/yl powd.
SnCl ₂ •2H ₂ O	225.63	38	652	2.71	al., eth., acet., glac. ac.	wh powd.
SnCl ₄	260.50	-33	114	2.23	eth.	Clr liq.
TiCl ₄	189.69	-25	136	1.73	HCl, al.	Yl liq.

* al=alcohol; chl=chloroform; eth.=diethylether; bz=benzene; acet=acetone; glac. ac.=glacial acetic acid

† wh=white; yl=yellow; clr=clear; powd=powder; liq=liquid

Data taken from the CRC Handbook of Chemistry and Physics, 61st Ed., CRC Press, Cleveland (1981)

5.1.1. Alder Ene Product

The Alder Ene product, prepared in the absence of a catalyst, was analyzed to provide a comparison with the catalytic products generated in this chapter. The reaction was allowed to proceed for 4.5 hours at 227°C. The system was exposed to air instead of an inert atmosphere to: i) reduce vaporization of maleic anhydride due to the flow of nitrogen across the surface of the reaction, and ii) enhance the free radical trapping nature of hydroquinone due to the presence of oxygen (Flory, 1953). The maleic anhydride reagent was added at 1.8 mole equivalence with respect to the vinylidene concentration. Initially, the reaction mass was yellow with the addition of the comonomer (maleic anhydride) and subsequently darkened over time. The presence of black solid upon conclusion of the reaction indicated the presence of poly(maleic anhydride), as observed by Walch and Gaymans (1992) and Tessier and Maréchal (1984b, 1990). The black solid was confirmed by FT-IR analysis to be poly(maleic anhydride) with a broad peak absorbance at 1780 cm⁻¹, spanning 1810 cm⁻¹ to

1760 cm^{-1} . The dark colouring of the final product and the extent of poly(maleic anhydride) was dramatically decreased when hydroquinone was present (1 wt %).

Characterization of the product was achieved by FT-IR spectroscopy and acid-base titrimetry. Figure 5.1 compares the FT-IR spectra of the virgin Glissopal 1000 polyisobutylene and the Alder Ene product in the wavenumber region of 700-2000 cm^{-1} . The vinylidene region of the spectra, 886-892 cm^{-1} , showed a decrease in absorbance from the virgin material to the product. Since the vinylidene isomer of the double bond was a feasible product of the reaction (a pendant vinylidene), it was not possible to use this functional group to determine the extent of reaction. This argument will come up repeatedly within this thesis,

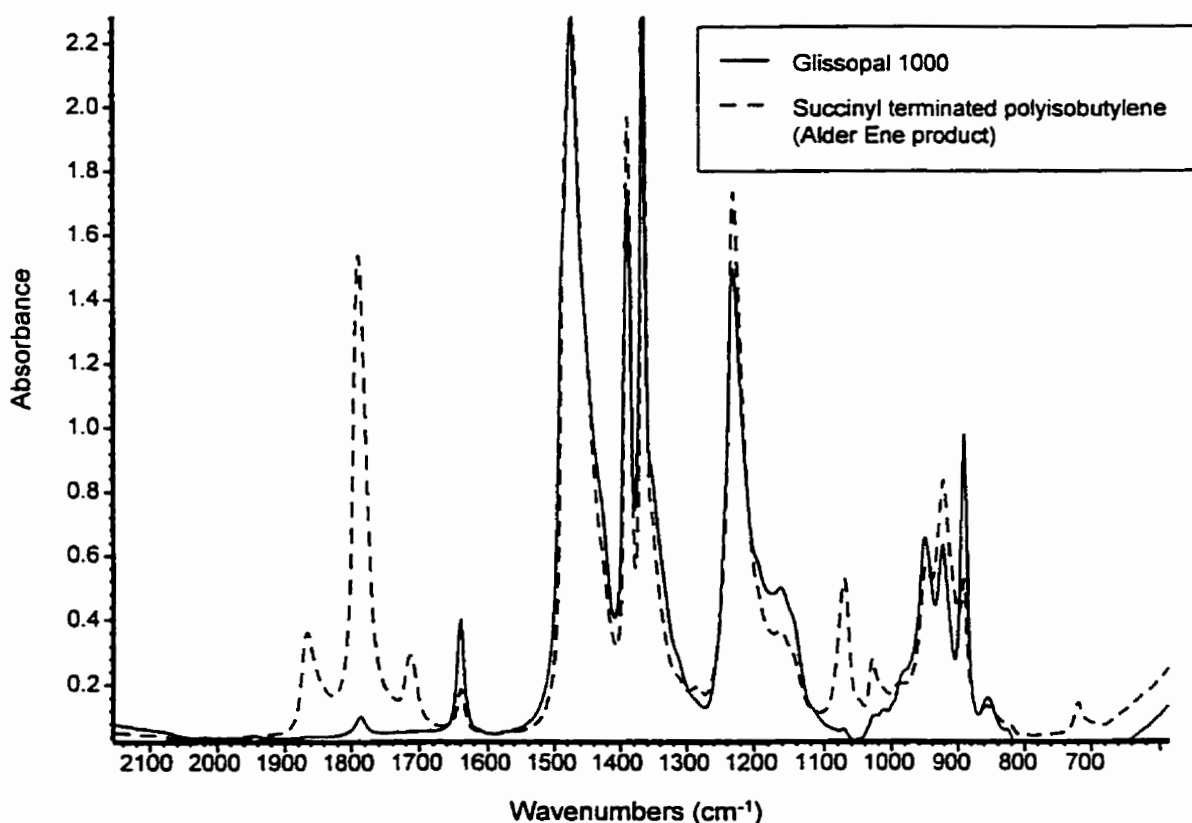
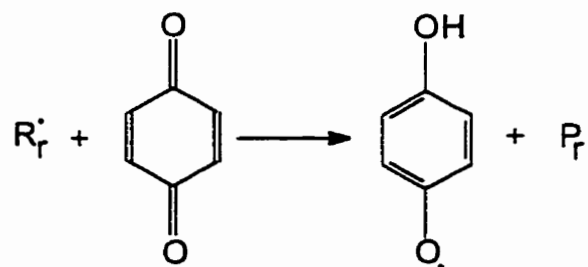


Figure 5.1. FT-IR spectra of Glissopal 1000 (polyisobutylene) compared to the succinyl terminated Ene product

and although one would expect this new pendant vinylidene to produce different vibrations, there were not studies in the literature to support a different peak assignment nor any new peaks in the polymer (at least not observable from the polymer backbone bands). The terminal succinyl anhydride attached on the product, yielded a broad absorbance in the infrared spectrum ranging from 1750-1814 cm^{-1} and centred at 1790 cm^{-1} . Most likely, the breadth of this peak included the presence of poly(maleic anhydride) grafts (1772 and 1780 cm^{-1}) and backbone anhydride incorporation (1784 cm^{-1}) due to the inevitable generation of free radicals at the elevated reaction temperature and in the presence of oxygen. Considering the possibility of free radical reactions occurring in spite of the presence of a free radical trapping agent such as hydroquinone, required an understanding of the chemistry of inhibitors.

The mechanism by which hydroquinone traps radicals depends on the generation of a quinone, a species produced via oxidation (Flory, 1953). In the quinone form, the free radical trapping agent undergoes a chain transfer reaction with a radical, most likely a macroradical (shown below):



where R_r^\cdot represents a living macroradical of chain length r and P_r represents a dead polymer of chain length r . The consumption of hydroquinone exhibits zeroth-order kinetics according to Flory (1953), indicating independence in concentration. However, due to the typically low

concentration of the radical trapping agent employed, not all free radical species present may be consumed. Also the quinone radical is not completely inert once formed. Therefore, some maleic anhydride will likely participate in grafting reactions instead of the Alder Ene mechanism. Once the inhibitor has been completely consumed, free radical reactions may proceed unabated. For an inhibitor species, a nitroxyl radical species would be preferential due to its regenerative nature (discussed in Chapter 2 and employed in subsequent chapters).

Titration of the Alder Ene product showed that there was 36.92 ± 1.41 mole percent incorporated anhydride. That value translates into an anhydride-isobutylene mole ratio of 0.0211, which compares closely with the infrared-determined anhydride-isobutylene ratio of 0.0197. After 4.5 hours, only 30 % conversion of the vinylidene groups to succinyl anhydride groups was obtained. Clearly, the Alder Ene reaction proceeds at a slow rate compared to typical reactions employed in reactive extrusion. Hence, the motivation to examine Lewis acids as catalysts in the reaction.

5.2. EXAMINING THE EFFECTS OF VARIOUS LEWIS ACIDS

This examination looked at the Lewis acids (SnCl_4 , TiCl_4 , and AlCl_3) classically employed in the Alder Ene reaction.

5.2.1. Stannic Chloride

A preliminary experiment with stannic chloride made use of 1 mole equivalence of the Lewis acid with respect to maleic anhydride for the same temperature as the Alder Ene product but for a reaction time of only one hour. The yellow colouring observed upon addition of maleic anhydride turned gray, almost clear, with the addition of stannic chloride

indicating rapid formation of the anhydride-Lewis acid adduct. After one hour of reaction, the system had become reddish brown with a large quantity of black poly(maleic anhydride) particulate observed on the bottom of the reactor. Through FT-IR analysis, conversion was estimated at 19 %, although the anhydride peak was shifted from 1790 cm^{-1} to 1784 cm^{-1} , possibly due to oligomeric or polymeric maleic anhydride grafted onto polyisobutylene or the Lewis acid remained adducted to the anhydride oxygen. The breadth of the anhydride absorbance spanned a range of wavenumbers from 1760 cm^{-1} to 1820 cm^{-1} which likely included any or all of the possible attached anhydride geometries (i.e. succinyl anhydride, and oligomeric and polymeric anhydride chains including their ketoolefin, and cyclopentanone forms). An absorbance at 1730 cm^{-1} , which was not seen in the non-catalyzed Alder Ene polymer from section 5.1.1, could be attributed to one of two sources: i) oxidative degradation due to the hydroquinone presumably being consumed by the Lewis acid, or ii) complex formation between the Lewis acid and anhydride species (shown in Figure 5.2) which was not removed by purification. The lack of a carboxylate absorbance ($\sim 1560\text{ cm}^{-1}$) in the spectrum of the sample produced in the presence of SnCl_4 tended to dismiss the probability of the latter reasoning for the peak at 1730 cm^{-1} . In spite of the low conversion, nearly complete consumption of the vinylidene group occurred, presumably

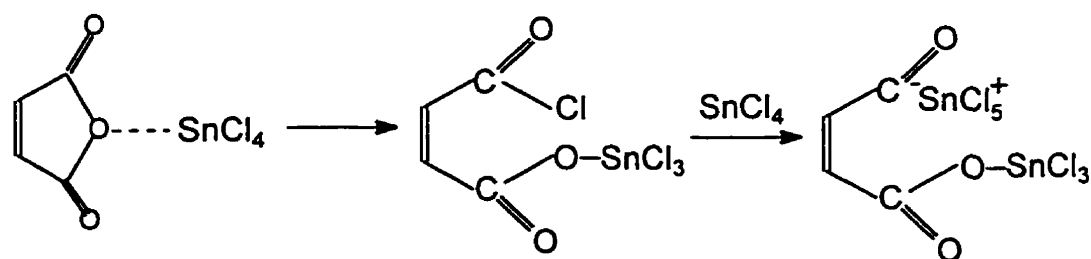


Figure 5.2. Proposed ring opening in the presence of a Lewis acid.

through isomerization at the elevated temperature. The observation of fumes upon addition of the Lewis acid pointed to the likelihood of isomerization via hydro-chlorination of the double bond. FT-IR analysis of a similar experiment performed in only 5 minutes, revealed 1.63 % conversion while the vinylidene group concentration had decreased to 50% of its initial value. Based on these findings, the use of strongly Lewis acids which evolve substantial quantities of HCl at elevated temperatures was evidently counterproductive since the rate of isomerization appeared to be considerably greater than the rate of the non-catalyzed Alder Ene reaction. To overcome these complications, it was necessary to examine Lewis acids with milder acidic properties and at lower concentrations, firstly to reduce isomerization and expense and secondly to demonstrate the catalytic nature of the Lewis acid which till this point had not be explored.

A 2² factorial screening experiment was performed to determine where the operating window must lie for the reaction. The reaction duration was 5 minutes, with temperature (166°C and 207°C) and SnCl₄ concentration (0.05 and 0.005 mole-eq. with respect to maleic anhydride) used as reaction parameters. FT-IR spectra of the four samples produced are shown in Figure 5.3. The succinyl anhydride concentration (in mol %) in each polymer was estimated from these spectra by applying equation (4.3) to the maximum peak absorbance (~1784 cm⁻¹) of each sample. The infrared estimated SAh concentrations and their standard deviations are listed in Table 5.2 (values in brackets are from titration data). The titration

Table 5.2. Effect of Temperature and Catalyst Concentration on SAh Content*

	0.005 mol-eq SnCl ₄	0.05 mol-eq. SnCl ₄
166°C	0 (0)	6.5±0.1 (3.4±0.1)
207°C	11.9±0.1(12.0±0.4)	21.1±0.2 (19.4±2.9)

* SAh=succinyl anhydride, concentration measured in mol %

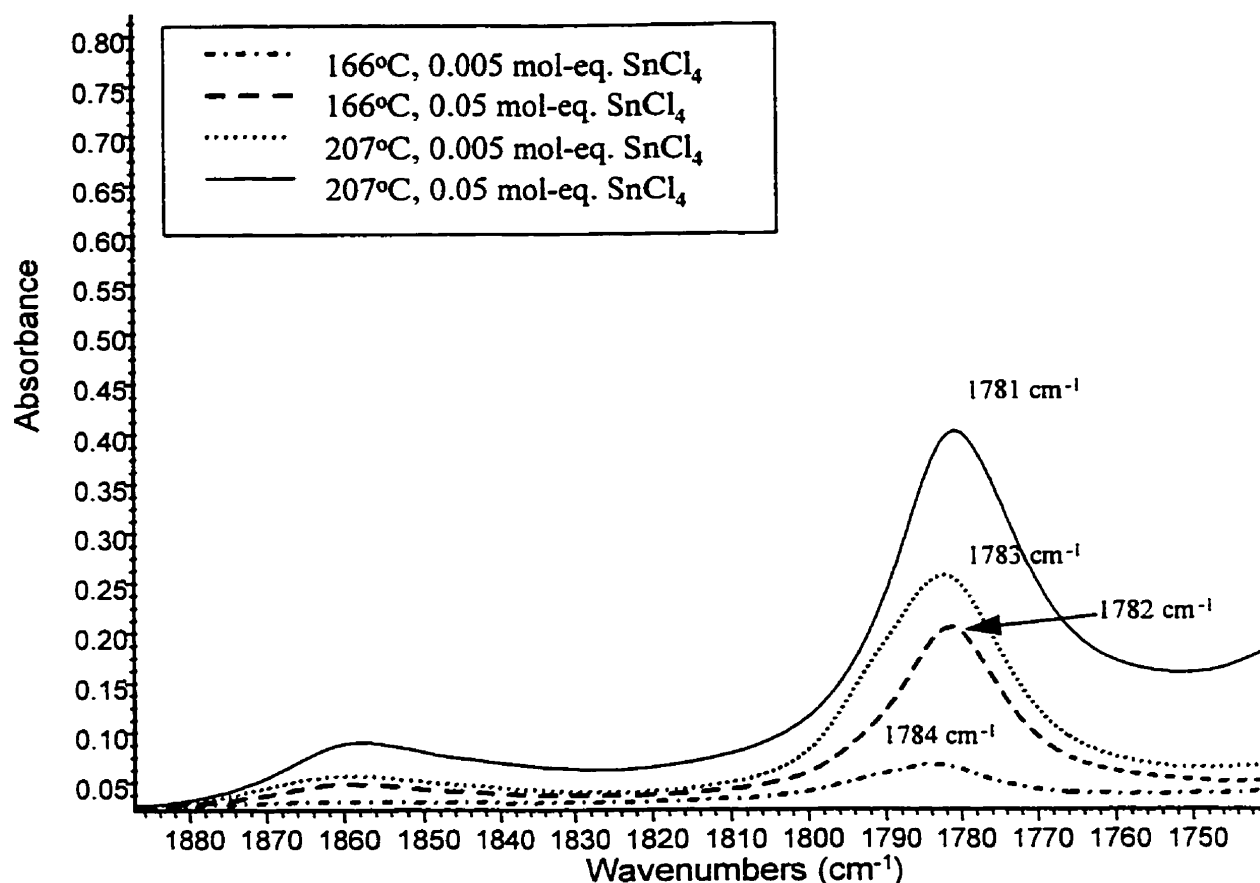


Figure 5.3. FT-IR spectra of a series of maleated polyisobutylenes produced by varying the temperature and catalyst concentration in the reaction (peak wavenumber included).

data increasingly deviates from the infrared measurements as the anhydride concentration drops below 10 mol %. The results indicate that the greater the temperature, the greater the extent of reaction. The findings demonstrated the applicability of the Alder Ene reaction in reactive extrusion. The effect of the catalyst concentration was much more complex. Reactions using 0.05 mole-eq. SnCl_4 yielded higher anhydride concentrations, however, the peaks were centred at 1783-1780 cm^{-1} . Using the lower concentration of Lewis acid, broadened the anhydride absorbance and introduced a distinct shoulder at 1792 cm^{-1} (which was the vibration of concern).

Quantitative analysis of the relative absorbance at 1792 cm^{-1} indicated that both samples produced at 207°C had the same extent of reaction. Unfortunately, this result may not be correct since spectroscopic analysis of polymers in general produces peak broadening for both infrared and NMR techniques. Interpreting the degree of succinyl anhydride incorporation onto polyisobutylene for the high catalyst concentration to be the same as the low concentration, in spite of the lack of a distinct absorbance peak, may be erroneous. However, no means of overcoming this resolution problem availed itself and, NMR which should give better resolution, did not appear to be analytically useful for the concentration of functionalities we sought to examine. This type of error will likely be prevalent throughout this thesis.

5.2.2. Titanium Chloride

Few experiments were actually done with titanium chloride as a catalyst due to the high reactivity of the species. A reaction was performed at 227°C in a similar manner to the Alder Ene product in section 5.1.1, employing titanium chloride at 1 mole equivalence with respect to maleic anhydride reactant. Upon addition of the Lewis acid, the system immediately turned dark brown, followed by rapid evolution of white fumes and excessive foaming of the polymer causing it to spill from the reactor. The reaction was rapidly terminated.

A second reaction was attempted by first adding 0.5 mole-eq. TiCl_4 into molten maleic anhydride (60°C). Once fuming had ceased, the reactant solution had gone from clear to pink in colour. The solution was added to the bulk system of polyisobutylene and allowed to react for 1 h at 190°C . No black particulate was observed immediately, however, over

time poly(maleic anhydride) was generated. The end product possessed only a very small concentration of succinyl anhydride, corresponding to 1.44 % conversion. The majority of the anhydride groups exhibited vibrations at 1780 cm^{-1} suggesting grafted polymeric or oligomeric maleic anhydride chains. Isomerization was prevalent, similarly to those reactions using stannic chloride, with the vinylidene concentration decreasing by 33 % over the duration of the reaction.

Clearly, titanium chloride was too reactive as a Lewis acid species to be useful at elevated temperatures. In addition, its high toxicity and moisture-sensitivity determined that this Lewis acid was not useful for our reaction system.

5.2.3. Aluminum Chloride

A reaction of polyisobutylene with maleic anhydride at 190°C was intended to contain 1 mole equivalence of AlCl_3 with respect to maleic anhydride. However, upon generation of yellow fumes with the graduated addition of the catalyst, only 0.06 mole equivalence of AlCl_3 was finally added. After allowing the reaction to proceed for 1 h, the product appeared dark brown with black particulate at the bottom of the system. Figure 5.4 shows the FT-IR spectrum of the non-catalyzed Alder Ene product with maleated polymers produced in the presence of stannic chloride and aluminum chloride. Examining the infrared spectrum of the aluminum catalyzed product, revealed a strong anhydride absorbance at 1784 cm^{-1} similar to the maleated polymer produced in the presence of stannic chloride. However, for the aluminum catalyzed material, a distinct shoulder was also observed at 1792 cm^{-1} indicating that a terminal succinyl anhydride group was also generated similar to the non-catalyzed Alder Ene product, along with the anhydride groups proposed in section 5.2.1.

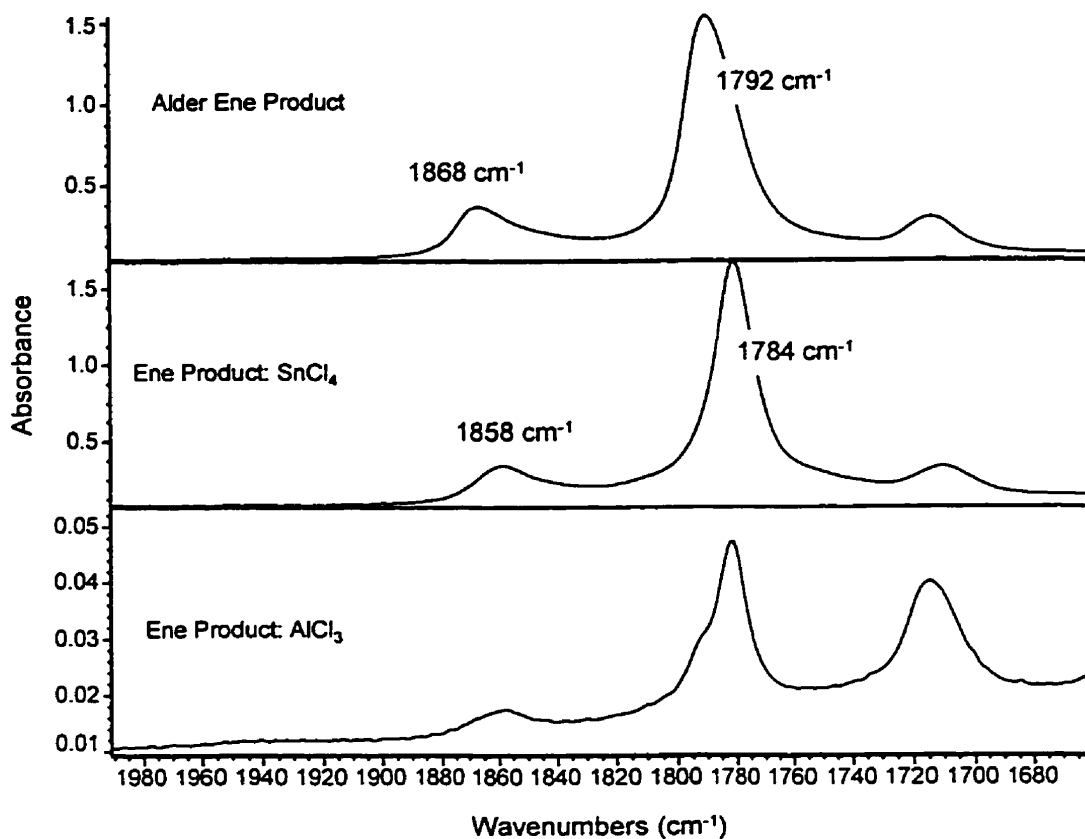


Figure 5.4. Comparing the anhydride absorbance peak in the region of carbonyl stretching vibrations

5.3. PRESENCE OF HYDROQUINONE IN THE CATALYZED REACTION

The possibility of an interaction between hydroquinone and a Lewis acid had not been considered initially. During an experimental set of runs employing stannic chloride, two concurrent reactions under identical conditions were initiated, yet only one received a fresh addition of hydroquinone immediately prior to the addition of maleic anhydride and the Lewis acid. The system with new hydroquinone exhibited a reddish-brown colouring upon completion of the reaction after 5 minutes, while the other system (where presumably the hydroquinone was consumed while attempting to heat the polymer to the desired reaction temperature) remained yellow in color.

To test the possible interaction of the Lewis acid with the inhibitor, hydroquinone (which appears as a white, crystalline solid) was introduced into two test tubes at room temperature followed by the addition of one of the two liquid Lewis acids examined in this study, either titanium chloride or stannic chloride. In the case of TiCl_4 , the reaction with hydroquinone was rapid with excessive fuming, leaving a dark red solid in the test tube. For SnCl_4 , the system appeared to be less reactive with regards to the evolution of fumes and the solid first turned yellow and only after a period of 10 minutes was there an indication of the solid turning dark red. These observations indicated that the hydroquinone used as an inhibitor in our system, was not inert to the reactants of the reaction. Based on Kurbanova et al. (1996) (discussed in section 2.6), it is also likely that in the presence of a Lewis acid, hydroquinone and maleic anhydride will react together. However, explaining the inclusion of the phenyl species into the polymer that was observed by FT-IR, will be addressed in the next chapter.

Since the majority of free radical trapping agents are phenyl based (eg. hydroquinone, 2,2'-di(p-hydroxyphenyl)propane, benzoquinone, butyl catechol), finding an effective species for our catalyzed Alder Ene reaction was difficult. Alternative thiol- or phosphorus-based species were also undesirable due to their suspected interference with the reaction (Smith, 1994). One chemical species, a derivative of the hindered amine light stabilizer family, TEMPO, which is a stable free radical nitroxide is examined in Chapter 6 and employed in all non-polyisobutylene experiments. Prior to using TEMPO, it was considered informative to examine the effects of dimethylformamide (DMF) and magnesium oxide (a Lewis base suggested by Coran and Patel (1983) as an acid scavenger) on the structure of the product.

The two reactions were performed at 207°C for 5 minutes, using 0.05 mole eq. SnCl₄ as a catalyst, with either DMF or MgO and they were compared to a run done in the absence of any additive species. Both reactions employing an additive species, exhibited peak broadening with a distinct shoulder at 1792 cm⁻¹ (unlike the sample with no additive), and with the anhydride peak still centred at 1784 cm⁻¹. Table 5.3 presents the relative peak absorbances for the anhydride and vinylidene group, including product appearance information. The ratio of 1792 cm⁻¹ to 1784 cm⁻¹ was greatest with the use of DMF which interfered with the homopolymerization of maleic anhydride, providing evidence that the 1784 cm⁻¹ was an indicator of an undesirable side reaction to the Alder Ene mechanism. The presence of MgO did not appear to reduce the degree of isomerization occurring. Based on the vinylidene measurements in Table 5.3, the use of DMF appeared to not only interfere with the mechanism for homopolymerization, but also affected the Lewis acid. It is possible that DMF was adducting with the metal.

Table 5.3. Effect of additives on the Alder Ene reaction

	No Additive	MgO Additive	DMF Additive
Product appearance	dark brown	Yellow	light brown
Relative succinyl absorbance	0.47	0.29	0.09
Relative vinylidene absorbance	0.20	0.17	0.34

5.4. METHOD OF ADDITION

The catalyst must complex with the maleic anhydride prior to the reaction with the vinylidene, so that the energy barrier for the desired mechanism is lowered. To better assist the formation of the complex, speed up the Ene reaction, and reduce polymer degradation/

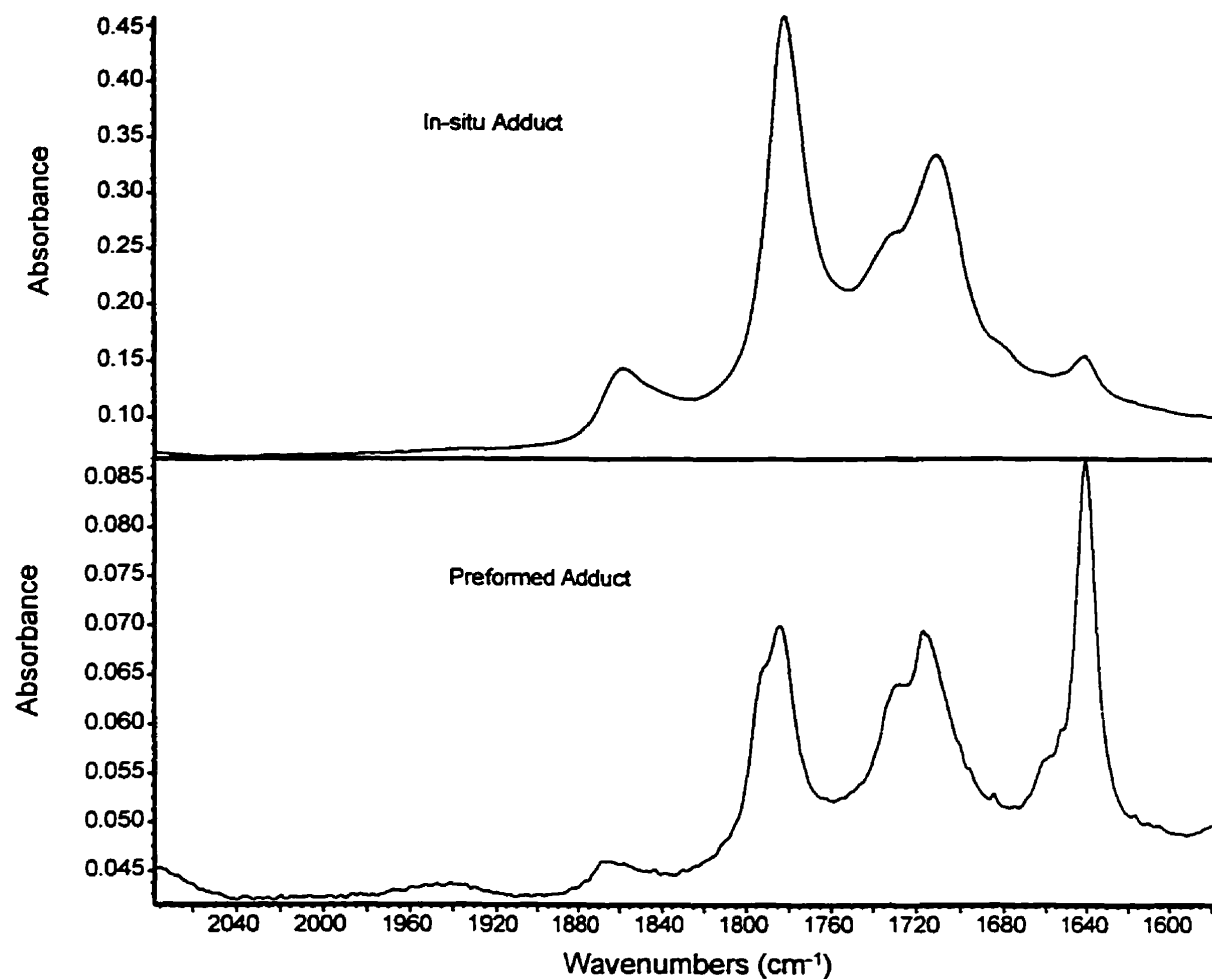


Figure 5.5. FT-IR spectra of two maleated polyisobutylenes in the region of the anhydride absorbance, comparing the effect of the method of enophile formation.

isomerization due to free acid being present within the system, it was proposed that the reactive species (*enophile*) be formed prior to its addition to the polymer. To do this, maleic anhydride was heated to 70°C and with the addition of the Lewis acid (SnCl_4) to the solution, it was allowed to stand for 2 minutes. Two reactions were carried out for 5 minutes at 207°C for comparison. One reaction used in-situ formation of the Lewis acid-anhydride adduct while the second system employed the pre-formed adduct. Figure 5.5 shows the FT-IR spectra of the two reaction products in the region of 1550-1980 cm^{-1} . The peak at 1650 cm^{-1}

corresponds to the stretching vibration mode of the vinylidene group, showing the difference in the two products in terms of the extent of reaction. The reaction employing a pre-formed adduct showed only a small reduction of the vinylidene group with the distinct anhydride absorbance present at 1784 cm^{-1} with a shoulder at 1792 cm^{-1} . The estimated conversion for the pre-formed reaction was 1.16 %. For the reaction that formed the enophile in-situ, the anhydride peak was comparatively large indicating 16.94 % conversion, though it was centred at 1783 cm^{-1} and lacked a 1792 cm^{-1} shoulder. The different scales used to display the anhydride region of the spectra properly for the two samples, made the in-situ polymer appears to have consumed all its vinylidene groups, yet the relative absorbance (A_{888}/A_{1390}) values were 0.17 and 0.20 (standard deviation was 0.01 for both values) for the pre-formed and in-situ reactions respectively (initial relative absorbance was 0.65 for the polyisobutylene vinylidene).

Therefore, the in-situ sample consumed a similar number of vinylidene groups compared to the pre-formed sample, and was determined to possess a similar concentration of bound succinyl anhydride compared to the SnCl_4 -catalyzed Alder Ene reaction that was carried out for 1 hour at a higher temperature. This may suggest that in the absence of a pre-formed adduct, homopolymerization of maleic anhydride would not be excluded from the reaction. Clearly, the rate of poly(maleic anhydride) growth was significantly greater than the non-catalyzed Alder Ene reaction. Although impossible to determine from this data, it seems likely that the grafted oligomeric or polymeric maleic anhydride chain proceeds through a free radical mechanism opposed to the Alder Ene attachment at the terminal vinylidene site. That would account for the vinylidene concentration being greater within the in-situ reaction since free radical grafting reaction have been observed to not react with sites

of unsaturation. A detailed kinetic study of in-situ versus pre-formed Lewis acid-anhydride enophiles shall be made in Chapter 6, and the remainder of the thesis will employ the pre-formed method. Interestingly, it will also be revealed in later chapters that the presence of a Lewis acid appeared to interfere with the ability of maleic anhydride to participate in free radical reactions including homopolymerization.

5.5. CONCLUDING REMARKS

It appeared that stannic chloride was more effective as a catalyst compared to TiCl_4 or AlCl_3 at high temperatures due to its reduced acidity, yet its acidity was still too high resulting in extensive isomerization of the vinylidene group. This Lewis acid species was also considered to be too toxic when considering health implications for an extrusion setup. It has been observed that isomerization and homopolymerization exhibited greater rates of reaction than the Alder Ene synthesis, therefore optimization of the reaction parameters shall be important to the subsequent work. The Lewis acid exhibited improved terminal succinyl anhydride incorporation at lower concentrations especially when the acid was adducted with maleic anhydride prior to the reaction (a pre-formed enophile). Phenyl-based inhibitors such as hydroquinone were identified as susceptible species to the Lewis acid employed in the reaction. Therefore, other sources of free radical trapping agents have to be sought. While MgO proved to be ineffective in preventing isomerization, DMF was useful for interfering with the polymerization of maleic anhydride. However, DMF may also slow the rate of a Lewis acid catalyzed reaction by adducting irreversibly to the metal centre.

Reviewing the different Lewis acids considered thus far, the weaker stannous chloride dihydrate Lewis acid is considered for future experiments. Hopefully the reduced acidity of

the species and its lower sensitivity to moisture will prove useful for high temperature maleation of polypropylene and EPDM via the Alder Ene reaction.

CHAPTER 6. MALEATION OF LOW MOLECULAR WEIGHT POLYPROPYLENE VIA THE ALDER ENE REACTION: CHARACTERIZATION AND PARAMETRIC STUDY

6.1. INTRODUCTION

Several different Lewis acids, (SnCl_4 , TiCl_4 , AlCl_3) were examined for the Alder Ene reaction using polyisobutylene (Chapter 5). However, the presence of HCl fumes often accompanied the addition of these catalysts to the reactor and black poly(maleic anhydride) particulate was observed in the product. A less reactive (and less toxic) Lewis acid was chosen, stannous chloride dihydrate ($\text{SnCl}_2 \cdot 2\text{H}_2\text{O}$), which had been used by other researchers for reactive modification of polypropylene in processing equipment (Coran and Patel, 1983; Kotlar and Borve, 1995). Interest in this Lewis acid aside from its catalytic performance was beyond the scope of this work, particularly regarding its actual structure at the reaction temperature and the structure of the proposed anhydride-acid adduct (proposed structure in Chapter 2). Numerous sets of conversion data from the experiments carried out, can be found in Appendix II. The addition of maleic anhydride and catalyst was observed to suppress the reactor temperature by 1-4°C (depending on the amount of reactants added) for reactions in this chapter, which the controller was not always able to correct over the duration of the reaction. This observation combined with evidence presented in subsequent sections, indicates that improvement in anhydride incorporation in the polymer should be attributed to the catalytic nature of the Lewis acid rather than an increase in the temperature due to the

highly reactive acid being introduced. Localized heating in the molten polymer could still be present, however, no indications of this phenomenon were observed.

The concentration of stannous chloride dihydrate ($\text{SnCl}_2 \cdot 2\text{H}_2\text{O}$) was measured with respect to maleic anhydride instead of the vinylidene group so that the catalyst concentration would be reflective of the enophile which now consists of the Lewis acid-anhydride adduct. Maleic anhydride concentration was always quoted in mole equivalence with respect to the vinylidene concentration. Attempts to distinguish the consequences of forming the anhydride-acid adduct (enophile) prior to injecting into the molten polymer opposed to forming the adduct in-situ, shall be discussed further in this chapter. Reaction runs with the introduction of solid catalyst from the catalyst bucket, shall be referred to as the heterogeneous reaction system, while reactions where the catalyst was dissolved into solution prior to its introduction, shall be referred to as the homogeneous reaction system. For heterogeneous reactions involving stannous chloride, higher concentrations of maleic anhydride (MAh) were used due to limitations in adding catalyst at 0.005 mole equivalence for MAh concentrations below 4 mole equivalence. The resulting functionalized polymer from the heterogeneous reaction system was always brown in colour. A finding in agreement with Deng (1990), who had noted that brown colouring of polymer was due to excess cationic species being present.

By dissolving the catalyst into solution, smaller concentrations of the Lewis acid may be used in the reaction which could not be achieved by the addition of solid $\text{SnCl}_2 \cdot 2\text{H}_2\text{O}$, thus resulting in a polymer that was off-white in colour instead of brown. The use of catalyst in solution also made possible the investigation of maleic anhydride concentrations below the

aforementioned limit of 4 mole equivalence. With the catalyst and molten maleic anhydride now being in similar phases, the introduction of the catalyst (now presumably $\text{SnCl}_2 \cdot 2\text{DMF}$ with DMF exchanging with the water ligands of the Lewis acid) solution into the anhydride species prior to the reaction should expedite the formation of the enophile adduct.

6.2. CHARACTERIZATION OF SUCCINYL TERMINATED POLYPROPYLENE

The amorphous polymer, Polypol-19, was sought to overcome certain limitations which crystallinity bears with respect to characterization. Semi-crystalline polymers typically exhibit a complete lack of solubility except under certain conditions (such as elevated temperatures) which may allow a solvent to overcome the crystallite structure of the material and completely penetrate the polymer matrix. This lack of solubility complicates molecular weight determination, functional group titration, and solution NMR analysis. The presence of crystallinity also increases the complexity of an IR spectrum with new diad/triad monomer interactions and produces a drifting effect in the spectrum baseline due to polymer crystallites scattering the laser of the instrument. With these considerations in mind, it was hoped that characterizing the attached succinyl anhydride in amorphous polypropylene would be greatly improved and that this information could be adapted to the higher molecular weight species discussed in the later chapters where characterization will be significantly more difficult. In order to properly characterize the structure of the Alder Ene product, it was important to understand the geometry (shown in Figure 6.1) of the two possible isomer products of a terminally maleated polypropylene with species (I) presumably being the favoured geometry based on the results of Tessier and Maréchal (1984a,b, 1990).

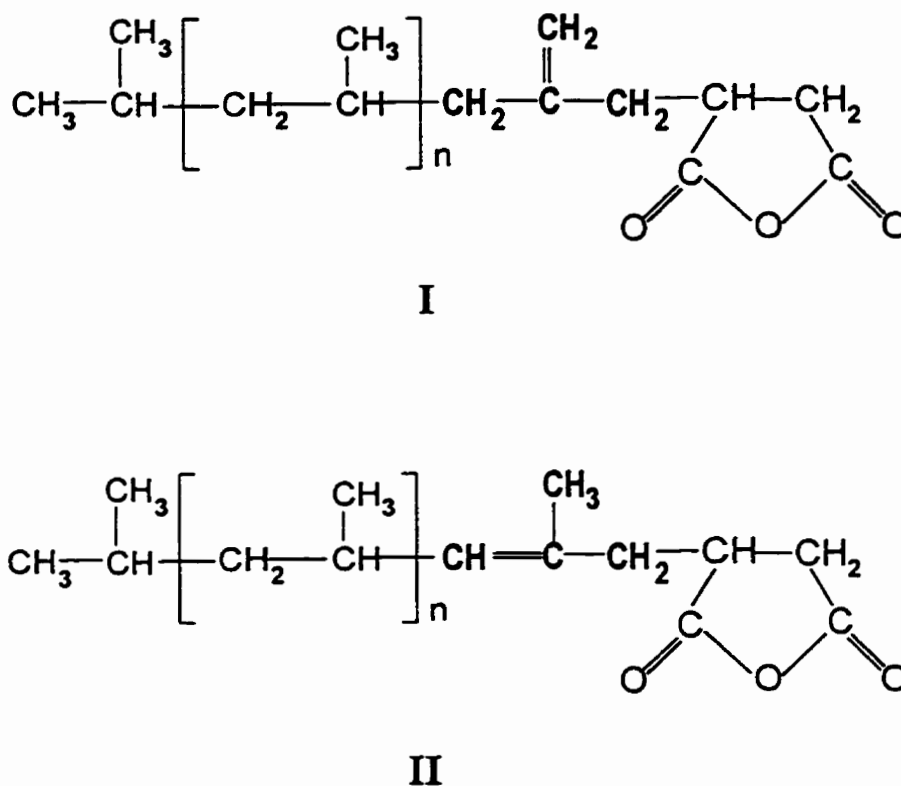


Figure 6.1. Isomeric structures of succinyl terminated polypropylene: (I) Exo double bond; (II) Endo double bond.

6.2.1. FTIR Analysis

Figure 6.2 shows the infrared spectrum of virgin polypropylene resin (Polypol-19) compared to the succinyl terminated polypropylenes (from a 5 minute SnCl₂ catalyzed reaction and a 24 h Alder Ene reaction without Lewis acid present) in the region of the vinylidene group. The figure includes a spectrum of a maleic anhydride and polypropylene mixture, to allow for improved identification of the changes made to Polypol-19 due to the Alder Ene reaction. Table 6.1. lists the wavenumbers of those vibrations unique to the respective samples, that were not observed in the virgin polymer. Of foremost importance in Figure 6.2, the strong vinylidene absorbance at 888 cm⁻¹ in the virgin resin showed a

Table 6.1. Characteristic IR wavenumbers (cm⁻¹) in several samples compared to Polypol-19

Polypol-19 and MAh	SnCl ₂ catalyzed Alder Ene Product	Alder Ene Product
635	728	663
700	1784	720
786	1792	920
863	728	1024
1053		1070
1589		1714
1566		1792
1650 (broadened)		1868
1706		
1780		
1790		
1853		

significant decrease upon the conclusion of the Alder Ene reaction in the presence of a Lewis acid catalyst and was completely consumed in the highly maleated sample which reacted for 24 h without the use of a catalyst. The decreased vinylidene concentration was similar to the findings of Walch and Gaymans (1994), who witnessed a complete absence of the vinylidene group in their product despite Tessier and Maréchal (1984ab) observing the functionality (through NMR) within the majority of their product. Walch and Gaymans (1994) suggested that the generated pendant vinylidene from the reaction was shifted to 920 cm⁻¹ due to its proximity to the attached anhydride group and therefore was obscured by the backbone absorbances of the polymer. As seen in Figure 6.2, the 920 cm⁻¹ absorbance was seen in the highly maleated product, yet is not visible in the catalyzed sample probably due to the low extent of reaction. The fact that the absorbance was not observed in the maleic anhydride and

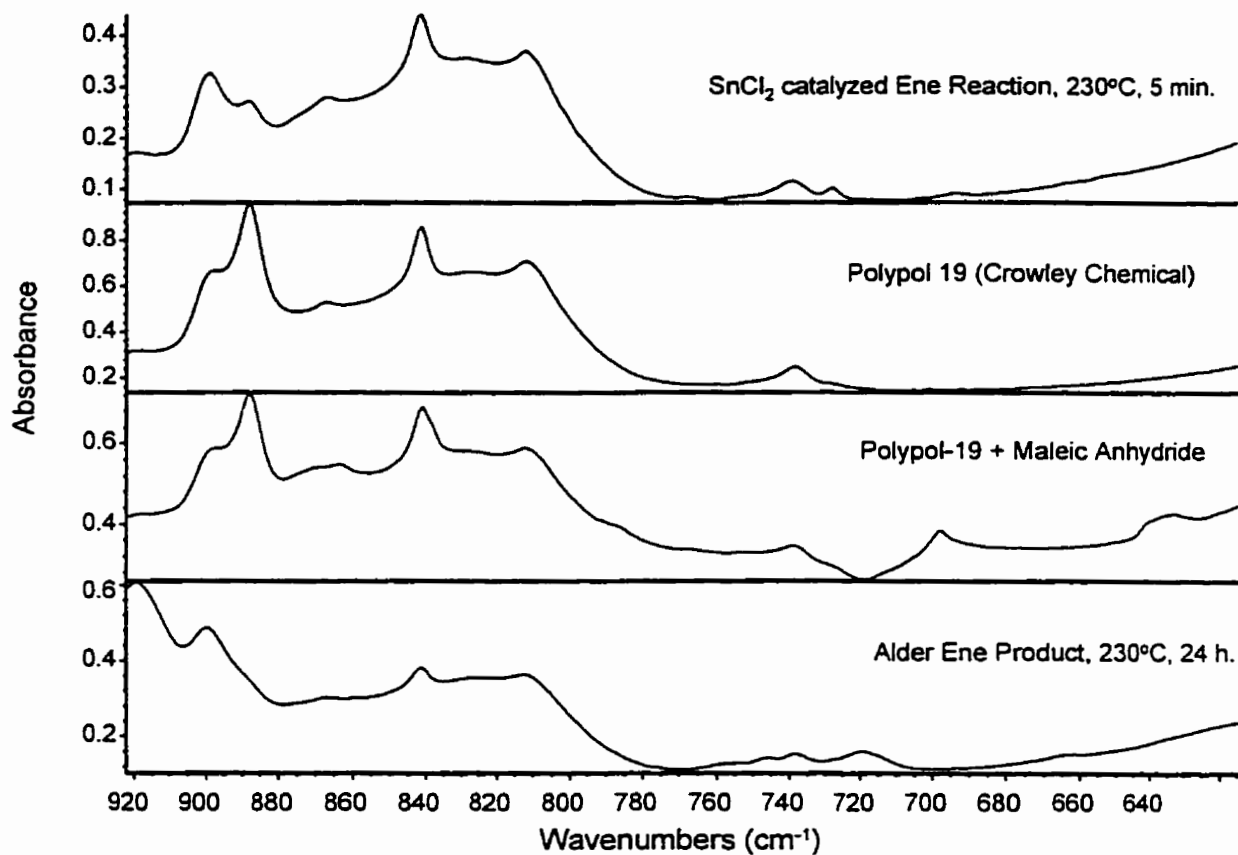


Figure 6.2. FTIR spectra comparing the virgin polypropylene and Ene product in the region of the vinylidene.

polypropylene mixture tends to lend credibility to this band assignment. Unfortunately, the band assignments made for maleic anhydride in section 2.6.3 from different authors, do not correspond to those observed in Figures 6.2 and 6.3, and Table 6.1, possibly due to differences in the diluent used.

Figure 6.3 shows the same polymers as in Figure 6.2, however, the region shown pertains to the carbonyl absorption. The peaks at 1745 cm^{-1} and 1780 cm^{-1} in the Polypol-19 indicate the presence of an anti-oxidant in the resin, which fortunately did not appear to interfere with the performance of the Lewis acid. The succinyl terminated polypropylenes in Figure 6.3 showed succinyl anhydride absorbances at 1792 cm^{-1} with a 1784 cm^{-1} shoulder.

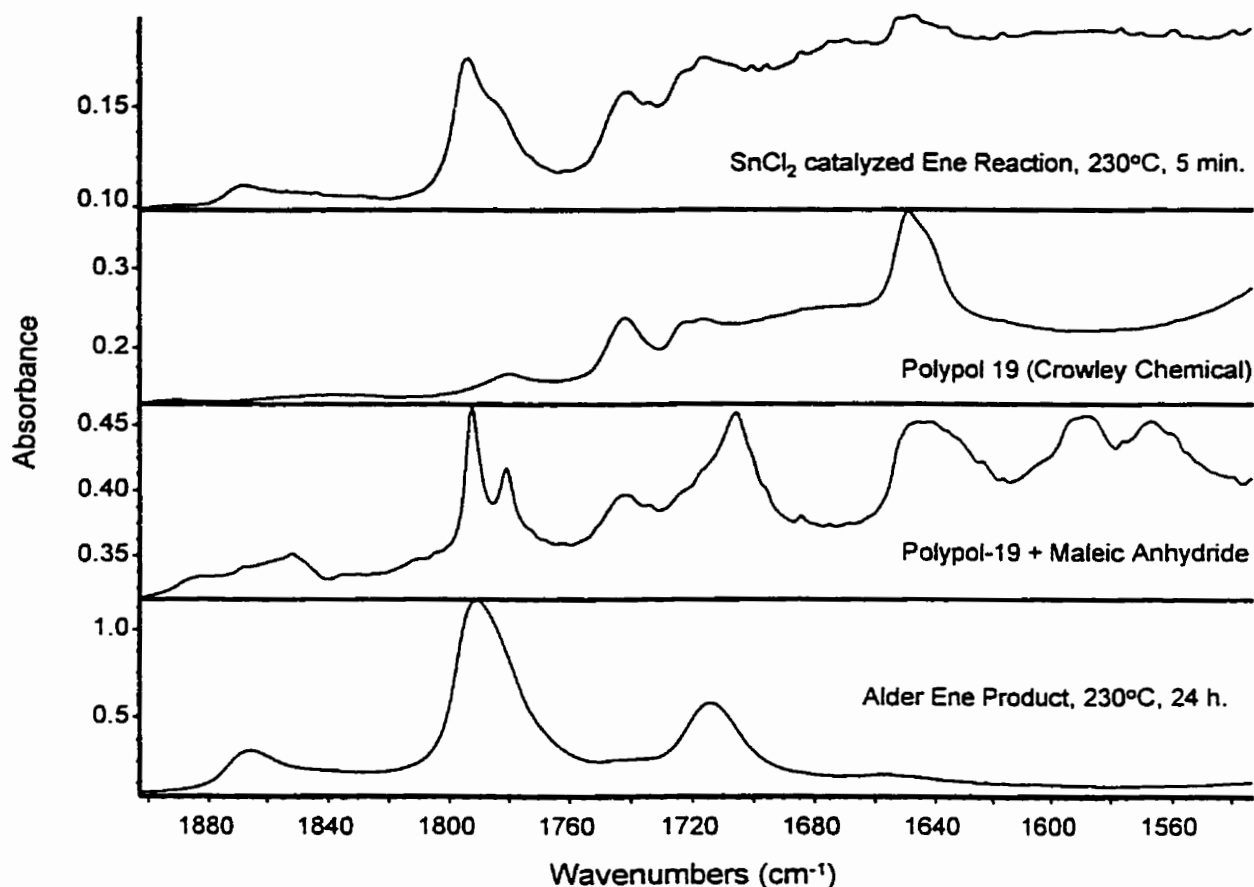


Figure 6.3. FTIR spectra comparing the virgin polypropylene and Ene product in the carbonyl region.

Compared to the maleic anhydride and polypropylene mixture, the anhydride bands corresponding to the polypropylene attached anhydride group exhibit extensive broadening, which is a general characteristic of any functionality present in a polymer. Interpreting the presence of the 1784 cm^{-1} band was complicated by conflicting views on the mechanism which maleic anhydride grafts to the polymer (De Roover et al., 1995; Heinen et al., 1996). However, both 1792 cm^{-1} and 1784 cm^{-1} are attributed to mechanical coupling of the carbonyl stretching modes within the anhydride (Marquardt, 1966). The intensity of the lower frequency band is increased in systems of increasing polarity or with increasing intermolecular hydrogen bonding (Nyquist, 1990). Therefore, maleic anhydride bound or

free in a polypropylene system should show a stronger high frequency band than low frequency band (which has been observed) unless highly localized concentrations of anhydride exist. Grafts of poly(maleic anhydride), if present in the polypropylene chain, would favour the low frequency band. An intensity ratio favouring the lower frequency has also been typically seen in products of free radical maleation. The presence of TEMPO was observed to maximize the intensity of the succinyl peak at 1792 cm^{-1} compared to the 1784 cm^{-1} absorbance for the samples in this thesis (discussed in section 6.4). Another absorbance which appeared to distinguish attached succinyl anhydride from free maleic anhydride was

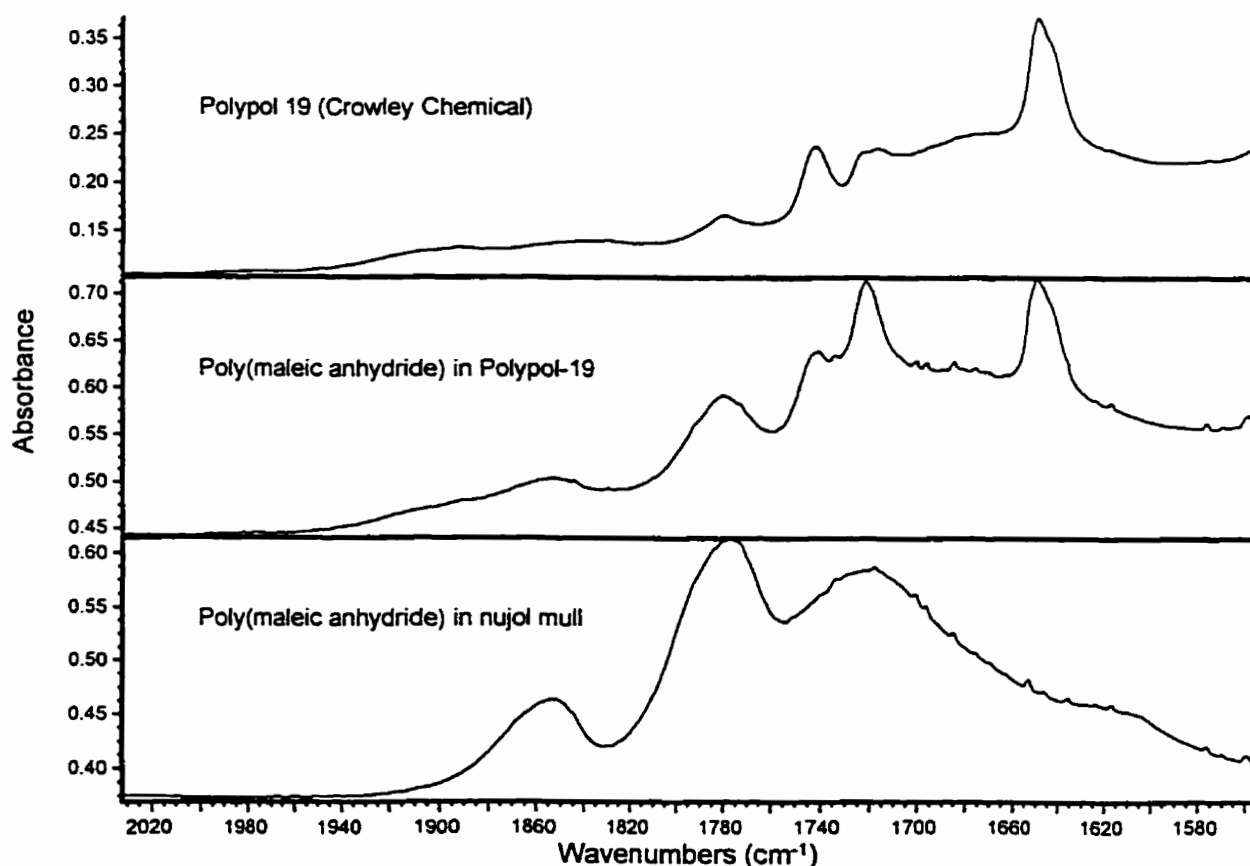


Figure 6.4. FTIR Spectra examining poly(maleic anhydride) in the carbonyl region.

the cyclic anhydride vibration that was found at 1868 cm^{-1} shifted from 1853 cm^{-1} when bound to a polymer. As presented in Figure 6.4, the absorbance at 1853 cm^{-1} for free maleic anhydride may also correspond to poly(maleic anhydride). The figure compares the infrared spectrum of poly(maleic anhydride) mixed into Polypol-19 with its separate components. The 1853 cm^{-1} absorbance band could prove invaluable for determining the degree of polymeric maleic anhydride in the product of any Alder Ene synthesis, provided it could be fully resolved from the surrounding absorbances. The polymeric maleic anhydride species displayed in Figure 6.4 was synthesized from a 50/50 w/w maleic anhydride-acetic anhydride solution at 90°C . The reaction was initiated using 5 wt % benzoyl peroxide (Aldrich, 97 % pure) in toluene, added dropwise for 1 h and then the system was maintained under nitrogen for 20 h. Due to the high solubility of the poly(maleic anhydride) in acetone and its nearly complete insolubility in toluene, the product was easily collected, washed and finally dried in a vacuum oven at 70°C for 8 h.

No chlorination of the Lewis acid-catalyzed product, due to isomerization, was observed, which would be characterized by a peak at 640 cm^{-1} . Detecting chloride vibrations required that the spectrum background include the sodium chloride disk to avoid overwhelming any chloride resonances that might be present in the polymer.

6.2.2. Intrinsic Viscosity

The intrinsic viscosity value of the virgin polymer was found to be 0.187 ± 0.003 dL/g while two succinyl terminated polypropylenes (from the heterogeneous system which should be the most severe in terms of the chance of degradation) with a low (0.005 mole eq.) and high (0.1 mole eq.) catalyst concentration were observed to have viscosity values, 0.170

± 0.037 dL/g and 0.105 ± 0.002 dL/g respectively. The intrinsic viscosities suggest that the polymer underwent degradation in the presence of high Lewis acid concentration.

6.2.3. NMR Analysis

Figure 6.5 presents a ^1H NMR spectrum of a succinyl anhydride terminated polypropylene (the Alder Ene product produced over a 24 h period from section 6.2.2) in hexane over a field range of 0-8 ppm. Deuterated hexane was used in place of toluene or benzene for this sample to determine if any maleic anhydride was present which otherwise

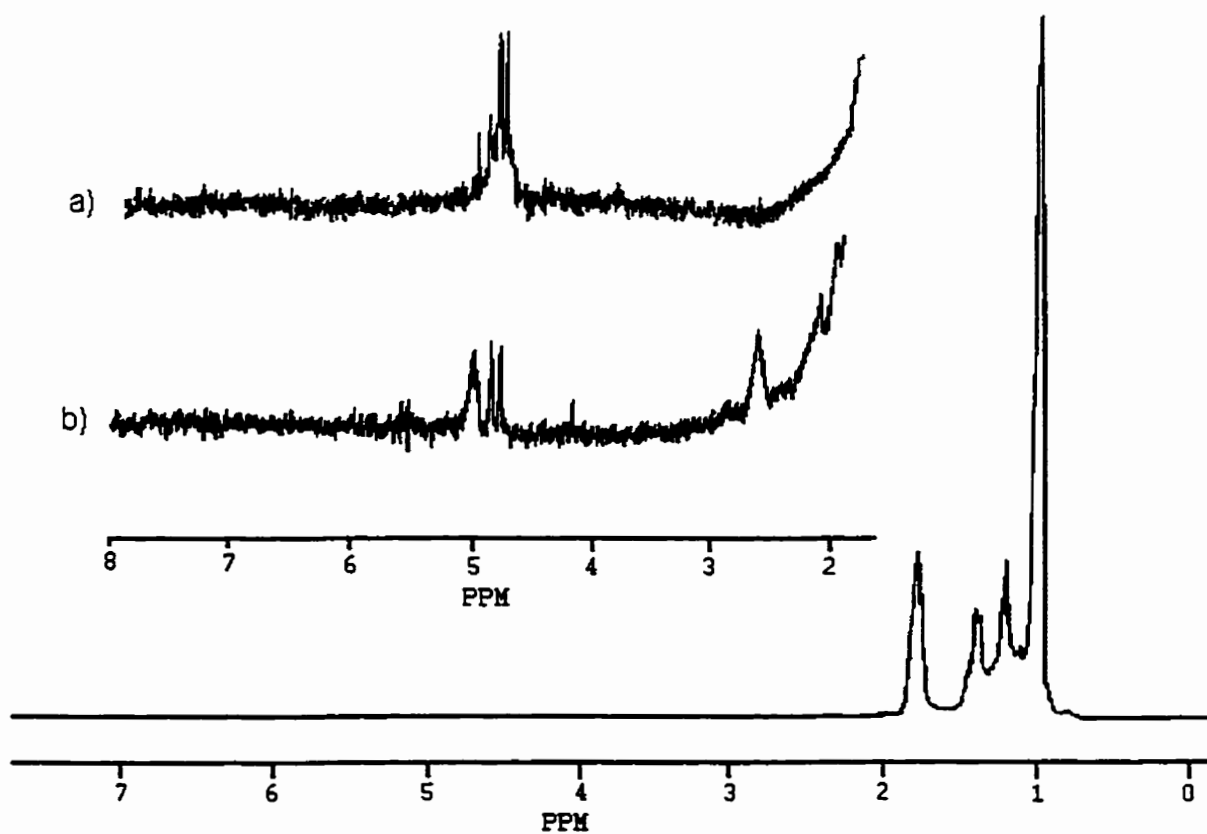


Figure 6.5. ^1H solution NMR spectrum of a) Polypol-19 and b) succinyl terminated polypropylene.

would have been obscured by the phenyl ring resonance of the solvents. The absence of a signal at 7.07 ppm indicated that the method of purification was effective in removing residual reactants from the product. No peaks were observed in the region of 9-15 ppm where carboxylic acids were anticipated. Peak assignments for the polypropylene backbone were observed in Figure 6.5 in the region of 0.5-1.7 ppm. Appendix III includes several NMR spectra of maleated Polypol-19 samples dissolved into benzene- d_6 as the solvent. No changes in the following chemical shift frequencies were observed due to solvent effects.

The terminal vinylidene was characterized by two fully resolved peaks at 4.78 ppm and 4.83 ppm corresponding to the two hydrogens at the chain end. Peak integration of the vinylidene relative to the polymer backbone indicated a decrease in the vinylidene content in the succinyl functionalized product compared to the virgin resin (compared in Figure 6.5a and 6.5b). The peak at 4.99 ppm could be assigned to either the pendant vinylidene or internal vinyl. It was probably due to the pendant vinylidene since the electronic structure of the group would not be very different from the terminal vinylidene though its protons would be expected to be slightly shifted downfield due to deshielding. The pendant vinylidene peak was observed to increase for the same product. The small resonance at 5.38 ppm was likely the internal vinyl, similar to the chemical shifts found for the internal vinyl of ethylidene norbornene in Chapter 8. The different isomers in the product confirmed the occurrence of the Alder Ene reaction. Terminal succinyl functional groups tend to have complex splitting patterns (Tessier and Maréchal, 1984ab, 1990) but generally are found in the region of 2-3 ppm which corresponds to the broad peak centred at 2.62 ppm in Figure 6.5. There was no evidence of polymerized maleic anhydride in the spectrum of the Ene product, by the lack of any broad peaks in the region of 4.5 ppm.

The peak assignment at 2.62 ppm was compared with a maleic anhydride grafted polymer synthesized using 1.0 wt % Lupersol 101 dialkyl peroxide (Elf AtoChem) for the same time and temperature as the Ene product (spectrum included in Appendix III). The succinyl anhydride peak was observed to shift downfield to 3.3 ppm, now that the anhydride group was positioned at a tertiary site. This result seems to suggest that the reaction product can involve exclusive terminal attachment without backbone grafting, if care is taken to prevent free radical formation.

A ^{13}C NMR spectrum of the Ene product is shown in Figure 6.6. The terminal succinyl CH and CH_2 groups of the cyclic anhydride should be observed in the region of 40

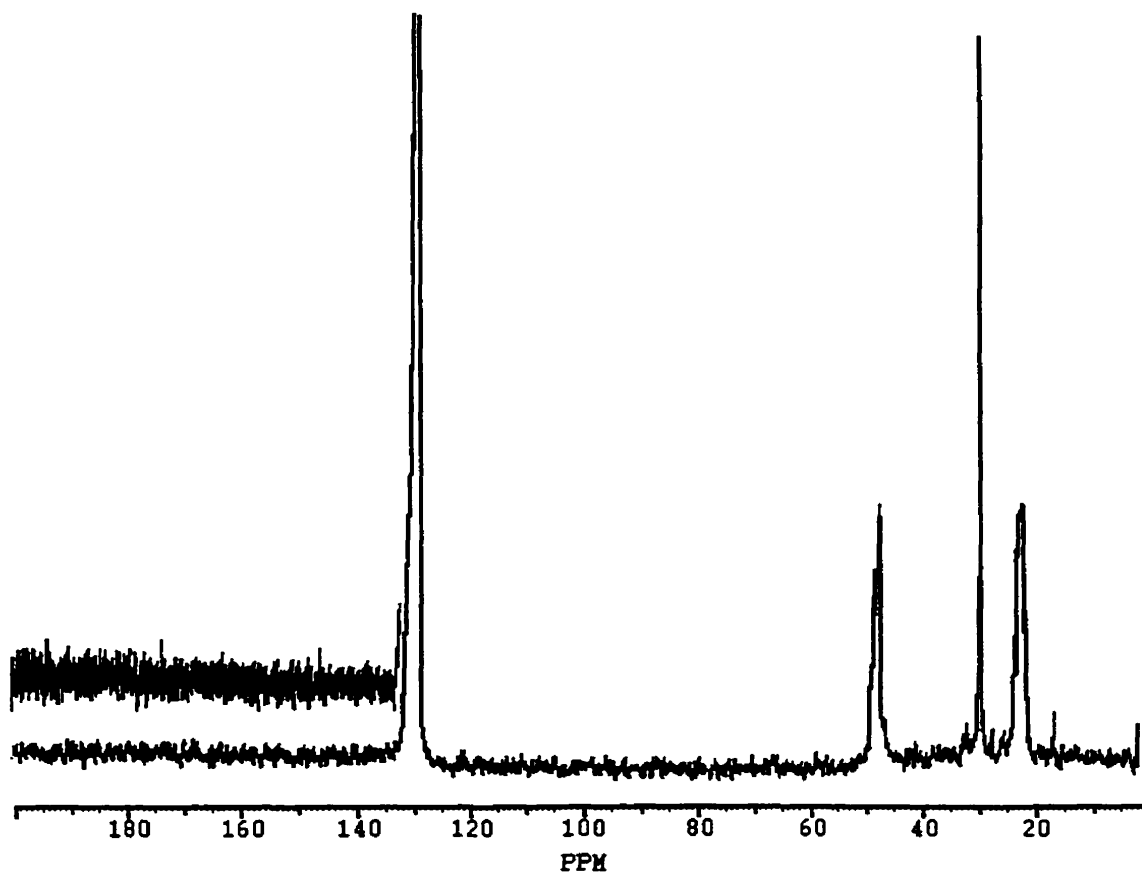


Figure 6.6. ^{13}C solution NMR spectrum of succinyl terminated polypropylene.

ppm and 34 ppm respectively (Tessier and Maréchal, 1984ab, 1990) whereas a tertiary grafted succinyl group should show chemical shifts at 63 and 53 ppm respectively (Tang and Huang, 1994). Carbonyl carbons of the succinyl group regardless of position, should produce chemical shifts of 169 and 174 ppm (Tessier and Maréchal, 1984ab, 1990; Tang and Huang, 1994). Figure 6.6 showed that the natural abundance of ^{13}C was insufficient to observe the low concentration (approximately 1 mole%) of succinyl groups attached to the polypropylene chain. According to the peak assignments of Shiono and coworkers (Shiono and Soga, 1992ab; Shiono et al., 1993) for polypropylene, the peak at 15.08 ppm corresponded to a propyl end group and the complex splitting patterns centred at 21, 28 and 46 ppm corresponded to the methyl, methine and methylene groups respectively. Vinyl groups could not be detected above the noise of the baseline.

6.3. COMPARING METHODS OF SUCCINYL ANHYDRIDE MEASUREMENT

The functional group concentration in free radical maleated polypropylene has been typically quoted as at least an order of magnitude higher (Gaylord and Mishra, 1983; Borsig et al., 1995) than the results of the catalyzed Alder Ene reaction over the same reaction time period. Therefore, a question of sensitivity presents itself with respect to the methods used to determine the concentration of the anhydride group when its quantity is relatively low. Looking at the three most utilized methods of determining functional group concentration, there are FT-IR, ^1H NMR and acid-base titrimetry, stated in decreasing order of sensitivity. Modern spectroscopic instruments are some of the most sensitive means available to researchers for measuring functional group content and these analytical techniques are limited to functional groups concentrations in the region of 10^{-2} wt % for IR and an order of

magnitude larger for NMR (proton). Based on this limitation in analytical detection of functional groups, terminal species on polymer chains beyond approximately 3000-4000 g/mol in length can not distinguished from noise with any accuracy by spectroscopic methods. Acid-base titration methods yield far lower sensitivity than spectroscopic techniques, compounding sources of error which include end-point detection (dye indicator or potentiometer), surface tension effects on reading the meniscus, and pH changes due to solution compositional changes (i.e. alcohol evaporation). Based on comparisons of the titration method with both IR and NMR methods, an estimated limit in functional group concentration for acid-base titrimetry would be an order of magnitude greater than ^1H NMR, at approximately 1 wt %.

Figure 6.7 attempts to demonstrate the lack of confirmation towards succinyl anhydride measurement among the two most common methods utilized in the literature for free radical maleated polypropylene, namely acid-base titrimetry and FT-IR analysis. An attempt to correlate the FT-IR calculated succinyl anhydride concentrations to those values determined by acid-base titrimetry, showed no agreement, although at least both sets of data were showing the same trend. A close examination of the values from each method, shows that the titration-calculated succinyl anhydride concentrations are three orders of magnitude higher than the infrared method. The difference in succinyl anhydride content between the two methods decreased as the concentration of the functionality increased. Table 6.2

Table 6.2. Evaluation of two terminally anhydride functionalized polypropylenes.

Samples	Glass Transition (°C)	FT-IR calculated SAh conc. (mol/g)	^1H NMR calculated SAh conc. (mol/g)	Titration calculated SAh conc. (mol/g)
1	-20	1.0×10^{-5}	1.5×10^{-4}	3.4×10^{-4}
2	-17	1.2×10^{-4}	1.2×10^{-4}	1.1×10^{-4}

SAh = succinyl anhydride

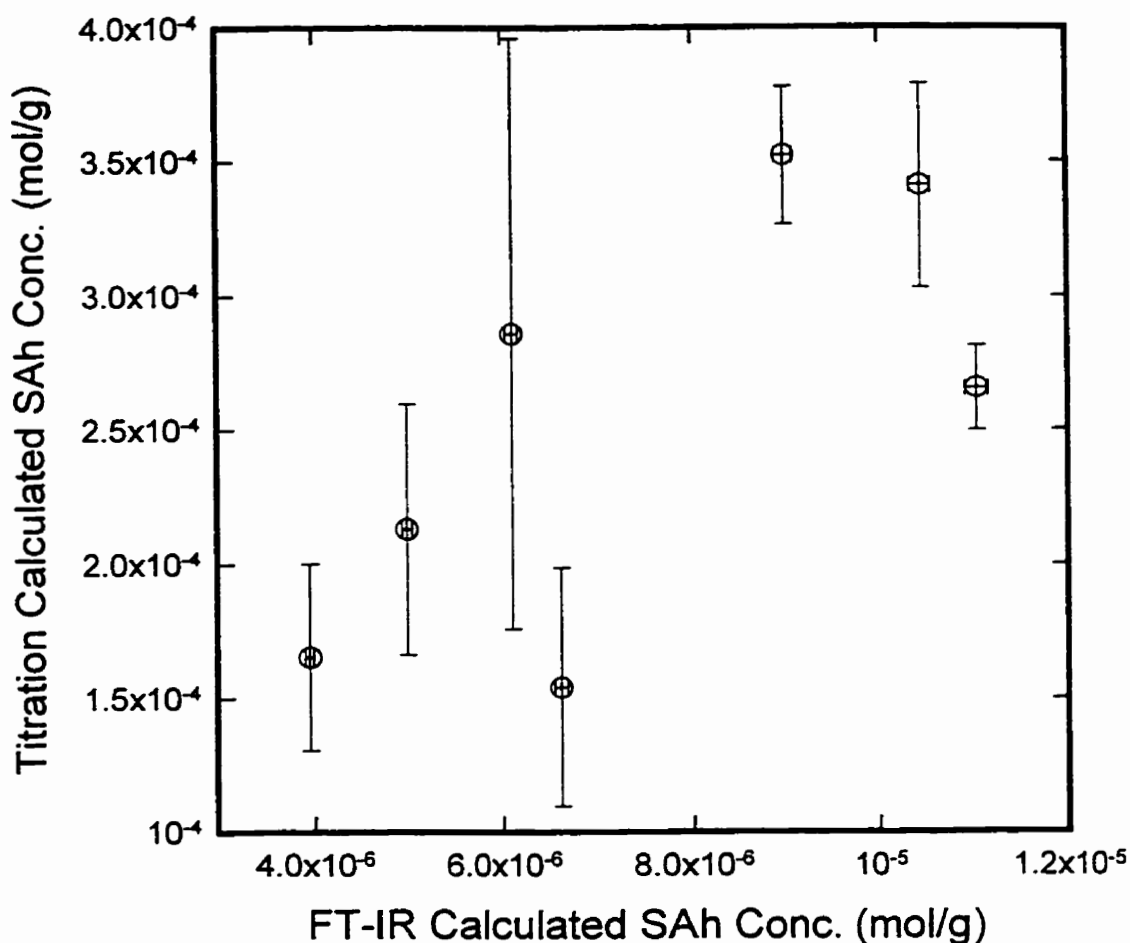


Figure 6.7. Evaluating the correlation between FT-IR and acid-base titrimetry as methods of measuring the concentration of the terminal functionality (standard deviation error bars)

compares two terminally maleated polymers, one with a relatively high concentration of the functional group. The agreement between the different methods of measuring change in the anhydride content was relatively high in sample 2, where the conversion was nearly 50 %, though the values among the different methods appeared considerable more disparate when the concentration was low (sample 1, which was indicative of the catalyzed Alder Ene product of this chapter). The standard error in the above values among the different methods of analysis were: 15% (titration), 10% (NMR), and 1% (FT-IR). The glass transition

temperature (T_g) can only indicate trends in the succinyl anhydride concentration, increasing in value with the polarity of the polymer. Figure 6.8 compares the two spectroscopic methods and the T_g among a set of polymers with differing terminal functionality. Since each sample was analyzed by ^1H NMR once, no error bars were included in the figure. The error in the T_g measurement was based on repetition of a single sample measured four times,

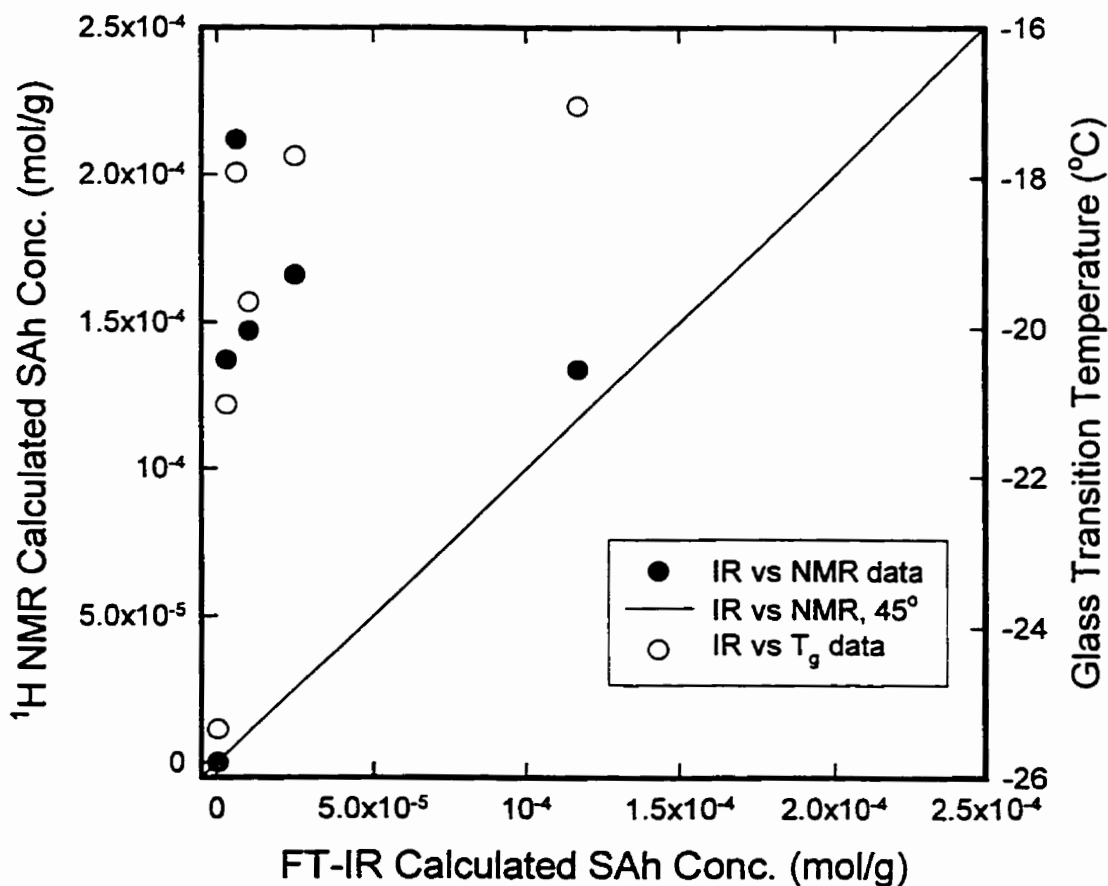


Figure 6.8. Comparing trends among FT-IR, ^1H NMR and T_g measurements of succinyl terminated polypropylene

yielding a deviation of 1.1°C. The glass transition temperature and the NMR measurements closely follow the trend of one another at low anhydride concentrations, possibly diverging at higher concentrations.

6.4. EFFECT OF FREE RADICAL INHIBITOR

The possible presence of free radicals generated during the reaction due to the presence of oxygen in the system and polymer degradation can lead to backbone grafting and/or homopolymerization of maleic anhydride. ¹H NMR analysis of a catalyzed reaction product with no inhibitor added, showed a strong broad peak in the region of 2.6 ppm and a weak peak at 3.3 ppm. The spectrum indicated that the presence of both free radical grafting and Alder Ene mechanisms were involved in the attachment of maleic anhydride onto the polypropylene chain. Hydroquinone, a common free radical inhibitor, was initially tested in an attempt to prevent maleic anhydride from being grafted onto the chain backbone. However, FT-IR analysis of samples ran with hydroquinone and Lewis acid, showed a phenyl group at 1610 cm⁻¹ attached to the polymer (spectrum shown in Figure 6.9) that was not observed in samples lacking this combination of phenyl group and Lewis acid (Figures 6.3-6.4). It was, therefore, concluded that no free radical inhibitors which possessed a phenyl group could be used in the work, which dismissed all common inhibitor candidates. It was desirable to search for an alternative free radical trapping agent which would not reduce the effectiveness of the catalyst, which led to TEMPO, a stable nitroxyl radical, commonly used in living free radical research. A series of seven runs were performed in the reactor using a 0.1 mole equivalence of SnCl₂•2H₂O with respect to the maleic anhydride reactant, with the TEMPO concentration ranging from 0-175 ppm. Figure 6.10 shows the relative FTIR

absorbances for each sample at 888 cm^{-1} (vinylidene) along with the titration data which determined maleic anhydride content in the polymer. Figure 6.10 indicated that the vinylidene concentration reached a minimum at 75-80 ppm TEMPO, while the anhydride content decreased to a plateau at the same concentration range. During radical addition of maleic anhydride, the vinylidene has been found (Heinen et al., 1996) to not participate which explains the high vinylidene content at low TEMPO concentrations. The IR absorbance ratio, $1792\text{ cm}^{-1}/1784\text{ cm}^{-1}$, showed a corresponding maximum at approximately 75 ppm. However, on either side of the maximum, the ratio rapidly dropped below unity. It

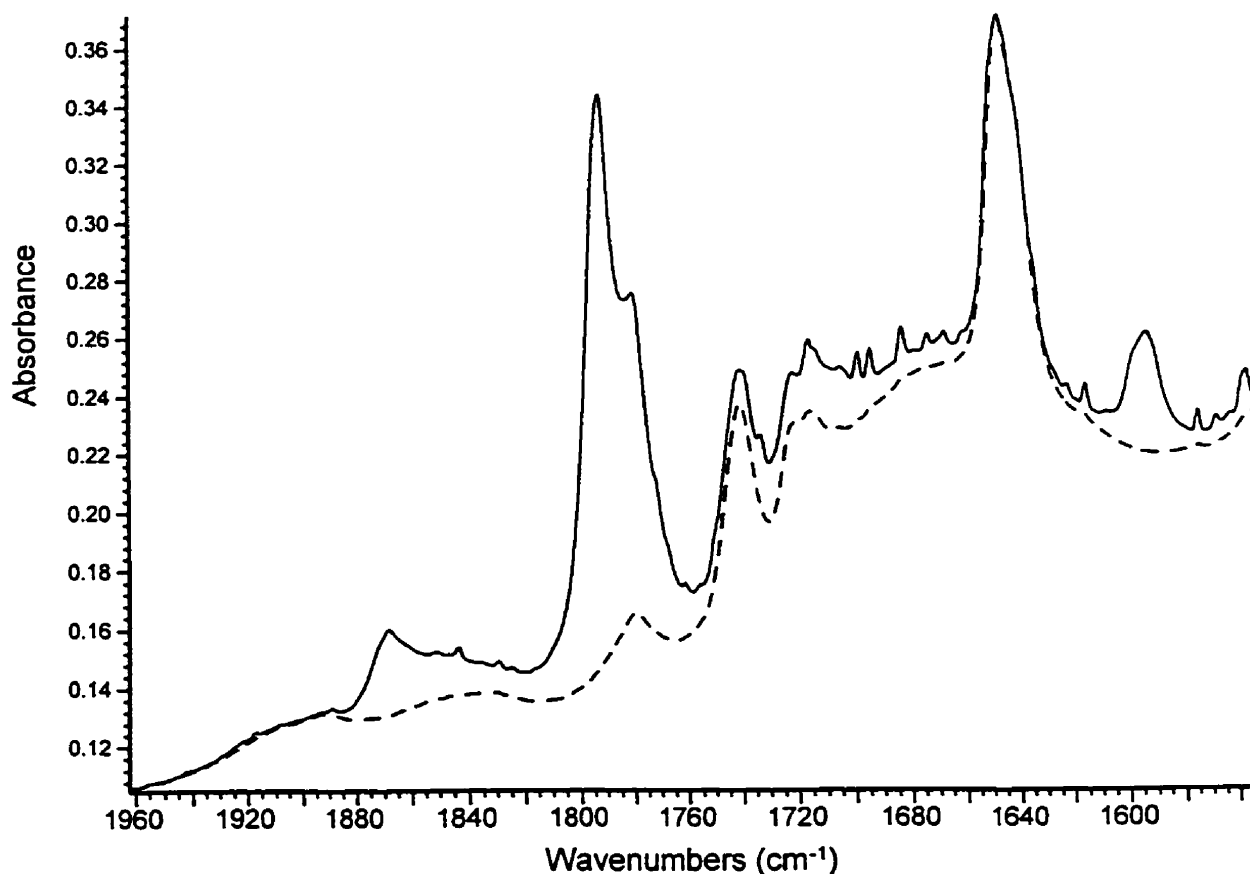


Figure 6.9. FT-IR spectra of a catalyzed Alder Ene product (solid line) reacted in the presence of hydroquinone with virgin Polypol-19 (dashed line) included for reference.

was apparent that an excess of TEMPO had a detrimental effect on the reaction similarly to reactions run without sufficient inhibitor. The stable free radical, in excess, may participate in the backbone grafted or homopolymerization (or both) of maleic anhydride. It is also possible that a high concentration of TEMPO could interfere with the catalyst. No evidence of bound TEMPO was observed in any NMR or FTIR spectra.

Since phenyl-based inhibitors can not be used in a Lewis acid catalyzed Alder Ene

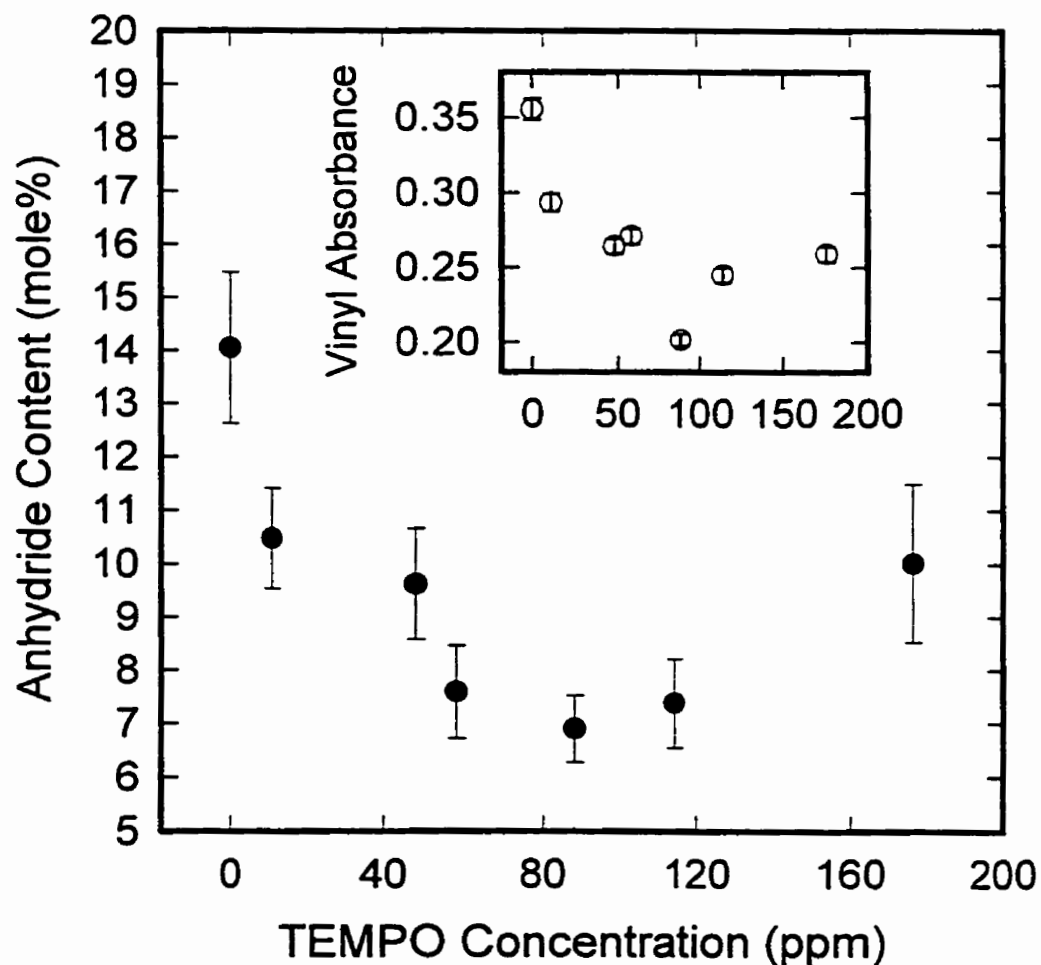


Figure 6.10. Effect of TEMPO Concentration in the Alder Ene Reaction on the Anhydride and Vinylidene Content in Polypropylene Product (standard deviation error bars).

reaction, it was necessary to question whether TEMPO provided comparable free-radical trapping efficiency to these more conventional species. The chosen free radical trapping agent, TEMPO, was compared to benzoquinone and butyl catechol under reaction conditions similar to those detailed in the experimental section, although no Lewis acid was present (hydroquinone was not tested since according to Flory (1953), hydroquinone does not perform well under a nitrogen atmosphere). This study of free radical trapping species assumed that the presence of a Lewis acid in the actual reaction did not affect the generation or consumption of radicals in any manner. Each experiment used 75 ppm of the respective free radical trapping agent. Looking at the relative peak heights for absorbances at 1792 cm^{-1} and 1784 cm^{-1} displayed in Table 6.3, one sees that TEMPO and benzoquinone behave in an equivalent manner with respect to both anhydride incorporation and the presence of side-reactions. The presence of butyl catechol in the reaction yielded higher relative absorbances for both monitored frequencies which could indicate the presence of homopolymerization. However, the absorbance ratio of 1792 to 1784 cm^{-1} was greater than either of the other trapping agents. Based on these measurements alone it would be difficult to determine if butyl catechol was more efficient at radical trapping, however, it was possible to conclude that all three of these chemical additives could reduce side reactions in the system.

Table 6.3. Inhibitor species in the Alder Ene reaction

Inhibitor	$\frac{1784\text{ cm}^{-1}}{974\text{ cm}^{-1}}$	$\frac{1792\text{ cm}^{-1}}{974\text{ cm}^{-1}}$	$\frac{1792\text{ cm}^{-1}}{1784\text{ cm}^{-1}}$
None	0.61	0.93	1.52
TEMPO	0.39	0.72	1.89
Benzoquinone	0.36	0.73	2.03
Butyl catechol	0.45	0.98	2.17

Therefore, with the effectiveness of TEMPO properly established, all further reactions discussed in this chapter (and the subsequent chapters) shall include 75 ppm of the stable nitroxyl radical species.

6.5. REACTION PARAMETERS

6.5.1. Effect of Temperature and Maleic Anhydride Reaction Parameters

Figure 6.11 shows the positive effect of both temperature and maleic anhydride concentration on the reaction conversion in the absence of catalyst (conversion was calculated from the mole ratio of succinyl anhydride bound onto the polymer chain with respect to the initial vinylidene content). For temperatures between 210-230°C, the increased functionalization of polypropylene was progressive. FT-IR measurements of products synthesized at 240°C and above showed a dramatic jump in the intensity of the relative 1792 cm^{-1} absorbance. The disjointed trend in the effect of temperature on the Alder Ene reaction suggested the occurrence of poly(maleic anhydride) oligomers (which would contribute to the 1792 cm^{-1} absorbance) began to become more dominant beyond 230°C. Based on the mass of black particulate (i.e. unbound poly(maleic anhydride) as identified by FT-IR spectroscopy) observed at the bottom of the reactor (prior to cleaning), which increased with temperature, the hypothesized side-reaction seems highly probable. However, no distinct FT-IR bands for the homopolymer were observable from the spectra of the maleated polymer samples.

To investigate the generation of poly(maleic anhydride), several products of the heterogeneous system were tested. These products were vacuum dried at 120°C for 16 h to

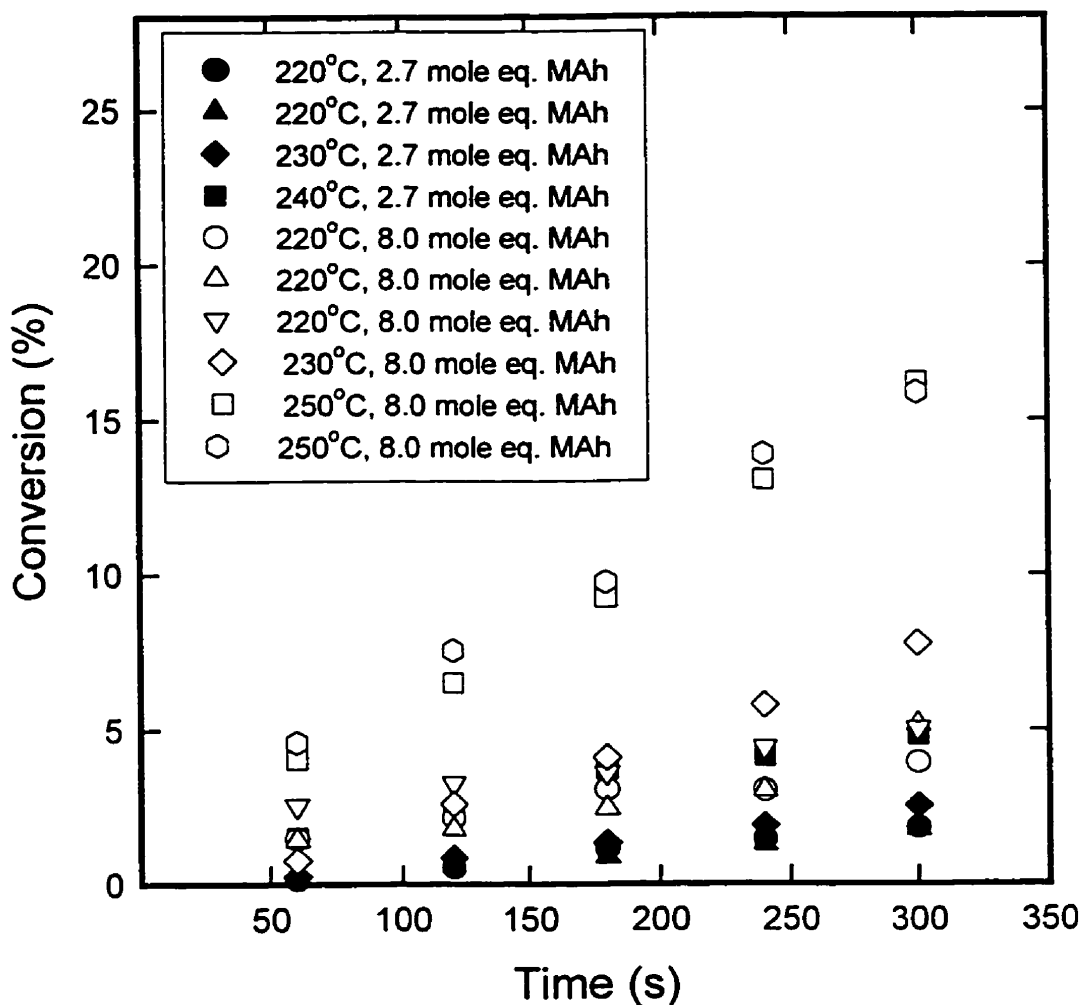


Figure 6.11. Conversion profiles as a function of temperature and maleic anhydride concentration in reactions with no catalyst present.

remove free maleic anhydride but not washed initially with acetone. The level of polymeric anhydride contamination (unbound to the polypropylene chain) was based on the change in the succinyl peak before and after repeated acetone washings. In the case of the catalyzed reaction system, the change in the succinyl anhydride absorbance was between 1 % (at 210°C) and 43% (at 250°C). For the uncatalyzed reaction system, the change in absorbance was noticeably greater at lower temperatures, i.e. 20 % (at 210°C) to 51 % (at 250°C). The

dark brown poly(maleic anhydride) has a high solubility in acetone yet remains practically insoluble in toluene (Trivedi and Culbertson, 1982). By collecting the acetone washing, evaporating the solvent and then washing with toluene, it was revealed that this method extracted only a small quantity of succinyl anhydride terminated polypropylene oligomers from the product. Clearly, the results suggest that the catalyst provides an inherent mechanism for suppressing the homopolymerization of maleic anhydride. Possibly, when maleic anhydride was incorporated into the Lewis acid-anhydride adduct, it was impossible for the species to participate in the excimer chain growth or the adduct has the ability to quench excimers.

The trend in temperature witnessed in the uncatalyzed reaction, has also been observed in those reactions using either a homogeneous or a heterogeneous catalyst system. Data from the heterogeneous system are shown in Figure 6.12. In this case, for similar maleic anhydride reactant concentration (8 mole eq. with respect to the vinylidene concentration) and Lewis acid concentration (0.5 % mole eq. $\text{SnCl}_2 \cdot 2\text{H}_2\text{O}$ with respect to maleic anhydride), the plot of succinyl anhydride absorbance versus time shows in a non-confounded manner, the influence of temperature on the degree of functionalization of the low molecular weight polypropylene species.

Based on the bimolecular nature of the reaction kinetics, increased maleic anhydride concentration was expected to increase the rate of reaction and, hence, result in higher conversions in the final product. However, based on the studies of free radical grafting (discussed in Chapter 2), increased maleic anhydride concentration would also be expected to decrease the occurrence of polymeric maleic anhydride formation due to excimer quenching.

The results observed at 250°C (and to some degree 240°C) in Figure 6.13, tend to confirm the previous assumption of poly(maleic anhydride) formation due to the decreasing anhydride concentration with increased maleic anhydride reacting, confirming results of the inhibitive nature of increased maleic anhydride concentration on the homopolymerization mechanism. Also, the concentration of maleic anhydride as a reactant in the heterogeneous system had a positive effect on the degree of succinyl anhydride functionalizing the polymer.

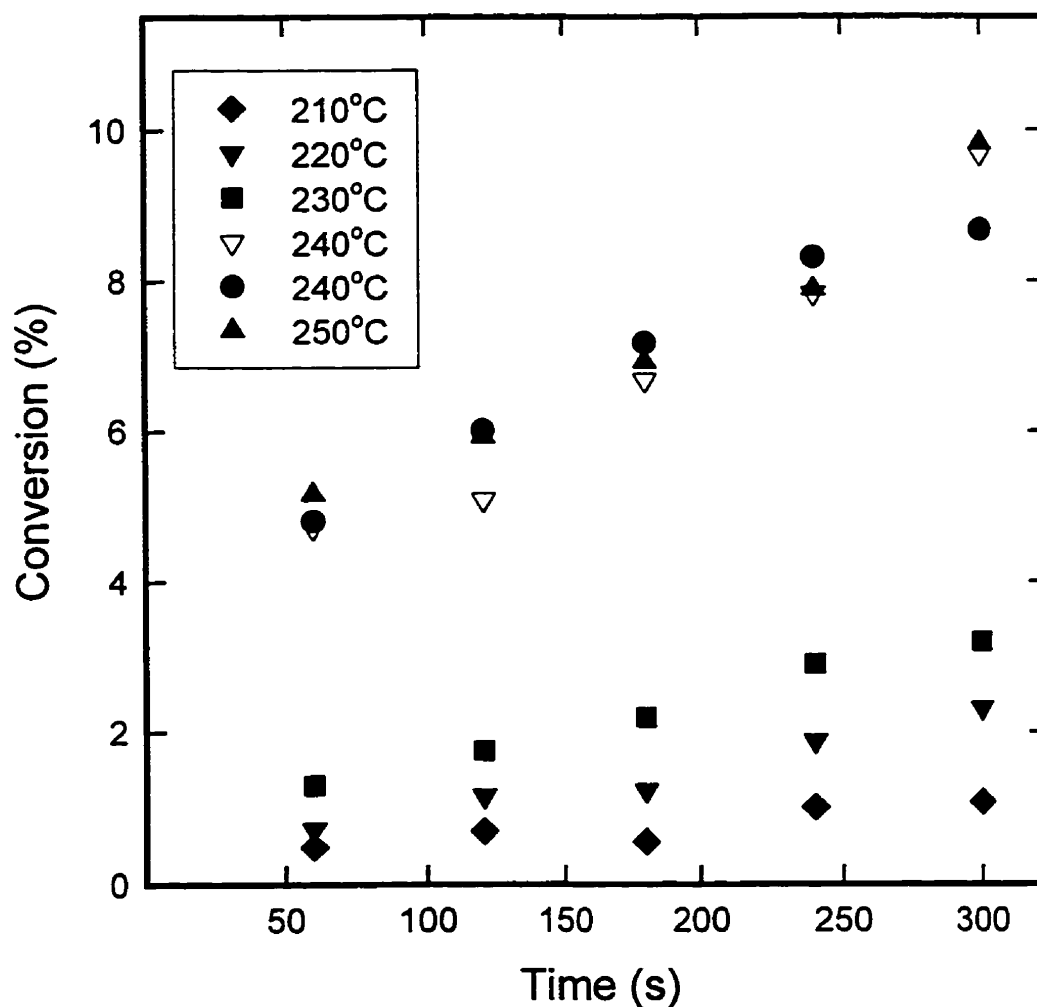


Figure 6.12. Effect of temperature in the Alder Ene reaction for reactions using 8 mole eq. maleic anhydride and 0.5 % mole eq. $\text{SnCl}_2 \cdot 2\text{H}_2\text{O}$.

Figure 6.14 shows that 12 mole equivalence of maleic anhydride gave the highest conversion for the product. A temperature/maleic anhydride concentration factor interaction can be observed in the figure which may again be attributed to the formation of maleic anhydride oligomers on the polypropylene chain.

Figure 6.13 also indicates the low reproducibility of the heterogeneous reaction

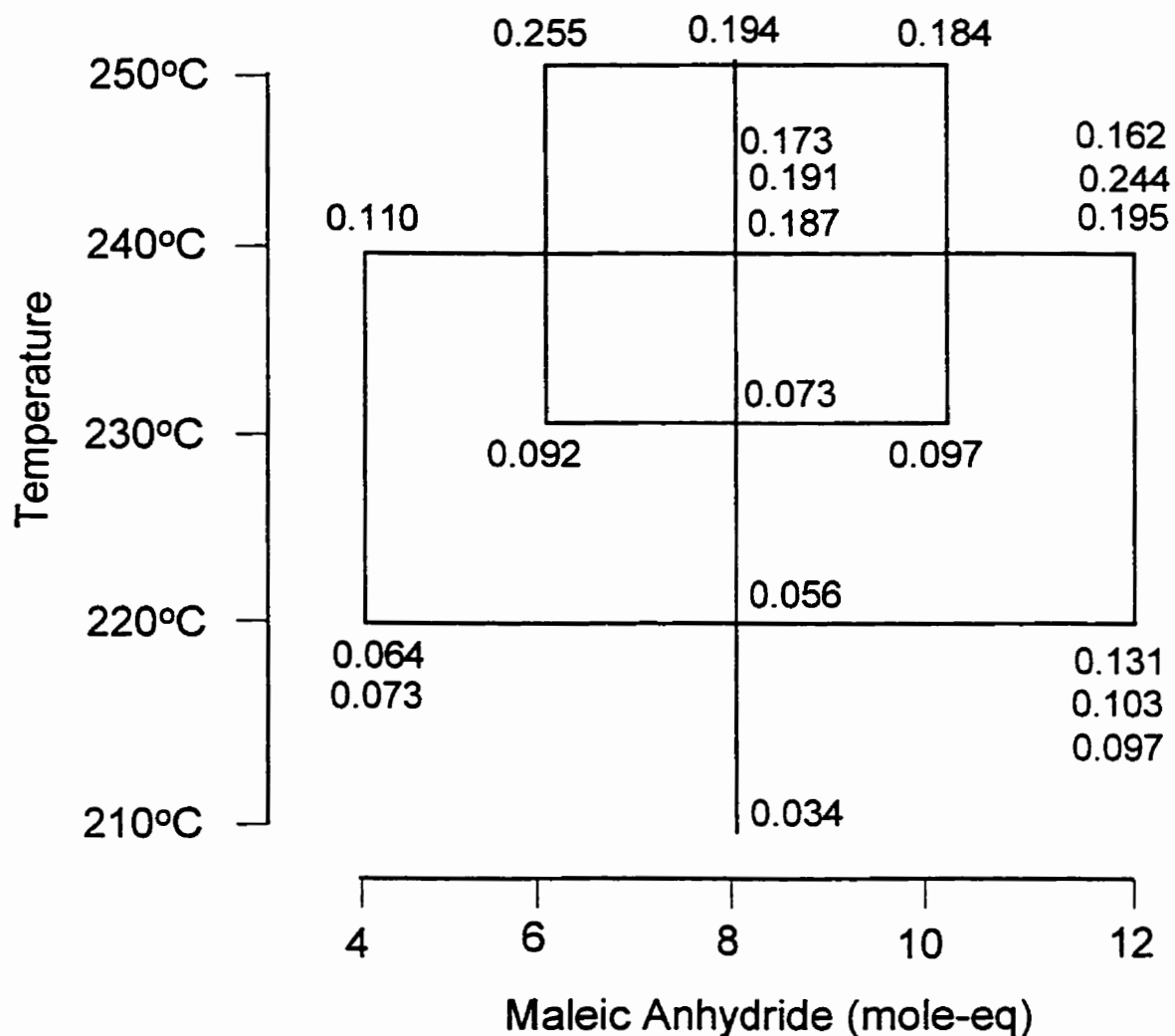


Figure 6.13. Relative succinyl anhydride absorbance values of 0.5 mol % SnCl₂ heterogeneous system using Polypol-19 after a 5 min. reaction, indicated on two response surfaces including a constant MAh concentration line for determination of the activation energy

system which was one of the major driving forces towards exploring a homogeneous reaction system. Causes for the high variance demand an understanding of the reactor itself. The contents of the catalyst bucket were isolated from the reactor by a teflon seal wound around the raised lip on the lid. This seal weakened with time due to prolonged exposure to high temperatures, and allowed polymer volatiles to enter the chamber and tackify the inner surface of the bucket. This was confirmed by the presence of Lewis acid adhered to the walls

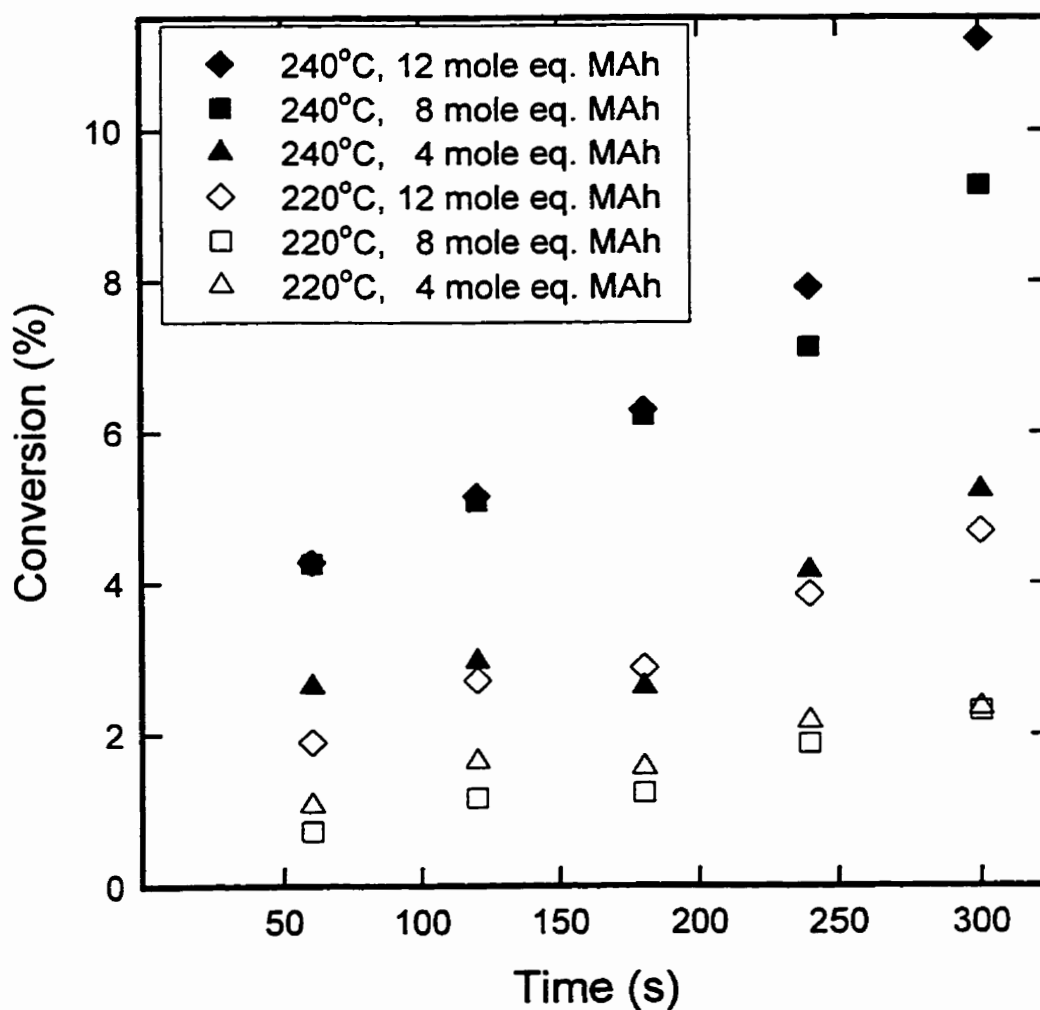


Figure 6.14. Effect of maleic anhydride concentration used in the catalyzed Alder Ene reaction (0.5 % mole eq. $\text{SnCl}_2 \cdot 2\text{H}_2\text{O}$) at 220°C and 240°C.

and lid of the bucket upon completion of the reaction. Therefore, inaccuracies in the exact quantity of Lewis acid added to the reaction abound for this reaction system.

6.5.2. Effect of Catalyst Concentration

The presence of Lewis acid was anticipated to increase the rate of reaction, though increasing the concentration of the acid was also expected to increase the rate at which the vinylidenes undergo isomerization prior to participating in the Alder Ene reaction. To determine if this theory was true, the reaction was run excluding maleic anhydride. Infrared analysis of the product showed the vinylidene content to decrease over the span of 5 minutes (more on isomerization in section 6.5.3). It should be noted that the concerted mechanism of the Alder Ene reaction is prohibitively slow with internal vinyls (that would result from isomerization) due to steric hindrance. Subsequently, a maximum in the Lewis acid concentration was anticipated as the effect of the catalyst was investigated. This investigation was begun with the heterogeneous reaction system where a lower limit on the catalyst concentration was imposed by the nature of the method for reasons discussed in the previous section.

Figure 6.15 shows the conversion for Lewis acid concentrations ranging from 0 to 0.10 mole equivalence with respect to the maleic anhydride reactant. The experimental series used 75 ppm TEMPO in each run. The expanded section of Figure 6.15 shows that a maximum exists at 0.001 mole equivalence of $\text{SnCl}_2 \cdot 2\text{H}_2\text{O}$. The plot shown in Figure 6.16 gives the mole percentage of anhydride in the polymer based on titration analysis. The maleic anhydride content titrated, was comparable to values found in free radical grafted polypropylene. A substantial increase in the anhydride functionality bound to the polymer

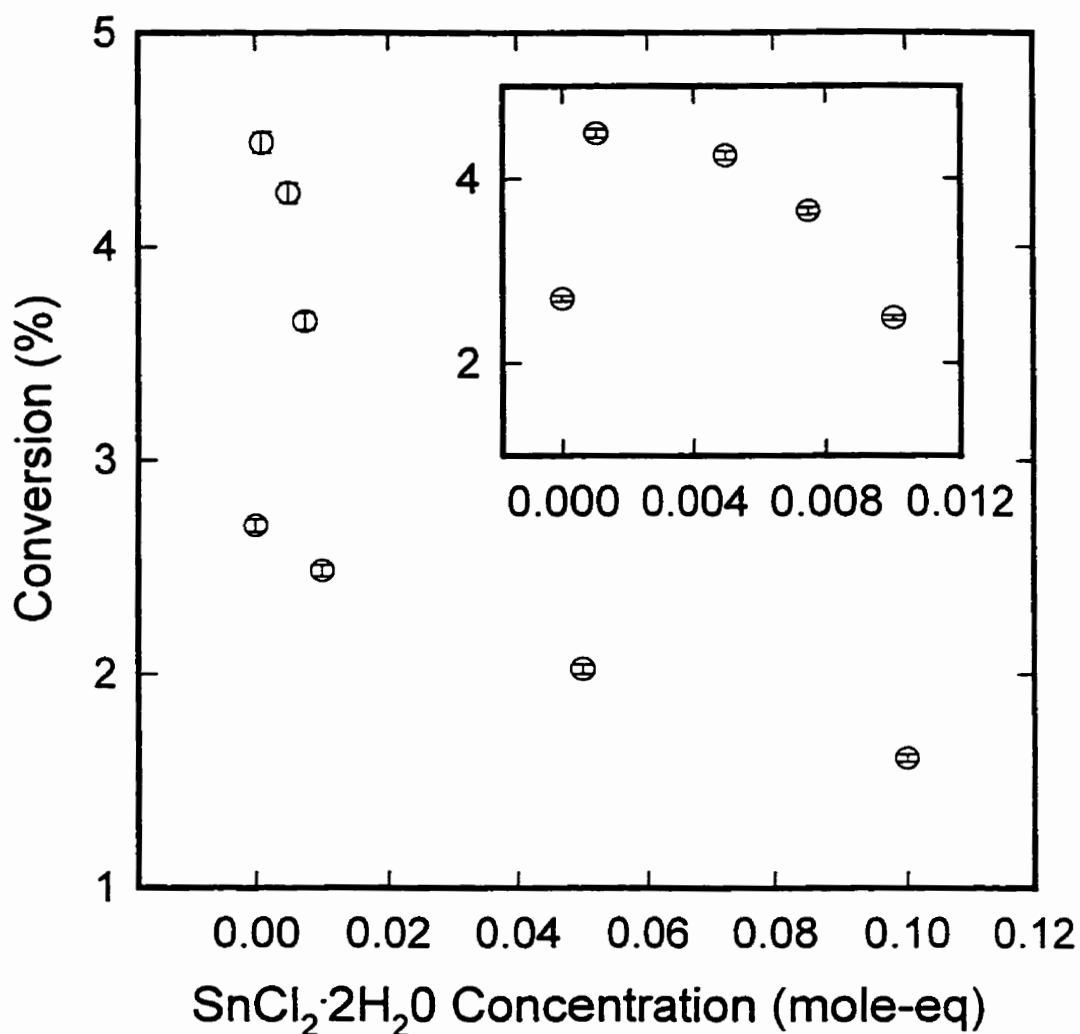


Figure 6.15. Effect of Lewis acid concentration on the conversion (FT-IR with standard deviation error bars) in the Alder Ene product (region of optimal anhydride incorporation has been expanded).

was observed relative to the sample produced without the Lewis acid present in the reaction. The anhydride concentration within the polypropylene appeared to be greatest in the region of 0.005-0.0075 mole equivalence of SnCl₂·2H₂O with respect to the maleic anhydride reactant. The titration data represent the total anhydride content including those groups which had undergone hydrolysis despite precautions taken.

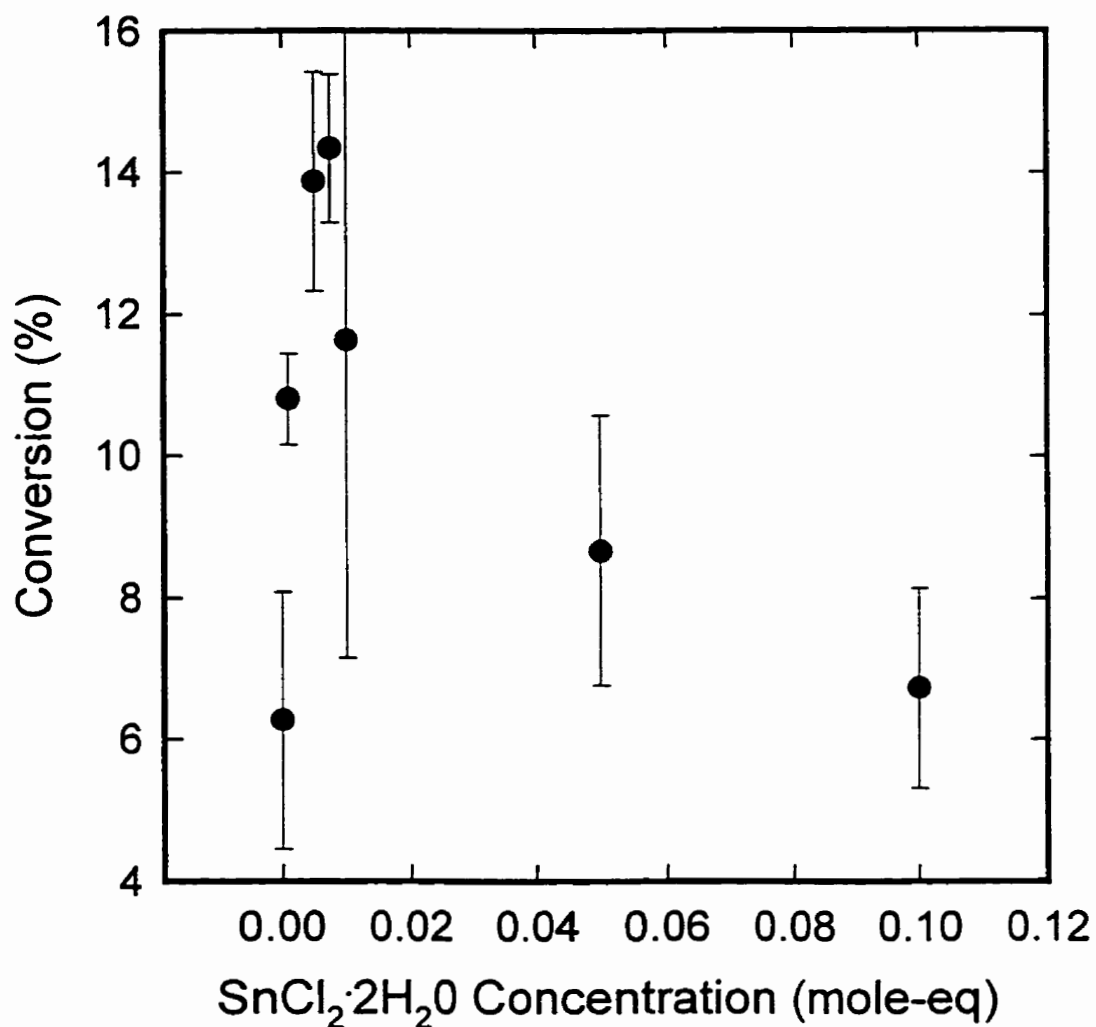


Figure 6.16. Conversion based on titrated succinyl anhydride group in the Alder Ene product with respect to the Lewis acid concentration (standard deviation error bars).

The difference in the maximum value of succinyl anhydride attached to the polypropylene between Figure 6.15 and Figure 6.16 was possibly lies in the infrared results where the dicarboxylic acid formed by hydrolysis was neglected. The difference in the measured conversion between the two figures, reiterates the point made in section 6.3 where the insensitivity of the titration method to the low succinyl anhydride concentrations may

produce erroneous conclusions. In spite of this lack of sensitivity, the similar trends in the two methods of analysis suggest that the maximum was probably within the region outlined by these two analysis techniques. It was for this reasoning that reactions in the heterogeneous system used a catalyst concentration of 0.5 % mole equivalence for experiments examining the parametric effect of temperature and maleic anhydride concentration in the previous section.

Figure 6.17 shows the glass transition temperature for each sample in the Lewis acid run series. Increasing anhydride functionality with respect to the alkyl nature of the polymer increases intermolecular interactions in the species, reducing mobility in the chains and therefore increasing the transition temperature. Based on this assumption and assuming that no unbound comonomer was present within the polymer sample, the increase in the material T_g is indicative of an increase of succinyl groups in the polypropylene. Figure 6.17 established the region where the Lewis acid had maximum effect on the Alder Ene reaction and it generally showed the same trend observed in Figures 6.15 and 6.16.

To study catalyst concentrations below 0.5 % mole eq., $\text{SnCl}_2 \cdot 2\text{H}_2\text{O}$ had to be introduced in a DMF solution which was then combined with the molten maleic anhydride prior to injection into the reactor (homogeneous system). The quantity of DMF was kept constant since it had been observed that DMF has an effect on the reaction (Thompson et al., 1998b), possibly due to DMF interfering with the formation of poly(maleic anhydride) segments (Gaylord and Mehta, 1982, 1988) during the reaction or hindering the formation of an anhydride-Lewis acid adduct should DMF have a higher affinity for the metal. In the homogeneous reaction system, it was observed in all runs that the reaction for the first two

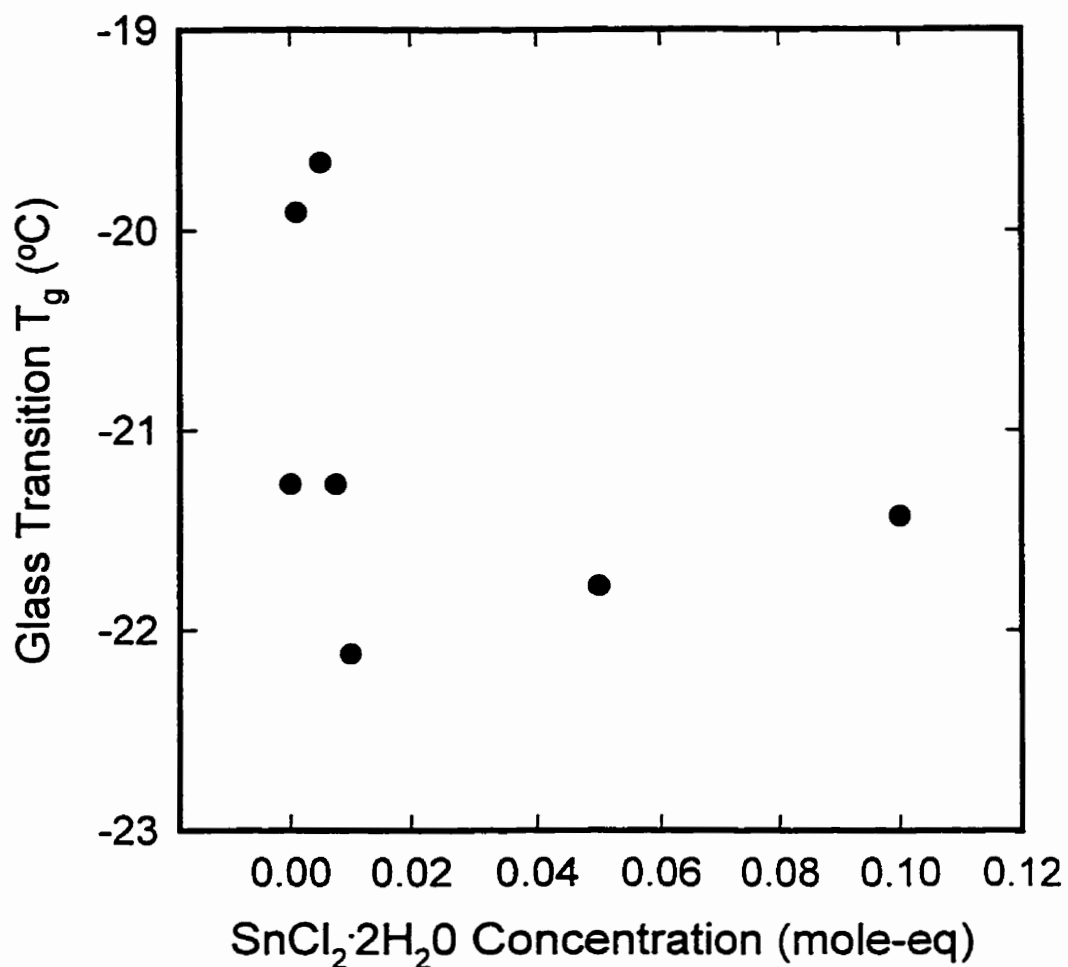


Figure 6.17. Effect of Lewis acid concentration on the glass transition temperature of the Alder Ene product.

minutes exhibited a slower rate than for subsequent times. This occurrence was more easily observed at higher temperatures where the rate of reaction changed more dramatically after this “induction period”. This trend was not observed in the uncatalyzed reactions leading us to believe that this “induction period” corresponded to the formation of the enophile adduct, a process much slower than originally anticipated. Once sufficient adduct was present in the reaction system, the rate of reaction increased leading to improved incorporation of the

anhydride as seen in Figures 6.18 through 6.20. This phenomenon was also not observed in the heterogeneous system, presumably due to further mass transfer/interfacial limitations between maleic anhydride and the catalyst which are not present to the same extent in the case with the catalyst being dissolved into DMF.

In the first two minutes of the reaction at the highest temperature examined (240°C), during the “induction period”, the extent of reaction was very similar for all concentrations of

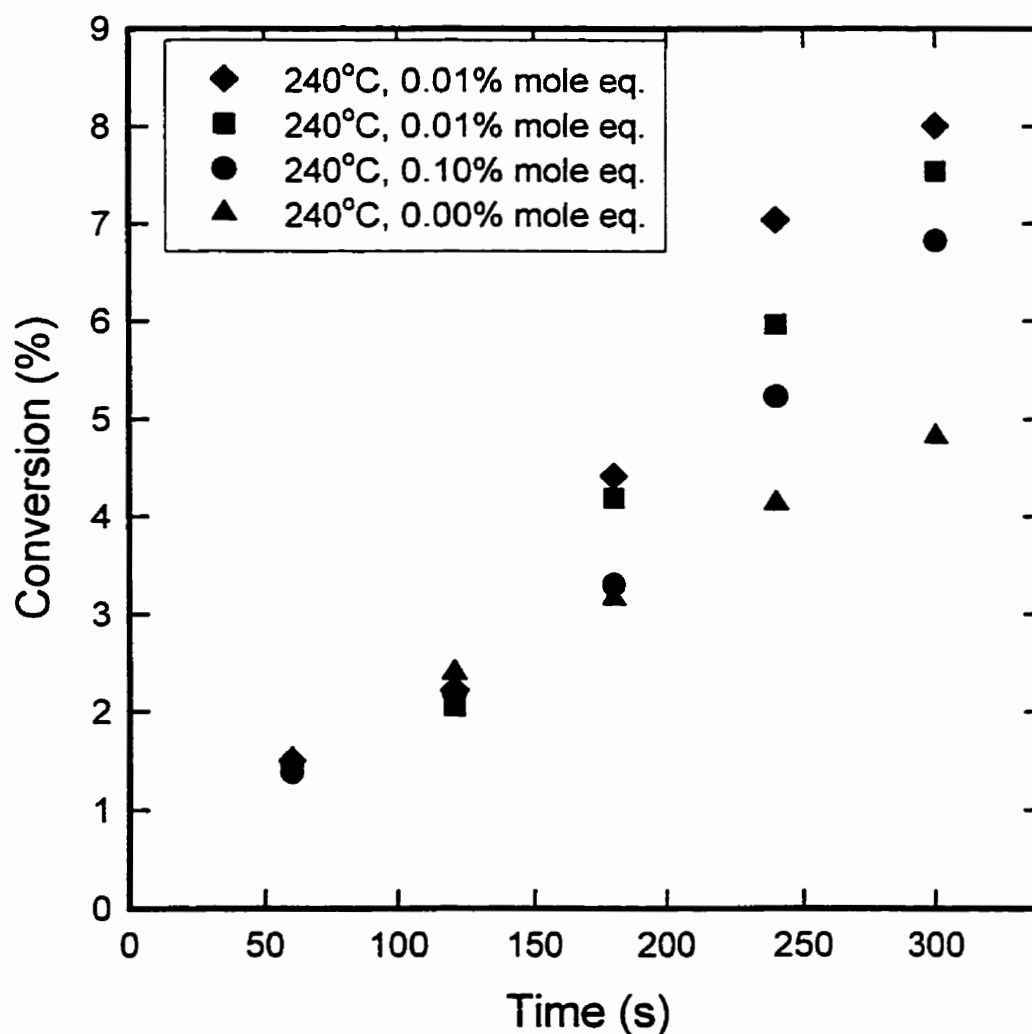


Figure 6.18. Varying the $\text{SnCl}_2 \cdot 2\text{H}_2\text{O}$ concentration for reactions using 2.7 mole eq. maleic anhydride at 240°C.

the Lewis acid in the homogeneous reaction system (Figure 6.18). Figure 6.18 shows the similarity in conversion for catalyst concentrations of both 0.01 and 0.1 % mole eq. $\text{SnCl}_2 \cdot 2\text{H}_2\text{O}$ at 240°C. At 220°C, the optimal homogeneous reaction system was immediately discernible. As seen in Figure 6.19, the 0.01 % mole eq. catalyzed reaction produced the highest amount of anhydride incorporation, while there was no distinction between the higher catalyst concentration (0.1 %) and the uncatalyzed reaction product. The

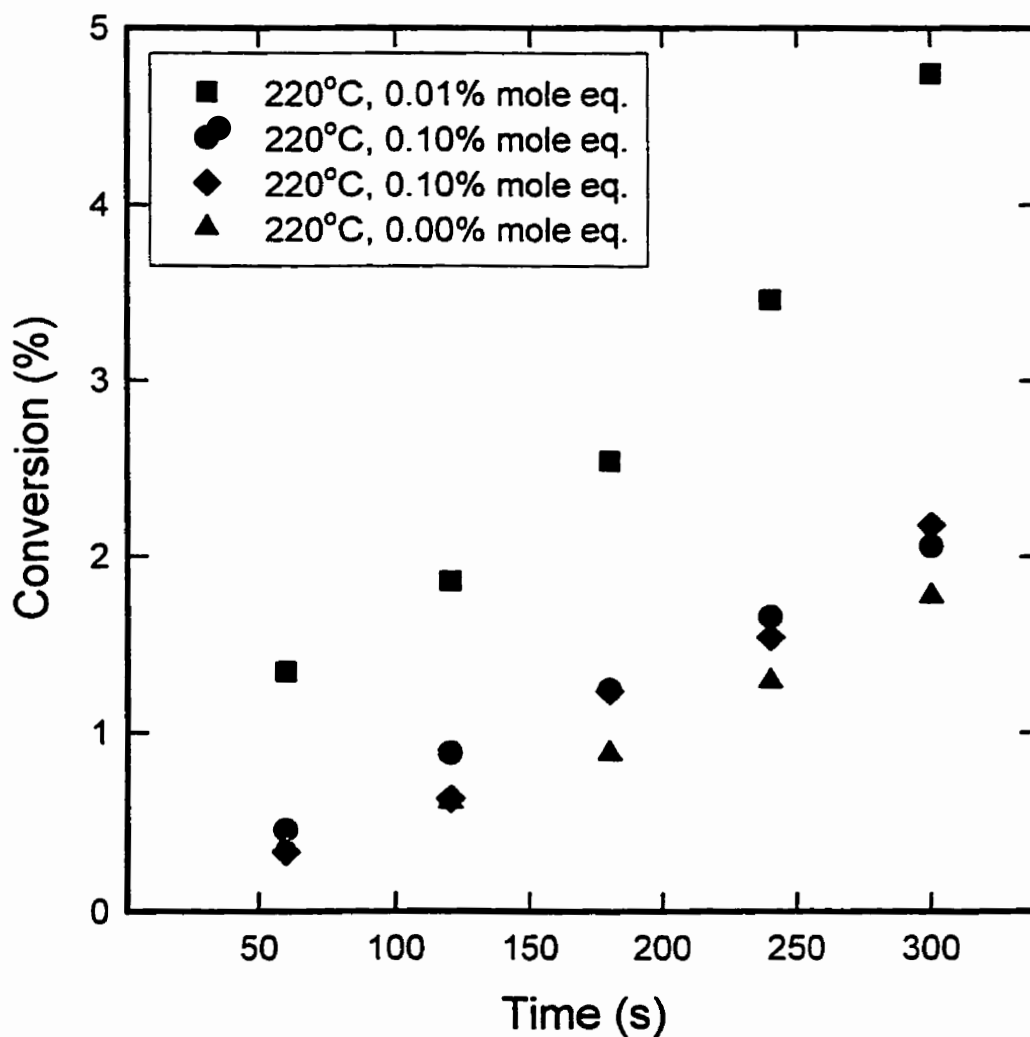


Figure 6.19. The effect of $\text{SnCl}_2 \cdot 2\text{H}_2\text{O}$ concentration at 220°C for the reaction using 2.7 mole eq. maleic anhydride.

“induction period” was less visible in Figure 6.19 since the rate of reaction did not change dramatically after the first two minutes, although it was discernible from those values corresponding to the reaction using 0.01 % mol-eq. Lewis acid. Therefore, temperature was not a factor in the duration of the “induction period”, simply the period reflected the rate of the uncatalyzed reaction for each temperature till sufficient Lewis acid-anhydride enophilic species had been generated to change the energetics of the reaction.

For all temperatures, the 0.01 % catalyst concentration yielded improved succinyl anhydride incorporation compared to 0.1 % for the same maleic anhydride concentration as shown in Figure 6.20, with differences being more significant at temperatures below 240°C. Presumably less side reactions, i.e. anhydride homopolymerization and vinylidene isomerization, were taking place at the milder reaction conditions.

The catalyst concentration was also observed to have an effect on the poly (maleic anhydride) particulate content. As the concentration of the catalyst was increased, the quantity of black particulate at the bottom of the reactor was noticeably reduced. Presumably, such observations could infer that the Lewis acid-anhydride adduct was not susceptible to free radical reactions, inhibiting the generation of anhydride excimers which have been discussed in section 6.5.1. Unfortunately, further examination of this interesting facet of the Lewis acid-anhydride adduct was beyond the intended scope of this work, though, analytical analysis of this phenomenon could be performed with the use of high temperature electron spin resonance (ESR) spectroscopy. These opposing effects of the Lewis acid on the FT-IR measured succinyl anhydride concentration (since polymeric maleic anhydride will contribute to the 1792 cm^{-1} absorbance which was used as an indicator of

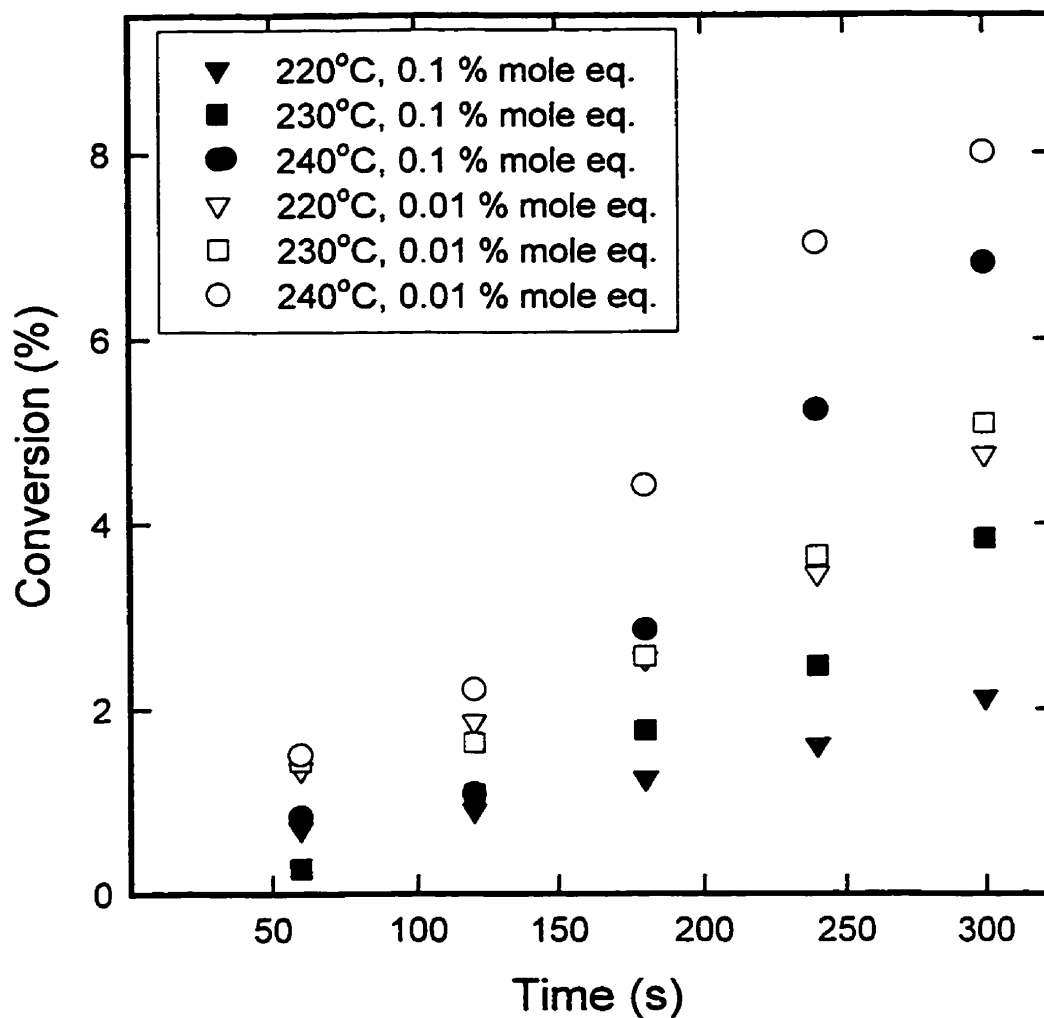


Figure 6.20. Effect of temperature and $\text{SnCl}_2 \cdot 2\text{H}_2\text{O}$ concentration on the reaction conversion at 2.7 mole eq. maleic anhydride.

succinyl anhydride attachment) could explain the minimum relative absorbance observed in Figure 6.21 at 230°C. The value shown in Figure 6.21 for 0.05 % mole-eq. stannous chloride could not have been an artifact due to the reproducibility observed in the homogeneous experiments. The reproducibility in data (as seen in Figure 6.21) was relatively high compared to those results presented in Figure 6.13 for the heterogeneous system. There was less chance for experimental error in the homogeneous method.

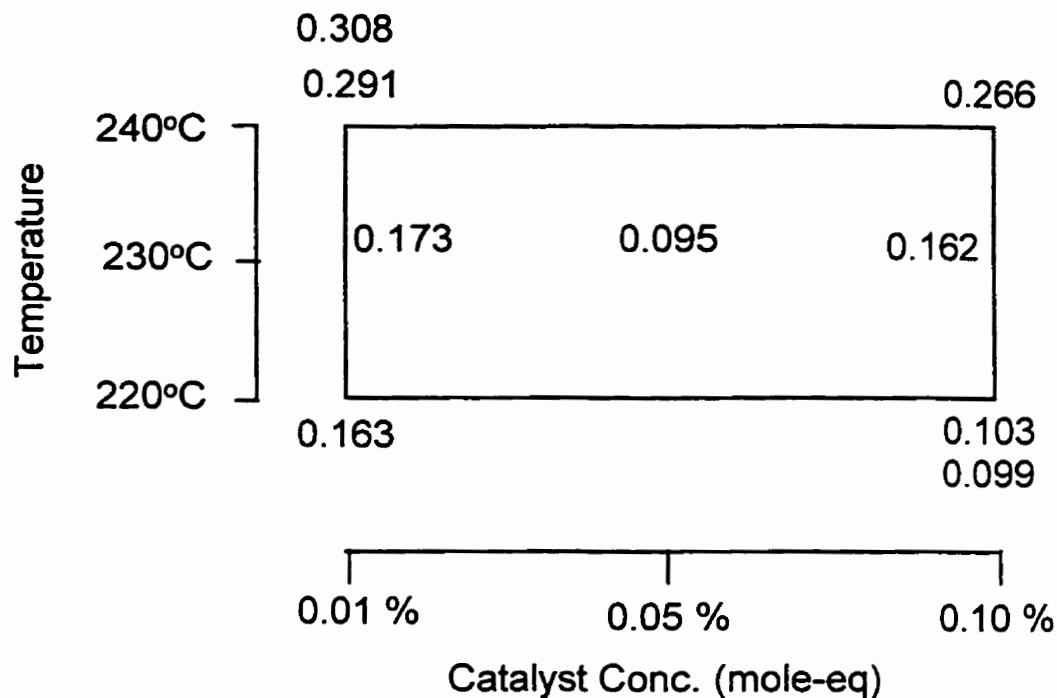


Figure 6.21. Relative succinyl anhydride absorbance values of 2.8 mol-eq MAh homogeneous system using Polypol-19 after a 5 min reaction

From all analysis techniques, the presence of a catalyst appears to be valuable in this type of reactive modification of polypropylene.

6.5.3. Isomerization

Given the low extent of reaction, the major source of double bonds pertained to the unreacted polypropylene, and therefore, it was reasonable to attribute fluctuation in the vinylidene absorbance to isomerization instead of isomeric double bond generation via the Alder Ene reaction. Figure 6.22 shows the variance in the vinylidene group IR absorbance for reactions performed both in the presence of maleic anhydride (0, 0.01 and 0.1% mole eq. $\text{SnCl}_2 \cdot 2\text{H}_2\text{O}$ based on 2.7 mole eq. maleic anhydride) and in the absence of maleic anhydride (0.05 and 0.5% mole eq. $\text{SnCl}_2 \cdot 2\text{H}_2\text{O}$ based on similar reactant ratios). Considering the

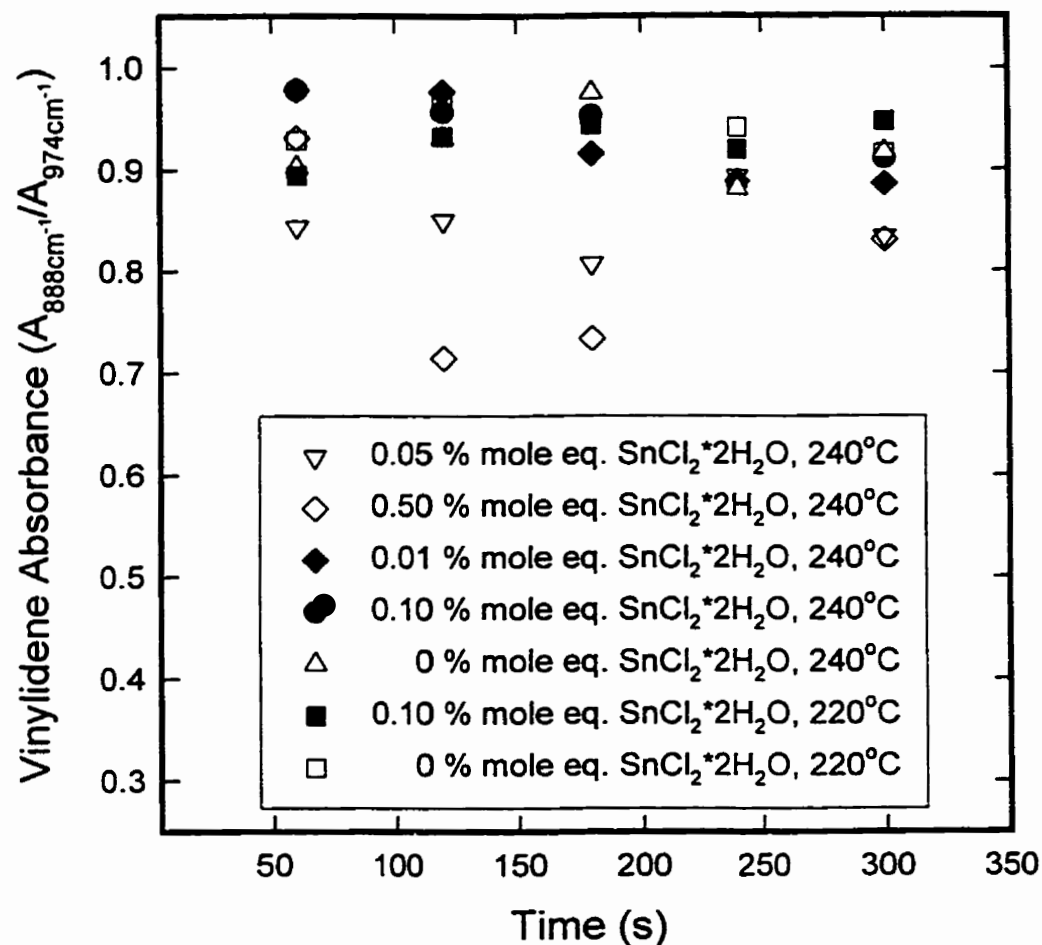


Figure 6.22. Variance in the relative vinylidene infrared absorbance due to isomerization as it is affected by temperature and catalyst concentration (no maleic anhydride present in reactions using 0.05 % and 0.5 % mole eq. SnCl₂·2H₂O).

measurement variance and sample homogeneity variance on the vinylidene group absorbance (Box et al., 1978), which were determined to be 5.679×10^{-5} and 1.112×10^{-4} respectively on an average infrared measurement of 0.476, it may be concluded that the scatter in the measured vinylidene group absorbance was not an artifact of the analysis technique. The scattering of absorbance results was greatest at higher temperatures and for those reactions with a higher concentration of catalyst (0.5 % mole eq. SnCl₂·2H₂O). Clearly, monitoring

vinylidene concentration would not be useful for kinetic rate estimation. Furthermore, kinetic rate constants based on this reaction system can be anticipated to be less reliable at higher temperatures and higher catalyst concentrations.

6.6. HIERARCHICAL DESIGN FOR ERROR ANALYSIS OF THE IR METHOD

The previous sections have disclosed the sensitivity of the different methods of quantifying succinyl anhydride content, revealing the FT-IR method as the most sensitive method available. To reveal the most significant source of variance in the IR measurement of the succinyl anhydride group, a hierarchical design (Box et al., 1978) was used. Three sources of variance were analyzed in the hierarchical design, i.e. experimental repeats, sample homogeneity with regards to creating polymer films, and infrared measurement of the film. To determine if the manner which the catalyst was added to the reaction affected the product, samples of both method were analyzed individually and compared. Table 6.4 presents the average response (i.e. relative succinyl anhydride absorbance) and the pooled estimates of variance for the different factors. Each factor was represented by a letter according to those designated by Box et al. (1978): batch (B), sample homogeneity (S), and IR measurement (T).

Table 6.4. Results of the Hierarchical Analysis

Variable	Solid Addition of Catalyst	Solution Addition of Catalyst
Response, \bar{Y}	1.28×10^{-1}	8.36×10^{-2}
batch variance, σ_B^2	1.76×10^{-3}	1.58×10^{-4}
sample variance, σ_S^2	1.80×10^{-4}	2.38×10^{-4}
testing (IR) variance, σ_T^2	4.86×10^{-5}	3.04×10^{-5}

Variance in the infrared measurements proved to be an order lower in magnitude compared to the other two factors, testifying to the good reproducibility of the spectroscopic technique and its instrumentation. Both batch-to-batch variance and sample homogeneity exhibited similar values of variance in the hierarchical design from those experiments using catalyst in solution. However, experiments using the solid catalyst method demonstrate considerably more variance in batch-to-batch reproducibility possibly due to the complications involved in complete addition of the solid catalyst from its bucket and consistency in weighing the species at low masses. Regardless of the differences between the two methods of catalyst addition, the variance of the three tested factors were quite low. These findings provide some confidence to the kinetics analysis in the following section, where the majority of all calculations were made using the infrared method of succinyl anhydride measurement.

6.7. KINETICS OF THE ALDER ENE REACTION

The kinetics of the Alder Ene reaction for maleic anhydride with various alkenes has been reported (Benn et al., 1977) to be second-order overall, first order with respect to the individual reactants. A second-order rate constant could be obtained for the succinyl group by plotting $\ln\left(\frac{\Theta - X_{\text{succinyl}}}{\Theta(1 - X_{\text{succinyl}})}\right)$ versus time, where X_{succinyl} is the mole fraction of anhydride in the product and Θ is the mole ratio of maleic anhydride with respect to vinylidene. Figure 6.23 presents the IR spectra of a single experiment sampled every minute for 5 minutes. It was characteristic to observe the vibration band at 1784 cm^{-1} remain essentially constant throughout the experiment, while the succinyl anhydride band at 1792 cm^{-1} increased. The exact nature of the 1784 cm^{-1} band was not understood, particularly

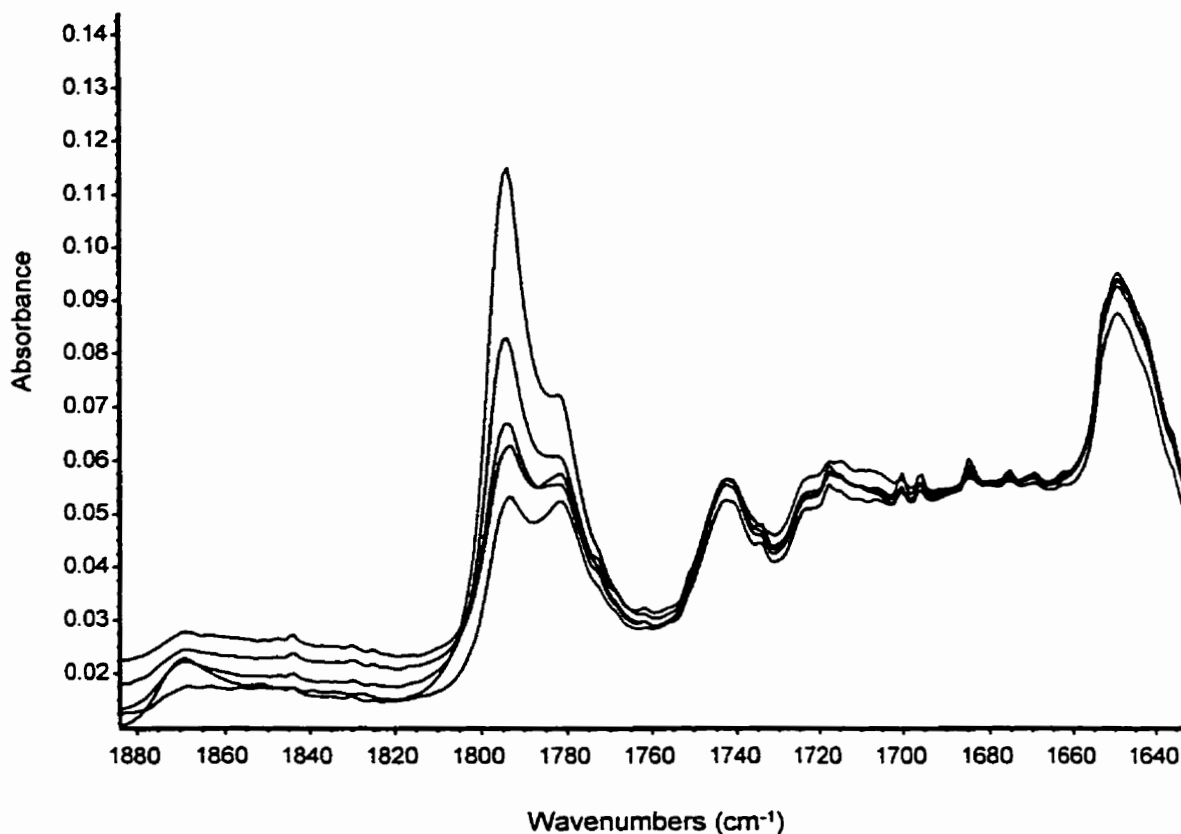


Figure 6.23. FT-IR monitored reaction with increasing succinyl concentration in minute increments (lowest peak at 1792 cm^{-1} corresponds to 1 minute elapsed, 2, 3, 4, highest peak at 5 minutes).

since it was immediately present, which could indicate a rapid free radical reaction such as homopolymerization. However, the band did not increase significantly over time which casts doubt into what role homopolymerization actually plays. Clearly, the interpretation of mechanical coupling among these bands does not fully describe the nature of the anhydride functionality. Figure 6.24 shows the FT-IR data for the sample run with a 0.005 mole equivalence $\text{SnCl}_2 \cdot 2\text{H}_2\text{O}$ with respect to maleic anhydride (heterogeneous). The correlation constant, R^2 , for a linear fit to the data was 0.99. In fact, only two samples, 0.05 and 0.10

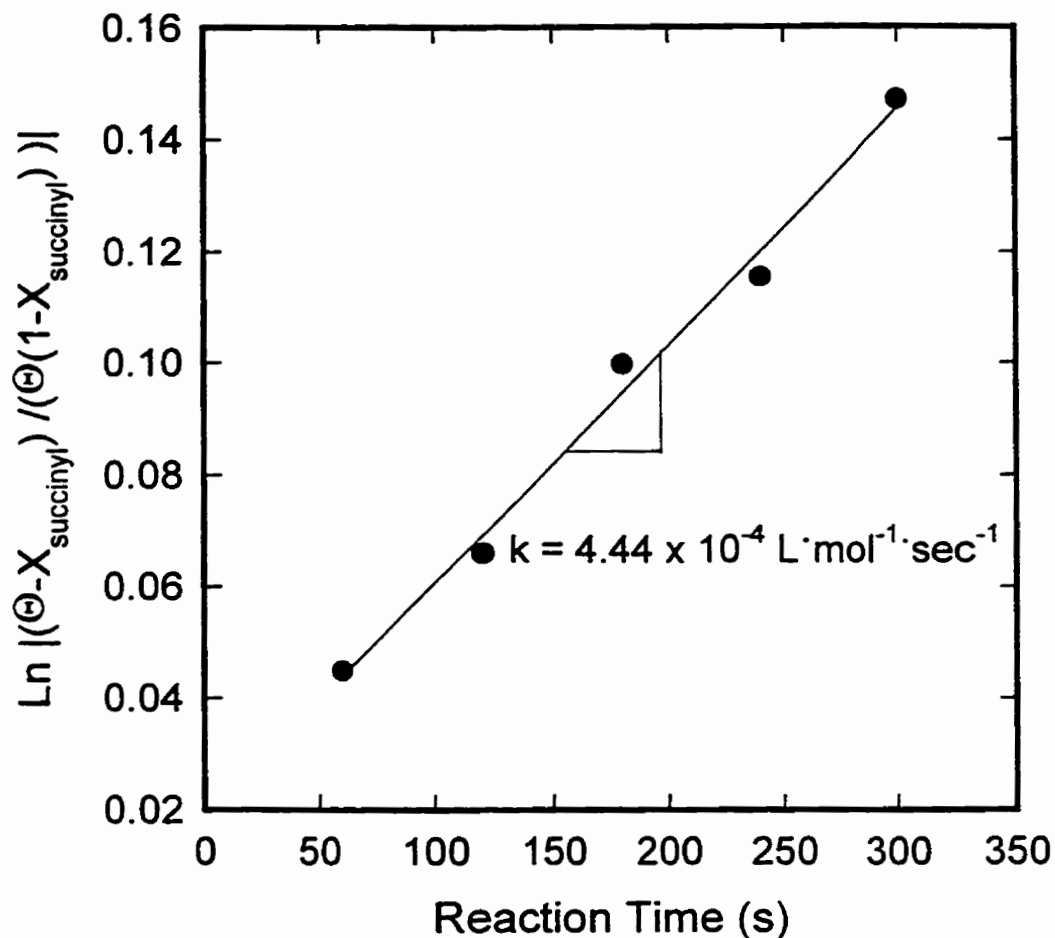


Figure 6.24. Best linear fit to FTIR measurements assuming second-order reaction kinetics.

mole equivalence Lewis acid, out of the entire heterogeneous series, examining different catalyst concentrations gave a correlation constant dramatically less than 0.98 (0.45-0.5). This observation indicates that Lewis acid concentrations significantly larger than the optimum, deviate from second-order kinetics denoting reactions aside from the Alder Ene reaction are occurring. Figure 6.25 presents the rate constants calculated for the series including their 95% confidence interval, excluding the higher acid concentration rate constants which strongly deviated from a second-order system. Figure 6.25 includes the

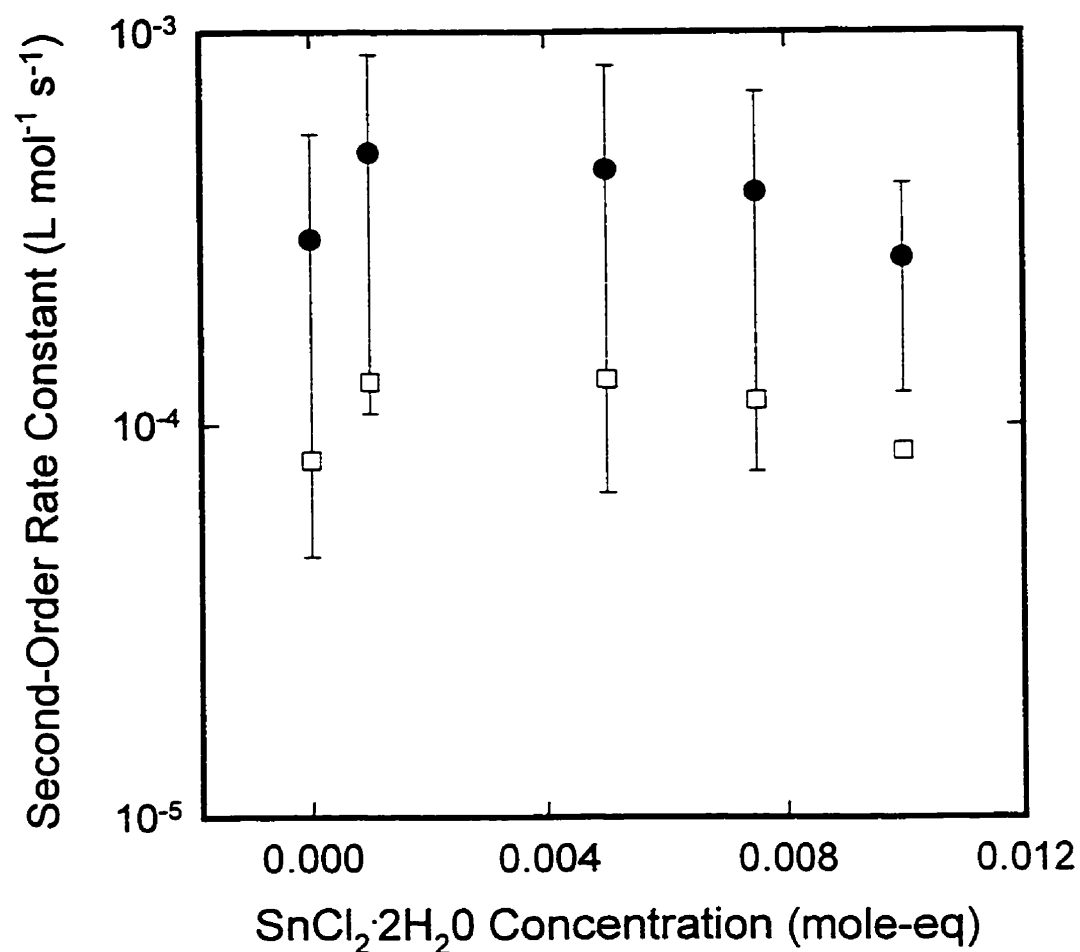


Figure 6.25. Second-order rate constants for the catalyzed Alder Ene reaction (95% confidence interval error bars). Determined from titration data (circles) and FT-IR data (squares).

second-order rate constants determined using FT-IR data, which shall remain the method of calculation for subsequent kinetics analysis. These values from the FT-IR method are consistently lower (eg. $4.44 \times 10^{-4} \text{ L mol}^{-1} \text{ s}^{-1}$ for the titration method at 0.5 %, 230°C became $1.307 \times 10^{-4} \text{ L mol}^{-1} \text{ s}^{-1}$ using eqn. 4.7), however, they remain within the confidence interval of the titration data with the exception of the constant value for 0.01 mole-eq. SnCl₂.

For the heterogeneous series, calculation of the activation energy was done at 0.005 mole-eq. Lewis acid. The conversion data for the heterogeneous catalyzed system and those

runs performed without Lewis acid, could be used to fit to a second-order kinetic model with all cases giving a covariance coefficient, R^2 , better than 0.85. To achieve a reasonable fit with the second-order kinetic model (eqn. 4.9) to the homogeneous reaction data, only the latter four time values (i.e. 120 - 300 s) were used in estimating the reaction rate constant. The rate of the reaction was greatest for the catalyst concentration of 0.01 %, and while 0.1 % was significantly greater than the uncatalyzed reaction, there was little benefit in running

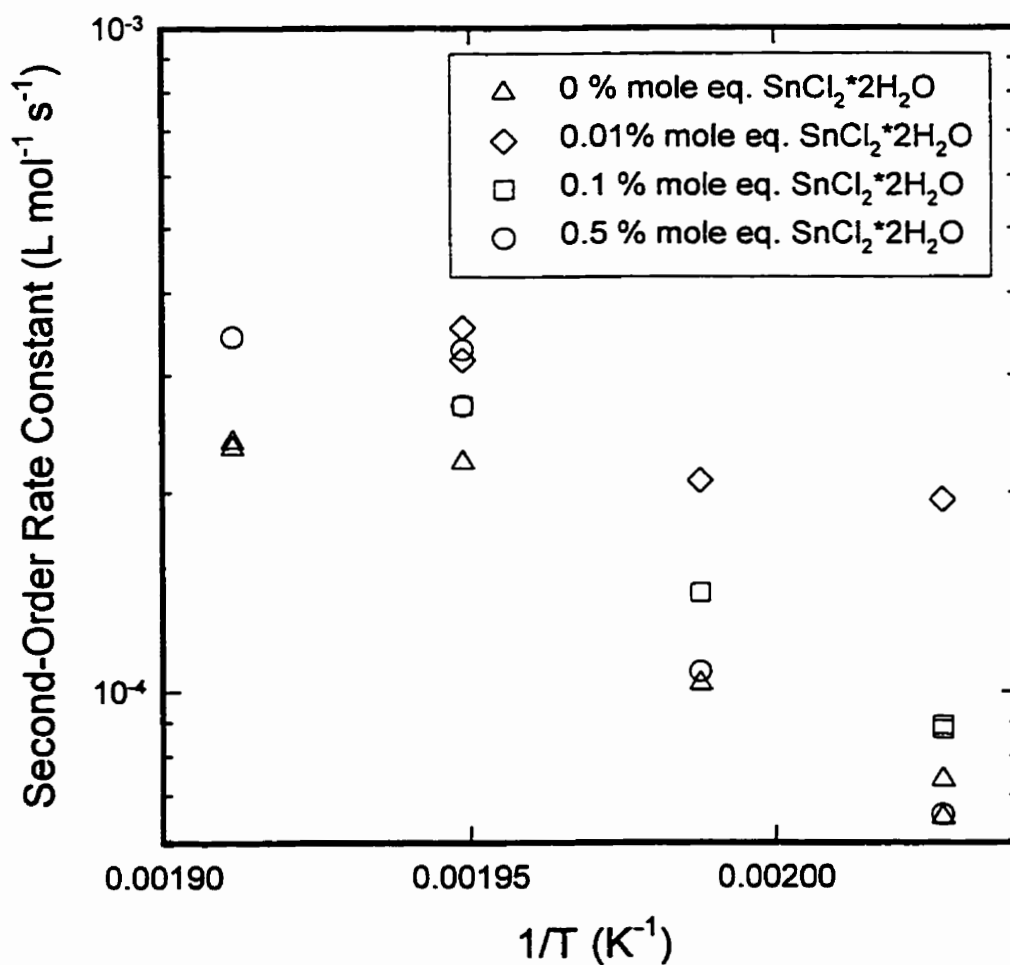


Figure 6.26. Plot of second-order kinetic rate constants versus temperature for four catalyst concentrations in the reaction of maleic anhydride with the vinylidene of polypropylene.

with a catalyst at this concentration (Figure 6.26). Standard error in the rate constant for the homogeneous reaction system was estimated to be 9% based on repeats, while in the heterogeneous system, the standard error was 15% indicating a greater lack of homogeneity in the product from the heterogeneous system corroborating the findings of the hierarchical experiment discussed in section 6.6. As the temperature was increased, the benefits of the catalyst appeared to be much lower, presumably due to interference from poly(maleic anhydride) formation and isomerization. No conclusions could be properly drawn for rates at 240°C and higher. Indeed, the kinetic plot (Figure 6.26) shows that there was no linear relationship for the rate constant between temperatures of 220°C and 240°C. Estimated activation energy for different catalyst concentrations are shown in Table 6.5, however, confidence in these calculated activation energy values was generally poor as demonstrated by the standard error with the exception of those runs using 0.1% mole eq. $\text{SnCl}_2 \cdot 2\text{H}_2\text{O}$. Benn et al. (1977) have shown that the activation energy of the Alder Ene reaction should be in the region of 90 KJ /mol for small alk-1-ene molecules (olefins between C_6 and C_{12}). These findings, in comparison to our activation energies calculated for high molecular weight species, lend some confidence to the given values since the viscosity of the present reaction system would lead to higher activation values. This leads to the point that the kinetic rate

Table 6.5. Estimated activation energies for different catalyst concentrations

Catalyst Concentration (% mole eq.)	Activation Energy (J/mol)	Standard Error (J/mol)
0	91896	11055
0.01	60561	17560
0.1	115430	7637
0.5	133554	24449

constants and activation energies calculated are not absolute values and they probably include mass-transfer limitations. However, the choice of Polypol-19 was made on the premise of minimizing viscous mixing issues. A sufficiently low molecular weight polypropylene will exhibit flow characteristics similar to wax at room temperature and possess a viscosity near water at high temperature (for example, $\log \eta(\text{Pa}\cdot\text{s})=2.573-0.04337\cdot\log[T(\text{Kelvin})]$, data supplied by Crowley Chemical). A material which possesses this rheological character should ensure that kinetic phenomenon pertaining to the Alder Ene reaction are not significantly diffusion dependent.

6.8. STANNOUS CHLORIDE VS. RUTHENIUM CHLORIDE

Ruthenium chloride is a mild catalyst like $\text{SnCl}_2\cdot 2\text{H}_2\text{O}$ and has been typically used above 200°C . Its insensitivity to the presence of water (Alderson et al., 1965) makes its use relatively simple compared to Lewis acids such as AlCl_3 , TiCl_4 , SnCl_4 and even $\text{SnCl}_2\cdot 2\text{H}_2\text{O}$ where the presence of moisture must be avoided.

Ruthenium chloride was compared to stannous chloride in a set of reactions at 240°C . The catalysts (0.05 % mole equivalence with respect to maleic anhydride) were dissolved in 20 μL of either alcohol for the ruthenium chloride species (1-dodecanol, Aldrich Chemicals) or DMF for stannous chloride, and added to 2.7 mole equivalence of molten (70°C) maleic anhydride with respect to vinylidene present in the polypropylene. Samples were collected every minute for 5 minutes in the manner discussed in the experimental section (4.2.2). No ester absorption was observed in the IR of the product despite alcohol being present with an anhydride. No evidence of significant grafting of poly(maleic anhydride) was seen in the infrared spectra of the ruthenium chloride product, despite the lack of DMF in the reaction.

The calculated conversion upon completion of the reaction was 9.66 % (ruthenium chloride) and 7.32 % (stannous chloride). Comparison of the kinetic rate constant using a second-order rate equation showed that ruthenium chloride (2.755×10^{-4} L/mol s) provides significant rate enhancement with respect to stannous chloride (1.933×10^{-4} L/mol s). The robustness of ruthenium chloride towards moisture is a useful property with regards to a catalyst for the Alder Ene reaction, and its improved reaction rate compared to stannous chloride based on the kinetics of the system, demonstrate its advantage.

6.9. CONCLUDING REMARKS

An anhydride terminated polypropylene was produced using a Lewis acid catalyzed Alder Ene reaction. It has been shown that the maleic anhydride incorporation onto the polymer was terminally positioned provided free radical reactions were inhibited. A stable free radical trapping species, TEMPO, has been found to be a useful inhibitor at concentrations in the region of 75-80 ppm, preventing the radical grafting of maleic anhydride onto the polymer backbone. The presence of a Lewis acid catalyst ($\text{SnCl}_2 \cdot 2\text{H}_2\text{O}$) was observed to have a catalytic effect for both heterogeneous and homogeneous reaction systems. With solid catalyst provided to the reaction, the maximum anhydride incorporation was observed at a stannous chloride concentration of 0.005 mole equivalence with respect to the maleic anhydride reactant. Among the homogeneous reaction experiments, the lowest catalyst concentration (0.01 % mole-eq.) examined, yielded the maximum anhydride incorporation, possibly indicating that even lower stannous chloride concentrations would bring about an even higher degree of conversion. In general, increased temperature and maleic anhydride concentration had a positive effect on improving the incorporation of the

succinyl anhydride moiety at the terminal site in polypropylene. Lower Lewis acid concentrations, likewise, improve the functionality of the product. Increasing the parameters of maleic anhydride and catalyst concentration appeared to have an inhibitive quality on the occurrence of homopolymerization of maleic anhydride. Finally, ruthenium chloride produces slightly improved levels of anhydride incorporation in polypropylene compared to stannous chloride.

The overall order for the rate equation governing the kinetics of the Alder Ene reaction was not shown to change due to the addition of a solid catalyst. However, it has been found that the use of a second-order kinetic equation was not valid over the entire time domain of the present homogeneous reaction system, unlike uncatalyzed and heterogeneous reactions. The induction period observed over the first two minutes of the reaction, was possibly due to the slow formation of the anhydride-Lewis acid adduct. Should this assumption prove valid then the catalyst of the heterogeneous reaction formed the adduct considerably slower. The formation would have been so slow that the adduct enophile had only a minor and gradually increasing contribution to the Alder Ene reaction compared to maleic anhydride being used as the enophile. Similarly, the mechanistic pathway was too complicated to apply a simple kinetic model to the Alder Ene reaction at temperatures beyond 230°C, particularly with side-reactions like isomerization and homopolymerization of the maleic anhydride demonstrating increasing dominance.

CHAPTER 7. MALEATION OF POLYPROPYLENE THROUGH REACTIVE EXTRUSION VIA THE ALDER ENE REACTION

7.1. INTRODUCTION

Three experimental designs were examined in this work. The first experimental design was a 2^{5-1} fractional factorial (Table 7.1) at a screw speed of 20 rpm and 20 g/min feed rate to identify the effects of several factors on the succinyl anhydride concentration, attributable to the reaction. The factors examined were vinylidene concentration, maleic anhydride concentration, stannous chloride concentration, barrel temperature and method of double bond generation. The second experimental design was a 2^4 full factorial (Table 7.2) examining the effect of mixing on the reaction conversion through the factors of screw speed and feed rate, and the contributions of catalyst concentration and the method of vinylidene generation. In this design, the maleic anhydride concentration was fixed at 4 mole eq. with respect to the vinylidene group and the barrel temperature was 210°C. These first two experimental sets used the same screw design (configuration 1 in Figure 4.7). Three additional experiments were run using screw configuration 1. The first run, denoted as 36G, attempted to dramatically increase the degree of channel fill by running at a feed rate of 40 g/min while the screw operated at 10 rpm. The temperature of the barrel was 220°C, and the reactants were PD100 (detailed in section 4.2.4.2), 4 mole eq. maleic anhydride and 0.05 % mol eq. SnCl_2 . Samples 37G and 38G used the same conditions as 9G and 12G respectively, however, the Lewis acid was now ruthenium chloride dissolved in 2-octanol.

The screw design used for the third experimental set (configuration 2 in Figure 4.7) was expected to increase the degree of channel fill within the intensive mixing regions. The

Table 7.1. Experimental set 1: Examining reaction parameters

Sample No. [‡]	Vinylidene Conc.	MAh Conc. (mole eq.) [*]	Temp (°C)	SnCl ₂ Conc. (% mole eq.) [†]	SAh Conc. (wt %)	Conversion (%)
1G ^t	4.92x10 ⁻⁵	2	200	0.01	1.67x10 ⁻²	3.45
2G ^t	2.33x10 ⁻⁵	4	200	0.01	1.47x10 ⁻²	6.44
3G ^t	2.33x10 ⁻⁵	2	220	0.01	1.49x10 ⁻²	6.52
4G ^t	4.92x10 ⁻⁵	4	220	0.01	2.65x10 ⁻²	5.48
5G ^t	2.33x10 ⁻⁵	2	200	0.05	1.45x10 ⁻²	6.32
6G ^t	4.92x10 ⁻⁵	4	200	0.05	2.10x10 ⁻²	4.35
7G ^t	4.92x10 ⁻⁵	2	220	0.05	2.16x10 ⁻²	4.48
8G ^t	2.33x10 ⁻⁵	4	220	0.05	1.60x10 ⁻²	6.99
9G ^p	3.01x10 ⁻⁵	2	200	0.01	1.53x10 ⁻²	5.20
10G ^p	4.84x10 ⁻⁵	4	200	0.01	1.80x10 ⁻²	3.80
11G ^p	4.84x10 ⁻⁵	2	220	0.01	1.80x10 ⁻²	3.80
12G ^p	3.01x10 ⁻⁵	4	220	0.01	1.80x10 ⁻²	6.11
13G ^p	4.84x10 ⁻⁵	2	200	0.05	1.67x10 ⁻²	3.51
14G ^p	3.01x10 ⁻⁵	4	200	0.05	1.62x10 ⁻²	5.50
15G ^p	3.01x10 ⁻⁵	2	220	0.05	1.74x10 ⁻²	5.90
16G ^p	4.84x10 ⁻⁵	4	220	0.05	2.14x10 ⁻²	4.51
17G ^t	2.33x10 ⁻⁵	4	200	0.01	1.48x10 ⁻²	6.47
(2G)						
18G ^t	4.92x10 ⁻⁵	2	220	0.05	1.98x10 ⁻²	4.11
(7G)						
19G ^p	4.84x10 ⁻⁵	2	200	0.05	1.61x10 ⁻²	3.40
(13G)						

* maleic anhydride mole eq. with respect to vinylidene concentration.

† stannous chloride mole eq. with respect to maleic anhydride concentration.

‡ sample superscript indicate degradation method: t=thermal, p=peroxide.

Table 7.2. Experimental set 2: Mixing performance

Sample No. ‡	Screw Speed (rpm)	Feed Rate (g/min.)	Catalyst Conc. (% mole eq.)*	SAh Conc. (wt %)	Conversion (%)
20G ^t	20	20	0.01	1.59x10 ⁻²	6.97
21G ^t	40	20	0.01	1.62x10 ⁻²	7.08
22G ^t	20	40	0.01	1.48x10 ⁻²	6.47
23G ^t	40	40	0.01	1.60x10 ⁻²	7.00
24G ^t	20	20	0.05	1.64x10 ⁻²	7.16
25G ^t	40	20	0.05	1.60x10 ⁻²	7.00
26G ^t	20	40	0.05	1.56x10 ⁻²	6.84
27G ^t	40	40	0.05	1.58x10 ⁻²	6.92
28G ^p	20	20	0.01	1.70x10 ⁻²	7.44
29G ^p	40	20	0.01	1.67x10 ⁻²	7.30
30G ^p	20	40	0.01	1.70x10 ⁻²	7.43
31G ^p	40	40	0.01	1.45x10 ⁻²	6.32
32G ^p	20	20	0.05	1.71x10 ⁻²	7.47
33G ^p	40	20	0.05	1.68x10 ⁻²	7.36
34G ^p	20	40	0.05	1.41x10 ⁻²	6.19
35G ^p	40	40	0.05	1.57x10 ⁻²	6.87

*stannous chloride mole eq. with respect to 4 mole eq. MAh.

‡ Sample superscript indicate degradation method: t=thermal, p=peroxide (lower vinylidene concentration used for both series)

kneading blocks in the second configuration were mostly left-handed as opposed to the use of neutral kneading blocks in the first screw configuration. Thus, the second screw design increased the residence time as well as mixing for the reaction. The third experimental design was developed from results of the previous two experimental sets. It was a 3³⁻¹ fractional factorial design (Table 7.3) examining the main factors of barrel temperature, catalyst concentration and maleic anhydride concentration. The screw speed and polymer

Table 7.3. Experimental set 3: Studying important reaction factors for non-linearity

Sample No.	SnCl ₂ Conc. (% mole eq.) [†]	Temp (°C)	MAh Conc. (mole eq.) [*]	SAh Conc. (wt %)	Conversion (%)
40G	0	210	1	1.82x10 ⁻²	3.78
41G	0	220	2	2.26x10 ⁻²	4.69
42G	0	230	3	2.37x10 ⁻²	4.92
43G	0.005	210	3	2.05x10 ⁻²	4.25
44G	0.005	220	1	1.82x10 ⁻²	3.78
45G	0.005	230	2	2.26x10 ⁻²	4.68
46G	0.01	210	2	1.84x10 ⁻²	3.81
47G	0.01	220	3	2.06x10 ⁻²	4.28
48G	0.01	230	1	1.97x10 ⁻²	4.08
49G (41G)	0	220	2	2.14x10 ⁻²	4.43
50G (41G)	0	220	2	2.22x10 ⁻²	4.61
51G(46G)	0.01	210	2	1.76x10 ⁻²	3.64
Coefficients [‡]	-0.21	0.31	0.30		4.26

* maleic anhydride mole eq. with respect to vinylidene concentration.

† stannous chloride mole eq. with respect to maleic anhydride concentration.

‡ regression coefficients for a 3³⁻¹ fractional factorial design

feed rate were fixed at 30 rpm and 30 g/min respectively. The only source of polypropylene was TD380 (detailed in Chapter 3) for the third experimental set.

7.2. RESULTS AND DISCUSSION

Due to the variance in the vinylidene group concentration among the different experimental sets, quoting the extent of reaction in terms of conversion of vinylidene groups would be more meaningful. The conversion will be calculated based on a ratio of the concentration of succinyl anhydride detected over the initial concentration of vinylidene in the polymer.

The difficulties in measuring functionalities below 1 wt % in polymer complicate the analysis of the modified polypropylene. However, it was necessary to determine the structure of the functional group attached to the polymer, whether it was terminally attached via the Alder Ene reaction or bound along the backbone due to free radicals present due to oxidation. To assist structural analysis, each maleated sample of the third experimental set, i.e. 40-48G, was reacted with 1-hexadecylamine (Aldrich Chemicals) in refluxing xylene under a nitrogen blanket for 2 h. It was hoped that by increasing the size of the functionality, discerning the anhydride attachment site would become easier. Full conversion was confirmed by the disappearance of the succinyl anhydride vibration in the infrared spectra. However, the presence of imide, carboxylic acid and amide groups were detected indicating that not all attached chains proceeded to the imide functionality. For comparison, a sample of TD380 (55E) was maleated for 24 h at 190°C in 1,2,4-trichlorobenzene followed by chain extension via 1-hexadecylamine in the manner described above. Characterization of the maleated form of 55E, prior to chain extension, was not necessary since the structure of a terminally functionalized polymer has already been performed previously (Thompson et al., 1998b). This sample is compared to the other chain extended ones in later sections. The question that needed structural confirmation was whether maleation was exclusively achieved through the Alder Ene reaction or if the presence of oxygen due to the partially filled channel of a twin screw extruder, was sufficient to lead to backbone grafting.

To properly identify a material referenced in this chapter, each sample designation shall be included, although, the actual reaction conditions by which it was produced will not be included for ease of reading. The reader is referred to the tables in this chapter to determine the conditions at which each sample was produced.

7.2.1. Characterization of Maleated Polypropylene

7.2.1.1. Molecular Weight Distribution

Figure 7.1 shows the molecular weight distributions (MWD) of two degraded polymers (TD380 and PD075) and four maleated species for each of the two degraded polypropylenes. The distributions for the maleated polymers showed no significant difference from the unmodified material. This was the case for all modified polymers

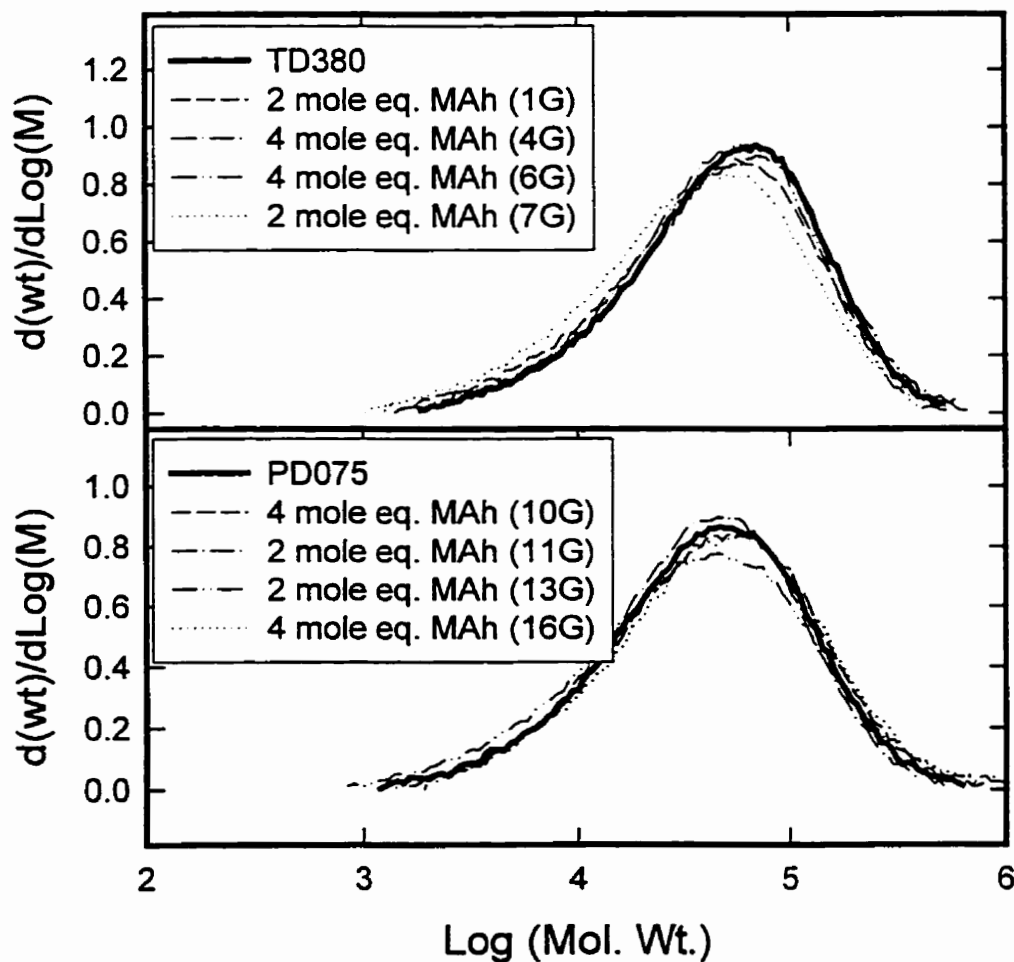


Figure 7.1. Effect of maleic anhydride concentration on the MWD of the maleated polypropylenes.

including several repeated MWD measurements. Thus, the occurrence of β -scission was minimized during extrusion despite the presence of oxygen. Also, these observations indicated that neither degradation method exhibited a greater susceptibility to chain transfer from the maleic anhydride species. Based on the findings, it is arguable that free radical grafting of maleic anhydride did not significantly occur since the degree of scission should have been related to the concentration of maleic anhydride reactant due to its propensity to initiate β -scission through the chain transfer reaction.

The usefulness of the chain extended samples to distinguish the manner by which the maleic anhydride was attached to the polymer was based on their individual reaction mechanisms. Maleation via the Alder Ene reaction will be greatest among polymer chains of lower molecular weight where there are more reactive sites and an improved chance of polymer/comonomer interaction. Therefore, maleated polymer produced through the Alder Ene reaction reacted with hexadecylamine attachments should bring about a measurable change to the lower molecular weight fraction of the polymer distribution. Maleation via free radical grafting, based on hydrogen abstraction from the polymer backbone, is a random process statistically favouring higher molecular weight chains of a polymer distribution provided we accept the notion that the anhydride group reacts with a tertiary macroradical opposed to a primary macroradical. Thus, branching through reaction of the radical-grafted maleated polymer with hexadecylamine would bring about the majority of change to the weight fractions in the high molecular weight region of the distribution. Figure 7.2 compares two chain extended polymers (41E and 47E) against their maleated counterpart and sample 55E as an example of the effects of high maleation through the Alder Ene reaction.

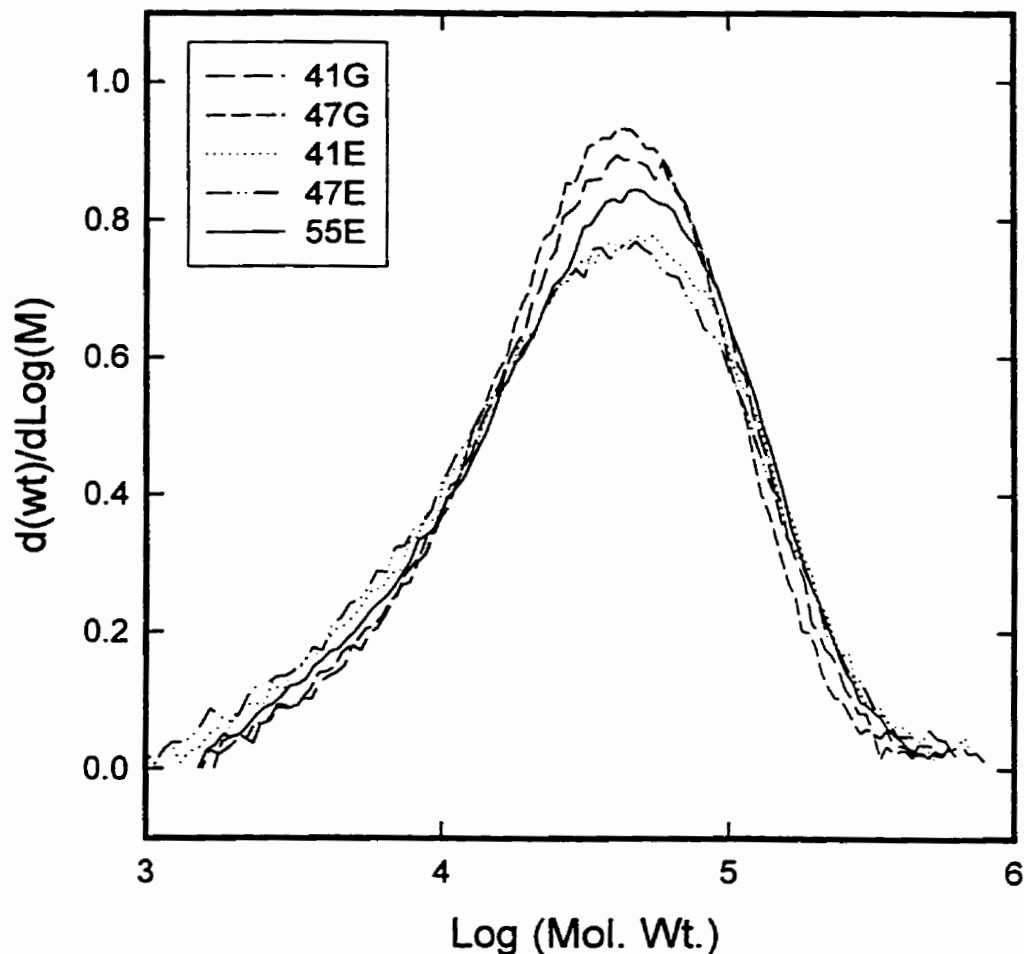


Figure 7.2. Differences in the MWD between two maleated polypropylenes (41 and 47G) and their hexadecylamine grafted counterparts (41 and 47E). Sample 55E was a highly maleated polypropylene sample grafted with hexadecylamine, used for comparison.

Examining the MWDs in Figure 7.2, the low end fraction of both chain extended samples is slightly increased compared to their maleated counterparts. Also, sample 55E does show the expected change in the weight fraction of the low molecular weight chains, lower than samples 41E and 47E since the higher molecular weight fraction would also have been increased. Unfortunately, the error attributed to the measured distributions from the GPC does not provide significant differentiation between the MWDs.

The presence of KF6100 polypropylene in the diluted samples produced a shoulder in the main distribution (as shown in Figure 7.3). The high molecular weight shoulder in the distribution will significantly increase the viscosity of the polymer, affecting the degree of mixing and the solubility of maleic anhydride in the molten material. The effect of viscosity on the reaction shall be discussed in subsequent sections, however, the higher molecular weight tail should have been more susceptible to chain degradation. Figure 7.3 overlays the MWD of four maleated polypropylene from Table 7.2, chosen to represent the

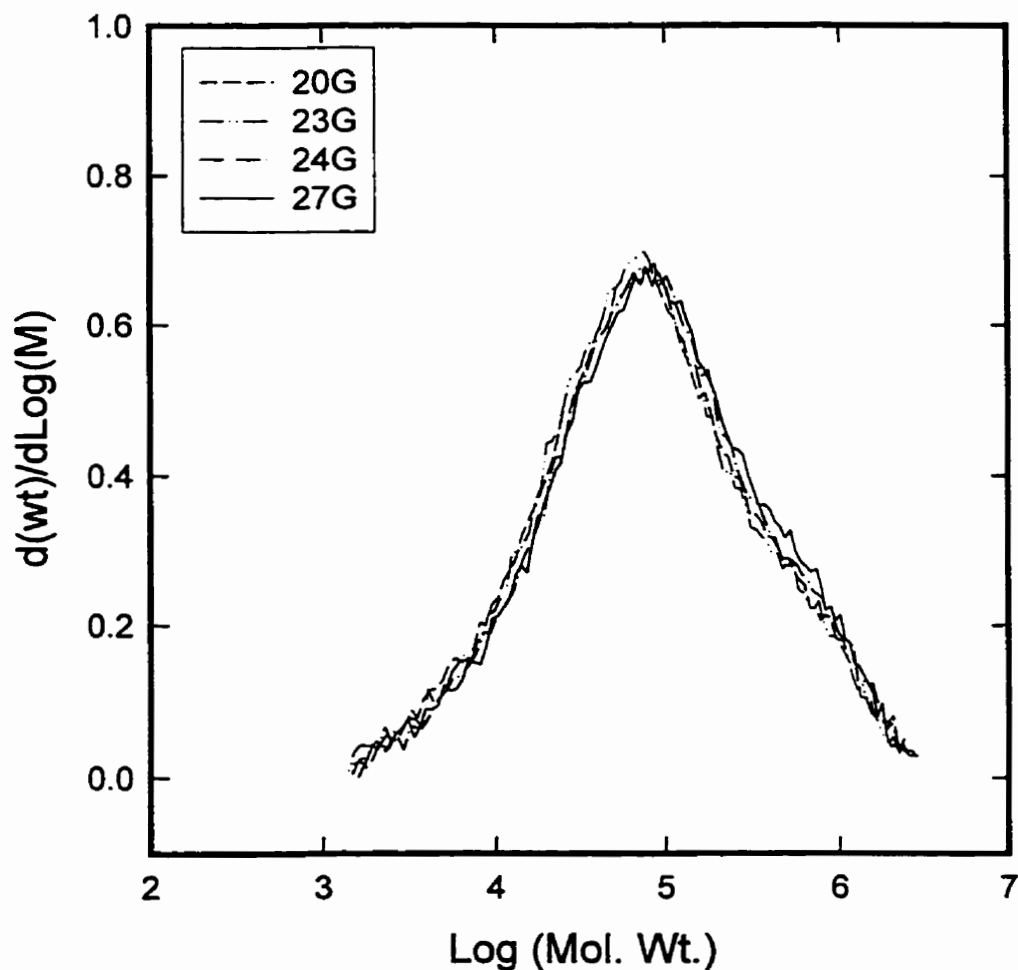


Figure 7.3. Effect of processing conditions on the MWD of the maleated polypropylenes.

extreme cases of screw speed, feed rate and catalyst concentration employed. Fortunately, it appeared that the molecular weight distribution remained unchanged.

7.2.1.2. Infrared Analysis

Figure 7.4 shows four maleated polypropylenes, samples 9G and 12G produced in the presence of stannous chloride and samples 37G and 38G, produced in the presence of ruthenium chloride. The anhydride absorbance at 1792 cm^{-1} was quite small and the corresponding 1865 cm^{-1} vibration was not detectable. The structure of the succinyl

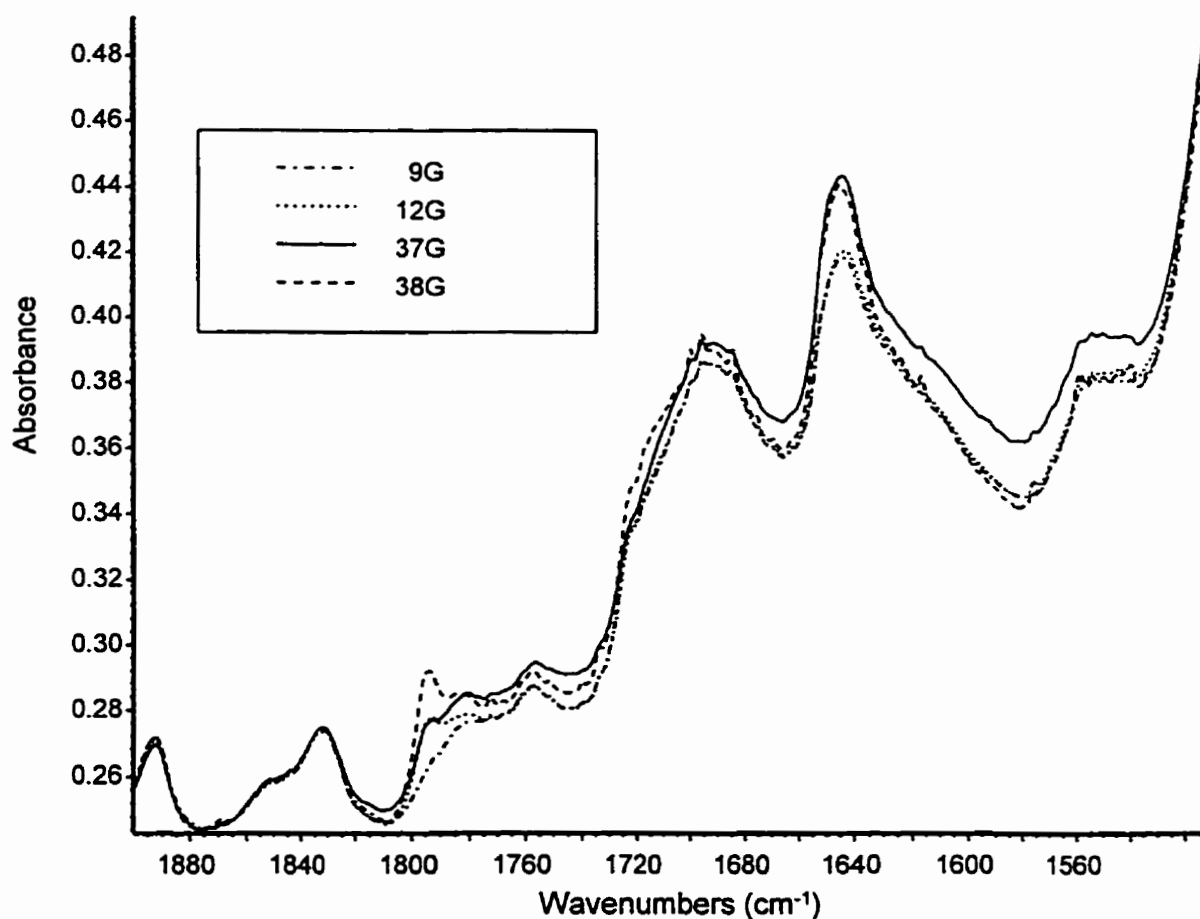


Figure 7.4. Carbonyl region of the FT-IR spectra for several maleated polypropylenes produced in the presence of either stannous chloride (9 and 12G) or ruthenium chloride (37 and 38G).

anhydride moiety was best determined from the maleated polypropylene with the highest succinyl anhydride incorporation, i.e. sample 38G where the 1784 cm^{-1} anhydride vibration appeared as a shoulder in the 1792 cm^{-1} peak. Both 1792 cm^{-1} and 1784 cm^{-1} vibrations are attributed to mechanical coupling of the carbonyl stretching modes within the anhydride (Marquardt, 1966) as discussed in Chapter 6. Therefore, maleic anhydride bound as single, isolated units should show a stronger high frequency band than low frequency band unless high localized concentrations of anhydride exist. Grafts of poly(maleic anhydride), if present in the polymer chain, would favour the low frequency band. Conversion among all experimental sets varied between 3-7 % based on the infrared calibration curve (eqn 4.7). It was due to the low concentration of succinyl anhydride in the product that classical titration methods could not be used to quantify the extent of reaction.

7.2.1.3. NMR Analysis

Due to the low concentration of succinyl anhydride bound to the polypropylene chain, ^{13}C NMR yielded no information concerning the structure of the anhydride moiety. Consequently, any analysis of the maleated samples had to be based on proton analysis. Figure 7.5 shows the ^1H NMR spectra for the maleated 42G sample and its chain extended counterpart, sample 42E. Peak assignments for the polypropylene backbone lie between the region of 1-2 ppm. The terminal vinylidene was characterized by two fully resolved peaks at 4.76 ppm and 4.81 ppm corresponding to the two hydrogens at the chain end. Evidence of the alkyl segment of the hexadecylamine chain extender, was seen as two small doublets at 0.8 and 1.2 ppm not seen in sample 42G. The maleated polymer (sample 42G) showed

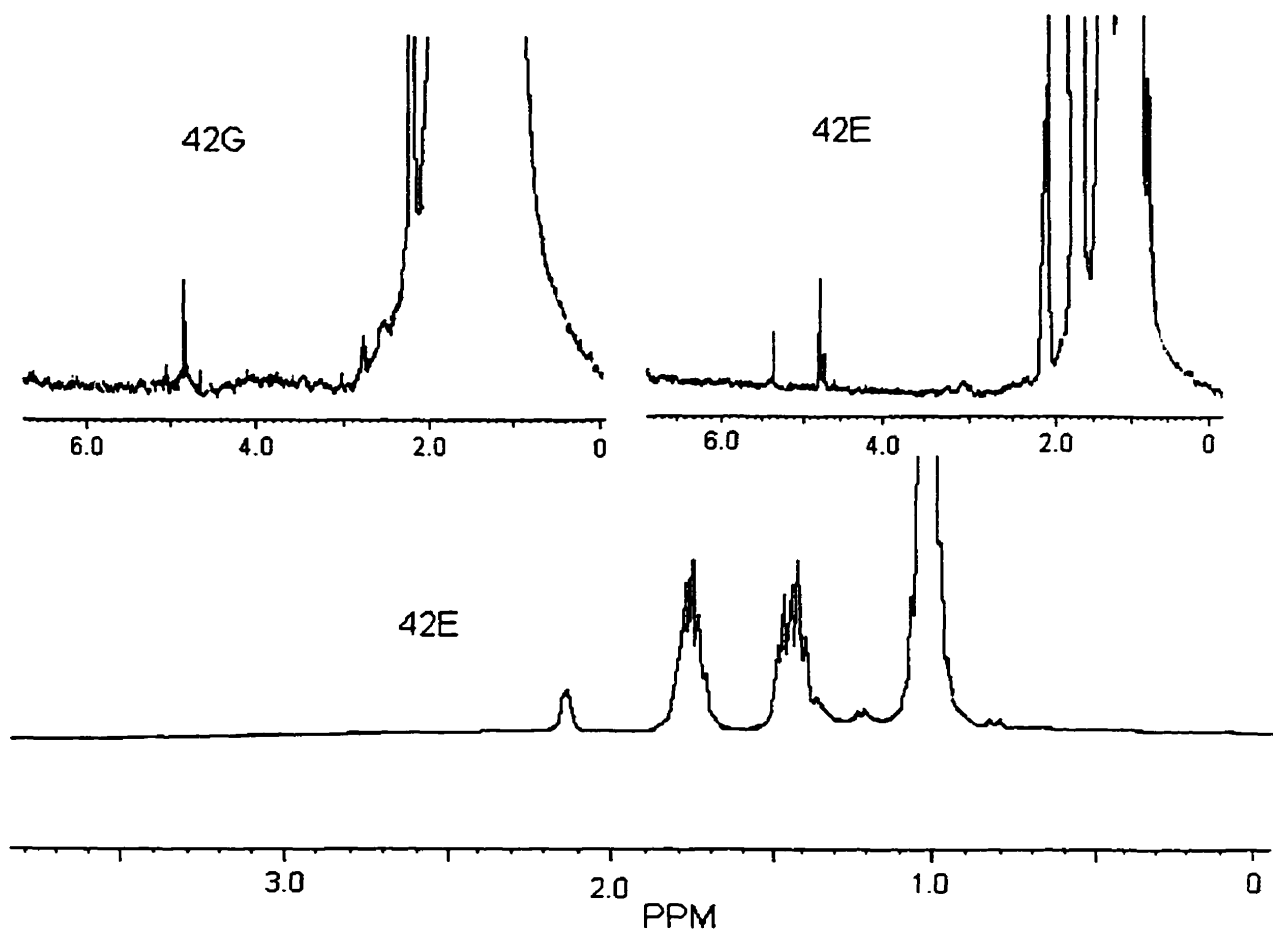


Figure 7.5. ¹H NMR spectra of a maleated sample (42G) and its hexadecylamine grafted product (42E) in the region of 0–6 ppm for the upper two plots, with the alkyl region (0–3 ppm) of 42E expanded in the lower view.

succinyl anhydride resonances at 2.6 and 2.82 ppm which fit within the succinyl anhydride region given by Russell and Kelusky (1988) and Thompson et al. (1998b). Succinyl anhydride groups reacted along the backbone due to free radical grafting, were found to exhibit peak resonances shifted downfield to 3.3 ppm according to their tertiary site instead of the primary site corresponding to a terminal position (Thompson et al., 1997). No indication of free radical grafting is seen in Figure 7.5. The noise in the baseline made it difficult to identify the internal vinyl at 4.98 ppm (Thompson et al., 1997) which may have

occurred in one of the isomer products. However, at least a very small peak appears to be present. There appeared to be sufficient evidence to conclude that maleic anhydride had been predominantly attached onto polypropylene as single units via the Alder Ene reaction. The proton spectrum of the chain extended sample in Figure 7.5, does not show the succinyl anhydride resonances mentioned above. However, four new peaks are distinguishable from the baseline. The two peaks centred at 3.1 and 3.3 ppm were similar to those observed in 1-alkylmaleimides corresponding to the N-CH₂- protons. The presence of two peaks likely correspond to both amide and imide functionalities being present, as seen by infrared analysis. A broad peak observed at 9.0 ppm which is not shown in Figure 7.5, confirmed the amide hypothesis, showing a carboxylic acid functionality is present in the polymer. The resonance at 5.4 ppm, obviously a double bond, can not be explained.

7.2.2. Thermal Transition Properties

An attempt was made to determine the nature of the succinyl anhydride attachment through comparison of the maleated polymer (40-48G) to the hexadecylamine grafted samples (40-48E) with respect to changes in crystalline structure. Unfortunately, the exact behaviour of chain extension or branching on the crystallinity within our polymer will be difficult to predict from other works due to the block copolymer nature of the product and its inclusion of a polar group (carboxylic acid-amide linkage) within the chain. Therefore, maleated polymers produced by the two methods (free radical vs. Alder Ene) were reacted with hexadecylamine and their transition properties were measured.

A commercial grade maleated polypropylene produced by peroxide-induced grafting (FUSABOND™ P MZ-203D , DuPont Canada) was reacted with 1-hexadecylamine in a

manner already described for the maleated product of this work. Examining the crystallization transition for a side-chain grafted product showed no significant difference in the crystallization temperature, 113.1°C and 113.9°C, with only a small change in the enthalpy, 72.4 J/g and 77.1 J/g, of the grafted FUSABOND and the maleated sample respectively. For comparison, sample 55E (highly maleated Alder Ene polypropylene reacted with hexadecylamine) showed an increase in the crystallization temperature, from 110.3°C to 116.1°C while the enthalpy of crystallization increased from 68.0 J/g to 99.7 J/g, from the maleated to the chain extended sample respectively. Clearly, the hexadecyl alkyl chain was involved in crystallization when it is located at the terminal site of the polymer chain, despite chain irregularities due to the polar linkage. Figure 7.6 shows the crystallization thermograms for several polymers from series G and E. The narrow, uniform shape to the distributions ensured more accurate transition calculations of peak temperature and enthalpy than values determined from the crystal melt transition.

Figure 7.7 shows the crystallization transition properties of several alkyl grafted samples compared to their original maleated samples. The alkyl grafted products exhibited an increase in the peak transition temperature of approximately 10°C from 102°C for the maleated samples (G series) to 112°C for the hexadecyl grafted polymers (E series). Some of the maleated samples of series G had hydrolyzed prior to analysis resulting in an increase of their transition temperature to approximately 110°C with $T_c^E - T_c^G$ now only 2°C (as shown in Figure 7.7). The latter $T_c^E - T_c^G$ fits within the extremes outlined by the Alder Ene (sample 55E) and free radical grafted (FUSABOND) examples which also began in the hydrolyzed form. These results suggest that the hexadecyl chain was positioned at the

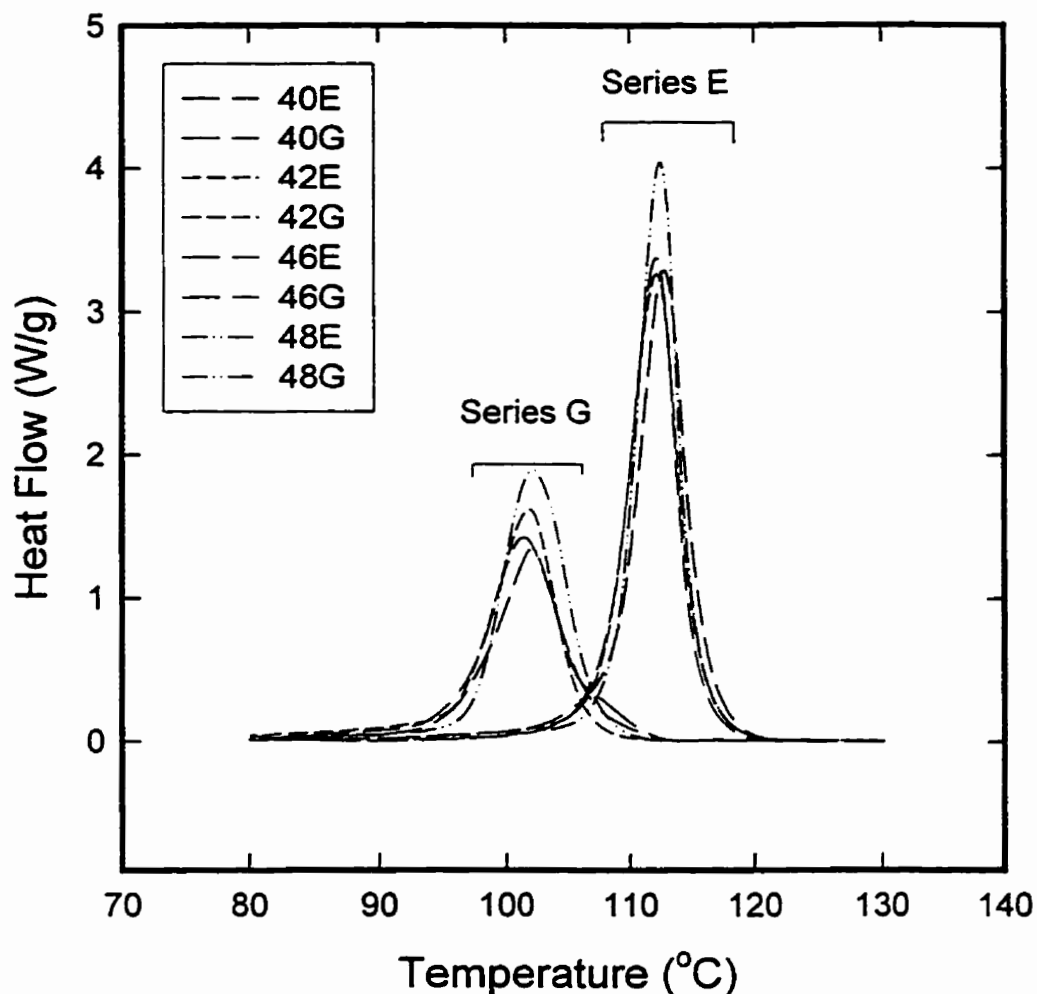


Figure 7.6. DSC crystallization thermograms of select samples from series G and E.

terminal site similar to sample 55E, just at lower concentration. No correlation was observed between $T_c^E - T_c^G$ and the succinyl anhydride concentration. The average increase in the crystallization enthalpy between series G (anhydride form) and E was 32 J/g, while between series G(acid form) and E, it was considerably lower at 8 J/g.

The crystal melting transitions are shown in Figure 7.8 where the endotherms appear quite broad including two transitions which correspond to α - and β -crystallite structures in

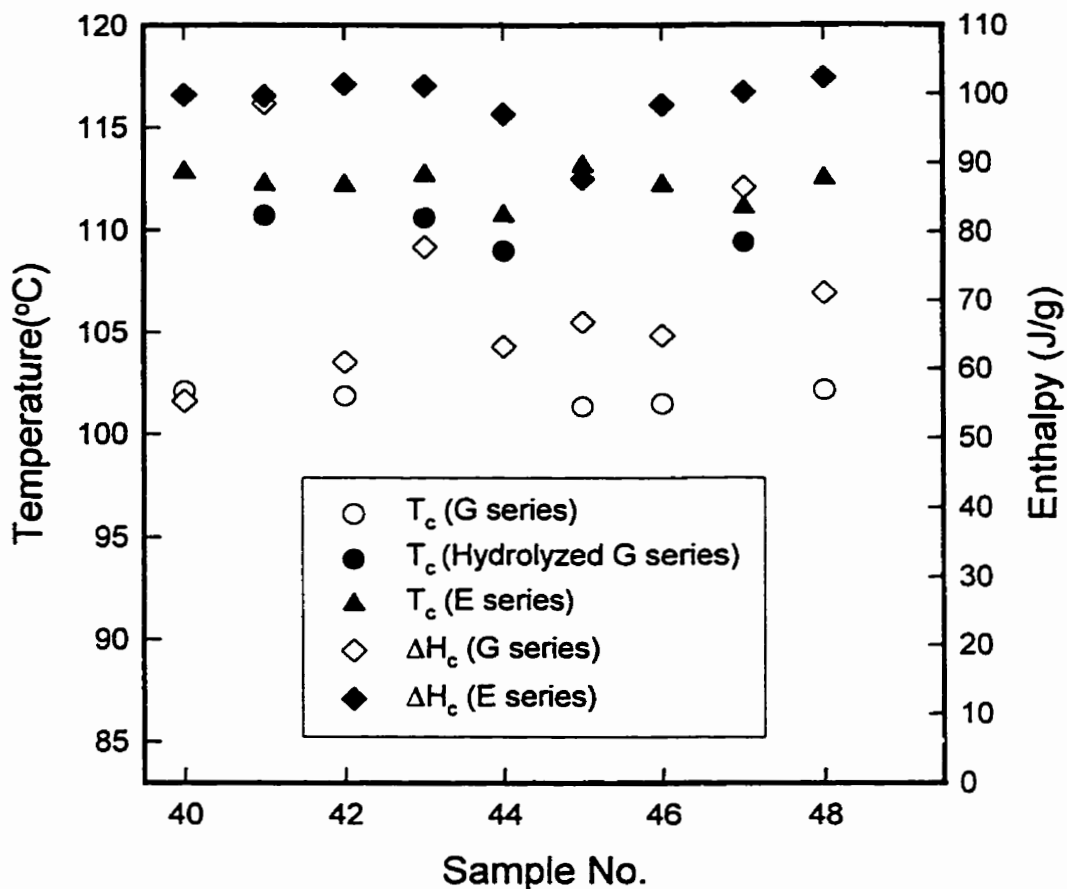


Figure 7.7. Crystallization transition properties (T_c and ΔH_c) for the maleated polypropylenes (G series) and their hexadecyl chain extended products (E series).

the polymer. The figure indicates that the higher temperature transition seen in both series G and E samples, increases in intensity and becomes better resolved for the chain extended samples.

7.2.3. Effect of Reaction Parameters

Beginning with experimental set 1, the results in terms of conversion are listed in Table 7.1 with a pooled estimate of variance being 0.025 % conversion based on repeats. The average conversion for maleated polypropylene produced from thermally degraded polymer

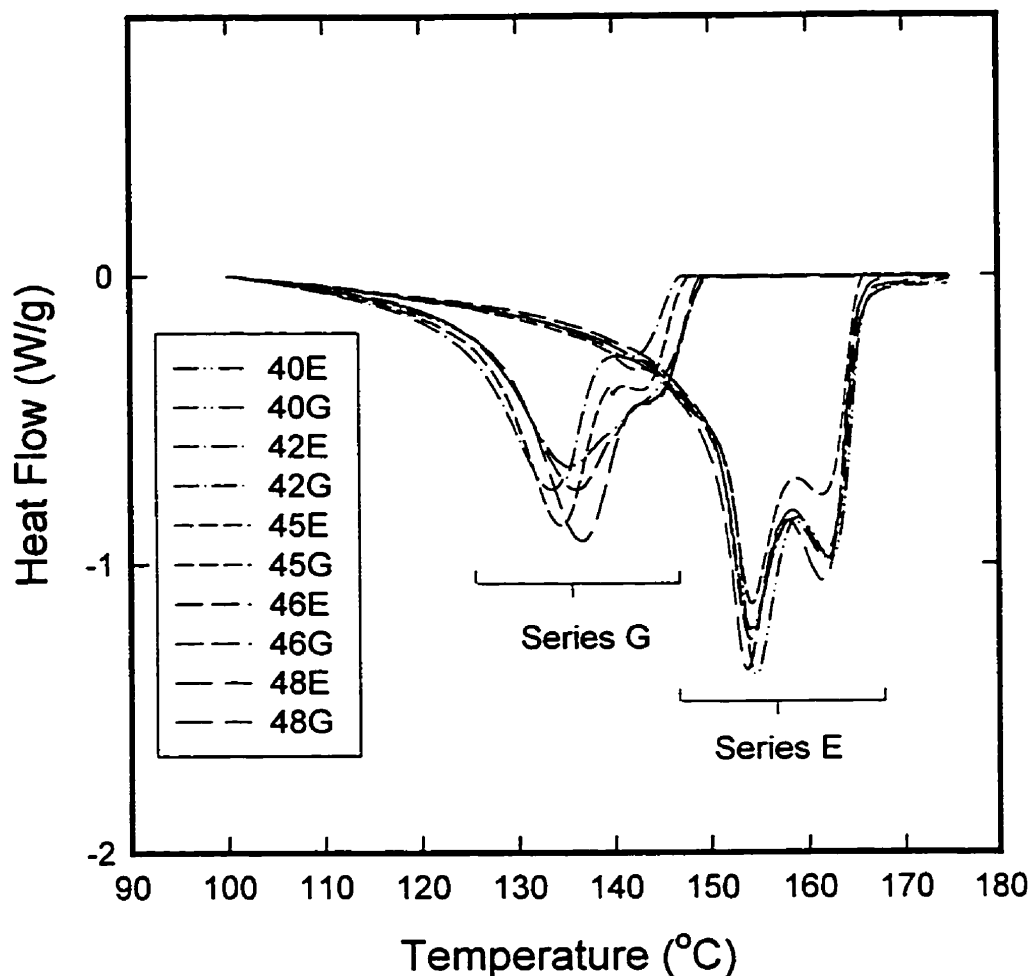


Figure 7.8. Crystal melting endotherms for several maleated and hexadecylamine grafted products.

compared to peroxide degraded material was 5.51 % and 4.79 % respectively. The significant difference between the two methods of generating the vinylidene group, showed that the peroxide method with its higher concentration of oxidation groups in the polymer, yielded inferior conversion. The result could be due to the Lewis acid forming adducts with these oxidation groups interfering with the generation of the anhydride-Lewis acid enophile, or the result could arise from the polymer forming a polar phase domain, thus, isolating the maleic anhydride from the vinylidene group of the hydrophobic hydrocarbon domain. Analysis of

the results of the fractional factorial for experimental set 1 showed that the vinylidene concentration was the most important factor in the reaction with a decrease of nearly 2 % conversion for the higher vinylidene concentration level compared to the lower level. Since the Alder Ene reaction exhibits bimolecular kinetics (Thompson et al., 1998ab; Benn et al., 1988), the contradiction the result offers must be attributed to mixing effects related to the high molecular weight virgin polypropylene being used to dilute the vinylidene group. The high molecular weight peak of the broadened distribution in the dilute polymer will improve channel fill in the mixing regions of the extruder where the shear was sufficiently high to breakup the maleic anhydride domain thus increasing the interfacial area between the two reactants. Both temperature and maleic anhydride reactant concentration showed a positive effect on the conversion of the vinylidene group to a succinyl anhydride moiety. Catalyst concentration was the only factor without significance to conversion, with an average increase in conversion of 0.1% for the higher catalyst level. Categorizing the catalyst effect further, for the thermally degraded polymer with high vinylidene concentration (and low viscosity) conversion did not change, yet for the thermally degraded polymer with the low vinylidene concentration (and high viscosity) conversion increased by 0.17% for the higher Lewis acid level. For the peroxide degraded polymer, the trend mentioned for the thermally degraded polymer was exactly opposite. Clearly, the effect of mixing and the method of vinylidene generation were both important parameters.

The final experimental set (using screw configuration 2) examined several reaction factors in the absence of mixing effects to ensure that the effect of the Lewis acid was not being concealed. Prior to analyzing the experimental design for significant effects, the product samples were used in a hierarchical (nested) design (Box et al., 1978) to elucidate

significant sources of variance in the measurement of the succinyl anhydride group. Three sources of variance were analyzed in the hierarchical design according to the letter designations of Box et al. (1978): batch (B), sample homogeneity (S), and IR measurement (T). Table 7.4 presents the conversion and the pooled estimates of variance. Variance in the infrared measurements proved to be the lowest one, testifying to the good reproducibility of the spectroscopic technique. The higher batch-to-batch and sample variance are indicators of the homogeneity of the extrusion process. It appears that a greater effort in dispersive mixing will be necessary to provide a more uniform product with respect to succinyl anhydride incorporation.

Table 7.4. Results of the hierarchical analysis

Sample No.	Response \bar{Y}	batch variance σ_B^2	sample variance σ_S^2	testing (IR) variance σ_T^2
40G	3.78	2.87×10^{-1}	2.36×10^{-3}	1.89×10^{-3}
41G	4.70	1.52×10^{-2}	5.36×10^{-2}	9.93×10^{-4}
42G	4.93	3.39×10^{-1}	4.56×10^{-2}	1.58×10^{-3}
43G	3.57	2.26×10^{-1}	2.62×10^0	2.18×10^{-3}
44G	3.78	4.13×10^{-2}	9.05×10^{-3}	1.11×10^{-3}
45G	4.68	5.18×10^{-3}	4.56×10^{-2}	6.87×10^{-4}
46G	3.82	1.67×10^{-3}	7.97×10^{-3}	1.06×10^{-3}
47G	4.29	4.18×10^{-2}	2.43×10^{-3}	2.17×10^{-3}
48G	4.04	8.04×10^{-3}	3.69×10^{-2}	3.21×10^{-2}

The 3^{3-1} fractional factorial in Table 7.3, provided a means of determining the main effects without confounding interactions. Based on repeats, the pooled estimate of variance was determined to be 0.017 % conversion. Through analysis of the conversion data for

experimental set 3, regression coefficients (given in Table 7.3) for the model showed that all three factors were significant, with positive effects observed for temperature and maleic anhydride concentration with respect to the succinyl anhydride incorporation. The Lewis acid concentration had a negative effect on the Alder Ene reaction, increasing the succinyl anhydride concentration with decreasing catalyst concentration. The trend confirmed the observations made within experimental set 1 for the same material (TD380), but did not demonstrate the importance of the Lewis acid similar to the observations made for a low molecular weight polypropylene maleated via the Alder Ene reaction in a batch reactor (Thompson et al., 1998ab and Chapter 6). If experimental set 1 was an indication, improved mixing was necessary to observed similar behaviour as seen within the batch reactor.

7.2.4. Effect of Screw Speed and Feed Rate

Experimental set 2 examined the effects of screw speed and feed rate on the degree of mixing during extrusion along with catalyst concentration (since it was the principle parameter under study) and the method of polymer degradation. Analysis of the complete factorial design (results included in Table 7.2), showed the feed rate as the only significant factor in the experiment, increasing the extent of reaction with decreasing feed rate. By looking at the experimental set according to the levels for the method of degradation, a screw speed-catalyst concentration interaction was also observed and it appears that the effect of feed rate on conversion was greater among those samples produced using peroxide-induced chain scission. The increased contribution of feed rate to conversion in the case of the peroxide degraded polymer was probably, once again, due to the molecular weight of the polymer with PD100 being higher than TD380 (prior to dilution with virgin KF6100). The

difference in the molecular weight distribution between the two degraded materials was small, particularly in comparison with the final diluted material of either degradation method, but that was probably why the method of vinylidene generation was not revealed as a significant effect.

7.2.5. Comparing Estimated to Measured SAh Content

Through estimation of the succinyl anhydride concentration bound to the polypropylene samples, it was possible to examine the quality of mixing in comparison to the batch reaction where the rate constants were derived. Since the degraded polymer was structurally similar to Polypol-19 (Chapter 6), the solubility of the reactant and the reactive site would be similar. The differences would be mainly found in the presence of oxygen over the reaction system and the mixing characteristics of the two reactors. It is reasonable to presume that the mixing remained constant among all reactions in the batch reactor for the kinetic data.

Estimating the conversion using the kinetic data of Chapter 6, required several assumptions and some extrapolation of the data, thereby introducing significant sources of error to the values. Rate constants below 220°C, had to be extrapolated using the Arrhenius equation with activation energy values for the appropriate catalyst concentration as previously disclosed. The reaction time and mean residence time were considered to be equivalence. No compensation for the distance between the feed section and the injection stem was made due to the error inherent in the calculation of the mean residence time. Since the minimum residence time, t_0 , will be the only reasonably accurate measurement made using coloured tracers, it was necessary to under-estimate the mean residence time by

assuming the laminar flow theory for a single screw extruder was applicable. This was essentially due to a lack of analytical residence time distribution calculations for a co-rotating intermeshing twin screw extruder. Therefore, the mean residence time was calculated as, $\bar{t} = \frac{1}{3} \cdot t_0$. Figure 7.9 shows that all estimated conversion values were below those conversions calculated from the measured FT-IR data. Since the actual melt temperature of the polymer in the extruder was not known, the estimated conversion values in Figure 7.9 possess deviation bars accounting for a temperature variance of 5°C from set-point. Thermal and peroxide degraded polypropylene samples were differentiated in the figure to determine if the method of degradation had an effect on the difference between the two conversion data sets. At least from this graph, no visible differences were observed, however, with nearly an order of magnitude difference between the measured and estimated values, it was also not possible to recognize that the estimated values did not follow the trend of the conversion values from the FT-IR measured data. Interestingly, the data for the second screw configuration (diamond symbols in the figure) exhibited similar deviations from the measured data as those values from screw configuration 1 (triangle symbols), however, the values were much more localized. The other localized cluster of data points was for those measurements which varied the screw speed and feed rate (circle symbols). However, in this case it has already been shown that the operating parameters did not exhibit the same degree of importance as the reaction parameters (at least for the range investigated). Therefore, with the reaction parameters fixed, as was the case with the samples between 20-35G, all polymers should observe similar extents of reaction (both estimated and measured).

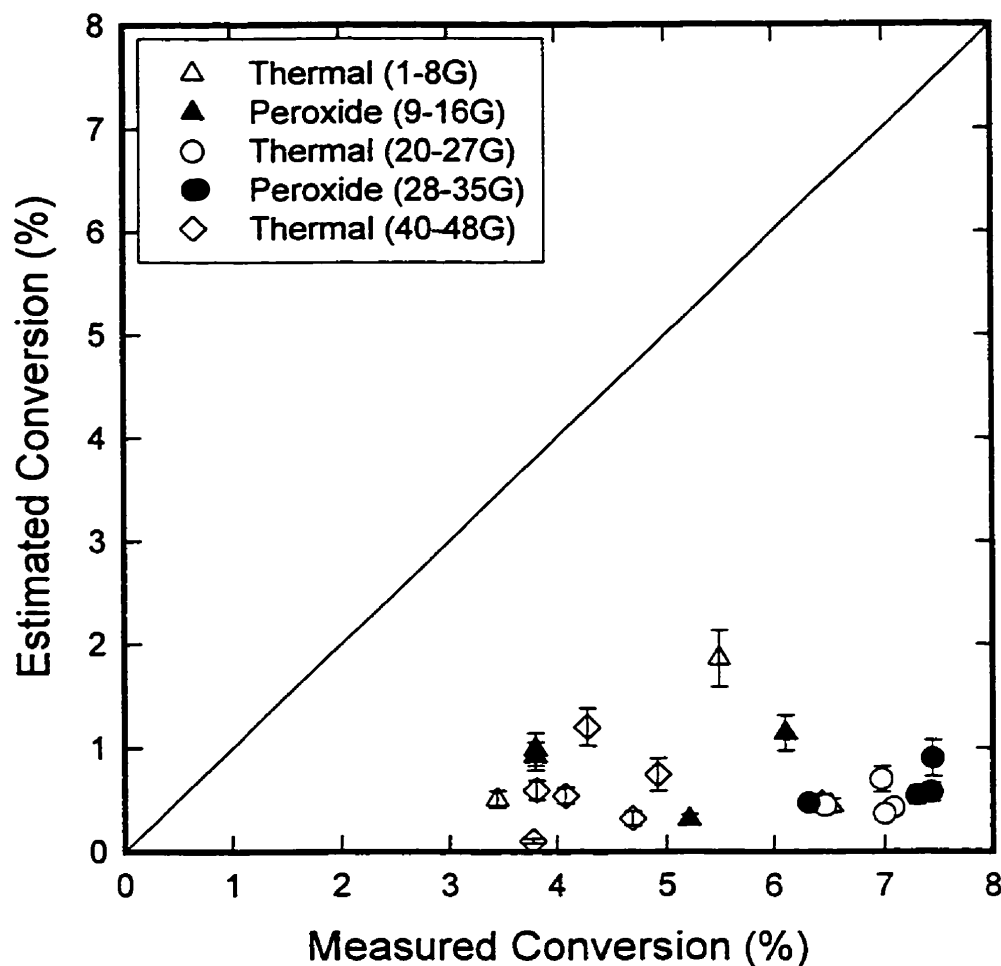


Figure 7.9. Comparing the kinetic-estimated conversion with the conversion values derived from FT-IR measurements (deviation bars for conversions within a $\pm 5^\circ\text{C}$ range).

Based on the above data, it was observed that the estimated conversion values did not follow the same trend as those values derived from measured data. Figure 7.10 looks more closely at the effect of several parameters on the difference between these two conversion values (presented as a single value, namely percent error) for samples produced in screw configuration (1). Similarly to Figure 7.9, peroxide and thermally degraded polypropylene samples were differentiated in Figure 7.10. The variability observed in the percent error in

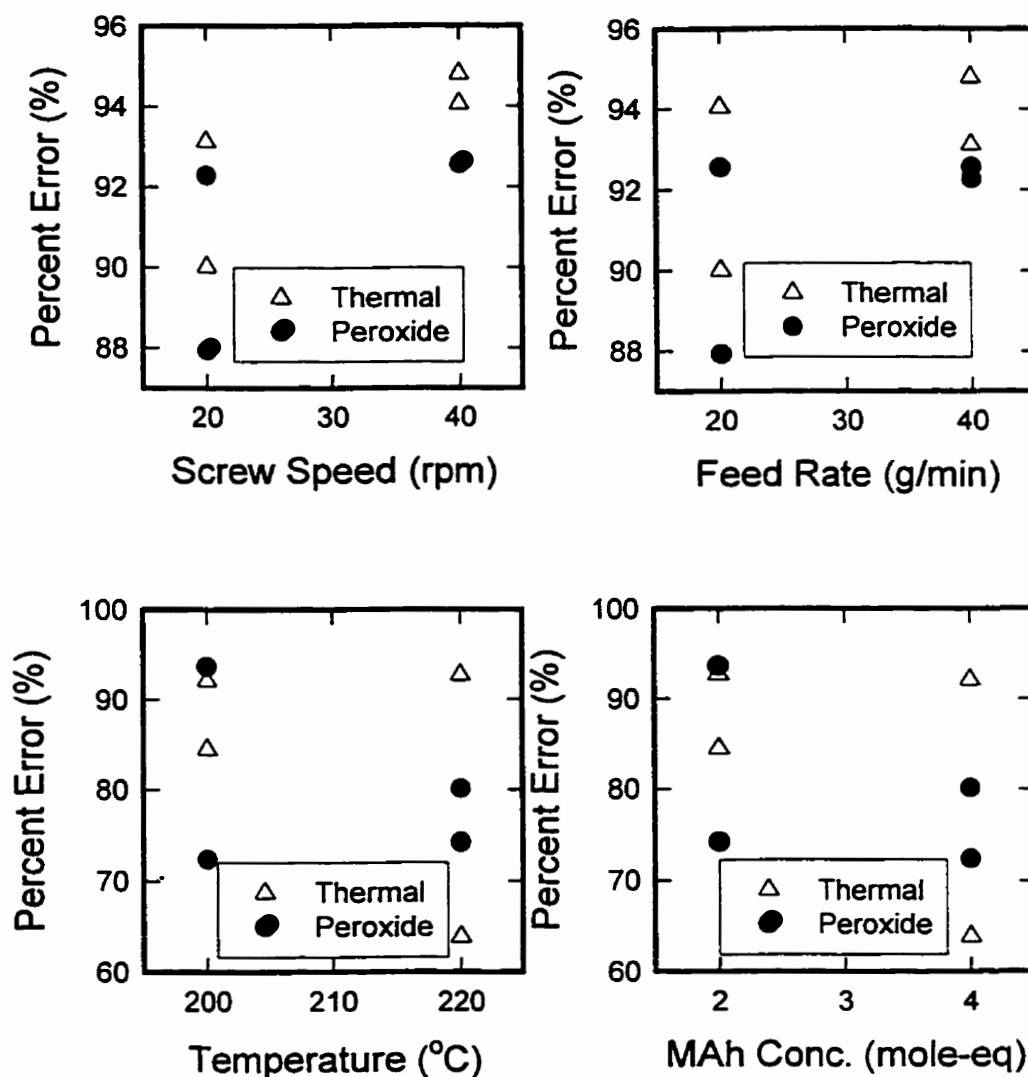


Figure 7.10. Effect of several reaction and operating parameters on the difference observed between measured and estimated conversion, given as percent error

Figure 7.10, may in part be due to the error introduced in deriving the estimated conversion (as discussed above). The variability may also be due to interactions between the factors and effect of the high molecular weight tail among several of the samples, which has been shown in section 7.2.5 to have a strong effect on the extent of reaction. Examining the data, the higher data point for each method of degradation at the different factor levels, was

consistently the maleated polypropylene sample derived from the broadened distribution (KF6100 diluted samples). It would be expected that the percent error remained constant between the different levels examined for each factor, if the kinetic rate equation was accounting for the variance in values observed. For the reaction parameters of temperature and maleic anhydride concentration, that certainly may be true, however, for the operating parameters of screw speed and feed rate, the percent error appeared to increase towards the higher factor level of each. These results stress longer residence times in comparison to greater mixing efficiency for minimizing the percent error.

7.2.6. Ruthenium chloride vs. Stannous chloride

Two maleation runs (9 and 12G) were reproduced using ruthenium chloride in place of stannous chloride. The FT-IR spectra of the samples has already been shown in Figure 7.4. Conversion of the vinylidene in samples 37G and 38G was 6.26 % and 7.15 % respectively, showing a 16 % improvement over those materials produced in the presence of stannous chloride. The improved catalytic nature of ruthenium chloride compared to stannous chloride was also observed in previous work using a low molecular weight polypropylene (Thompson et al., 1998a). Ruthenium chloride does not form an adduct with the anhydride oxygen similar to stannous chloride, rather it coordinates with the vinyl group (Alderson et al., 1965; Cramer, 1965), evidently producing a superior enophile for the Alder Ene reaction with respect to the vinylidene group of polypropylene. Unlike stannous chloride, the robustness of ruthenium chloride towards moisture, is a useful property with regards to a catalyst being used for reactive extrusion and the improved rate of reaction resulting from its presence demonstrates its advantage to our system.

7.3. CONCLUDING REMARKS

Maleation of polypropylene through reactive extrusion via the Alder Ene reaction has been shown to produce a terminal functionality without significant chain scission. Increased temperature and maleic anhydride reactant concentration were found to improve the extent of the reaction, while the contribution of a Lewis acid species ($\text{SnCl}_2 \cdot 2\text{H}_2\text{O}$) could not be conclusively determined due to mixing effects. With improved mixing in the extruder, due to increased melt viscosity or increased feed rate, the degree of conversion was increased. Ruthenium chloride was found to increase the extent of the reaction by 16 % in comparison to stannous chloride as a catalyst in the Alder Ene reaction.

CHAPTER 8. MALEATION OF ETHYLENE-PROPYLENE-DIENE TERPOLYMER THROUGH REACTIVE EXTRUSION VIA THE ALDER ENE REACTION

8.1. INTRODUCTION

The *ene* moiety of the Alder Ene mechanism is a double bond with an allylic hydrogen (as discussed in Chapter 2), which in the present case was the hindered unsaturation of 5-ethylidene-2-norbornene. The *enophile* was maleic anhydride or a Lewis acid-maleic anhydride adduct, similar to the reaction systems of the previous chapters. In order to provide evidence that maleic anhydride attachment has resulted from the Alder Ene mechanism instead of a free radical reaction (likely due to thermo-oxidative degradation), it was important that the structure of the attached succinyl anhydride moiety be determined. Since characterization of a functional group below 1 wt % is difficult, it is generally necessary to rely on indirect evidence from a variety of characterization techniques. No consideration of maleated products resulting from reaction with the vinylidene of degraded EPDM, was made since the low concentration of this reactive site would make structural determinations impossible.

The Alder Ene reaction was carried out in several types of processing equipment including a batch mixer, a single screw extruder and a twin screw extruder. Due to the relatively high concentration of *ene* groups in EPDM compared to polypropylene, it was hoped that sufficient maleation would result to determine the extent to which free radical reactions participate/interfere with the attachment of maleic anhydride onto the polymer in conventional polymer processing equipment.

The majority of the analysis in this chapter shall be focused on the results from the twin screw extruder experiments. Two sets of experiments were performed, each with a different screw configuration. Tables 8.1 and 8.2 outline the experimental parameters used in each set and include the measured succinyl anhydride content of each resulting sample.

Table 8.1. Experimental conditions for screw configuration 3²

Sample No.	Screw speed (rpm)	MAh Reactant (mole eq.)*	Catalyst (mole eq.)†	SAh Conc. (wt %)
13F	30	2.25	0	1.077
14F	30	2	0	0.88
15F	30	1	0	0.69
16F	30	0.5	0	0.43
17F	30	2	0	0.81
18F	30	1	0	0.69
19F	30	0.5	0	0.50
20F	20	2	0	0.79
21F	20	1	0	0.61
22F	20	0.5	0	0.33
23F	30	2	0.01 % SnCl ₂	0.91
24F	30	1	0.01 % SnCl ₂	0.51
25F	30	0.5	0.01 % SnCl ₂	0.36
26F	30	2	0.01 % RuCl _n	0.91
27F	30	1	0.01 % RuCl _n	0.53
28F	30	0.5	0.01 % RuCl _n	0.37

SAh = bound succinyl anhydride, MAh = maleic anhydride reactant

‡ fixed EPDM feed rate, 20 g/min.

* mole equivalence with respect to the double bond concentration.

† mole equivalence with respect to maleic anhydride concentration.

8.2. CHARACTERIZATION OF MALEATED EPDM

Attempts to determine the structure of the maleated EPDM produced via the Alder Ene reaction are discussed in this section. Characterization involved only products from the twin screw extruder experiments due to their improved reaction conditions compared to

Table 8.2. Experimental parameters for screw configuration 4

Sample No.	Catalyst Conc. (% mole eq.)†	Catalyst Type	Temperature (°C)	MAh Reactant (mole eq.)‡	SAh Conc. (wt %)
30F	0	SnCl ₂ ·2H ₂ O	210	0.5	0.074
31F	0	SnCl ₂ ·2H ₂ O	230	1	0.203
32F	0	SnCl ₂ ·2H ₂ O	220	2	0.154
33F	0.005	SnCl ₂ ·2H ₂ O	220	0.5	0.115
34F	0.005	SnCl ₂ ·2H ₂ O	210	1	0.104
35F	0.005	SnCl ₂ ·2H ₂ O	230	2	0.319
36F	0.01	SnCl ₂ ·2H ₂ O	230	0.5	0.159
37F	0.01	SnCl ₂ ·2H ₂ O	220	1	0.149
38F	0.01	SnCl ₂ ·2H ₂ O	210	2	0.150
39F	0	RuCl _n ·xH ₂ O	230	0.5	0.181
40F	0	RuCl _n ·xH ₂ O	220	1	0.164
41F	0	RuCl _n ·xH ₂ O	210	2	0.201
42F	0.005	RuCl _n ·xH ₂ O	210	0.5	0.117
43F	0.005	RuCl _n ·xH ₂ O	230	1	0.229
44F	0.005	RuCl _n ·xH ₂ O	220	2	0.176
45F	0.01	RuCl _n ·xH ₂ O	220	0.5	0.122
46F	0.01	RuCl _n ·xH ₂ O	210	1	0.103
47F	0.01	RuCl _n ·xH ₂ O	230	2	0.189
48F	0	AlCl ₃	220	0.5	0.174
49F	0	AlCl ₃	210	1	0.135
50F	0	AlCl ₃	230	2	0.249
51F	0.005	AlCl ₃	230	0.5	0.299
52F	0.005	AlCl ₃	220	1	0.168
53F	0.005	AlCl ₃	210	2	0.133
54F	0.01	AlCl ₃	210	0.5	0.115
55F	0.01	AlCl ₃	230	1	0.251
56F	0.01	AlCl ₃	220	2	0.149

SAh = bound succinyl anhydride, MAh = maleic anhydride reactant

† mole equivalence with respect to maleic anhydride concentration.

‡ mole equivalence with respect to double bond concentration.

samples from the preliminary screening experiments in the batch mixer and single screw extruder. To properly identify a material referenced in this chapter, each sample designation shall be included, though, the actual reaction conditions by which it was produced shall not

be included for ease of reading. The reader is referred to the above tables to determine the conditions at which each sample was produced.

8.2.1. Molecular weight distribution data

Figure 8.1 shows the MWD of two not extruded samples (virgin EPDM and virgin/purified EPDM) as well as the distributions of three maleated EPDMs compared to an unmodified EPDM control sample which had been extruded at 210°C and subsequently purified. The fact that the high molecular weight fractions of the virgin/purified EPDM distribution are so much greater than the other purified samples is surprising, possibly attributable to an error in the analysis software. The maleated EPDMs in Figure 8.1, were produced through a catalyzed Alder Ene reaction as described in Chapter 4, at temperatures between 210-230°C in the twin screw extruder. Within the limits of instrumental error, the overlapping nature of the latter four curves demonstrated that the degree of chain scission was independent of maleic anhydride concentration as would be expected of maleation in the absence of free radicals. At least this observation was valid for samples produced in the presence of Lewis acid catalysts (shown more clearly in Figure 8.2 with a distribution for each catalyst type presented). The molecular weight distribution of samples maleated in the absence of a catalyst, established temperature and maleic anhydride concentration effects which are discussed in a later section.

A lack of significant difference in the molecular weight distribution of those maleated samples produced at 270°C (shown in Figure 8.3) in the twin screw extruder, indicate that even at elevated temperatures there was no evidence of a correlation between maleic anhydride concentration and the degree of scission and/or cross-linking. Comparison of the

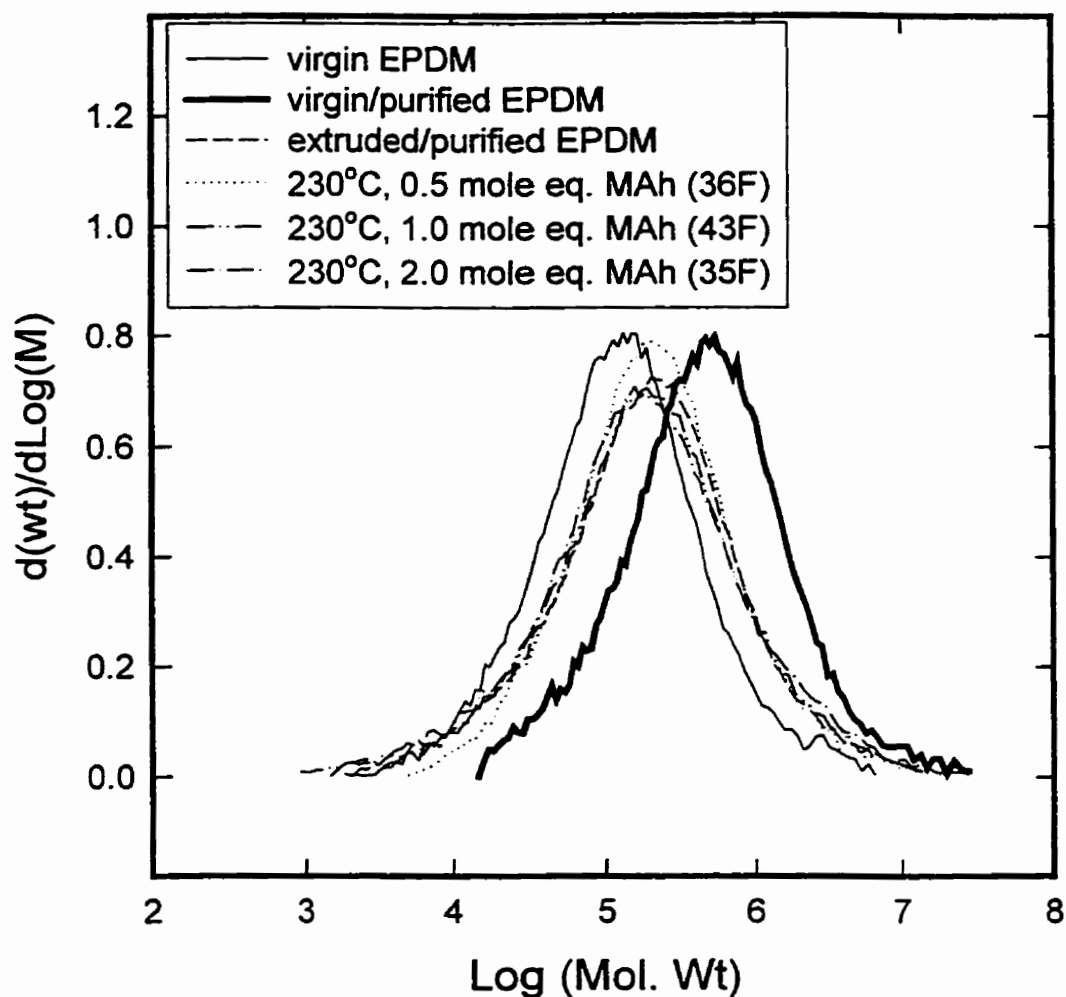


Figure 8.1. Changes in the molecular weight distribution of EPDM resulting from chain scission (due to processing) and fractionation (due to purification).

distributions in Figure 8.2 and Figure 8.3 shows that samples produced at the higher temperature had a greater weight fraction of high molecular weight chains and lower weight fraction of the lower molecular weight chains. However, since the energy requirements for the screw configuration used at 270°C were different from the screw used for reactions at 210-230°C, the difference between Figures 8.2 and 8.3 need not be due to temperature. A lack of gel was observed during cleaning, indicating that cross-linking did not occur to any

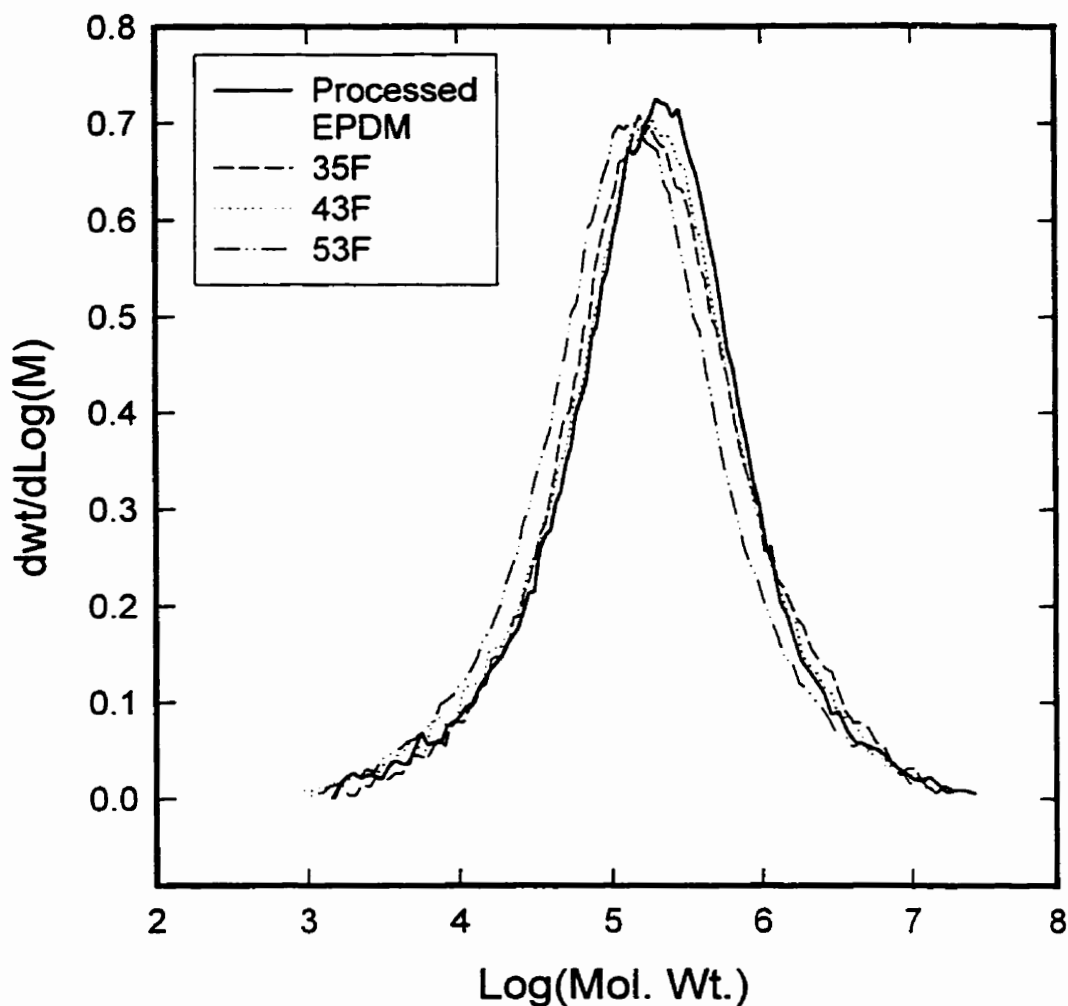


Figure 8.2. Molecular weight distributions of maleated EPDMs via the catalyzed Alder Ene reaction at 210-230°C with unmodified EPDM included for comparison.

significant extent, since termination by disproportionation should be more energetically favoured at higher temperatures. The consistency in the change of the MWD within a specific screw configuration, indicate that there was a small amount of scorching and/or degradation of the rubber, which was attributed to melt processing and not related to the presence of maleic anhydride. Therefore, it was possible to surmise that any grafting of maleic anhydride on account of thermo-oxidative reactions were negligible. The low degree

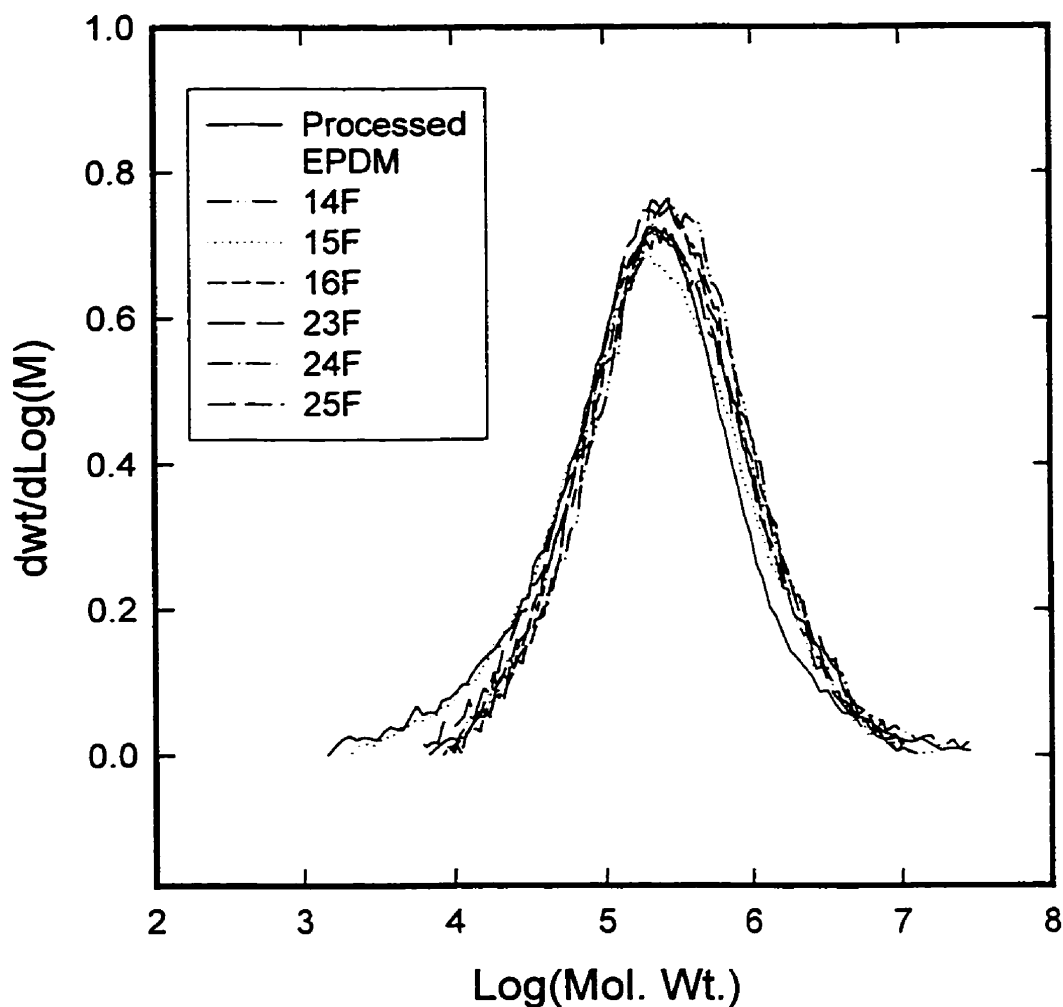


Figure 8.3. Molecular weight distributions of maleated EPDMs via both catalyzed and uncatalyzed Alder Ene reactions at 270°C with unmodified EPDM included for comparison.

of scission and cross-linking inferred by the similarity in the molecular weight distributions among the different processing conditions, was presumably due to the excellent weatherability (i.e. oxygen and ozone resistance) of EPDM. Due to the presence of chain scission, spectroscopic analysis for double bonds in the EPDM samples will likely include vinylidenes as a result of degradation. However, the vinylidene group was not anticipated as

an isomer of the Alder Ene reaction in the present system and therefore, should not interfere with our analysis.

Figure 8.1 also showed through the inclusion of the MWD of the virgin EPDM as-received, that the procedure of dissolving EPDM into hot xylene and precipitating with an excess of acetone, provided a fractionated product with respect to its lower molecular weight fractions. This phenomenon of fractionation was corroborated during rheological analysis, where the storage modulus (G') of the cleaned sample showed a significant increase at low frequencies and a slight decrease at high frequencies compared to the virgin rubber. Fractionation during purification of maleated EPDM was also observed by Coutinho and Ferreira (1994), who found that low molecular weight EPDM fractions remained in solution during acetone extraction. While this phenomenon reduces the measurable succinyl anhydride in the polymer, purification of the product remained a necessity. From the stance of molecular weight determination as well as other characterization methods, purification must be done prior to analysis to avoid misinterpretation due to oligomeric and polymeric maleic anhydride contaminants which can not be removed by other means. Thus, it was necessary to assume that the degree of fractionation remains consistent for a constant xylene/acetone ratio despite the varied concentration of the bound polar group which might change the solubility of the rubber in polar solvents like acetone. Based on molecular weight determination of all product samples, this assumption appeared to be valid.

8.2.2. Infrared Analysis

Figure 8.4 shows the succinyl functionalized EPDM from reactions with (sample 55F) and without (sample 50F) Lewis acid present, in comparison with the purified virgin

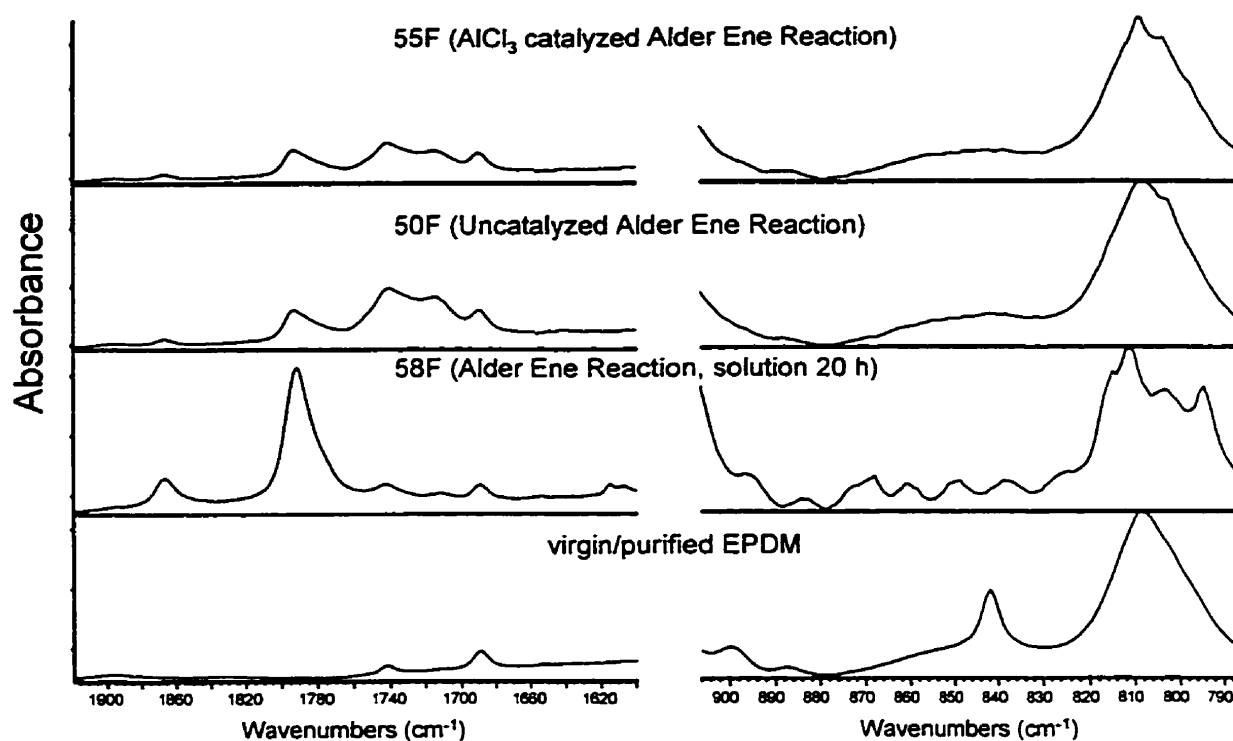


Figure 8.4. Infrared spectra of maleated and virgin EPDM in the carbonyl (1600-1900 cm^{-1}) and fingerprint (900-800 cm^{-1}) regions.

resin and a maleated EPDM (sample 58F) which was produced by the Alder Ene reaction in solution over a 20 h period. In the carbonyl absorption region, the functionalized EPDMs showed succinyl anhydride vibrations at 1792 cm^{-1} with a 1784 cm^{-1} shoulder and at 1868 cm^{-1} . Both 1792 cm^{-1} and 1784 cm^{-1} vibrations are attributed to mechanical coupling of the carbonyl stretching modes within the anhydride (Marquardt, 1966) as discussed in Chapter 6. Based on the interpretation of anhydride vibration modes, it was possible to conclude that the maleic anhydride was bound in our product as single succinyl anhydride units. Based on the infrared calibration curve (eqn 4.8), all maleated samples possessed succinyl anhydride concentrations in the range of 0.1-1 wt %.

Identification of the double bond vibrations in EPDM was much more difficult than the succinyl group, due to limited published infrared peak assignments for the internal, hindered vinyl in ENB and its possible isomers either due to isomerization or the Alder Ene reaction. Determination by difference between IR spectra of the virgin EPDM and an epoxidated EPDM (synthesized by reacting for 2 h. in xylene at 90°C using m-chloroperoxybenzoic acid), identified the internal ENB vinyl at 1689 and 804 cm^{-1} . The difficulty in distinguishing any =C-H out-of-plane deformation bands in the region of 800 cm^{-1} to 1000 cm^{-1} , made it necessary to rely on the C=C stretching band region between 1600-1700 cm^{-1} to discern changes in the double bond (Tosi et al., 1972; Levine and Haines, 1970) due to the reaction mechanism. It was expected that the resulting double bond of the Alder Ene mechanism would either be within the norbornene ring (-CH=CR', ~1600 cm^{-1}) or as a terminal vinyl (-HC=CH₂, ~1630 cm^{-1}). The spectrum of the highly maleated EPDM (0.72 wt %, sample 58F) showed a reduced internal vinyl band at 1689 cm^{-1} and a new broad peak centred at 1620 cm^{-1} with a shoulder at 1603 cm^{-1} indicating that the terminal isomer was favoured in the Alder Ene product although both structures exist. Due to the small extent of the reaction in the extruded samples, only the 1620 cm^{-1} band was distinguishable in samples 50 and 55F though too small to be seen clearly in Figure 8.4. The small absorbance observed at 1653 cm^{-1} in all samples including the virgin EPDM, was probably due to the vinylidene group which did not appear to vary in intensity.

8.2.3. NMR Characterization

Characterization of the maleated EPDM by ¹³C NMR spectroscopy to identify the structure of the attached anhydride group, proved inconclusive presumably due to insufficient

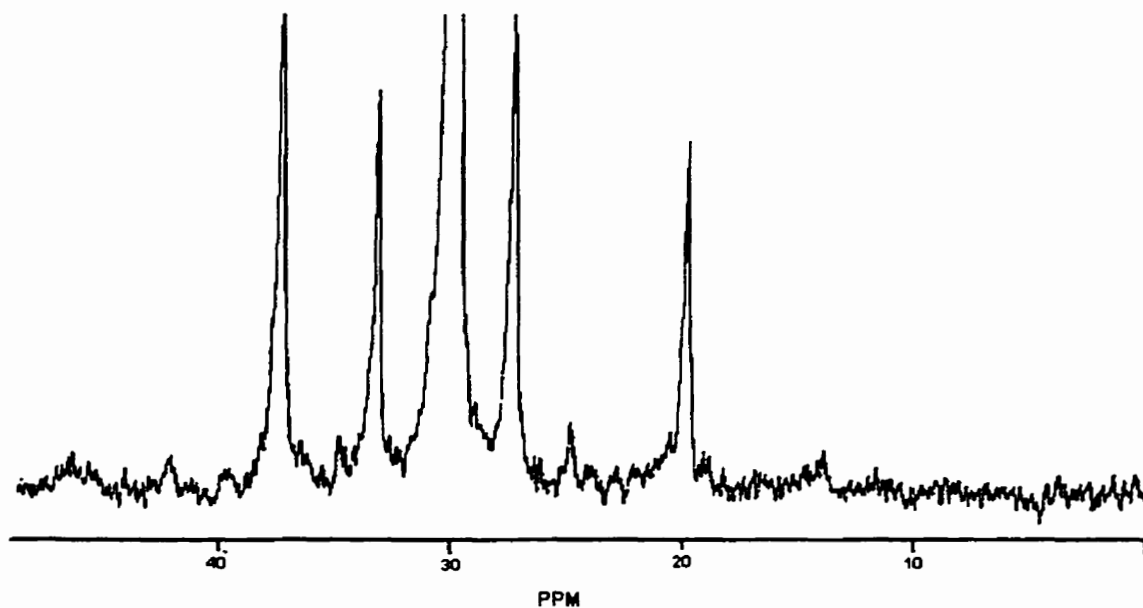


Figure 8.5. ^{13}C NMR spectrum of maleated EPDM (Sample 43F) in the backbone region

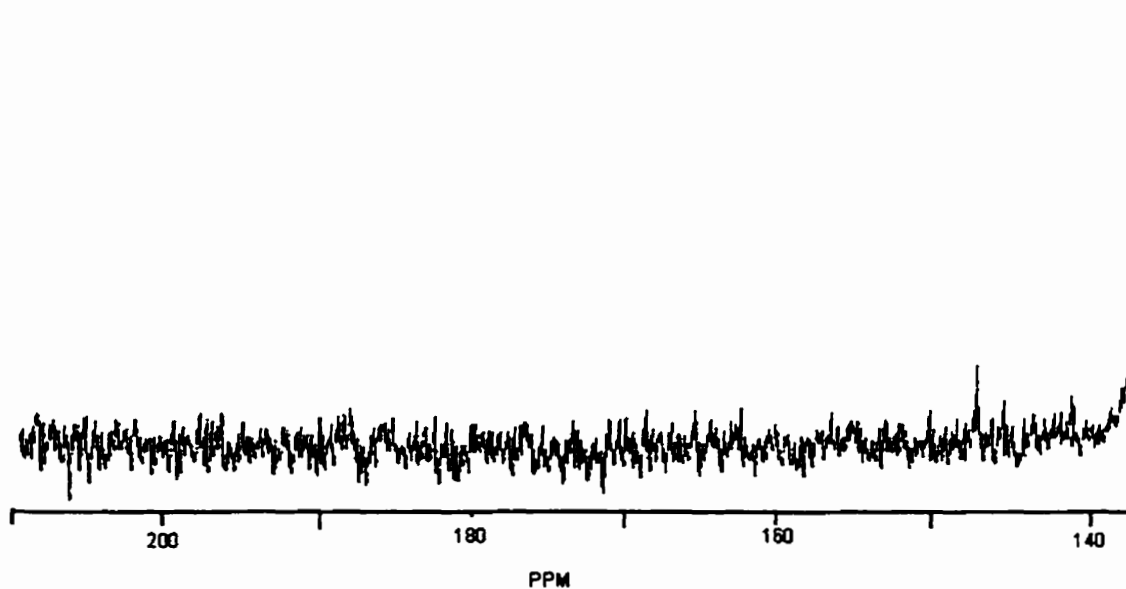


Figure 8.6. ^{13}C NMR spectrum of maleated EPDM (sample 43F) in the unsaturated region (edge of the trichlorobenzene peak seen at right-hand side of figure)

functional group mobility to resolve the low concentration of bound anhydride (backbone resonances shown in Figure 8.5 with the unsaturation presented in Figure 8.6). For

comparison, the characteristic ENB double bond resonance at 147.2 ppm was just noticeable from base-line noise. Unfortunately, ^1H NMR characterization of maleated EPDM samples (in Figure 8.7) did not clearly resolve the nature of the anhydride group either. The proton spectrum of EPDM shows a resonance at 2.84 ppm pertaining to the ENB species. However, in the maleated samples the resonance appears slightly broader. It is suspected that at least one of the succinyl proton resonances lies slightly upfield from the ENB resonance. This was most easily seen in the spectrum for 43F, where the succinyl group is considerably lower in concentration resulting in the peak being resolved at 2.80 ppm. Russell and Kelusky (1988) identified the methine and two methylene proton resonances of a grafted single succinyl

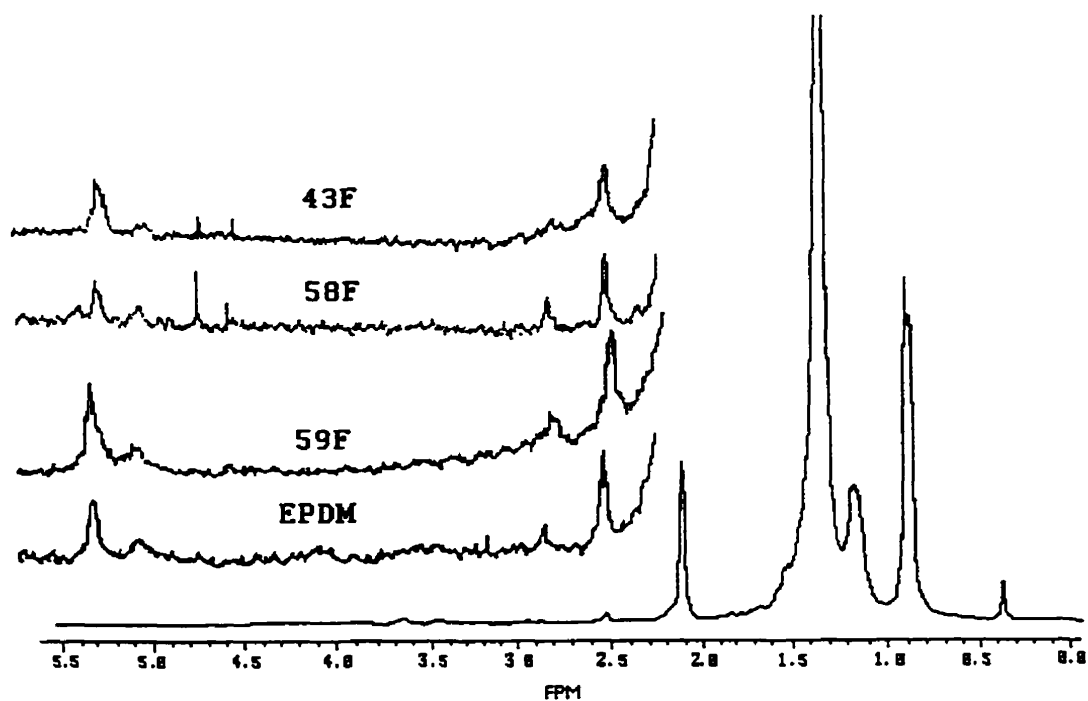


Figure 8.7. ^1H NMR spectrum of EPDM with overlapping spectra scaled to show the succinyl anhydride and double bond resonances of several maleated samples. Top-to-bottom: (43F) Lewis acid catalyzed, extruded product; (58F) highly maleated Alder Ene solution product; (59F) peroxide-induced maleated EPDM; (EPDM) virgin EPDM.

anhydride ring on n-eicosane to be in the region of 3.30, 3.20 and 2.83 ppm respectively. These values varied depending on the solvent used and the site of attachment. The finding of Russell and Kelusky (1988) tends to lend some credibility to the hypothesized location of the succinyl anhydride in maleated EPDM, bearing in mind that the location of attachment will be different between EPDM and n-eicosane. No carboxylic acid or poly(maleic anhydride) species were detected in Figure 7. The succinyl anhydride group does not appear to be useful for discriminating between free radical induced grafting and Alder Ene reaction. However, the nature of the unsaturation appeared to be much more informative.

The maleated sample (59F) produced in hot trichlorobenzene (180°C) with Lupersol 101 (Elf AtoChem) dialkyl peroxide showed the two characteristic peaks of the internal vinyl of ENB at 5.4 and 5.1 ppm, at similar intensities compared those of the virgin EPDM. The result agreed with previous observations (Coutinho and Ferreira , 1994; Sheng and Hu, 1996) that the double bond of the diene does not participate in radical reactions with EPDM. The spectrum of the peroxide-induced maleated product showed no new double bond geometries, including the vinylidene group. The samples produced by the Alder Ene reaction (samples 43F and 58F) in Figure 8.7, displayed new vinylidene resonances at 4.86 and 4.64 ppm which are attributed to degradation of the rubber either during extrusion or due to prolonged exposure to high temperatures as was the case with sample 58F which was produced in solution at 214°C for 20 h. Identification of the vinylidene resonances was based on NMR analysis of an extruded EPDM sample that was not maleated, yet exhibiting similar peaks. Looking at the spectrum of sample 58F in Figure 8.7, two more double bond resonances can be distinguished at 4.99 and 4.95 ppm. Understanding the structure of the two possible Alder

Ene products will assist in the assignment of these peaks to one of the two possible double bond isomers. In figure 8.8, two structures of the functionalized EPDM are proposed, depending on which allylic hydrogen (A or B) participates in the Alder Ene reaction. The double bond of isomer A should give a resonance in the region of 6-6.5 ppm, and would be unlikely due to the imposed ring strain that would result. The formation of a terminal vinyl would appear in the region of 4.7-5.1 ppm matching our two peaks observed in sample 58F, and though the proximity of the anhydride ring to the norbornane ring will increase steric hindrance, isomer B would be the most likely product. From the infrared analysis (section 8.2.2), isomer A was also present, though too low obviously for detection by NMR.

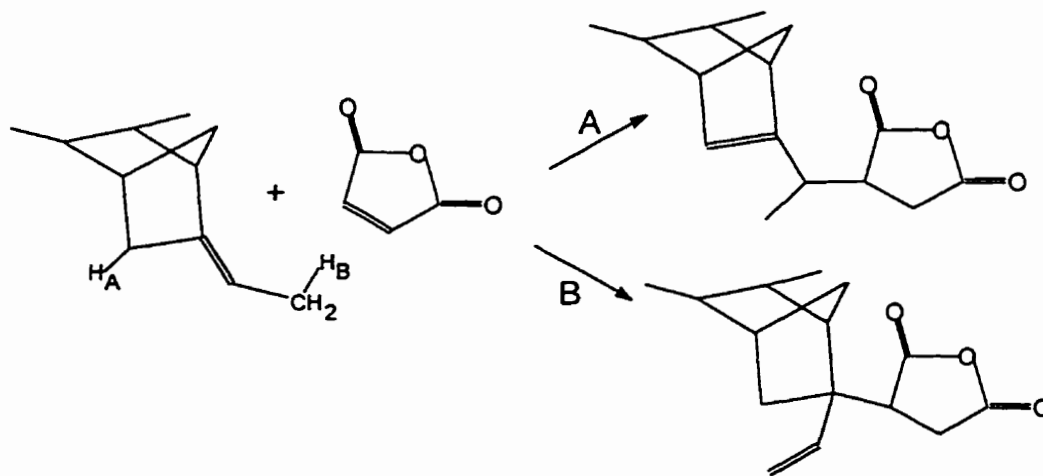


Figure 8.8. Two proposed structures of a succinyl anhydride EPDM adduct resulting from a concerted mechanism involving either allylic hydrogen A or B.

8.3. EXPERIMENTS IN THE BATCH MIXER

The unsaturation in the EPDM used in this work, i.e. 5-ethylidene-2-norbornene, was an internal vinyl, which may have been too hindered for high levels of maleation via the

Alder Ene mechanism. While it is possible that isomerization of the vinyl at the processing temperatures may yield a terminal vinylene for the reaction, there was not evidence in the literature to support this occurrence. A less hindered vinyl (EPDM containing butadiene as its termonomer) had been observed by Roncetti and Banzi (1992) to exhibit greater reactivity compared to the internal vinyl of ethylidene norbornene towards maleic anhydride in an Alder Ene reaction, so much that the catalyst concentration was unimportant when the vinyl was contained on the butadiene termonomer. To investigate the manner which the unsaturation geometry influences the Alder Ene reaction, two diene termonomers were examined: 5-ethylidene-2-norbornene (Royalene EPDM) and 1,4-hexadiene (Nordel EPDM).

A simple experimental set (2^2 factorial) was examined in a batch mixer at 270°C (60 rpm) comparing two Lewis acid catalysts (ruthenium and stannous chloride) with the two diene termonomers. An uncatalyzed Alder Ene sample using Royalene was included to demonstrate whether the catalysts were hindering or enhancing the reaction. The experimental parameters and the measured succinyl anhydride content for each product, are presented in Table 8.3. Ruthenium chloride exceeded stannous chloride in catalytic activity during the reaction (which will be discussed in more detail in section 8.7) and appeared to be less affected by the structural geometry of the unsaturation. For both Lewis acids, the less sterically hindered geometry of the hexadiene termonomer yielded superior succinyl anhydride incorporation compared to the ethylidene norbornene species. Hardly surprising results, considering the bulky nature of the enophile. The torque plots of the first four samples (01F to 04F) are shown in Figure 8.9 (sample 05F overlaps the torque plot of 01F). Stannous chloride appeared to have a degradative effect on the Royalene EPDM compared to

ruthenium chloride. Since the Nordel plots did not even overlap in the fusion region of the graph, no conclusions can be drawn from the results shown.

Table 8.3. Comparison of Nordel and Royalene EPDM with two Lewis acids.

Sample No.	Material*	Temperature (°C)	Lewis Acid Type	Parts Acid	$A_{1792}/A_{1385} \times 10^3$
01F	Royalene	270	RuCl_3	0.05	2.01
02F	Nordel	270	RuCl_3	0.05	2.31
03F	Royalene	270	SnCl_2	0.05	0.68
04F	Nordel	270	SnCl_2	0.05	1.14
05F	Royalene	270	none	0	1.86

* 1 part maleic anhydride per 100 parts polymer used, 140 g. polymer mass used in each run

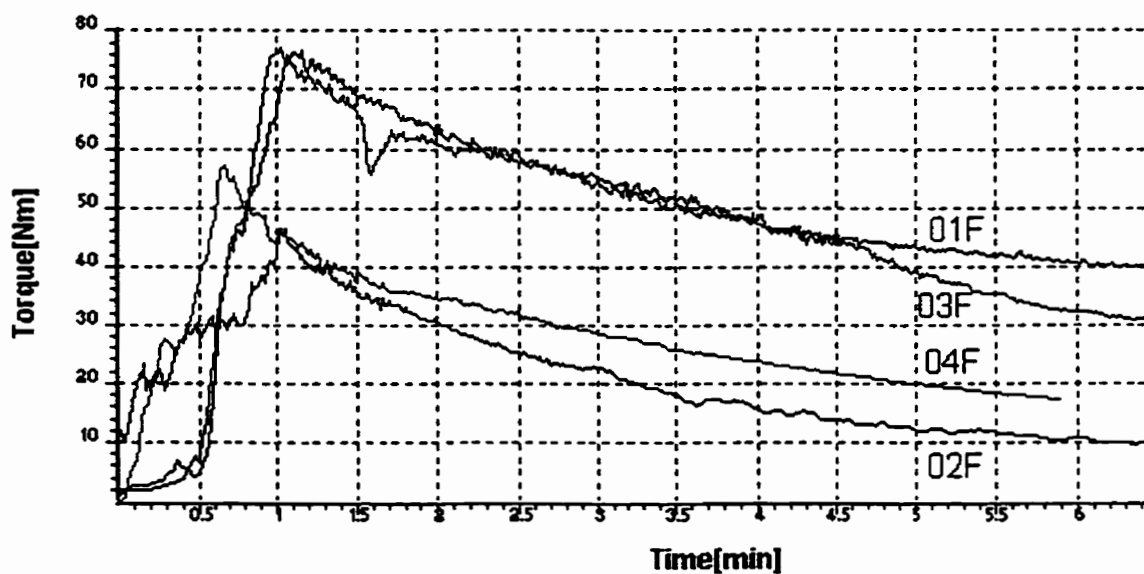


Figure 8.9. Torque plots of the maleation experiments for Royalene and Nordel EPDM

8.4. EXAMINING EXTRUSION OPERATING PARAMETERS

The unsaturation available for reaction in the ethylidene norbornene termonomer, has been shown to exhibit strong steric effects on the Alder Ene mechanism with stannous chloride (which was primarily used in this work). Therefore, it was necessary to optimize the reaction by understanding the influence of reaction and processing parameters. To begin the investigation, reactions were performed in the single screw extruder to screen several of these parameters in a reactor that possessed simpler mixing and with less oxygen present than the twin screw extruder (the ultimate scale-up for this thesis). Unfortunately, due to the bulk density of EPDM being inappropriate for the feed throat and hopper geometry of the single screw extruder, the pellets would “bridge” at the entrance to the extruder rather than falling down into the screw. Therefore, achieving steady state processing conditions for pure EPDM was not possible. To increase the bulk density of the material and, henceforth, achieve steady state, the EPDM rubber was blended with Montell KF6100 polypropylene in a ratio of 50/50 w/w (weight basis). Choudhary et al. (1991) have examined binary blends of EPDM (Nordel 2760) and isotactic polypropylene (MFI=3.0 g/10 min.) with varying elastomer content (0-30 wt %) in a Betol single screw extruder (melt temperature 210°C). They observed an increase in viscosity, elongation at break and impact strength (by 1333%) for the extrudate. Some degree of macromolecular inter-penetration between the two phases was shown via T_g variance of the EPDM dispersant (Choudhary et al., 1991; Wenig and Wasiak, 1993). Based on solution experiments, Wenig and Wasiak (1993) postulated that a narrow inter-penetration region existed at the interface of the two immiscible polymer phases, produced primarily by polypropylene molecules entering the EPDM phase. Da Silva and Tavares (1996)

demonstrated by ^{13}C NMR that for atactic PP/EPDM blends prepared in a Brabender and Haake plastograph, the system was miscible for polypropylene contents below 45 %. Thus, it can be anticipated that the polymer system shall exhibit two phases which may reduce the homogeneity of the reactants observed in the reactor depending on how maleic anhydride partitions itself. Also, due to the presence of the polypropylene resin, the ENB vinyl concentration shall be diluted for the Alder Ene reaction.

Table 8.4 presents the results from this set of experiments, preliminary to full scale reactive extrusion in the twin screw extruder. For the sake of comparison, the succinyl anhydride concentration was also predicted from the kinetic data provided in Chapter 6 for the low molecular weight polypropylene (Polypol-19). The reaction times were calculated using the extruder volume and material density properties that are included in the table and assuming the reaction time was 39 % of the material residence time based on the location of the injector. The measured succinyl anhydride data were calculated using a yet undisclosed

Table 8.4. Varying factor levels for maleic anhydride and Lewis acid concentration

Sample No.	Screw Speed (rpm)	Estimated [†] Reaction time (s)	MAh (mole eq.)	Measured SAh Conc. (wt %)	Standard Error (wt%)	Predicted SAh [‡] Conc. (wt %)
06F	50	400	1	0.016	0.005	0.030
07F	70	277	1	0.010	0.005	0.021
08F	30	677	1	0.023	0.006	0.050
09F	50	400	2	0.018	0.006	0.059
010F	70	277	2	0.015	0.005	0.041
011F	30	677	2	0.020	0.006	0.099

all reactions carried out at 230°C, 0.01 % mole-eq. $\text{SnCl}_2 \cdot 2\text{H}_2\text{O}$

MAh = maleic anhydride; SAh = succinyl anhydride

[†] based on 750 mL extruder volume, $\rho(230^\circ\text{C})=731.2 \text{ kg/m}^3$ estimated in capillary rheometer

[‡] calculated using rate constant, $k(230^\circ\text{C}, 0.01 \text{ \% mole-eq. SnCl}_2)=2.0824 \times 10^{-4} \text{ L/mol}\cdot\text{s}$ (chapter 6)

calibration curve. The procedure of generating the curve was identical to eqn (4.8) except the polymer film was a 50/50 w/w mixture of EPDM and polypropylene. The calibration curve was,

$$C_{SAh} = 4.7812 \times 10^{-6} \cdot \frac{A_{1792 \text{ cm}^{-1}}}{A_{459 \text{ cm}^{-1}}} - 4.9322 \times 10^{-7} \quad (8.1)$$

where C_{SAh} was the concentration of succinyl anhydride (mol/g) calculated from its IR absorbance at 1792 cm^{-1} relative to an internal reference band at 459 cm^{-1} . Despite the significant differences between the Polypol-19 and EPDM/PP reaction systems namely the degree of viscous mixing, presence of oxygen, differing solubility of maleic anhydride in EPDM and PP, geometry of the unsaturation and presence of multiple phases in the case of EPDM/PP, the values of the measured and estimated anhydride content agreed better than expected. Considering the FT-IR measured data in Table 8.4 by itself, the results do not show significant difference from one another. For comparison, an Alder Ene reaction was performed in the extruder at 230°C , 50 rpm and 2 mole-eq. MAh without catalyst, yielding a succinyl anhydride concentration of 0.0150 wt % (12F). No effect of catalyst, reaction time or maleic anhydride concentration was observed from these results. Inadequate mixing may be obscuring the significance of these other effect.

From the present knowledge on the maleic anhydride functionalization of EPDM, if free radical reactions were attributed with the attachment of the anhydride groups, then significant side-reactions (i.e. cross-linking and more predominately scission) would be expected. Due to the high viscosity of the polymer matrix for the maleated samples, it was possible to examine the viscosity curves of these materials using a capillary rheometer (Kayeness Galaxy V). This method of analyzing the structure of the polymer product was

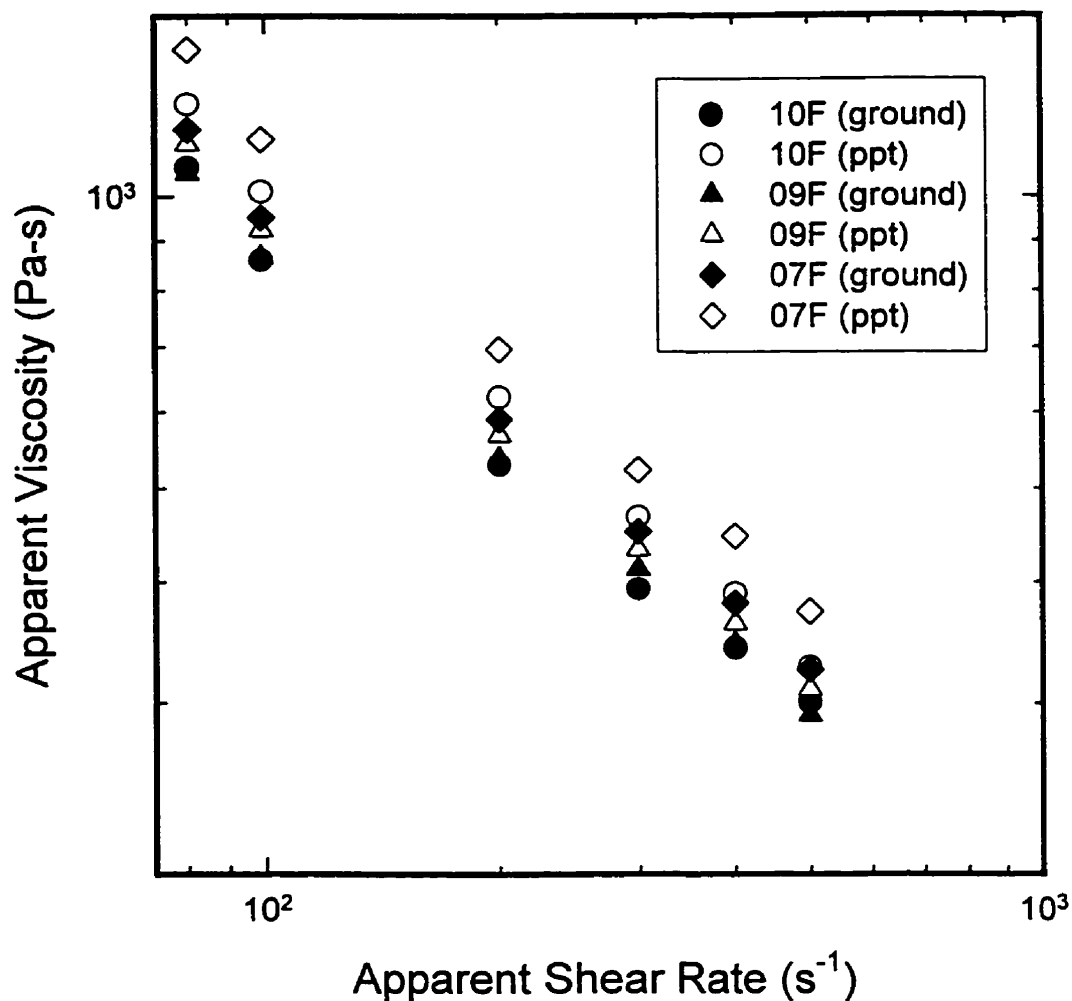


Figure 8.10. Comparison of viscosity between ground extrudates from several experiments with their solvent purified samples (ppt) for evidence of cross-linking.

not utilized anywhere else in this thesis since Polypol-19 and the degraded polypropylene lacked sufficient viscosity to remain in the barrel for testing and EPDM was too elastic in its pure state to produce accurate results on account of melt fracture. The maleated samples were tested at 230°C over a span of shear rates from 80 to 500 s⁻¹. Since the viscosity data in Figures 8.10 and 8.11 are in apparent values, it was necessary to include the specifications of the capillary die used (0.508 mm diameter, L/D=20) for those wishing to reproduce these

results. Figure 8.10 shows the viscosity curves of three samples, comparing the material directly from the extruder (ground) with the soluble EPDM/PP fraction (ppt) collected from dissolving the product into hot xylene, filtering the solution through a 200 mesh stainless steel filter and precipitating with an excess of acetone. The data in the figure show that the sol fraction of the EPDM/PP had a higher viscosity than the ground material, presumably due to some small degree of polymer fractionation occurring during precipitation. It was possible

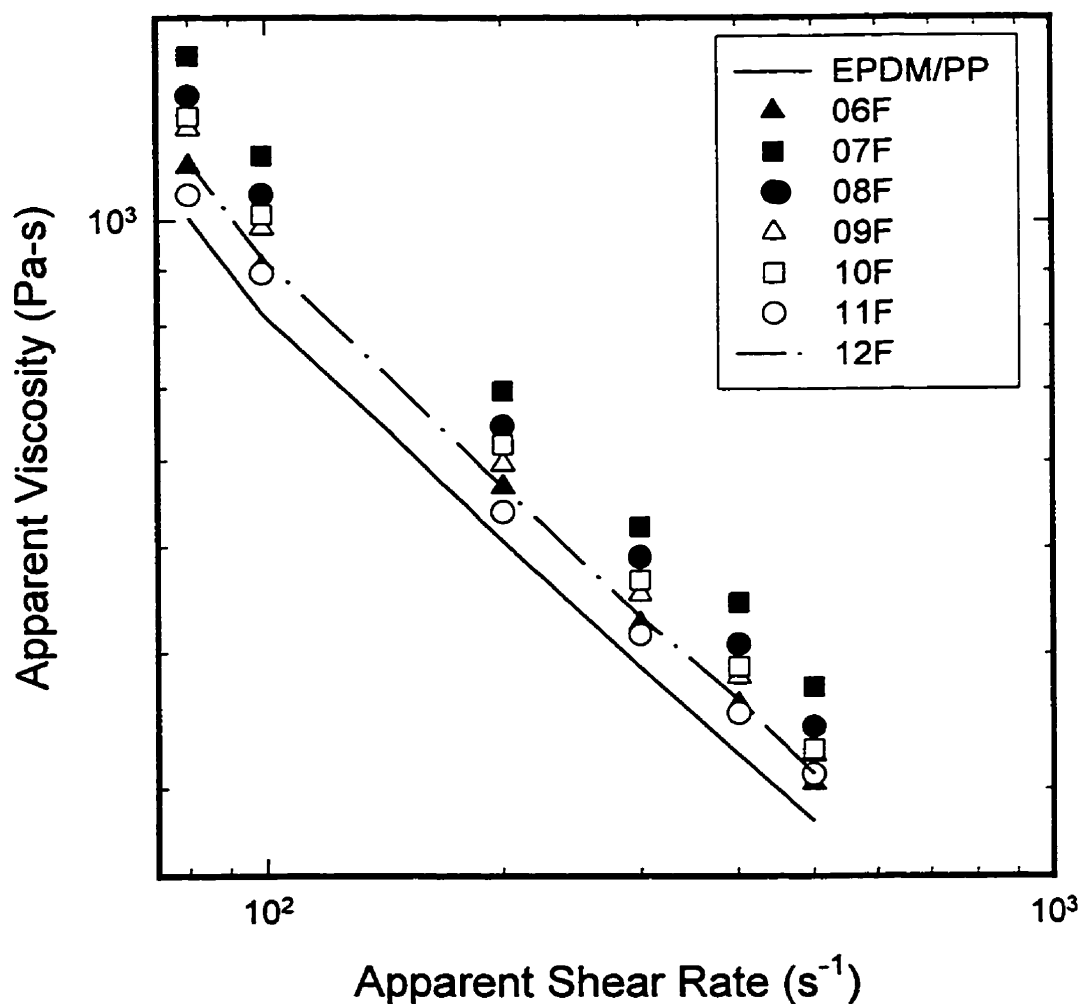


Figure 8.11. Comparing the viscosity curves of the maleated EPDM/PP samples (ppt) along with the virgin blend (ppt) to identify any occurrence of scission

to state that no significant quantity of cross-linking had occurred in the product, provided that one assumes the lubrication effect of free maleic anhydride in the ground sample and the fractionation effect from the precipitation of the samples, did not obscure its presence. All the maleated samples from the extrusion experiments (in precipitated form) were examined in Figure 8.11 including a virgin EPDM/PP blend which had been extruded using the same temperature profile at 50 rpm and cleaned (precipitated) for comparison. All the samples exhibited an increase in viscosity above the virgin EPDM/PP and in the absence of significant cross-linking, that finding must be attributed to hydrogen bonding through the maleic anhydride groups. No general correlation was observed for the viscosity curves with respect to the degree of maleation measured by the FT-IR method. However, in light of those infrared measurements being unable to discriminate the effects of the different parameters, such a revelation should not be considered important. Interestingly, those samples maleated with a higher maleic anhydride concentration (which should produce a higher degree of succinyl anhydride incorporation based on second-order kinetic) exhibited lower viscosity values than those samples produced with the lower maleic anhydride concentration. Such an observation could be caused by either i) branching caused by the high quantity of Lewis acid used in those samples produced with high maleic anhydride reactant, or ii) the higher maleic anhydride concentration quenched the excimer formation more effectively and reduced the quantity of oligomeric and polymeric maleic anhydride segmented grafted to the EPDM chains, thereby, decreasing the number of hydrogen bonds. Based on branching theory, the side chains would have to exceed a critical chain length, so as to not reduce the viscosity of the polymer by increasing its free volume (Ferry, 1980). Due to the black colouring of the

extrudate from the extruder, the presence of poly(maleic anhydride) was certainly possible yet no evidence of the homopolymer was observed in the infrared spectrum.

Ultimately, these rheological results indicate that side reactions with respect to scission and cross-linking did not participate significantly in the maleation of EPDM. In their absence, it would be reasonable to assume that maleation due to free radical reaction was likewise insignificant.

8.5. EFFECT OF SCREW SPEED IN THE TWIN SCREW EXTRUDER

The first experimental series in the twin screw extruder detailed in Table 8.1, varied screw speed among other parameters to determine its effect on the extent of reaction. It was intended that the greater mixing inherent to the twin screw extruder would provide the means to determine the effect of the screw speed on the succinyl anhydride content in the product, compared to the results in the single screw extruder. Due to torque limitations in the machinery and the high elastic energy of the rubber, a greater range in the screw speed was not possible. The screw design of configuration 3 provided more regions along the screw channel which would flood-fill and hence, provide greater mixing to enhance dispersion of maleic anhydride into EPDM. Varying screw speed at a fixed mass flow rate, may affect several aspects of the reaction including residence time, degree of mixing and channel fill; none of these phenomena are independent. The concentrations of succinyl anhydride bound to EPDM, as determined by IR, for the first experimental series were included in Table 8.1. The estimated variance of the experiment was 1.497×10^{-3} wt % based on repeats, indicating that screw speed and maleic anhydride concentration effects were significant, yet differences between the two Lewis acids were not observable. Comparing the measured succinyl

anhydride concentration with the estimated values from kinetic data shall be done in section 8.8. Examining the results (in Table 8.1) pertaining to samples prepared without catalyst, the lower screw speed examined (20 rpm) consistently yielded a lower succinyl anhydride incorporation. These results indicate that the effect of screw speed on residence time was not necessarily important compared to its effect on the dispersion of maleic anhydride into EPDM. Two phase systems such as maleic anhydride and EPDM, will likely induce homopolymerization of maleic anhydride, diminishing the presence of the reactant for the Alder Ene reaction. The effects of the Lewis acid and maleic anhydride reaction parameters shall be discussed in subsequent sections.

8.6. EFFECTS OF TEMPERATURE AND MAH CONCENTRATION

It had been previously observed with polypropylene wax (Thompson et al., 1998a) that maleation via the Alder Ene reaction at temperatures above 230°C exhibited side-reactions such as isomerization and homopolymerization of maleic anhydride. Therefore, it was not unexpected to observe black poly(maleic anhydride) particulate in those runs performed at 270°C with sample colouration varying from dark brown to black. Most maleated EPDMs synthesized at this temperature possessed a small gel content, as observed during cleaning, typically less than 5 wt %. The GPC measurements of the samples processed at this temperature consistently showed the high-end tail of the distributions shifted to higher molecular weights independent of maleic anhydride, catalyst type or catalyst concentration (already mentioned in section 8.2.1). The increase in the higher molecular weight fraction was presumably due to the cross-linking reaction, while the loss of low molecular weight fractions have already been attributed to solvent fractionation during

purification. The concentrations of succinyl anhydride incorporated into EPDM for reactions at 270°C were given in Table 8.1, with values being nearly three times higher than at temperature between 210 to 230°C. The strong dependency of the reaction on the concentration of maleic anhydride reactant was observed from the data, with anhydride incorporation being approximately 0.8, 0.6 and 0.4 wt % for maleic anhydride reactant concentrations of 2.0, 1.0 and 0.5 mole equivalence in relation to the initial concentration of the internal vinyl group of ENB, respectively.

For samples prepared below 270°C, no insoluble fractions were observed in the xylene solution indicating the absence of gel in the product. Figure 8.12 shows the molecular weight distributions of four maleated samples prepared in the absence of catalyst in comparison with a sample of unmodified EPDM control which had been extruded at 210°C and subsequently purified. The molecular weight distribution appeared to shift towards lower molecular weights with increased temperature and lower maleic anhydride reactant concentration. The increased maleic anhydride concentration was observed to act as a lubricant during processing, through a reduction of the torque. This lubrication effect would likewise reduce viscous dissipation within the EPDM and, hence, decrease the rate of degradation, explaining the results witnessed. As already mentioned, this phenomenon was not observed in those reactions occurring at 270°C in the twin screw extruder.

The experimental series shown in Table 8.2 was setup as a 3^{4-1} fractional factorial design which provides a method of determining the main factors affecting the concentration of attached succinyl anhydride in EPDM, without confounding with two factor interactions. The estimated variance of the experiment was 4.850×10^{-5} wt % based on repeats. Comparing the infrared measured succinyl anhydride concentration with the estimated values from

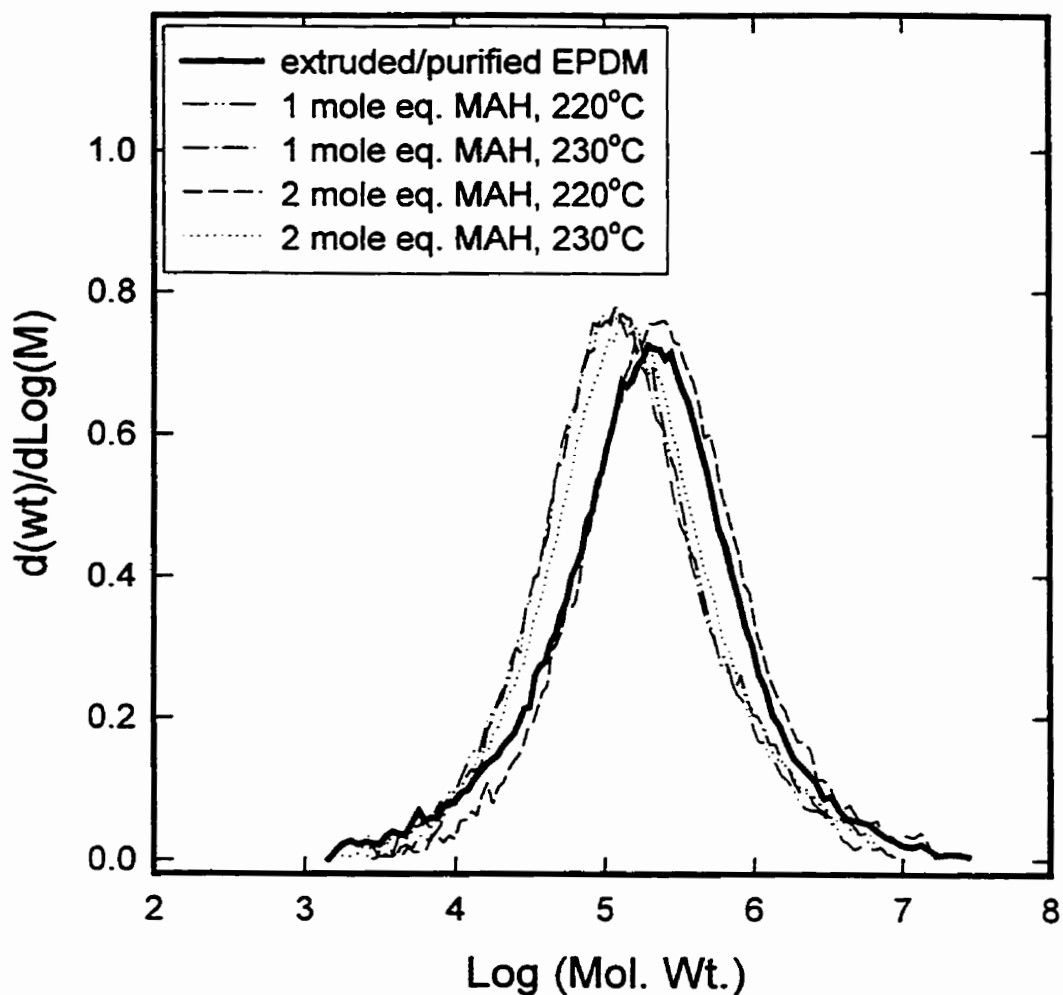


Figure 8.12. Effect of temperature and maleic anhydride concentration on the molecular weight distribution through scission that occurred during uncatalyzed maleation of EPDM.

kinetic data shall be done in section 8.8. Based on IR determination of the anhydride functionality in the maleated product, temperature was determined to be the strongest factor affecting the extent of reaction with the concentration of maleic anhydride reactant also being important. Both factors had a positive influence on the reaction, increasing bound succinyl anhydride concentration with increased temperature and/or maleic anhydride concentration. The bound succinyl anhydride concentration among the experimental series ranged from 0.1

to 0.3 wt % (values included in Table 8.2). Due to the bimolecular nature of the reaction, succinyl anhydride incorporation into EPDM appeared to be sensitive to the concentration of double bonds in EPDM, as observed experimentally (in Table 8.5) within a set of repeats for samples 30 to 32F. The minor lot-to-lot variance of ENB in the supplied EPDM, typical of any polymerization process, was sufficient to have an effect on the extent of the reaction. As shown in Table 8.5, there was a consistent increase by approximately 0.03 wt % for maleated

Table 8.5. Repeated runs showing the vinyl effect on SAh incorporation

Sample No.	EPDM Lot No.	SAh Conc. (wt %)
30F	1	0.060
30F	1	0.061
30F	2	0.098
31F	1	0.170
31F	2	0.206
31F	2	0.217
32F	1	0.134
32F	2	0.166
32F	2	0.153

SAh = succinyl anhydride

EPDM based on material designated as EPDM Lot #2 (6.5 wt % ENB) compared to Lot #1 (3.9 wt % ENB). The estimated ENB values were based on ^1H NMR analysis of the two lots and assumed that the mole composition of ethylene to propylene (74/26) remained constant.

8.7. EFFECT OF LEWIS ACIDS

As mentioned previously, Figure 8.12 demonstrated the effect of temperature and maleic anhydride concentration in the absence of any catalyst species, on the molecular weight distribution of the maleated product. Unlike the observed chain scission among these maleated samples, rubber functionalized in the twin screw extruder at 210-230°C in the

presence of a Lewis acid did not demonstrate significant variance of its molecular weight distribution from the unmodified EPDM extrudate (as shown in Figures 8.1 and 8.13). This phenomenon appeared to be independent of catalyst concentration among a Lewis acid

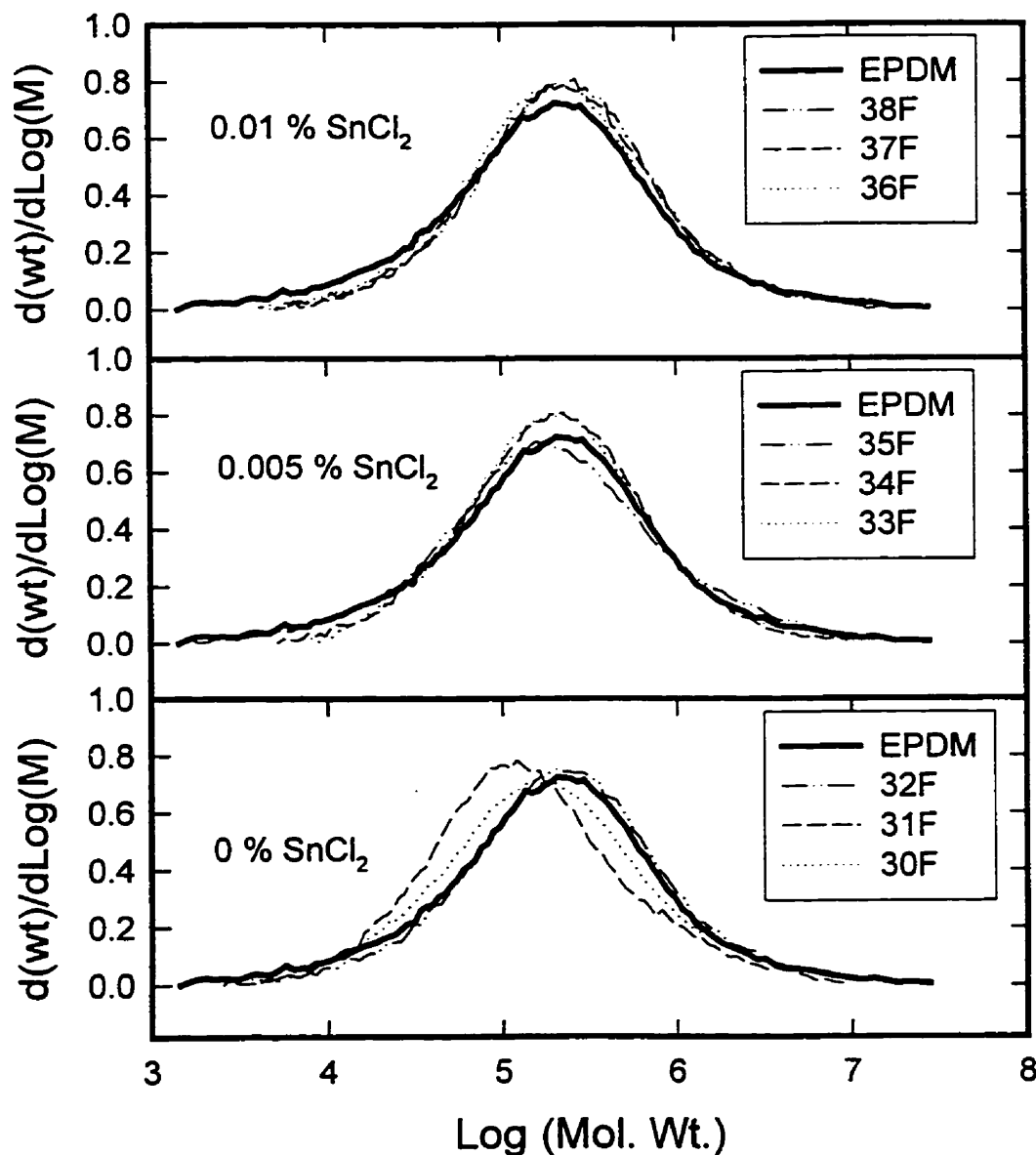


Figure 8.13. Changes in the molecular weight distribution of maleated EPDMs within the stannous chloride dihydrate series, grouped according to Lewis acid concentration.

species, however, aluminum chloride appeared to produce more scission in the product presumably due to it being a stronger acid. This phenomenon had been observed in previous work (Thompson et al., 1998a,b), where the presence of catalyst appeared to inhibit the ability of maleic anhydride to participate in free-radical reactions which normally would result in chain scission through chain-transfer, and homopolymerization of the comonomer.

In the first experimental series done in the twin screw extruder, the presence of stannous chloride or ruthenium chloride appeared to have no effect on the reaction, however, due to the evidence of maleic anhydride homopolymerization at 270°C, it is difficult to anticipate the actual influence of the metal species at that temperature. Based on analysis of the 3⁴ fractional factorial design for the second set of experiments (Table 8.2), the presence of a Lewis acid was considerably less important than temperature and maleic anhydride reactant concentration on the extent of reaction. Among the three Lewis acid species examined, the order of importance was AlCl₃ > RuCl₄·xH₂O > SnCl₂·2H₂O, with the reaction favouring lower Lewis acid concentrations. The catalytic behaviour of stannous chloride at high temperatures in the Alder Ene reaction between maleic anhydride and polypropylene has been observed in previous studies (Thompson et al., 1998a,b). However, the findings above demonstrate the possibility of optimizing the reaction by examining other Lewis acid species where the optimal species would presumably be reaction system specific.

8.8. COMPARING ESTIMATED TO MEASURED SAH CONTENT

To produce reasonable estimates of the degree of succinyl anhydride incorporated into EPDM through reactive extrusion in the twin screw extruder from the kinetic data in Chapter 6, several assumptions had to be made. From those maleated EPDMs produced at 270°C,

only samples produced in the absence of catalyst or using 0.01 % mole-eq. stannous chloride could be used. Using the determined minimum residence times provided in Chapter 4 for the two screw speeds, two mean residence times were derived using $\bar{t} = \frac{4}{3} \cdot t_0$ from the theory of laminar flow in a single screw extruder (Tadmor and Gogos, 1979). Therefore, for screw speeds of 20 and 30 rpm, the mean residence time shall be 600 s and 467 s respectively (independent of temperature, reaction, or polymer). Due to the significant error inherent to these estimated time, they were not reduced to account for the location of the injector and therefore, the mean residence time shall be treated as the reaction time for the experiments. The kinetic rate constants for the reactions were derived from the activation energy already calculated for the two catalyst systems. Since the actual kinetic data never exceeded temperatures of 250°C, these rate constants were extrapolations. Despite all these sources of error including the simple fact that the reactive system does not bear any similarities to those which the kinetic data were derived from, the estimated succinyl anhydride values were reasonable. Figure 8.14 plots the measured versus the predicted SAh content, showing the estimated values as being lower than the measured values (similar to the polypropylene system). Both Figures 8.14 and 8.15 include deviation bars to account for a possible 5°C variance in temperature, since the melt temperature is not known.

Similarly to the calculations above, only those samples produced from the second set of experiments in the absence of catalyst or using 0.01 % mole-eq. stannous chloride could be used. With a fixed screw speed and feed rate in these experiments, only a single mean residence time (reaction time), $\bar{t} = 400$ s, was applicable for each calculation (using single screw extrusion theory). Rate constants for temperatures of 220°C and 230°C were taken

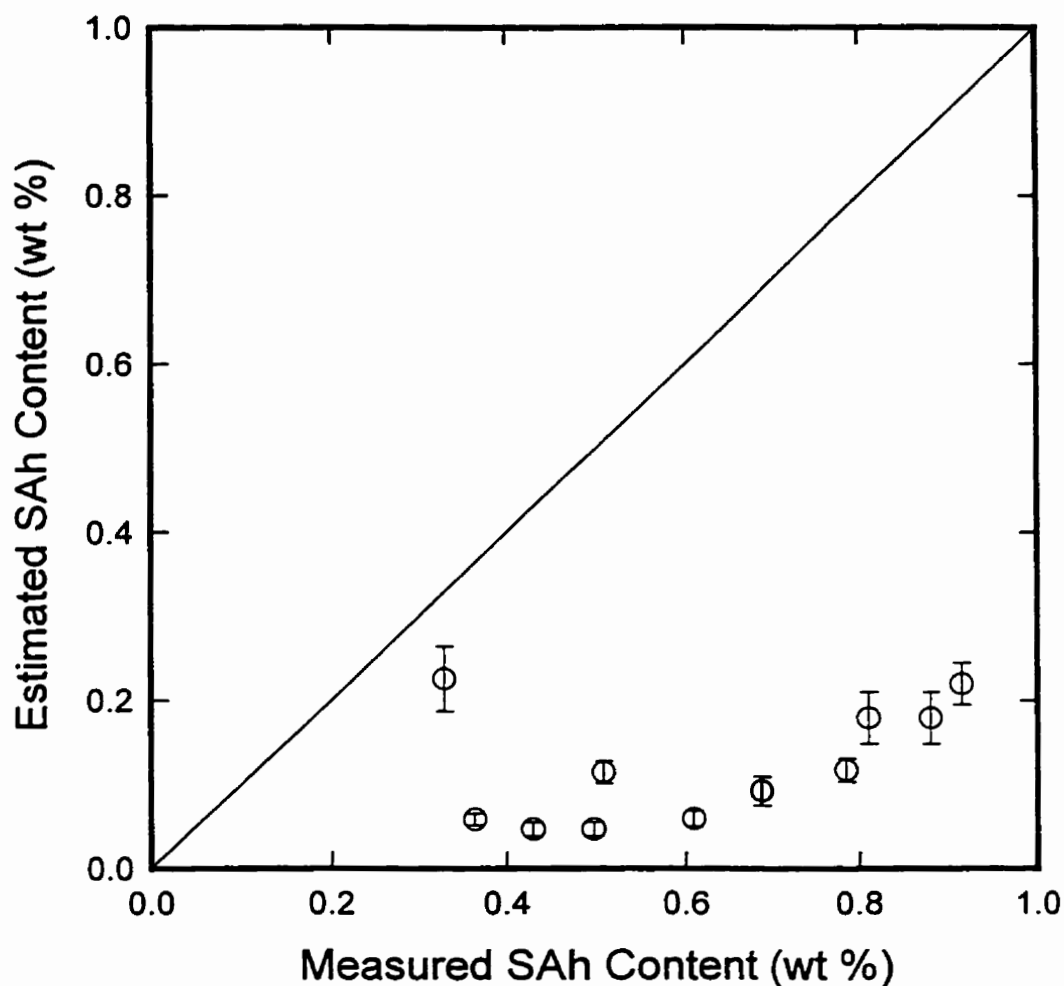


Figure 8.14. Correlation between the FT-IR measured succinyl anhydride (SAh) content and the predicted SAh content estimated from kinetic data in Chapter 6 for the first set of experiments in the twin screw extruder (deviation bars for conversions within a $\pm 5^\circ\text{C}$ range).

directly from the kinetic data in Chapter 6, however, the constant at 210°C had to be determined using the appropriate activation energy. The sources of errors were identical to those previously mentioned and yet, once again, the results were reasonable compared to the measured SAh content (Figure 8.15) although more under-predicted in value compared to the results in Figure 8.14.

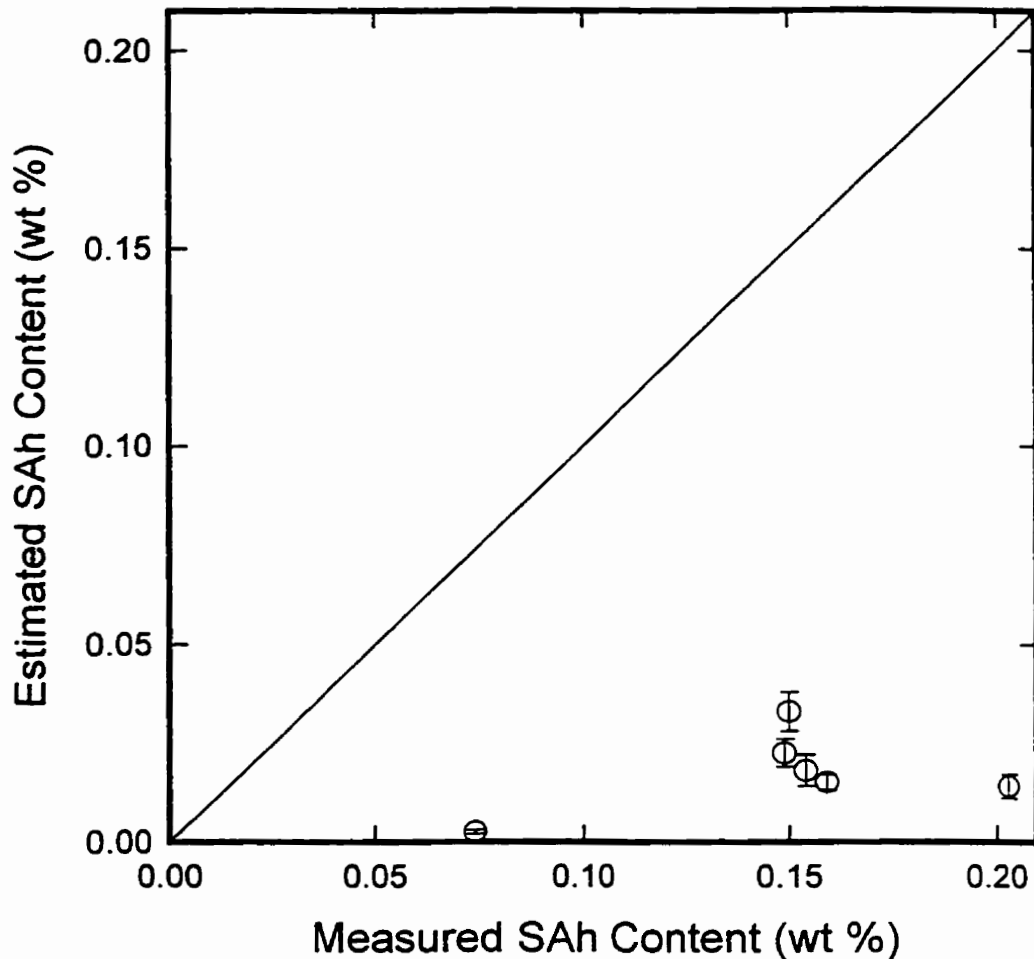


Figure 8.15. Correlation between the FT-IR measured succinyl anhydride (SAh) content and the predicted SAh content estimated from kinetic data in Chapter 6 for the second set of experiments in the twin screw extruder (deviation bars for conversions within a $\pm 5^\circ\text{C}$ range).

The increased divergence between estimated results and those determined using FT-IR data, for the second set of experiments in the twin screw extruder compared to the first set was likely indicative of a decrease in the degree of mixing. Decreased mixing efficiency can be easily understood since screw configuration 4 was essentially designed for conveying.

8.9. GLASS TRANSITION TEMPERATURE

The measured glass transition temperature (T_g) for virgin EPDM was $-40.82 \pm 0.16^\circ\text{C}$ while EPDM which had been processed in the twin screw extruder exhibited a T_g of $-40.62 \pm 0.4^\circ\text{C}$. The glass transition temperature was measured for those maleated EPDM samples produced in the temperature range of 210 to 230°C, to avoid interference resulting from the presence of cross-linking. Repeated glass transition measurements for a single maleated sample showed that measurement error was quite large, with a span of values over 1.3°C possibly due to the calculation routines used by the software to determine the inflection point of the glass transition. Greco et al. (1987) stated that a positive linear relationship was observable between grafted maleic anhydride content and the glass transition temperature, however, their data points were too few for the variance in values they were observing, to be making such conclusions. In this work, the measured glass transition temperatures could not be related to the functionality of the rubber directly. Through attempts to correlate the data with any of the reaction parameters, only a weak relationship was observed with the concentration of maleic anhydride reactant as shown in Figure 8.16. The glass transition temperature in the figure appears to decrease with increasing maleic anhydride concentration which has been determined previously to have a relationship with increased succinyl anhydride functionalization of EPDM, though it would appear not to be a direct correlation. The highly maleated (0.72 wt %) EPDM produced by long-term Alder Ene reaction in solution, had a $T_g = -42.74^\circ\text{C}$, which lies within the proposed relationship between glass transition temperature and EPDM functionality. Such a trend would be opposite to the finding of Greco et al. (1987) for free-radical grafted EPDM where increased polarity was

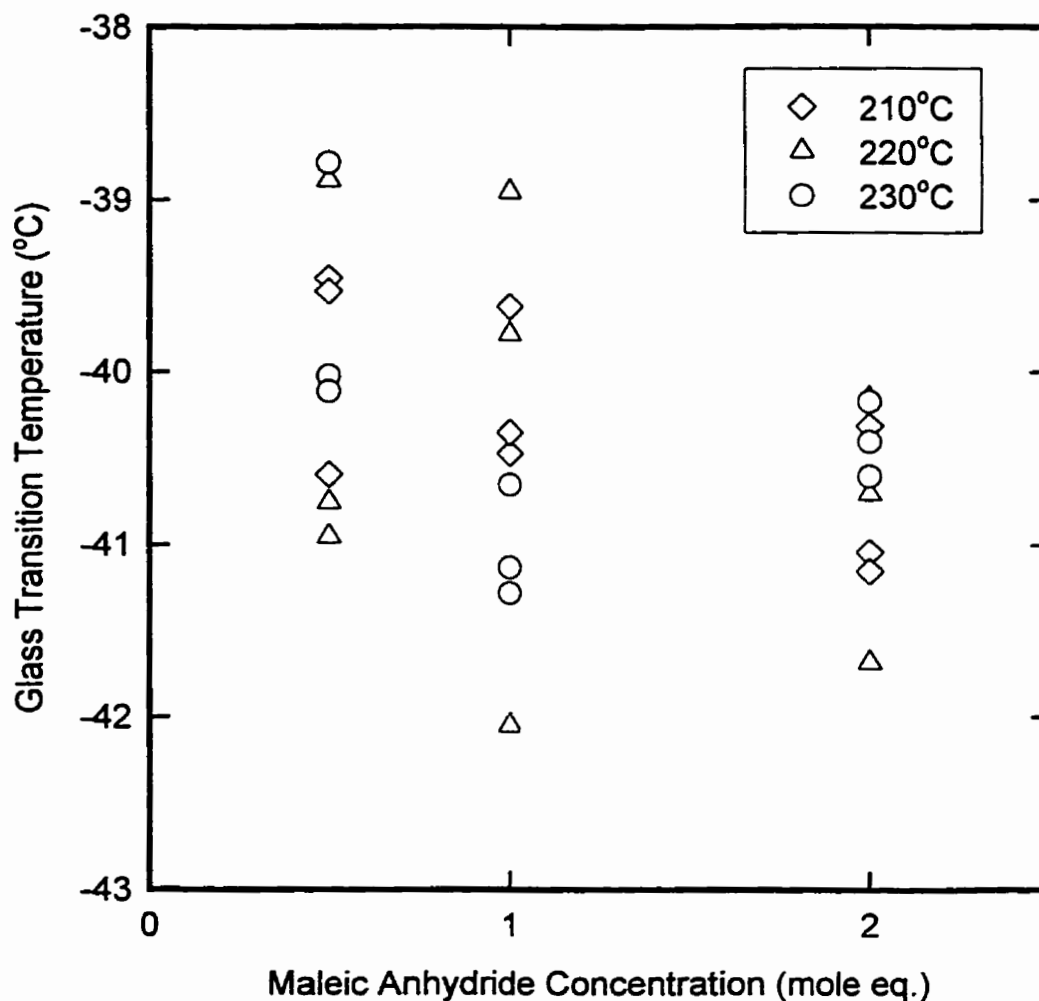


Figure 8.16. Glass transition temperature measured for samples 30-56F from the twin screw extruder

thought to decrease chain mobility (and free volume). However, in the section (8.11) on rheology, attached anhydride groups were revealed to decrease chain mobility not increase it.

8.10. NEUTRALIZATION OF MALEATED EPDM

To ensure that the measured torque gain observed was not due to ZnO/stearic acid behaving as a filler, EPDM resin which had been processed in the extruder at 210°C without maleation, was compounded using 10 phr ZnO and 1 phr stearic acid under the same

procedure as employed for neutralization of the maleated samples. On average no significant torque gain was observed in the absence of bound succinyl anhydride groups. Figure 8.17 shows the relative torque data for three maleated EPDM samples along with the fit of the model, $Y = B_0(1 - e^{-B_1 t})$ where B_0 and B_1 were constants, Y was the relative torque response

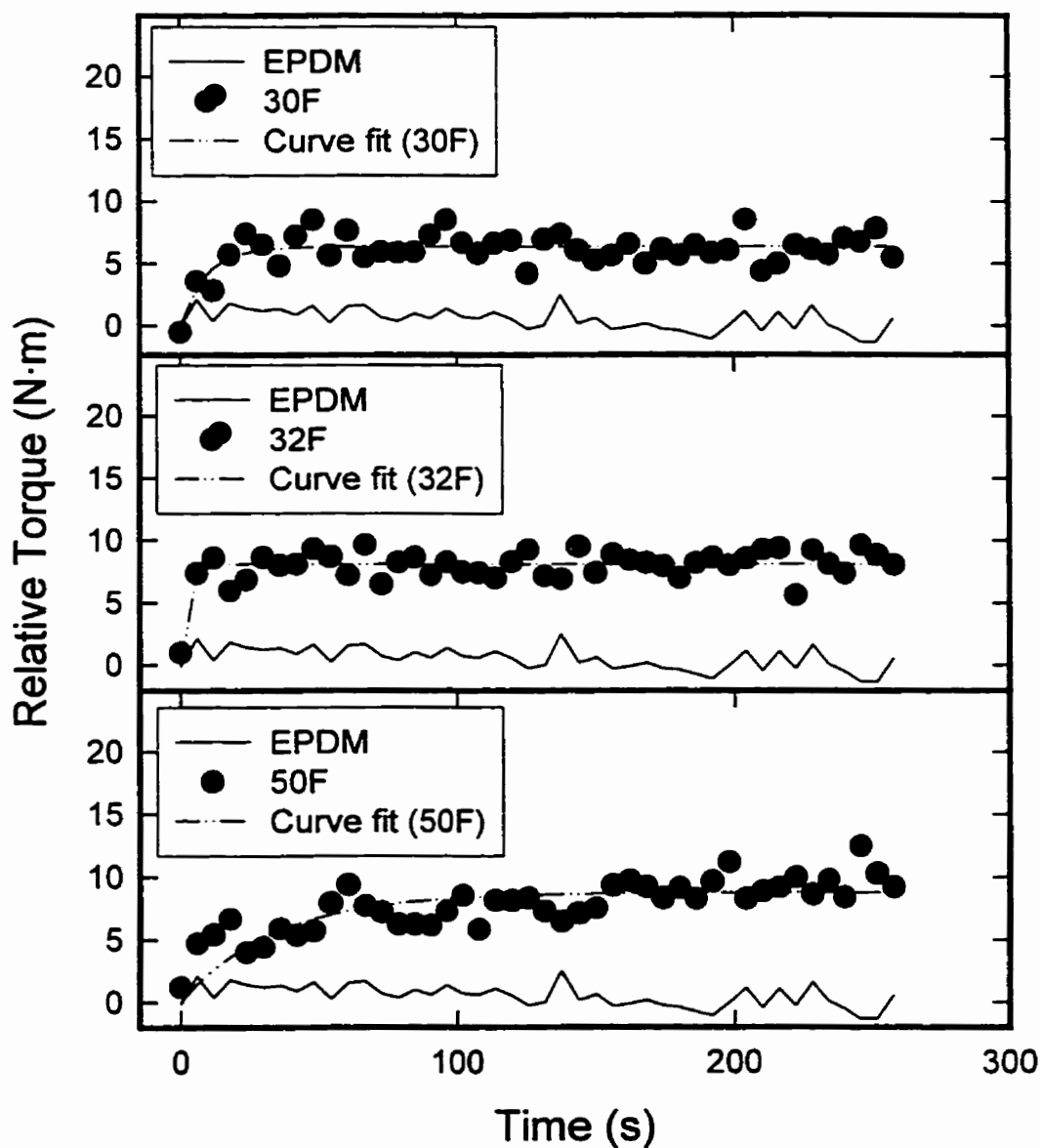


Figure 8.17. Relative torque plots of virgin EPDM and three maleated EPDMs versus neutralization time, using the steady-state torque within the range $t=-300$ to $t=0$, as a baseline.

and t was the neutralization time which would be zero at the onset of the measured torque exceeding the previously determined base-line. Figure 8.18 shows the relative torque value (as predicted by the model) for each sample from Table 8.2, calculated at $t=300$ s. The existence of a correlation between the succinyl anhydride content determined by infrared analysis (eqn. 4.8) and the relative torque value is evident from the plot.

Figure 8.18 divides the data among the different catalyst species used in the

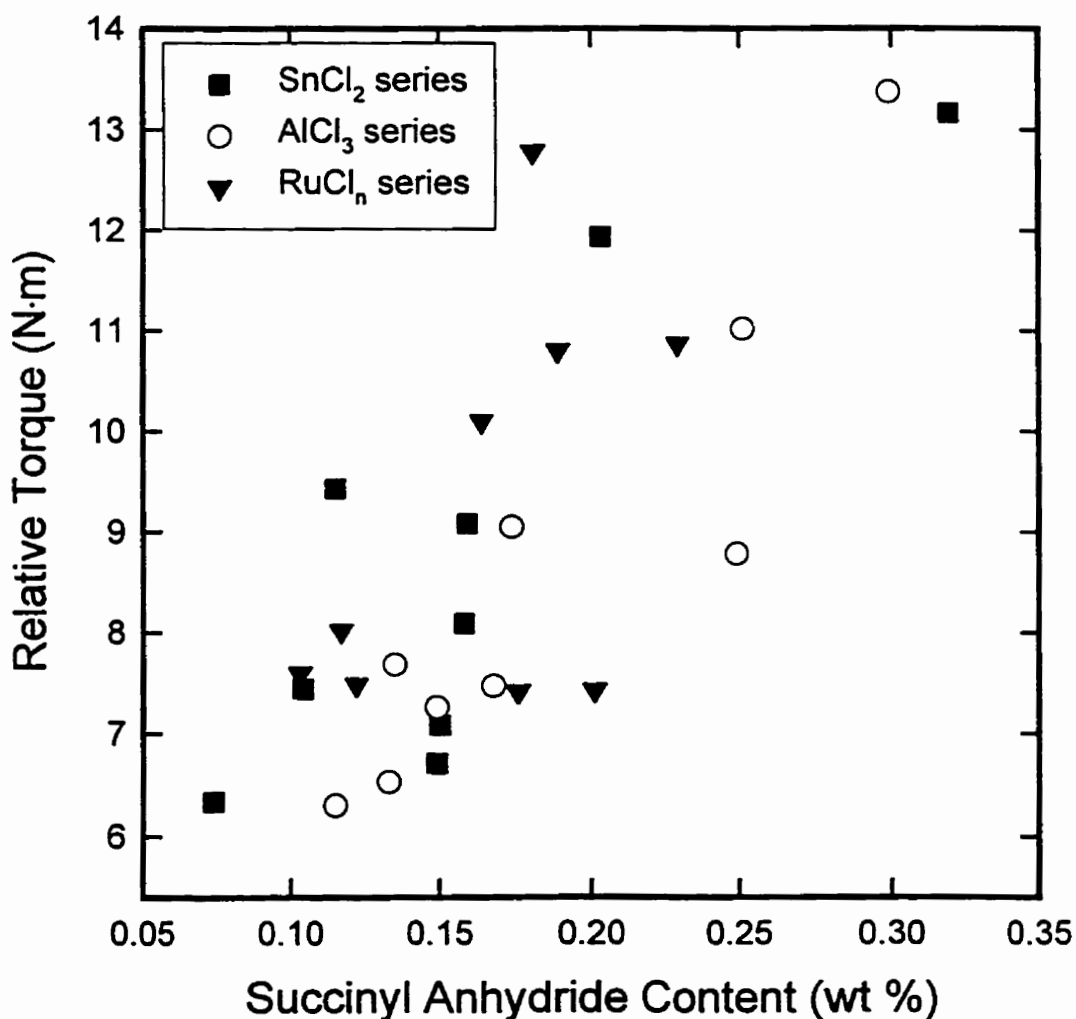


Figure 8.18. Relative torque calculated at $t=300$ s from a model fitted to the Rheocord data.

experimental series for presentation purposes, however, it should be noted that the effect of reaction parameters on the relative torque gain in influencing the degree of functionalization were no different from those determined by the infrared calibration method. Thus, confirming the exclusive relationship between the observed degree of cross-linking and the extent of maleation despite the scatter in data shown in Figure 8.18. The scatter is probably due to errors which naturally arise from calculating the anhydride content in the EPDM sample by the infrared calibration method. These errors would include limitation of the Beer-Lambert law across a wide concentration range, sample inhomogeneity, the small degree of hydrolysis which could not be taken into account due to overlapping absorbances for the carboxylic acid band, and loss in infrared beam transmission due to varied sample opaqueness which changes with maleic anhydride concentration through a phenomenon which is not understood in the literature. The torque measurements shall also include errors, particular since the samples were not purified first, rather the free maleic anhydride was expected to vaporize during the first 5 minutes of mixing due to the open nature of the batch mixer. It was assumed that any reaction between the EPDM and remaining MAh would be consistent among the samples and any residual MAh present upon addition of ZnO would not increase the system torque. The latter appeared to be true based on an experiment performed using EPDM with 1 mole-eq. MAh added immediately ahead of the ZnO, with no torque increase observed similar to the virgin EPDM. The former assumption would be more difficult to prove, however, there must be some credibility to the assumption since the torque data confirmed those results determined by FT-IR with respect to the important reaction parameters.

8.11. DYNAMIC MECHANICAL ANALYSIS

Rheological data for virgin EPDM is presented in Figure 8.19 showing the storage and loss moduli and the complex viscosity. The cross-over modulus (G_c) for EPDM at 230°C corresponded to 1.2×10^5 Pa at $\omega_c=21$ rad/s. The cross-over modulus was only observed in those rubber samples which had not been maleated. Among the maleated samples, $G'(\omega)$ was always greater than $G''(\omega)$ with similar slopes. Processing the EPDM in

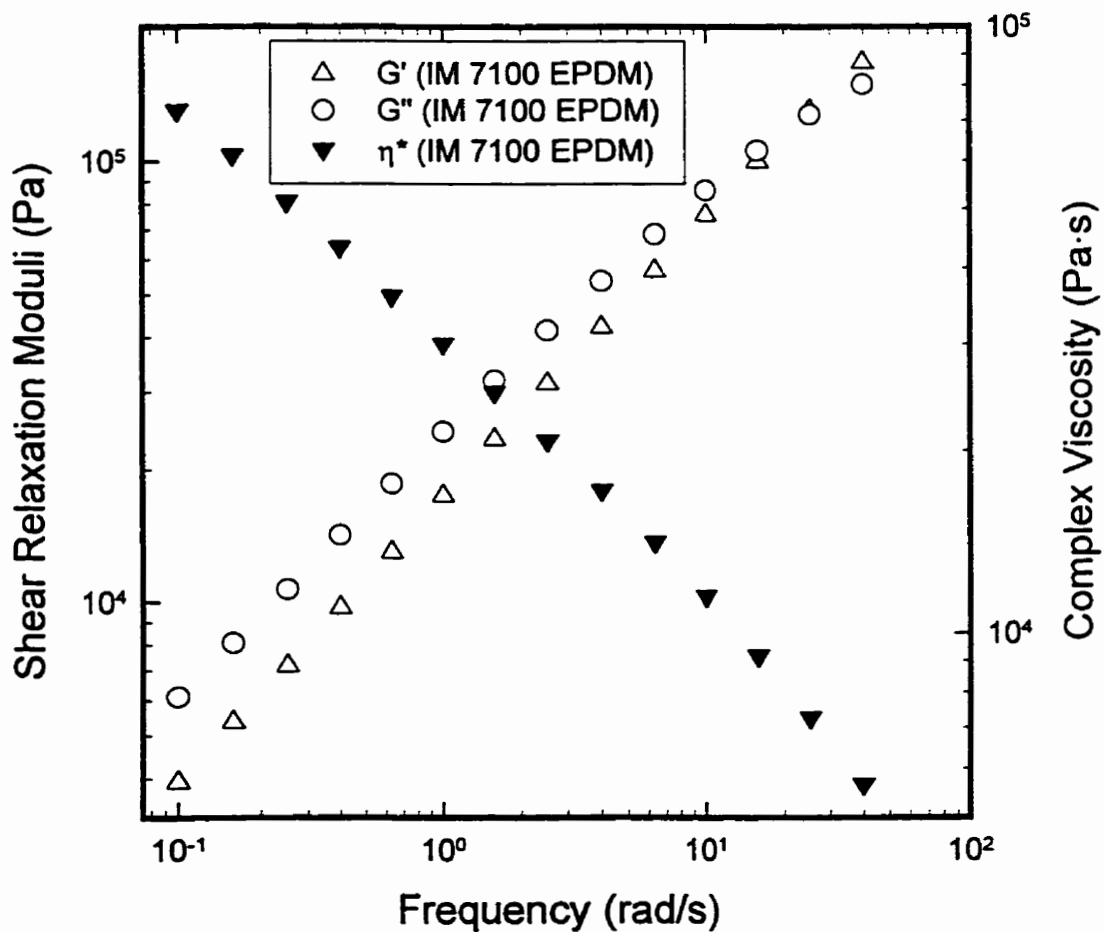


Figure 8.19. Relaxation moduli and complex viscosity of virgin EPDM at 230°C.

the twin screw extruder (210°C) shifted the cross-over modulus to a frequency of $\omega_c=25$ rad/s with negligible change in the G_c . The shifted cross-over observed in the processed EPDM was indicative of a decrease in the Maxwell zero-shear viscosity, presumably caused by a low degree of chain scission (Wu and Su, 1991). A Cole-Cole plot (Figure 8.20 on logarithmic scales) confirmed this low degree of scission with the processed EPDM essentially described by the master curve for EPDM. The plots of two unmodified EPDM samples in Figure 8.20

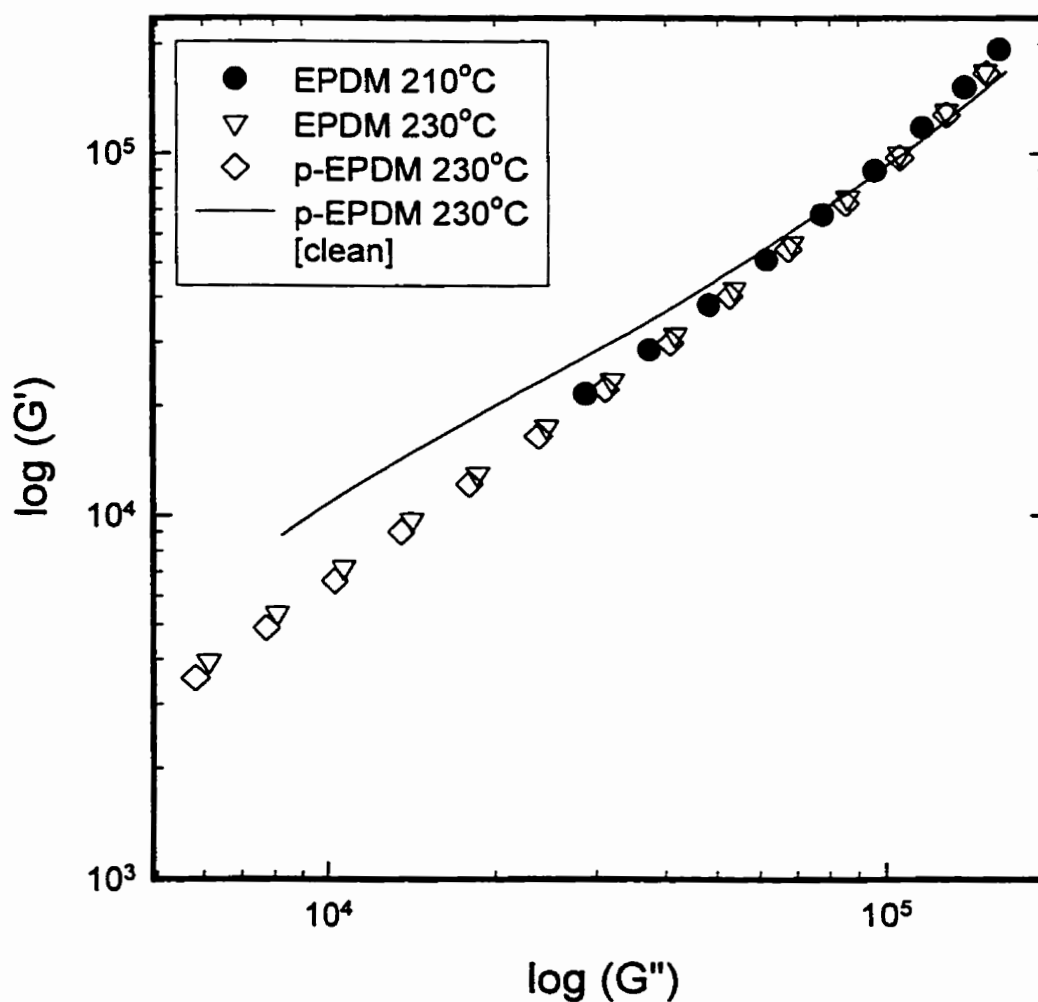


Figure 8.20. Cole-Cole plot of virgin EPDM and processed EPDM (p-EPDM) examining the effects of processing and purification of the rubber.

reiterate those findings of section 8.2.1, showing the effect of cleaning on the MWD of the polymer. Fractionation due to cleaning, had a more dramatic effect than processing on the material rheology, with the G' - G'' curve indicating a shift of the molecular weight distribution for the purified sample compared to other EPDM samples. The G' data for the cleaned EPDM exhibited higher values at the low frequencies, characteristic of a higher molecular weight polymer with increased elastic energy due to higher entanglement density. The high frequency reduction of the G' indicates a loss of segmental chain motion due to the loss of the small molecules.

The rheological properties of several maleated EPDM samples produced at 230°C (from Table 8.2, screw configuration 4), were analyzed yielding interesting results. The samples from Table 8.1 (270°C, screw configuration 3) could not be included in this study by parallel plate rheometry since initial strain sweep experiments could not identify a linear strain region to perform the analysis. Among the samples chosen from Table 8.2, similar G' values at the low frequency region demonstrated that the extent of degradation did not change. Thereby, confirming earlier observations that the MWD of the maleated EPDMs exhibited independence of maleic anhydride reactant concentration, and that any effect of catalyst concentration on chain scission, was small. At the high frequency region, the G' appeared to vary with no correlation to the concentration of succinyl anhydride incorporated into EPDM, rather the relationship might be much more complicated, similar to the capillary rheometer analysis in section 8.4. To properly examine the rheological results, the maleated samples were separated based on the presence of catalyst and displayed as Cole-Cole plots in Figure 8.21 (absence of catalyst in the reaction) and Figure 8.22 (presence of catalyst in the reaction).

The curves in Figures 8.21 and 8.22 of the maleated EPDM samples appear to converge in the high moduli region of the plot, confirming the independence of rheological measurements from large scale molecular structures (Shroff and Mavridis, 1994) in the high moduli region when the relaxation time is eliminated. The individual samples become much more disparate in the lower moduli region, with varying G' for a constant value of G'' .

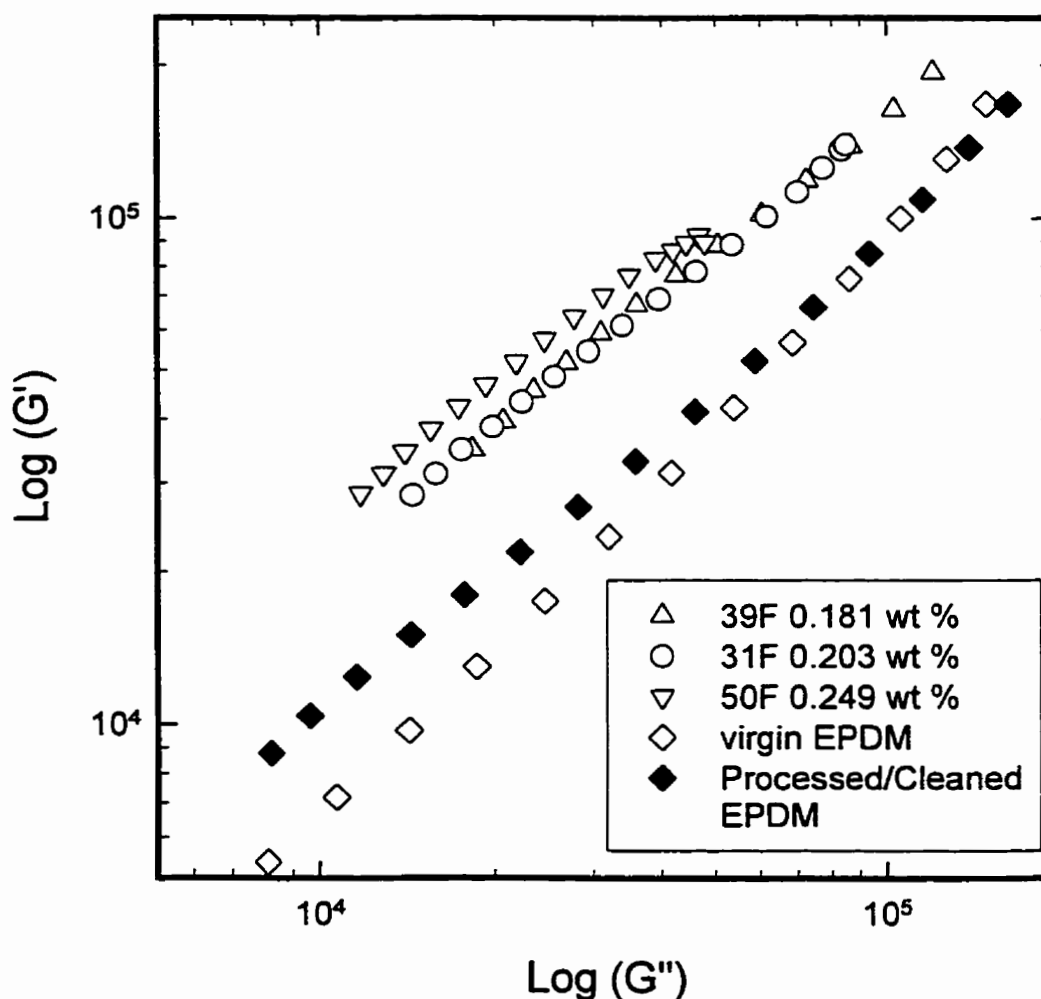


Figure 8.21. Cole-Cole plot (logarithmic scale) of the maleated EPDM sample produced at 230°C from Table 8.2 in the absence of catalyst.

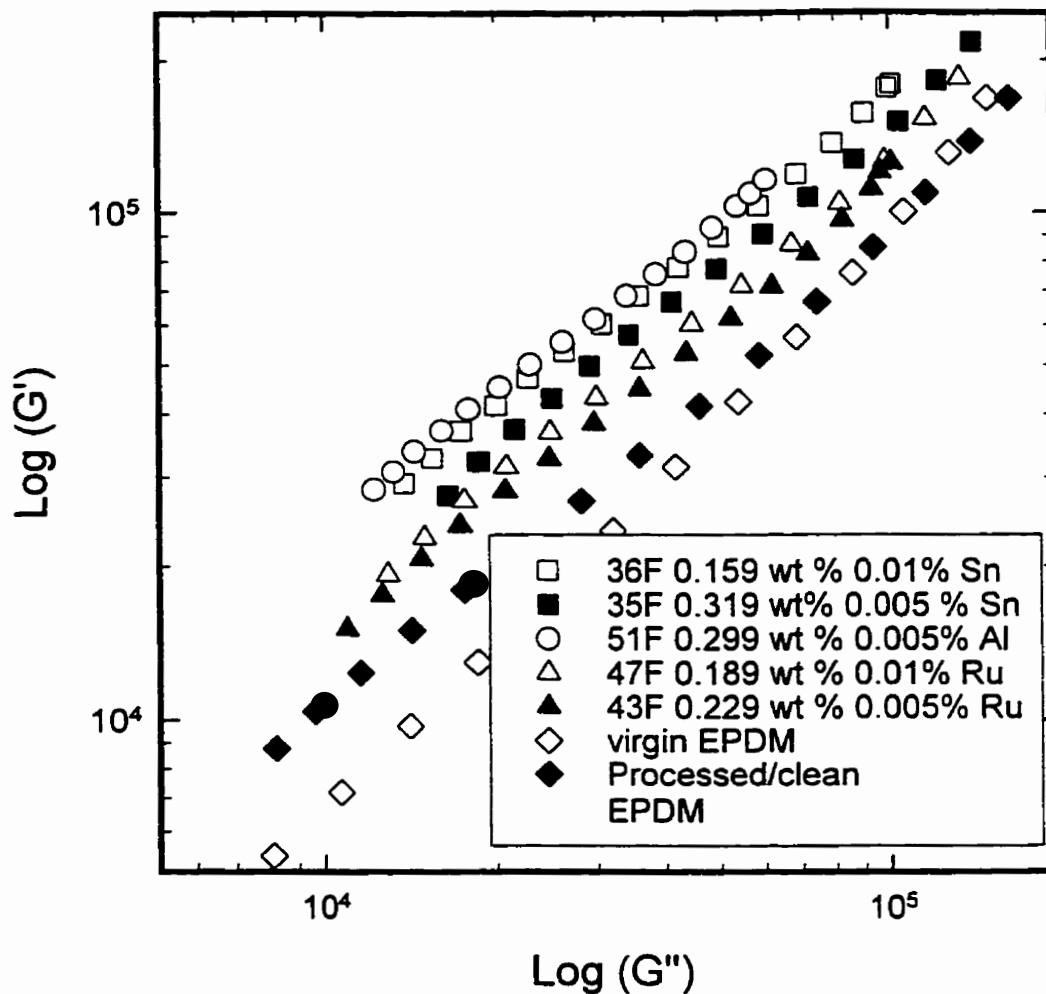


Figure 8.22. Cole-Cole plot (logarithmic scale) of the maleated EPDM sample produced at 230°C from Table 8.2 in the presence of a Lewis acid.

Among those maleated samples prepared in the absence of catalyst, there appeared to be an increase in the elastic state of the rubber with increasing succinyl anhydride concentration (shown in Figure 8.20). Samples 31F and 39F have similar concentrations measured by FT-IR, which was confirmed in the figure, while sample 50F showed a significant increase in elastic energy in correlation with succinyl anhydride content. These results suggest an increase in polar interactions between the EPDM chains due to the attached anhydride

moiety. The figure also corroborates the results of the infrared analysis, indicating that the calculated SAh concentrations increased according to an increase in maleic anhydride reactant concentration. Figure 8.22 examines those samples prepared with one of the three Lewis acid catalysts from Table 8.2. The only missing sample in the figure, from those maleated EPDMs produced at 230°C was sample 55F, since the material would not form a uniform sample disk for the RMS. The figure revealed a catalyst effect which was dependent on the concentration of catalyst used in the reaction and the type of Lewis acid employed. Samples prepared with aluminum chloride had the greatest elastic nature (as well as the greatest concentration of succinyl anhydride incorporated into EPDM among the catalyzed species examined). The use of ruthenium chloride, yielded products with the lowest elastic properties of the three Lewis acids. In this figure, the elastic properties of the material did not demonstrate any correlation to the succinyl anhydride content (or the maleic anhydride reactant concentration), however, all maleated samples exhibited greater G' values for a constant G'' than the unmodified rubber. Comparing the data between Figure 8.21 and 8.22, it also revealed that those maleated EPDMs produced in the presence of catalyst exhibited lower elasticity with respect to the materials produced in the absence of catalyst. These results introduced some concern whether the Lewis acid remained adducted to the anhydride (even after purification) interfering with the polar interactions. A similar suggestion was made in section 8.4 based on capillary viscosity measurements. However, secondary ion mass spectrometry (performed by Surface Sciences Western) did not detect any presence of the Lewis acids in the EPDM samples. It is also possible that this phenomenon observed, was due to branching of the EPDM product caused by the Lewis acids.

It was necessary to examine the rheological data in this chapter from the stance of what contributions poly(maleic anhydride) would make to the polymer. The synthesized poly(maleic anhydride) (discussed in Chapter 6) was compounded with EPDM (no polypropylene) at 220°C in a batch mixer for 5 minutes, a sample was extracted and then 10 ppm SnCl₂ in DMF was added to the mixer. After another 5 minutes, another sample was collected and both samples were cleaned to remove free poly(maleic anhydride) (pMAH). The torque measured by the Haake rheometer remained steady for the sample prepared without Lewis acid, and only began to decay slightly with the addition of stannous chloride. No evidence of cross-linking was observed during the runs. Figure 8.23 examines the difference in the infrared spectra between the EPDMs. The pMAH grafted EPDM showed a broad 1780 cm⁻¹ anhydride band and a carbonyl peak at 1714 cm⁻¹. Interestingly, the pMAH-g-EPDM sample which employed stannous chloride had a lower 1780 cm⁻¹ intensity and a greater 1714 cm⁻¹ intensity compared to the sample produced in the absence of Lewis acid. This may suggest that the Lewis acid was involved in ring opening of the cyclic anhydride. No evidence of cyclopentanone or ketoolefin repeat units were observed in the spectra. Examining a typical sample from the extruder (sample 036F), it was possible to see that the 1792 cm⁻¹ peak may include pMAH at 1780 cm⁻¹, however, the inclusion of the succinyl anhydride peak at 1868 cm⁻¹ (not seen with pMAH-g-EPDM) indicated that the majority of the bound anhydride groups were single units. The two pMAH grafted EPDMs were compared with virgin EPDM in the capillary rheometer for rheological analysis.

Figure 8.24 shows higher viscosity curves of the three EPDM samples, with virgin EPDM showing the greater viscosity over the two EPDMs containing pMAH branches. The

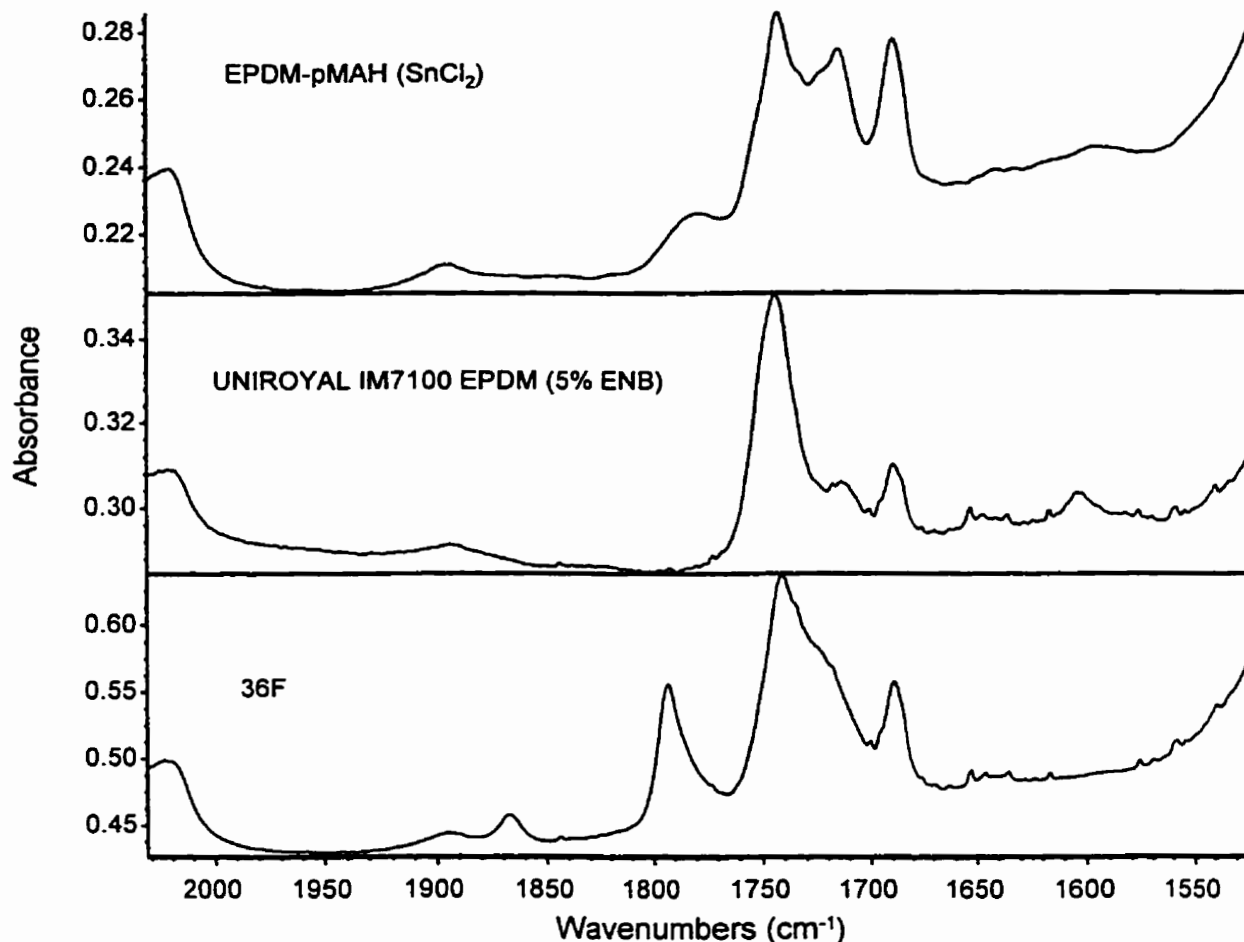


Figure 8.23. FT-IR spectra of EPDM samples to determine the presence of poly(maleic anhydride)

absence of sharkskin in the extrudate of the two branched samples indicated improved processibility compared to the virgin EPDM. The low shear rates used, compared to earlier analysis (Figures 8.10 and 8.11), were chosen to minimize melt fracture, though it was evidently present with the virgin EPDM at 200 s^{-1} . These polar pMAH branches were behaving similar to alkyl chain branches (for chains below the critical entanglement length), in their reduction of the viscosity by interfering with the entanglement density of the polymer. More interesting was the observed decrease in the viscosity of the sample produced in the presence of stannous chloride. Since the infrared spectra do not note a significant

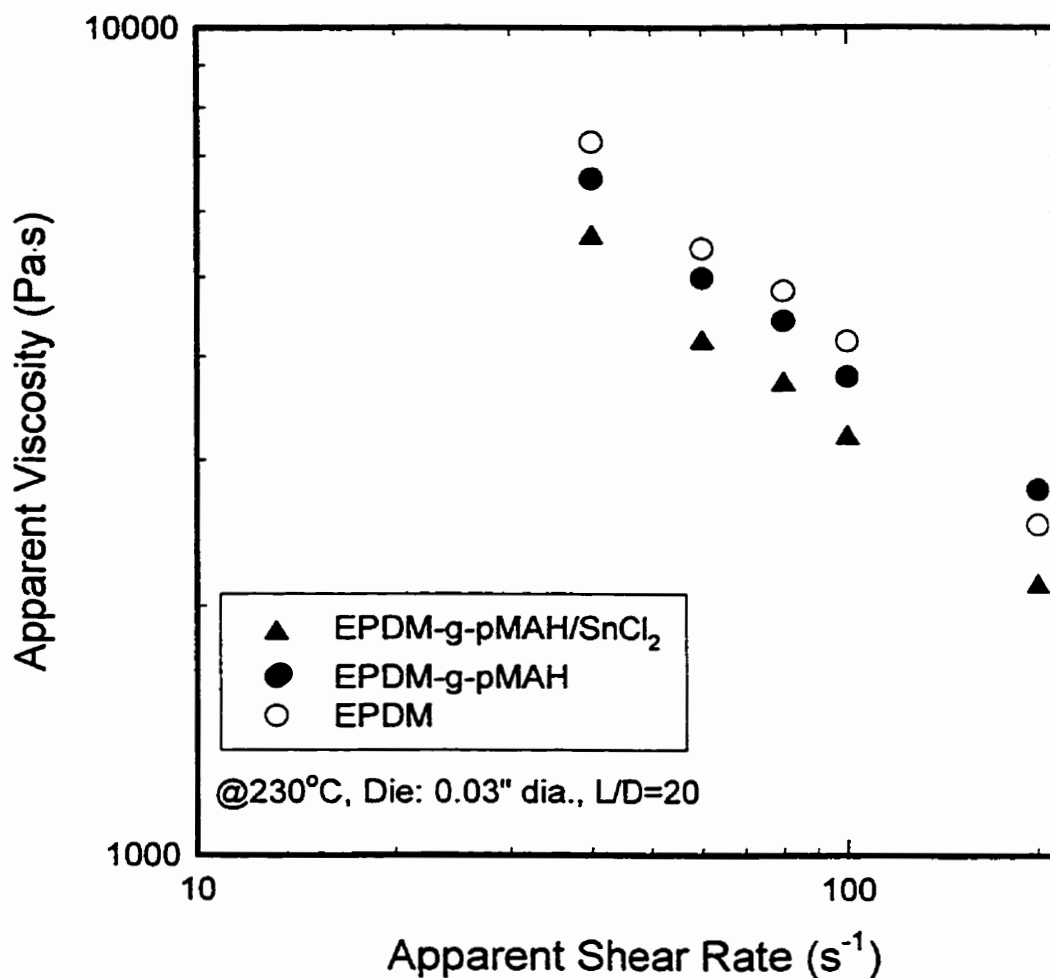


Figure 8.24. Apparent viscosity curves for two EPDMs grafted with poly(maleic anhydride) compared to the virgin resin.

difference (if any) in the grafted pMAH content between the samples prepared in the presence or absence of the Lewis acid, the change in viscosity must be due to the presence of the Lewis acid. The possibility of chain scission was examined by GPC and found to be very small in the sample with stannous chloride. Ultimately, these results indicate that the rheological results for the maleated samples from the twin screw extruder, could not be attributed to the presence of polymeric or oligomeric maleic anhydride branches, yet the

presence of a Lewis acid had a deleterious effect on the elasticity of the polymer product. The effect of the Lewis acid remains unclear.

There is unfortunately, no method of comparing these results with the rheological data (such as from Wu and Su, 1991) of maleated samples produced via free radical grafting, since the side reactions of scission and cross-linking dominate the structural changes observed in the product. It is therefore, impossible to confirm the effect of grafted anhydride groups on the structure of EPDM under deformation (and in the absence of catalyst).

8.12. CONCLUDING REMARKS

It has been observed that the Alder Ene reaction between maleic anhydride and the unsaturation of 2-ethylidene-5-norbornene in EPDM proceeds despite the hindered geometry of the double bond. However, the extent of reaction may be increased by using less hindered unsaturation such as the remaining double bond of the 1,4-hexadiene found in Nordel EPDM. The structure of the resulting succinyl-norbornyl anhydride group has been elucidated based on infrared, NMR, and molecular weight analysis of the maleated samples. No evidence of free radical grafting was observed based on the independence of the MWD with respect to maleic anhydride reactant concentration, an important parameter related to scission and cross-linking in free radical reactions due to the dominance of chain transfer termination with maleic anhydride. The extent of Alder Ene reactions at 270°C was approximately 1 wt % succinyl anhydride, three times greater than at temperatures between 210-230°C and appeared to improve with increased dispersion of maleic anhydride within EPDM due to increased screw speed. Comparing the measured SAh content with estimated values calculated from kinetic data in Chapter 6, confirmed that the absence of neutral or reverse

mixing block in screw configuration (4) for the twin screw extruder produced lower levels of mixing than screw configuration (3). Based on FT-IR measurements, temperature and maleic anhydride reactant concentration were determined to be important parameters in the optimization of the reaction, while the presence of a Lewis acid participating as a catalyst in the reaction had only a minor effect which improves with reduced concentration. Among the Lewis acids examined as catalysts for the reaction, aluminum chloride yielded the greatest succinyl anhydride content in the rubber. These parameter effects on the reaction were confirmed by relative torque measurements derived from ionic cross-link formation. Rheological analysis of the maleated samples was complicated by issues of purification, polar interactions and possible interference from residual Lewis acids in the purified product. Any scission or cross-linking of the EPDM chain was small and difficult to observe, indicating one significant advantage of the Alder Ene reaction over free radical methods, which is maleation without side-reaction (particularly in the presence of a Lewis acid). The moduli values from the maleated samples produced in the absence of catalyst, revealed that the elastic properties of the material increased with increasing anhydride functionality in the EPDM presumably due to the introduction of intermolecular polar forces.

CHAPTER 9. CONCLUSIONS AND RECOMMENDATIONS

9.1. CONCLUSIONS

This thesis has discussed an extensive set of Alder Ene reactions for the maleation of several polymers, both in the presence and in the absence of a Lewis acid catalyst. The reactions were carried out in a round bottom flask, a batch reactor, a batch mixer, a single screw extruder and a co-rotating intermeshing twin screw extruder. Polyisobutylene was used to carry out preliminary studies on the high temperature application of Lewis acids in the Alder Ene reaction. A low molecular weight polypropylene wax was chosen as a model material to study the kinetics of the reaction and identify reaction parameters useful for optimizing the reaction. The preparation of a vinylidene-rich polypropylene for the reaction via β -scission has been shown to be an effective route, with thermal degradation favoured over peroxide-initiated degradation due to the reduced presence of carbonyl functionalities in the polymer. Both methods of degradation have been shown to produce greater than one site of unsaturation per chain, demonstrating their advantage over commercial polymerization for producing an effective *ene* species in this work. Finally, EPDM was examined as a material with a high vinyl content useful for the reaction, that was also highly viscous making it more suited for reactive extrusion.

The structures of the succinyl anhydride adducted polymers has been characterized using numerous methods of analysis. No single method was found to provide conclusive evidence of the attached succinyl anhydride moiety, due to the current limitations in modern spectroscopic techniques with respect to level of detection. Unfortunately, the concentration

of the introduced functionality was too low to sometimes detect its presence and generally was incapable of distinguishing between grafted anhydride groups via the Alder Ene reaction in contrast to free radical reactions. The degree of functionalization was determined by infrared analysis, though an alternative method, explored with EPDM, also showed a direct correlation between the mechanical properties of an ionic network formed by neutralizing the maleated rubber, with the level of maleation. The reaction parameters of temperature and maleic anhydride concentration were found to be the most significant factors to this Alder Ene reaction. Increased temperature and maleic anhydride reactant concentration were found to improve the extent of reaction. Significant isomerization and homopolymerization side reactions have been observed in the batch reactor, beyond 230°C, indicating the presence of an optimal limit though this is likely to differ in the extruder. Increased maleic anhydride concentration may increase the succinyl anhydride content in the product and, it has also been attributed to lowering poly(maleic anhydride) side reactions possibly through quenching of the maleic anhydride excimer. A 'practical' optimum exists for maleic anhydride since higher levels of the comonomer in the polymer during the reaction, place a higher demand on the devolatilization zone to remove the unreacted comonomer else increased residuals will affect the performance of the product. Phenyl-based free radical trapping agents have been found to participate in the Alder Ene reaction when in the presence of a Lewis acid and therefore, were no longer employed. As a substitute, TEMPO has been found to act as an efficient free radical trap agent (with inhibitive properties similar to benzoquinone), preventing maleic anhydride from being grafted onto the backbone of polypropylene and EPDM.

The Lewis acid, primarily stannous chloride, has been proven to enhance the reaction, though confirmation of this observation was difficult in the extruder possibly due to mixing issues. Several Lewis acid species ($\text{SnCl}_2 \cdot 2\text{H}_2\text{O}$, $\text{RuCl}_n \cdot x\text{H}_2\text{O}$ [commercial $\text{RuCl}_3 \cdot x\text{H}_2\text{O}$] and AlCl_3) were tested as catalysts, and each was found to have a small effect on the degree of functionalization. This effect improved with reduced acid concentration. Among the Lewis acids examined, aluminum chloride gave rise to the greatest improvement of succinyl anhydride incorporation, at least into the rubber. Ruthenium chloride was found to improve the extent of reaction in Polypol-19, degraded polypropylene and EPDM. Employing the Lewis acid in phase with the reactant (maleic anhydride) was shown to produce higher conversion. Based on an observed "induction period" within conversion-time plots, the formation of the Lewis acid-anhydride enophile for the reaction was relatively slow with respect to the duration of the reaction. However, when the acid was employed as a solid creating a heterogeneous reaction (omitting the limited solubility of maleic anhydride within the examined polymers), the rate of formation of the acid-anhydride enophile was probably too low to observe an induction period. The applicability of the heterogeneous catalyzed system to second-order kinetics unlike the homogeneous catalyst system, provided immediate evidence of this phenomenon. In general, even in the absence of catalyst, the application of a second-order kinetic model to the measured succinyl anhydride results, was not valid over the entire temperature range studied due to side reactions, particularly vinylidene isomerization and homo-polymerization of maleic anhydride. The actual increase in functionalization due to the presence of a Lewis acid was diminutive, yielding a system with limited industrial value based on the cost of the metal species. However, the observed decrease in free radical side reactions, namely homopolymerization of maleic anhydride, in the presence of the Lewis

acid may reveal its true value in the maleation of polymers. The rheological results from the maleated EPDM series offered interesting insight. In the absence of a Lewis acid catalyst in the reaction, the elasticity of the rubber increased with increasing degree of succinyl functionalization. Likely, these polar groups were introducing intermolecular bonds with sufficient strength to produce rheological behaviour similar to cross-linking.

9.2. RECOMMENDATIONS

Another feasible comonomer for the Alder Ene reaction would be *m*-isopropenyl- α - α -dimethylbenzyl isocyanate (*m*-TMI). Dexter et al. (1986) reviewed the chemistry of this species, stating the *m*-TMI did not homopolymerize by free radical methods, rather it participated in free radical co-polymerization and may homopolymerize via cationic mechanisms. In this manner, the monomer behaves similar to maleic anhydride and therefore, should be viable in our reaction process. The molecule is shown in Figure 9.1, possessing both isocyanate and vinyl functionalities. The high boiling point of the monomer will complicate devolatilization for purification. However, its solubility in inert organics should improve mixing and rate of reaction. The reactivity of an isocyanate group would make a valuable functionality on polypropylene or EPDM, provided issues of oxidative degradation products concerning polypropylene can be overcome. Of course, precautions would have to be taken due to the toxic nature of isocyanates in general, though *m*-TMI is less toxic than hexamethylene diisocyanate (HDI) (Dexter et al., 1986).

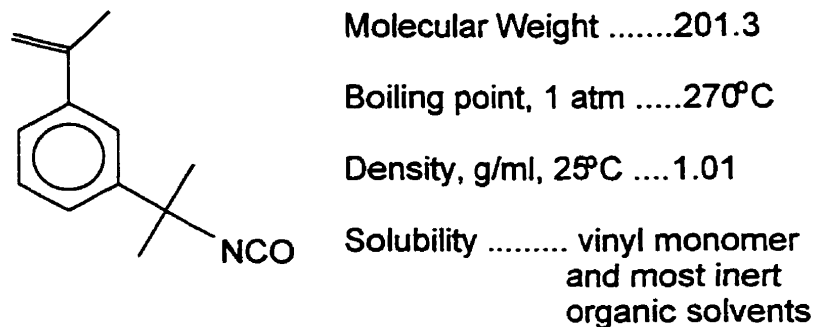


Figure 9.1. Structure and Select Properties of m-isopropenyl- α,α -dimethylbenzyl isocyanate (taken from R. W. Dexter et al., *J. Coat. Technol.*, 58, 43 (1986))

It would be advisable to characterize any radical formation during the catalyzed Ene reaction. Observation of the solution of the Parr reactor upon completion of both catalyzed and uncatalyzed Ene reactions, showed that the presence of a black poly(maleic anhydride) solid seemed to diminish along with the colouration of the product in the former case. The participation of the Lewis acid catalyst in preventing the formation of MAh excimers is unclear, though it appears to reduce the presence of undesirable side reactions. Based on this fact alone, the use of catalyst would appear to be beneficial. To prove this hypothesis, the reaction would need to be performed in a high-temperature ESR spectrometer. Our Lewis acid, $\text{SnCl}_2 \cdot 2\text{H}_2\text{O}$, and other useful Lewis acids such as the previously mentioned hydrates of RhCl_3 and RuCl_3 should be examined in this future work.

Stannous chloride was chosen primarily for its low toxicity, weak Lewis acidity, and on its inexpensive supply criteria. Ruthenium chloride, as mentioned in Chapters 6-8, has been shown to improve upon the conversion of the reaction, though not sufficiently to warrant the increase in reagent cost. The results of using several different catalysts in this thesis has identified the need to continue examining other Lewis acid species, since the rate

of reaction may improve dramatically with the proper choice of catalyst or catalysts. The following discusses a few suggested Lewis acids. Rhodium species were shown by Roncetti and Banzi (1992) to yield high conversion of the unsaturation in ethylidene norbornene and therefore, could be a possible candidate for analysis. Diethylaluminum chloride has been a classically employed Lewis acid for the Alder Ene reaction in the literature which has been found to act simultaneously as an acid scavenger, reducing the occurrence of isomerization and degradation. Though, the expense of this material may not compensate for any improvement in the extent of reaction results, from its use. The double salt, NaCl-AlCl_3 has been shown (Mori et al., 1984) to be a softer Lewis acid than AlCl_3 , minimizing degradation.

Finally, it has been observed during the course of this thesis that maleated EPDM behaves differently depending on the nature of the bound succinyl group. With the succinyl functionality in its anhydride form, the rubber possessed mechanical and processing properties similar to the virgin material. However, over the course of time, the anhydride functionality was hydrolyzed, at which point the material behaved very differently. Trials attempting to press films from the hydrolyzed material exhibited behaviour similar to a cross-linked rubber. The material was difficult to process and as seen in Chapter 8, had different thermal properties. Due to the great difficulty in reversing the hydrolysis process, the material was often unusable for analysis once the anhydride had changed to a dicarboxylic acid group. This was also noted in the functionalized polypropylene, though, less dramatically. No literature exists, to my knowledge, which explores the different mechanical, thermal and chemical properties of a maleated polymer in its two possible forms, dicarboxylic acid or cyclic anhydride.

CHAPTER 10. REFERENCES

- Achmatowicz, O., and Bialecka-Florjanczyk, E., "Mechanism of the Carbonyl-Ene Reaction", *Tetrahedron*, **52**, 8827 (1996)
- Adams, J. H., "Analysis of Non-volatile Oxidation Products of Polypropylene. I. Thermal Oxidation", *J. Polym. Sci. Part A-1*, **8**, 1077 (1970)
- Adams, J. H., and Goodrich, J. E., "Analysis of Non-volatile Oxidation Products of Polypropylene. II. Process Degradation" *J. Polym. Sci. Part A-1*, **8**, 1269 (1970)
- Albisetti, C. J., Fisher, N. G., Hogsed, M. J., and Joyce, R. M., "Thermal Addition of Monoolefins to Dienophiles", *J. Am. Chem. Soc.*, **78**, 2637 (1956)
- Alderson, T., Jenner, E. L., and Lindsay Jr., R. V., "Olefin-to-Olefin Addition Reactions", *J. Am. Chem. Soc.*, **87**(24), 5638 (1965)
- Andersen, P., "Downstream mixing in twin screw extruders", *SPE Extrusion Div. Newsletter*, **24**(1), 2 (1997)
- Bacski, R., "Structure of Poly(maleic anhydride)", *J. Polym. Sci.: Polym. Chem.*, **14**, 1797 (1976)
- Baranwal, K., "Mechanochemical Degradation of an EPDM Polymer", *Rubb. Chem. Technol.*, **41**, 1459 (1968)
- Benn, F. R., and Dwyer, J., "The Ene Reaction of Maleic Anhydride with Alkenes", *J. Chem. Soc. Perkin II*, 533 (1977)
- Bhadani, S. N., and Prasad, J., "Cathodic Polymerization of Maleic Anhydride with N-Methylpyridinium Iodide", *Makromol. Chem.*, **178**, 187 (1977)
- Bidaux, J-E., Smith, G. D., Bernet, N., Manson, J-A. E., and Hilborn, J., "Fusion Bonding of Maleic Anhydride Grafted Polypropylene to Polyamide 6 via In Situ Block Copolymer Formation at the Interface", *Polymer*, **37**(7), 1129 (1996)
- Borsig, E., Fiedlerova, A., and Hrcikova, L., "Influence of Maleic Anhydride on the Molecular Weight of Atactic Polypropylene at the Functionalization Reaction", *J. Macromol. Sci. Pure Appl. Chem.*, **A32**(12), 2017 (1995)
- D. Braun, El Sayed, I. A. A., and Pomakis, J., "Radical Homopolymerization of Maleic Anhydride", *Makromol. Chem.*, **124**, 249 (1969)

Burlett, D. J., and Lindt, J. T., "Reactive Processing of Rubbers", *Rubb. Chem. Technol.*, **66**, 411 (1993)

Busfield, W. K., and Hanna, J. V., "A ^{13}C NMR Study of End Groups and Stereoregularity Changes Induced by γ -Irradiation of Molten Polypropylenes", *Polym. J.*, **23**, 1253 (1991)

Caywood, Jr., S. W., "Adducts Containing Succinic Groups Attached to Elastomeric Copolymers", US Patent 4,010,223, E. I. DuPont (1977)

Chasmawala, M., and Chung, T. C., "Telechelic Polyisobutylene: A Facile Synthesis via the Cross-Metathesis Reaction and Trialkylborane-Containing Olefins", *Macromol.*, **28**(5), 1333 (1995)

Chiantore, O., Cinquina, P., and Guita, M., "Fractionation and Molecular Characterization of EPDM Rubbers", *Eur. Polym. J.*, **30**(9), 1043 (1994)

Choudhary, V., Varma, H. S., and Varma, I. K., "Polyolefin Blends: Effect of EPDM Rubber on Crystallization, Morphology, and Mechanical Properties of Polypropylene/EPDM Blends. I", *Polymer*, **32**(14), 2534 (1991)

Chien, J. C. W., and Tsai, M. W., "Zirconocenium Cation Catalysis of Propene Polymerization", *Makromol. Chem. Macromol. Symp.*, **66**, 141 (1993)

Coran, A. Y., and Patel, R., "Rubber-Thermoplastic Compositions. Part VIII. Nitrile Rubber Polyolefin Blends with Technological Compatibilization", *Rubb. Chem. Technol.*, **56**, 1045 (1983)

Coutinho, F. M. B., and Ferreira, M. I. P., "Optimization of Reaction Conditions of Bulk Functionalization of EPDM Rubbers with Maleic Anhydride", *Eur. Polym. J.*, **30**(8), 911 (1994)

Coutinho, F. M. B., and Ferreira, M. I. P., "Characterization of EPDM Rubber Modified with Maleic Anhydride (MAH) by Diffuse Reflectance FTIR (DRIFT)", *Polym. Test.*, **13**, 25 (1994)

Cramer, R., "Transition Metal Catalysis Exemplified by Some Rhodium-Promoted Reactions of Olefins", *Accts. Chem. Res.*, **1**, 186 (1965)

Cudby, M. E. A., "Cis Vinylidene Unsaturation in Polythene", *J. Polym. Sci. B: Polym. Lett.*, **3**, 73 (1965)

Curry, J., Jackson S., Strehler, B., van der Veen, A., "Free Radical Degradation of Polypropylene", *Chem. Eng. Progr.*, **84**(11), 43 (1988)

- Da Silva, N. M., and Tavares, M. I. B., "Characterization of EPDM/Atactic Polypropylene Blends by High-Resolution Solid-State NMR", *J. Appl. Polym. Sci.*, **60**, 663 (1996)
- Datta, A., and Baird, D. G., "Compatibilization of Thermoplastic Composites Based on Blends of Polypropylene with Two Liquid Crystalline Polymers", *Polymer*, **36**(3), 505 (1995)
- Datta, S., De, S. K., Kontos, E. G., and Wefer, J. M., "Ionic Thermoplastic Elastomer Based on Maleated EPDM Rubber. I. Effect of Zinc Stearate", *J. Appl. Polym. Sci.*, **61**, 177 (1996a)
- Datta, S., De, S. K., Kontos, E. G., Wefer, J. M., Wagner, P., and Vidal, A., "Dynamic Mechanical and Infra-red Spectroscopic Studies on Interaction Between Carbon Black and Ionic Thermoplastic Elastomer Based on Maleated EPDM Rubber", *Polymer*, **37**(15), 3431 (1996b)
- Dealy, J. M., and Wissbrun, K. F., "Melt Rheology and its Role in Plastics Processing", Von Nostrand Reinhold (1990)
- Dean, B. D., "EPDM-g-Polyethersulfone via Diels-Alder Chemistry", *J. Polym. Sci. Part A: Polym. Chem.*, **32**, 567 (1994)
- Dean, B. D., "High-Temperature Thermoplastic Elastomers via the Grafting Reaction of Polyarylate onto EPDM Rubber", *J. Appl. Polym. Sci.*, **47**, 2013 (1993)
- de Kock, R. J., and Hol, P. A. H. M., "Infrared Determination of Unsaturation in Polyethylene", *J. Polym. Sci. B: Polym. Lett.*, **2**, 339 (1964)
- Deng, X. M., Xiong, C. D., Cheng, L. M., and Xu, R. P., "Synthesis and Characterization of Block Copolymers from D,L-Lactide and Poly(ethylene glycol) with Stannous Chloride", *J. Polym. Sci.: Part C: Polym. Lett.*, **28**, 411 (1990)
- Denisov, E. T., "The Role and Reactions of Nitroxyl Radicals in Hindered Piperidine Light Stabilisation", *Polym. Deg. Stab.*, **34**, 325 (1991)
- De Roover, B., Sclavons, M., Carlier, V., Devaux, J., Legras, R., Momtaz, A., "Molecular Characterization of Maleic Anhydride-Functionalized Polypropylene", *J. Polym. Sci. Part A: Polym. Chem.*, **33**, 829 (1995)
- Dexter, R. W., Saxon, R., and Fiori, D. E., "m-TMI, A Novel Unsaturated Aliphatic Isocyanate", *J. Coat. Technol.*, **58**, 43 (1986)
- Dorman, D. E., Jautelat, M., and Roberts, J. D., "Carbon-13 Nuclear Magnetic Resonance Spectroscopy. Quantitative Correlations of the Carbon Chemical Shifts of Acyclic Alkenes", *J. Org. Chem.*, **36**(19), 2757 (1971)

- Dorn, M., "Modification of Molecular Weight and Flow Properties of Thermoplastics", *Adv. Polym. Technol.*, **5**(2), 87 (1985)
- Dreiblatt, A., Herrmann, H., and Nettelbreker, H. J., "On-line Quality Control for Improved Compounding", *Plast. Eng.*, **43**(10), 31 (1987)
- Duca, D. D., and Moore, Jr., E. P., "End-Use Properties", *Polypropylene Handbook*, Carl Hanser Verlag, Munich, 1996
- Dumoulin, M. M., Daigeneault, L. E., Gendron, R., and Dufour, J., "On-Line Rheology Control for the Peroxide Degradation of Polypropylene", *ANTEC*, **51**, 1448 (1993)
- Duvall, J., Sellitti, C., Myers, C., Hiltner, A., and Baer, E., "Interfacial Effects Produced by Crystallization of Polypropylene with Polypropylene-g-Maleic Anhydride Compatibilizers", *J. Appl. Polym. Sci.*, **52**, 207 (1994)
- Ebner, K., and White, J. L., "Continuous Thermal Degradation of Polypropylene in Single and Twin Screw Extruders" *ANTEC*, **51**, 499 (1993)
- Eisenberg, A., "The glassy state and the glass transition" in *Physical Properties of Polymers*, 2nd ed., Mark, J. E., Ed., American Chemical Society, Baltimore, 1993
- Ekman, K., Ekholm, L., and Nasman, J. H., "Preparation of a Novel HALS Polypropylene Stabilizer", *J. Polym. Sci: Part A*, **33**, 2699 (1995)
- Ferry, J. D., "Viscoelastic properties of polymers", Wiley and Sons, N. Y., 1980
- Flat, J. J., and Lambla, M., "Free Radical Grafting of Activated Monomers onto Polypropylene in an Extruder", *Polym. Processing Soc. Annual Meeting*, Seoul, Korea , p. 4 (1995)
- Florea, M., "New Use of Size Exclusion Chromatography in Kinetics of Mechanical Degradation of Polymers", *J. Appl. Polym. Sci.*, **50**(12), 2039 (1993)
- Flory, P. J., "Principles of Polymer Chemistry", Cornell University Press, N. Y., 1953
- Fritz, H. G., and Stöhrer, B., "Polymer Compounding Process for Controlled Peroxide-Degradation of PP", *Intern. Polym. Process.*, **1**, 31 (1986)
- Gabara, W., and Porejko, S., "Grafting in Reaction of Polyethylene and Poly(maleic anhydride)", *J. Polym. Sci: Part A-1*, **5**, 1539 (1967a)

- Gabara, W., and Porejko, S., "Grafting of Maleic Anhydride on Polyethylene. I. Mechanism of Grafting in a Heterogeneous Medium in the Presence of Radical Initiators", *J. Polym. Sci. Part A-1*, **5**, 1547 (1967b)
- Gaylord, N. G., and Mehta, M., "Role of Homopolymerization in the Peroxide-Catalyzed Reaction of Maleic Anhydride and Polyethylene in the Absence of Solvent", *J. Polym. Sci.: Polym. Lett. Ed.*, **20**, 481 (1982)
- Gaylord, N. G., and Mishra, M. K., "Nondegradative Reaction of Maleic Anhydride and Molten Polypropylene in the Presence of Peroxide", *J. Polym. Sci.: Polym. Lett. Ed.*, **21**, 23 (1983)
- Gaylord, N. G., Mehta, M., and Mehta, R., "Degradation and Cross-linking of Ethylene-Propylene Copolymer Rubber on Reaction with Maleic Anhydride and/or Peroxides", *J. Appl. Polym. Sci.*, **33**, 2549 (1987)
- Gaylord, N. G., "Use of Surfactants to Blend Polymers", *Chemtech*, **19**(7), 435 (1989)
- Golba, J. C., and Seeger, G. T., "Complex Blends Need Both Compatibility and SEC", *Plast. Eng.*, **43**, 571 (1987)
- Grassie, N., and Leeming, W. B. H., "Some Aspects of the Photo, Photothermal and Thermal Decomposition of Polypropylene under Vacuum", *Eur. Polym. J.*, **11**, 809 (1975)
- Grassie, N., and Scott, G., *Polymer Degradation and Stabilisation*, Cambridge University Press, London, 1985
- Greco, P., Lanzetta, N., Laurienzo, P., Maglio, G., Malinconico, M., Martuscelli, E., and Palumbo, R., "Acid and Base Functionalization of Ethylene-Propylene Rubber, 2", *Makromol. Chem.*, **188**, 961 (1987)
- Greco, R., Maglio, G., Musto, P., and Scarinzi, G., "Bulk Functionalization of Ethylene-Propylene Copolymers. II. Influence of the Initiator Concentration and of the Copolymer Composition and Chain Microstructure on the Reaction Kinetics", *J. Appl. Polym. Sci.*, **37**, 777 (1989)
- Gray, R. L., "A Novel Nonreactive HALS Boosts Polyolefin Stability", *Plast. Eng.*, **47**, 21 (1991)
- Harpell, G. A., and Walrod, D. H., "Organic Peroxides for Cure of Ethylene-Propylene Rubbers", *Rubb. Chem. Technol.*, **46**, 1007 (1973)
- Hashimoto, T., Suemoto, A., Okano, K., and Kodaira, T., "Synthesis of Aldehyde-Telechelic Poly(vinyl ether)s by the Reaction of Bifunctional Living Cationic Polymers with Water.", *J. Polym. Sci. Part A: Polymer Chem.*, **33**, 1921 (1995)

- Haslam, J., Willis, H. A., and Squirrell, D. C. M., *Identification and Analysis of Plastics*, Iliffe Books (1965)
- Heinen, W., Rosenmöller, C. H., Wenzel, C. B., de Groot, H. J. M., Lugtenburg, J., and van Duin, M., "13C NMR Study of the Grafting of Maleic Anhydride onto Polyethene, Polypropene, and Ethene-Propene Copolymers", *Macromol.*, **29**, 1151 (1996)
- Hinsken, H., Moss, S., Pauquet, J. R., and Zweifel, H., "Degradation of Polyolefins during Melt Processing", *Polym. Deg. Stab.*, **34**, 279 (1991)
- Ho, R. M., Su, A. C., Wu, C. H., and Chen, S. I., "Functionalization of Polypropylene via Melt Mixing", *Polymer*, **34**(15), 3264 (1993)
- Hoff, A., "Thermal Oxidation of Polypropylene in the Temperature Range of 120-280°C", *J. Appl. Polym. Sci.*, **29**, 465 (1984)
- Hoffmann, H. M. R., "The Ene Reaction", *Angew. Chem. Internat. Edit.*, **8**(8), 556 (1969)
- Huang, J. F., "A Kinetic Study of Polymerization of Propylene with Zirconocene Methylalumoxane Catalysts", Ph. D. Dissertation, University of Waterloo, Canada (1995)
- Hudec, P., and Obdrzalek, L., "The Change of Molecular Weights at Peroxide Initiated Degradation of Polypropylene", *Die. Angew. Makromol. Chem.*, **89**, 41 (1980)
- Immirzi, B., Lanzetta, N., Laurienzo, P., Maglio, G., Malinconico, M., Martuscelli, E., and Palumbo, R., "Acid and Base Functionalization of Ethylene-Propylene Rubber, I", *Makromol. Chem.*, **188**, 951 (1987)
- Ide, F., and Sasaki, I., "Producing Glass-Reinforced Polyolefin Compositions", US 4,003,874, Mitsubishi Gas Comp. (1977)
- Irwin, P. G., and Selwitz, C. M., US 3,412,111, Gulf Research and Development (1968)
- Jellinek, H. H. G., "Degradation and Depolymerization Kinetics" in *Aspects of Degradation and Stabilization of Polymers*, Elsevier Scientific Publishing, NY, 1978
- Jiang, A., and Hamed, G. R., "Crosslinking of Ethylene Propylene Diene Monomer (EPDM) by Buckminsterfullerene", *Polym. Bull.*, **38**(5), 454 (1997)
- Joshi, R. M., "The Free Radical Polymerization of Maleic Anhydride", *Makromol. Chem.*, **53**, 33 (1962)
- Kellou, M. S., and Jenner, G., "Radical Homopolymerisation of Maleic Anhydride", *Eur. Polym. J.*, **12**, 883 (1976)

Kim, B., and White, J. L., "Studies of Thermal/Peroxide Induced Degradation and Maleation of Polypropylene in a JSW Modular Twin Screw Extruder; Influence of Direction of Screw Rotation and Screw Configuration", *ANTEC*, **53**, 242 (1995)

Klemchuk, P. P., and Gande, M. E., "Stabilization Mechanisms of Hindered Amines", *Polym. Deg. Stab.*, **22**,241 (1988)

Kolbert, A. C., Didier, J. G., and Xu, L., "Mechanochemical Degradation of Ethylene-Propylene Copolymers: Characterization of Olefin Chain Ends", *Macromol.*, **29**(27), 8591 (1996)

Konar, J., Kole, S., Avasthi, B. N., and Bhowmick, A. K., "Wetting Behaviour of Functionalized Silicone and EPDM Rubber", *J. Appl. Polym. Sci.*, **61**, 501 (1996)

Kotlar, H. K., and Borve, K., "Reactivity and Function of Polypropylene-Phenol Formaldehyde Compatibilizers in Polypropylene Based Alloys", *ANTEC*, **53**, 1843 (1995)

Kowalski, R. C., US 3,563,972, ESSO (1971)

Kowalski, R. C., "Fit the Reactor to the Chemistry" in "Reactive Extrusion: Principles and Practice", M. Xanthos, ed., Hanser Publishers (1992), p. 37

Kurbanova, R. A., Mirzaoglu, R., Akovali, G., Rzaev, Z. M. O., Karatas, I., and Okudan, A., "Side-Chain Functionalization of Polystyrene with Maleic Anhydride in the Presence of Lewis Acids.", *J. Appl. Polym. Sci.*, **59**, 235 (1996)

Lambla, M., "Reactive Extrusion: A New Tool for the Diversification of Polymeric Materials", *Macromol. Symp.*, **83**, 37 (1994)

Lee, K-B., Kweon, J., Lee, H-J., and Park, H., "A ^{13}C NMR Determination of Monomer Compositions in Ethylene-Propylene Copolymers, Ethylene-Propylene-Butene-1, and Ethylene-Propylene-Diene Terpolymers", *Polym. J.*, **28**(8), 696 (1996)

Levine, I. J., and Hanes, R. G., "An Infrared Analysis for Ethylidenenorbornene in Ethylene-Propylene-Ethylidenenorbornene Rubber", *Rubb. Chem. Technol.*, **43**, 445 (1970)

Liang,, C. Y., and Pearson, F. G., "Infrared Spectra of Crystalline and Stereoregular Polymers. Part I. Polypropylene", *J. Mol. Spectros.*, **5**, 290 (1960)

Lin, J. S., Sheu, E. Y., and Jois, Y. H. R., "The Effect of Extruder Temperature and Maleated Polypropylene on Polypropylene/Nylon-6,6 Blend: A Small Angle X-ray Scattering Study", *J. Appl. Polym. Sci.*, **55**, 655 (1995)

- Lindeman, L. P., and Adams, J. Q., "Carbon-13 Nuclear Magnetic Resonance Spectrometry. Chemical Shifts for the Paraffins through C₉", *Anal. Chem.*, **43**(10), 1245 (1971)
- Liu, N. C., and Baker, W. E., "Basic functionalization of polypropylene and the role of interfacial chemical bonding in its toughening.", *Polymer*, **35**(5), 988 (1994)
- Lomonte, J. N., "Infrared Determination of Vinylidene Unsaturation in Polyethylene", *Anal. Chem.*, **34**(1), 129 (1962)
- Mapleston, P., "Resin Makers Broaden Properties", *Mod. Plast.*, **72**(9), 50 (1995)
- Mark, H. F., "Ethylene-Propylene Elastomer", Encyclopedia of Polymer Science and Engineering, 2nd ed., vol. 6, eds. Mark, H. F., Bikales, N. M., Overberger, C. G., and Menges, G., 1986
- Maréchal, P., Coppens, G., Legras, R., and Dekoninck, J-M., "Amine/Anhydride Reaction versus Amide/Anhydride Reaction in Polyamide/Anhydride Carriers", *J. Polym. Sci. Part A: Polym. Chem.*, **33**, 757 (1995)
- Marquardt, F. H., "The Intensity of Carbonyl Bands in the Infrared Spectra of Cyclic Anhydrides of Dicarboxylic Acids", *J. Chem. Soc. B*, 1242 (1966)
- Mauler, R. S., Galland, G. B., Samios, D., and Tokumoto, S., "Functional Group Determination in Hydroxylated Polymers", *Eur. Polym. J.*, **31**(1), 51 (1995)
- McGee, A. E., "Modified Olefin Polymers", US 5, 321, 094, ICI (1994)
- Mikami, K., Loh, T. P., and Nakai, T., "Diastereocontrol via Lewis Acid-Promoted Ene Reaction with Glyoxylates and its Application to Stereocontrolled Synthesis of a 22R-Hydroxy-23-carboxylate Steroid Side Chain", *Tetra. Lett.*, **29**(48), 6304 (1988)
- Moad, G., Rizzardo, E., and Solomon, D. H., "The Reaction of Acyl Peroxides with 2,2,6,6-Tetramethylpiperidiny-1-oxy", *Tetrahedron.*, **22**, 1165 (1981)
- Mülhaupt, R., Duschek, T., and Rieger, B., "Functional Polypropylene Blend Compatibilizers", *Makromol. Chem. Macromol. Symp.*, **48/49**, 317 (1991)
- Nelson, B. I., Dealy, J. M., and Patterson, W. I., "Control of a Polypropylene Visbreaking Process using a Novel In-line Rheometer", *ANTEC*, **51**, 1434 (1993)
- Nemes, S., Borbely, J., Borda, J., Deak, G., and Kelen, T., "Reactive Propylene Oligomers", *Polym. Bull.*, **29**, 135 (1992)
- Nowak, R. M., and Jones, G. D., US 3, 177, 269, Dow (1965)

- Nyquist, R. A., "Infrared Study of Maleic Anhydride in Solvent Systems", *Appl. Spectros.*, **44**(3), 438 (1990)
- Oostenbrink, A. J., and Gaymans, R. J., "Maleic Anhydride Grafting on EPDM Rubber in the Melt", *Polymer*, **33**(14), 3086 (1992)
- Oppolzer, W., "Asymmetric Diels-Alder and Ene Reactions in Organic Synthesis", *Angew. Chem. Int. Ed. Engl.*, **23**, 876 (1984)
- Ordelt, Z., "Attempted Diels-Alder Reaction of perChloro-1,3-butadiene and its Derivatives", *Chem. Abstr.*, **79**, 115026m (1973)
- Pabedinskas, A., Cluett, W. R., and Balke, S. T., "Modeling of Polypropylene Degradation during Reactive Extrusion with Implications for Process Control", *Polym. Eng. Sci.*, **34**(7), 598 (1994)
- Park, J-Y., Park, D-J., Ha, C-S., and Cho, W-J., "Synthesis and Properties of 2-Vinylnaphthalene-EPDM-Methyl Methacrylate Graft Copolymer", *J. Appl. Polym. Sci.*, **51**, 1303 (1994)
- Pinazzi, C., Danjard, J. C., and Pautrat, R., "Addition of Unsaturated Monomers to Rubber and Similar Polymers", *Rubb. Chem. Technol.*, **36**, 282 (1963)
- Prashad, M., Tomesch, J. C., and Shapiro, M. J., "Lewis Acid Catalyzed Stereoselective Ene Addition of Formaldehyde to 1,3-Diarylcyclopentenes - Synthesis of trans-2,5-Diaryl-2-cyclopentene-1-methanols", *Tetra. Lett.*, **30**(36) 4757 (1989)
- Pryor, W. A., "Introduction to Free Radical Chemistry", Prentice-Hall, N.Y., 1966
- Rado, R., "Controlled Decomposition of Polypropylene", *Intern. Chem. Eng.*, **2**(4), 482 (1962)
- Rao, G. S. S., Choudhary, M. S., Navqvi, M. K., and Rao, K. V., "Functionalization of Isotactic Polypropylene with Acrylic Acid in the Melt: Synthesis, Characterization and Evaluation of Thermomechanical Properties", *Eur. Polym. J.*, **32**(6), 695 (1996)
- Restaino, A. J., Mesrobian, R. B., Morawetz, H., Ballantine, D. S., Dienes, G. J., and Metz, D. J., "γ-Ray Initiated Polymerization of Crystalline Monomers", *J. Am. Chem. Soc.*, **78**, 2939 (1956)
- Rengarajan, R., Parameswaran, V. R., Lee, S., Vicic, M., and Rinaldi, P. L., "N.M.R. Analysis of Polypropylene-Maleic Anhydride Copolymer", *Polymer*, **31**, 1703 (1990)

Riddick, J. A., and Bunger, W. B., "Techniques in Chemistry: Organic Solvents", vol. II Wiley-Interscience, 1970, p. 836

Ripoll, J. L., and Vallee, Y., "Synthetic Applications of the Retro-Ene Reaction", *Synthesis*, **7**, 659 (1993)

Roncetti, L. and Banzi, V., "Process for Grafting Maleic Anhydride onto Unsaturated Polyolefinic Elastomers by Mass Reaction", US Patent 5,153,270, Ausimont S. r. I. (1992)

Rondestvedt, C. S., and Wark, B. H., "Mechanism of the Reaction of Mono-olefins with Dienophiles. II. A Possible Free-Radical Mechanism", *J. Org. Chem.*, **20**, 368 (1955)

Russell, K. E., and Kelusky, E. C., "Grafting of Maleic Anhydride to n-Eicosane", *J. Polym. Sci.: Part A: Polym. Chem.*, **26**, 2273 (1988)

Ryu, S. H., Gogos, C. G., and Xanthos, M., "Parameters Affecting Process Efficiency of Peroxide-Initiated Controlled Degradation of Polypropylene", *Adv. Polym. Technol.*, **11**(2), 121 (1992)

Sawaguchi, T., Ikemura, T., and Seno, M., "Preparation of α,ω -Diisopropenyloligopropylene by Thermal Degradation of Isotactic Polypropylene", *Macromol.*, **28**(24), 7973 (1995)

Sawaguchi, T., and Seno, M., "Preparation of Telechelic Oligomers by the Thermal Degradation of Syndiotactic Polypropylene", *Polym. J.*, **28**(9), 817 (1996)

Sawaguchi, T., and Seno, M., "Synthesis of Multiblock Copolymers of α,ω -Dihydrosilyl-polydimethylsiloxane with α,ω -Diisopropenyloligopropylenes with Different Stereoregularities", *J. Polym. Sci: Part A Polym. Chem.*, **34**(17), 3625 (1996a)

Schaufelberger, G. F., French 1, 346, 533, Union Carbide (1963)

Schulz, D. N., Turner, S. R., and Golub, M. A., "Recent Advances in the Chemical Modification of Unsaturation Polymers", *Rubb. Chem. Technol.*, **55**, 808 (1982)

Sharabash, M. M., and Guile, R. L., "Homopolymerization of Maleic Anhydride", *J. Macromol. Sci.-Chem.*, **A10**(6), 1017 (1976)

Sheng, J., and Hu, J., "Graft Polymerization of Styrene onto Random Ethylene-Propylene Diene Monomer", *J. Appl. Polym. Sci.*, **60**, 1499 (1996)

Shiono, T., and Soga, K., "Synthesis of Terminally Halogenated Isotactic Polypropylenes using Hydroalumination", *Makromol. Chem. Rapid Commun.*, **13**, 371 (1992a)

Shiono, T., and Soga, K., "Synthesis of Terminally Aluminum-Functionalized Polypropylene", *Macromol.*, **25**, 3356 (1992b)

Shiono, T., Kurosawa, H., Ishida, O., and Sogo, K., "Synthesis of Polypropylenes Functionalized with Secondary Amino Groups at the Chain End", *Macromol.*, **26**, 2085 (1993)

Siadat, B., Lundberg, R. D., and Lenz, R. W., "Preparation of an Ionomer Elastomer by Continuous Sulfonation in an Extruder and Neutralization in Static Mixers", *Polym. Eng. Sci.*, **20**(8), 530 (1980)

Sirinyan, K., Petzoldt, J., and Henning, W., "Coating Compositions with Improved Adhesion to Plastics", US 5,342, 890, Bayer, 1994

Skoog, D., West D. M., and Holler, F. M., "Fundamentals of Analytical Chemistry" 5th ed., Saunders College Publishing (1988) p. 234

Smith, M. B., *Organic Synthesis*, McGraw-Hill (1994)

Snider, B. B., "The Lewis Acid Catalysis of Ene Reactions", *J. Org. Chem.*, **39**(2), 255 (1974)

Snider, B. B., Rodini, D. J., Conn, R. S. E., and Sealfon, S., "Lewis Acid Catalyzed Reactions of Methyl Propiolate with Unactivated Alkenes", *J. Am. Chem. Soc.*, **101**, 5283 (1979)

Song, Z., and Baker, W. E., "Chemical Reactions and Reactivity of Primary, Secondary, and Tertiary Diamines with Acid Functionalized Polymers", *J. Polym. Sci. Part A: Polym. Chem.*, **30**, 1589 (1992)

Step, E. N., Turro, N. J., Gande, M. E. and Klemchuk, P. P., "Mechanism of Polymer Stabilization by Hindered-Amine Light Stabilizers (HALS). Model Investigations of the Interaction of Peroxy Radicals with HALS Amines and Amino Ethers", *Macromol.*, **27**, 2529 (1994)

Suwanda, D., Lew, R., and Balke, S. T., "Reactive Extrusion of Polypropylene. I. Controlled Degradation", *J. Appl. Polym. Sci.*, **35**, 1019 (1988)

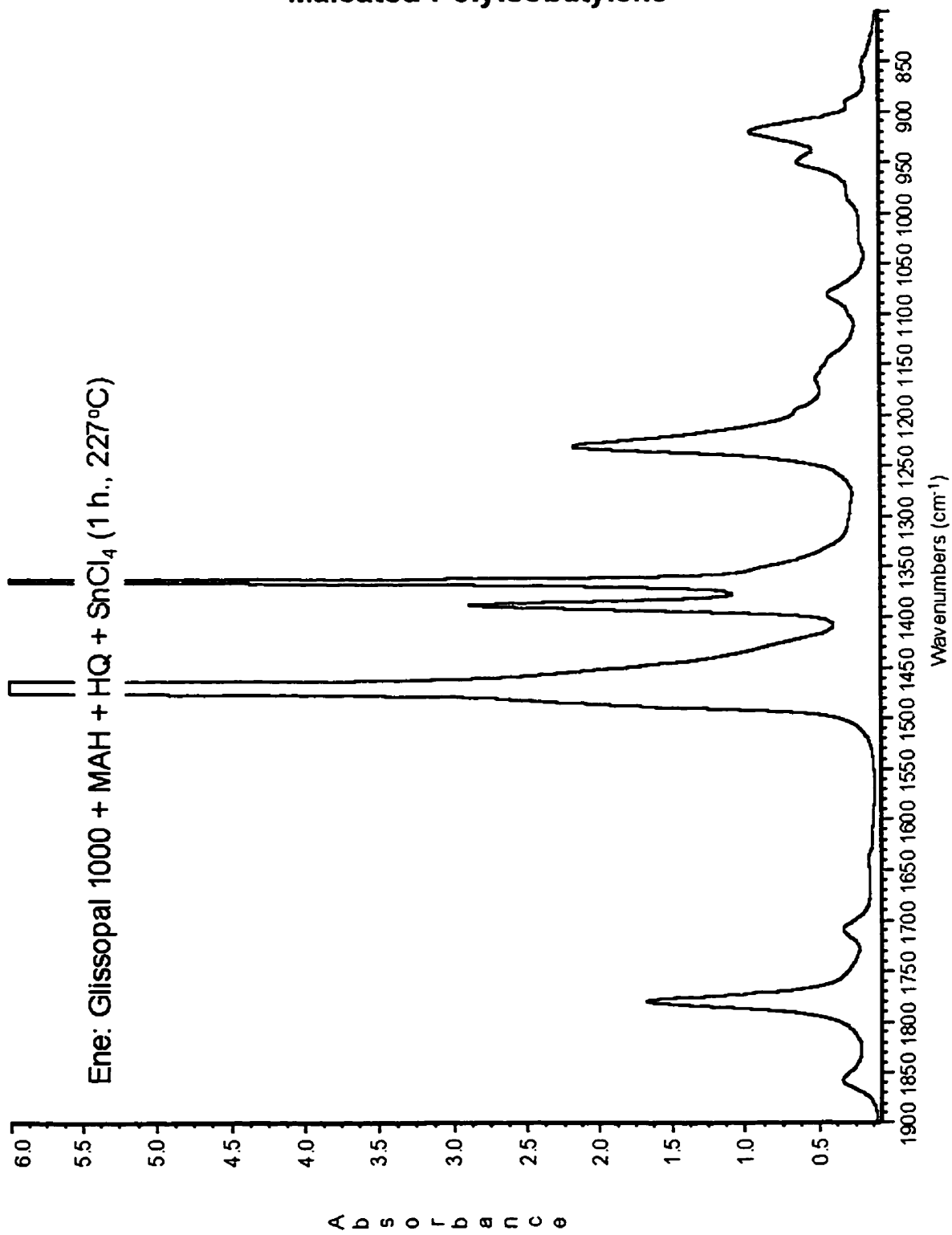
Tang, T., Li, L., and Huang, B., "Synthesis and Crystallization Behaviour of (PP-MA)-g-PEO", *Eur. Polym. J.*, **4**, 479 (1994)

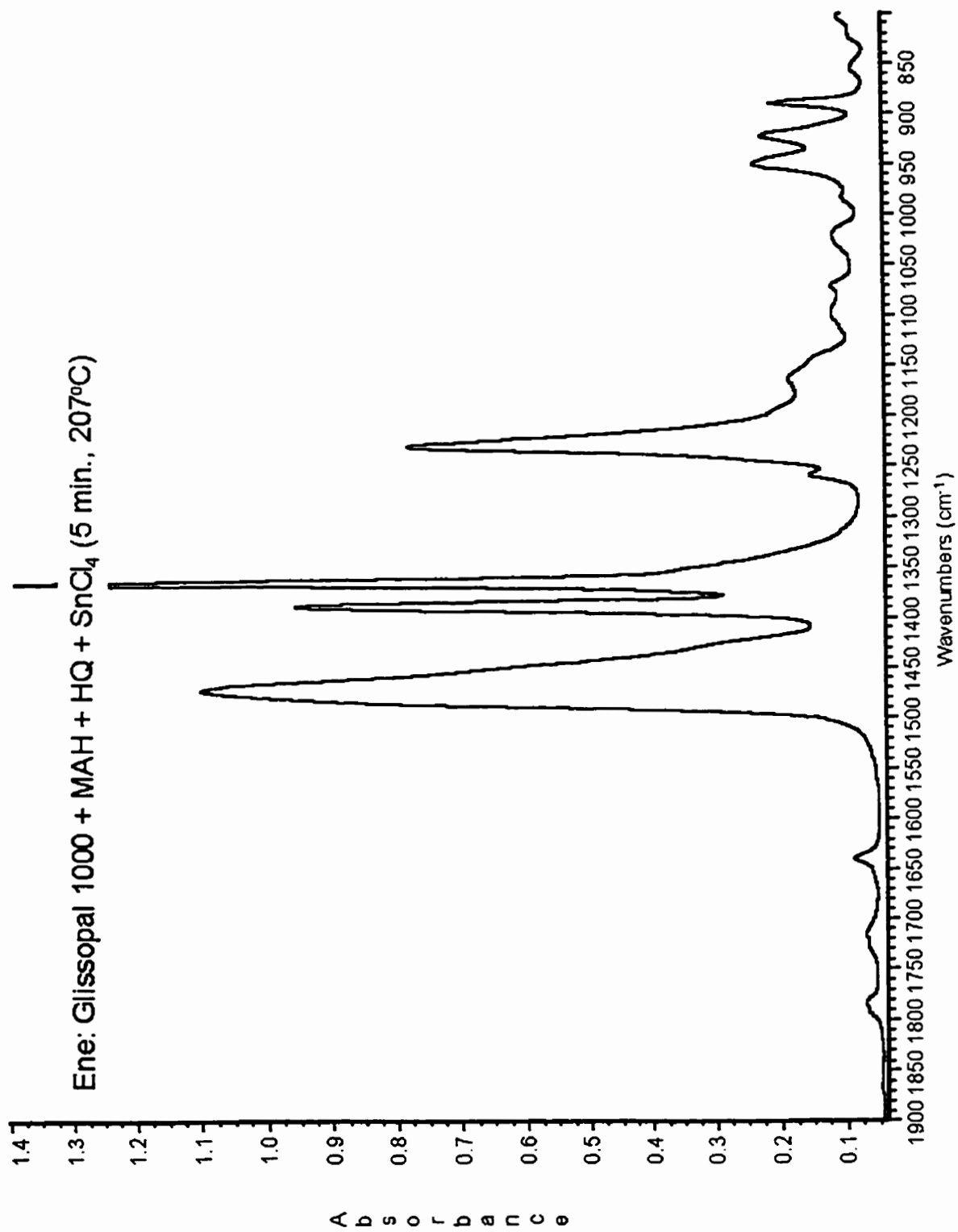
Tate, B. E., "The Decarboxylation of Itaconic Acid Polymers", *Makromol. Chem.*, **109**, 176 (1967)

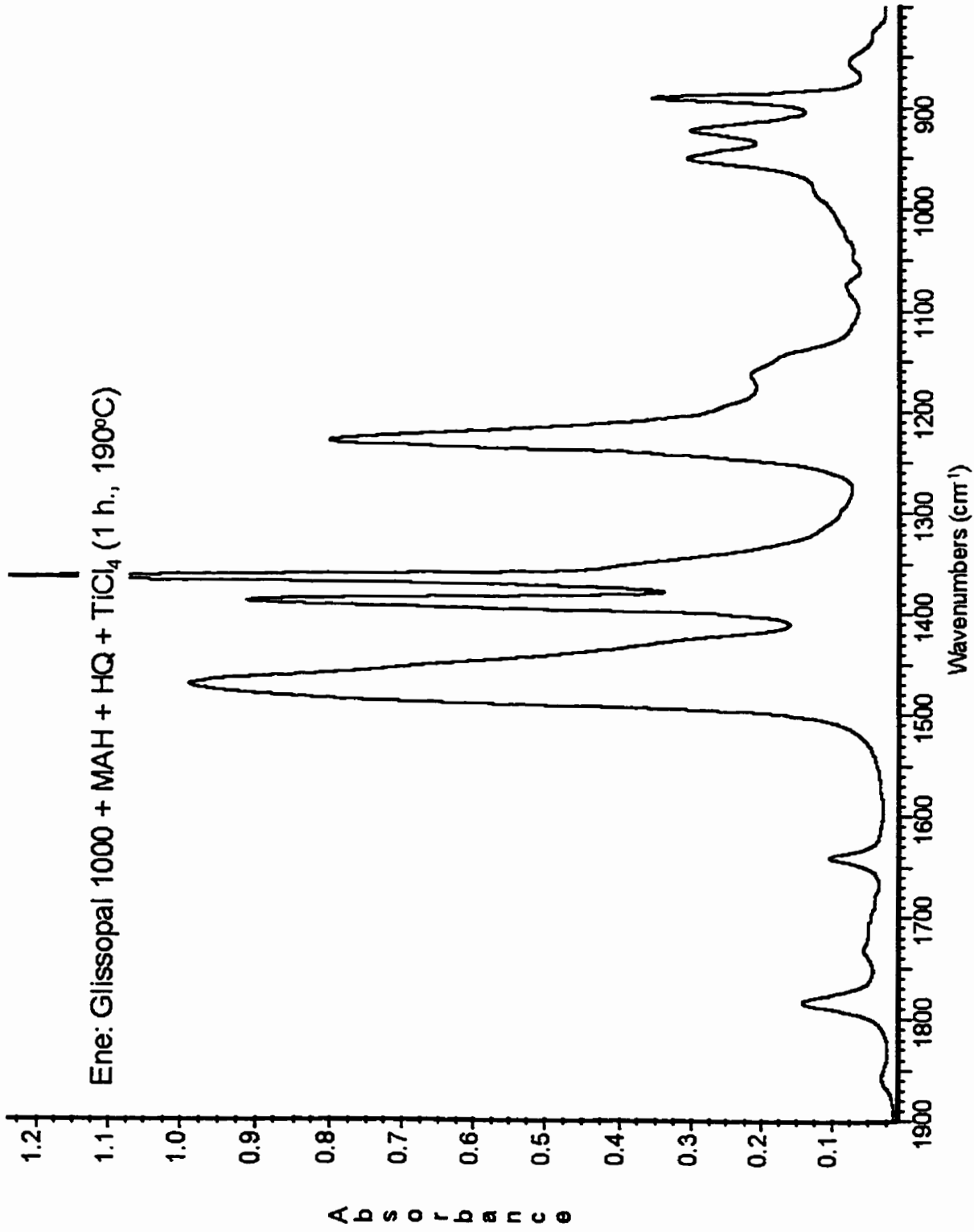
- Tessier, M., Maréchal, E., "Synthesis of Mono and Difunctional Oligoisobutylenes-III. Modification of α -Chlorooligoisobutylene by Reaction with Maleic Anhydride", *Eur. Polym. J.*, **20**(3), 269 (1984a)
- Tessier, M., Maréchal, E., "Synthesis of Mono and Difunctional Oligoisobutylenes-IV. Modification of α,ω -Chlorooligoisobutylene by Reaction with Maleic Anhydride: Preliminary Study on Block Polycondensation", *Eur. Polym. J.*, **20**(3), 281 (1984b)
- Tessier, M., Maréchal, E., "Synthesis of α -Phenyl- ω -anhydride Oligoisobutylene and α,ω -Dianhydride Oligoisobutylene", *Eur. Polym. J.*, **26**(5), 499 (1990)
- Thompson, M. R., Tzoganakis, C., Rempel, G. L., "A Parametric Study of the Terminal Maleation of Polypropylene Through the Alder Ene Reaction", *J. Polym. Sci. Part A: Polym. Chem.*, 1998a submitted
- Thompson, M. R., Tzoganakis, C., Rempel, G. L., "Terminal Functionalization via the Alder Ene Reaction", *Polymer*, **39**(2), 327 (1998b)
- Thompson, M. R., Tzoganakis, C., Rempel, G. L., "Evaluation of Vinylidene Content in Controlled-Rheology Polypropylene", *J. Polym. Sci. A: Polym. Chem.*, **35**, 3083-3086 (1997)
- Togo, S., Amagai, A., Kondo, Y., and Yamada, T., "Solvent-resistant Polyphenylene Ether Resin Composition", US 4,914,153, Mitsubishi (1990)
- Tosi, C., Ciampelli, F., and Cameli, N., "Spectroscopic Examination of Ethylene-Propylene-Norbornenic Diene Terpolymers", *J. Appl. Polym. Sci.*, **16**, 801 (1972)
- Triacca, V. J., Gloor, P. E., and Zhu, S., "Free Radical Degradation of Polypropylene: Random Chain Scission", *Polym. Eng. Sci.*, **33**(8), 445 (1993)
- Trivedi, B. C., and Culbertson, B. M., *Maleic Anhydride*, Plenum Press, NY (1982)
- Trost, B. M., Indolese, A. F., Muller, T. J. J., and Treptow, B., "A Ru Catalyzed Addition of Alkenes to Alkynes. A Transition-Metal-Catalyzed Formal Alder Ene Reaction", *ChemTracts-Org. Chem.*, **8**, 300 (1995)
- Tsuchida, E., Tomono, T., and Sano, H., *Makromol. Chem.*, **151**, 245 (1972)
- Tzoganakis, C., "Reactive Extrusion of Polymers: A Review", *Adv. Polym. Technol.*, **9**(4), 321 (1989)
- Tzoganakis, C., Vlachopoulos, J., and Hamielec, A. E., "Production of Controlled-Rheology Polypropylene Resins by Peroxide Promoted Degradation During Extrusion", *Polym. Eng. Sci.*, **28**(3), 170 (1988a)

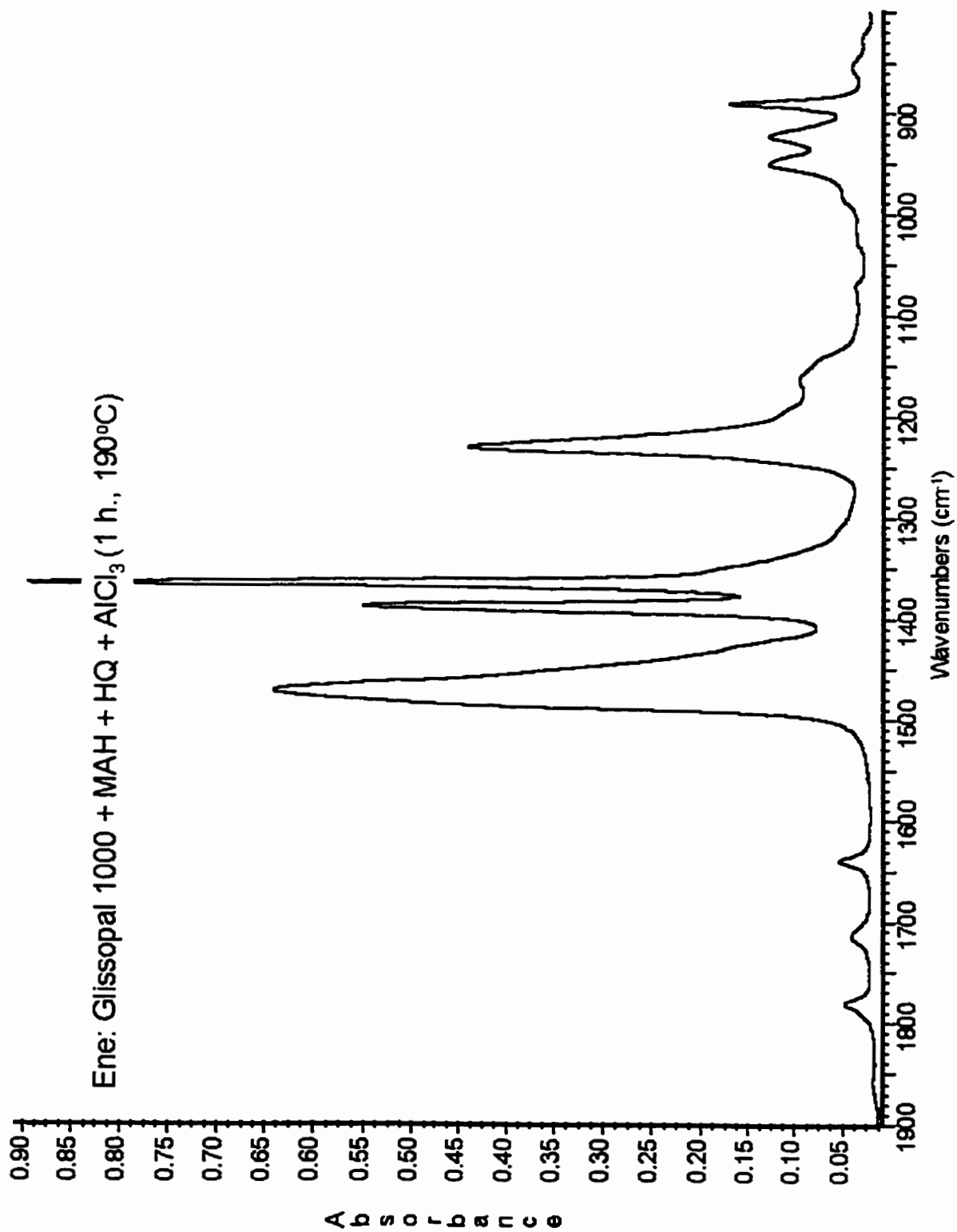
- Tzoganakis, C., Vlachopoulos, J., and Hamielec, A. E., "Modelling of the Peroxide Degradation of Polypropylene", *Intern. Polym. Process.*, **3**, 141 (1988b)
- Tzoganakis, C., Vlachopoulos, J., and Hamielec, A. E., "Controlled Degradation of Polypropylene", *Chem. Eng. Progr.*, **84**(11), 47 (1988c)
- van Gisbergen, J. G. M., Hoeben, W. F., and Meijer, H. E. H., "Melt Rheology of Electron-Beam-Irradiated Blends of Polypropylene and Ethylene-Propylene-Diene Monomer (EPDM) Rubber", *Polym. Eng. Sci.*, **31**(21), 1539 (1991)
- van Krevelen, D. W., *Properties of Polymers*, Elsevier Scientific Publishing, NY, 1976
- Walch, E., and Gaymans, R. J., "Telechelic Polyisobutylene with Unsaturated End Groups and with Anhydride Ene Groups", *Polymer*, **35**(8), 1774 (1994)
- Wenig, W., and Wasiak, A., "Interactions between the Components in Isotactic Polypropylene Blended with EPDM", *Colloid Polym. Sci.*, **271**, 824 (1993)
- Wu, C. H., and Su, A. C., "Functionalization of Ethylene-Propylene rubber via Melt Mixing", *Polym. Eng. Sci.*, **31**(23), 1629 (1991)
- F. Wild, M. Wasincioneck, G. Huttner, H. H. Brintzinger, *J. Organomet. Chem.*, **288**, 63 (1985)
- Yazdani-Pedram, M., Vega, H., and Quijadi, R., "Functionalization of polypropylene by grafting with itaconic acid", *Macromol. Rapid Comm.*, **17** (8), 577 (1996)
- Xanthos, M., *Reactive Extrusion: Principles and Practice*, Xanthos, M., ed., Hanser Publishers (1992)
- Xie, H-Q., Feng, D-S., and Guo, J-S., "Solution Maleation of EPDM and Blending of Acetal Copolymer with Rubber Using Maleated EPDM as Compatibilizer", *J. Appl. Polym. Sci.*, **64**, 329 (1997)
- Xu, G., and Lin, S., "Functional Modification of Polypropylene", *J. Macromol. Sci.-Rev. Macromol. Chem. Phys.*, **C34**(4), 555 (1994)
- Zoppi, R. A., and De Paoli, M-A., "Chemical Preparation of Conductive Elastomeric Blends: Polypyrrole/EPDM-II. Utilization of Matrices Containing Crosslinking Agents, Reinforcement Fillers and Stabilizers", *Polymer*, **37**(10), 1999 (1996)
- Zweifel, H., and Völker, T., "On the Mechanism of Anionic Polymerization of Maleic Anhydride, 2", *Makromol. Chem.*, **170**, 141 (1973)

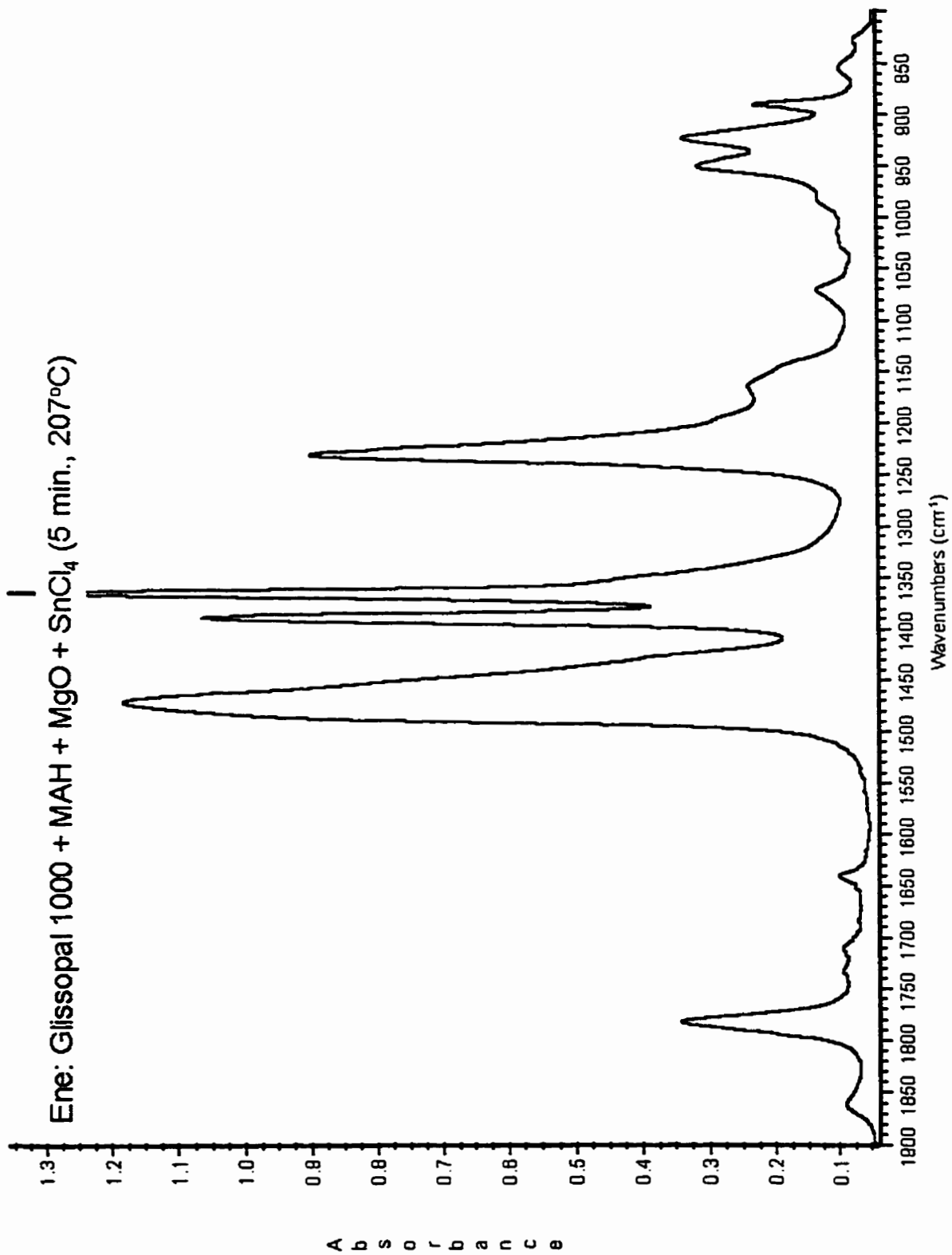
Appendix I: Maleated Polyisobutylene

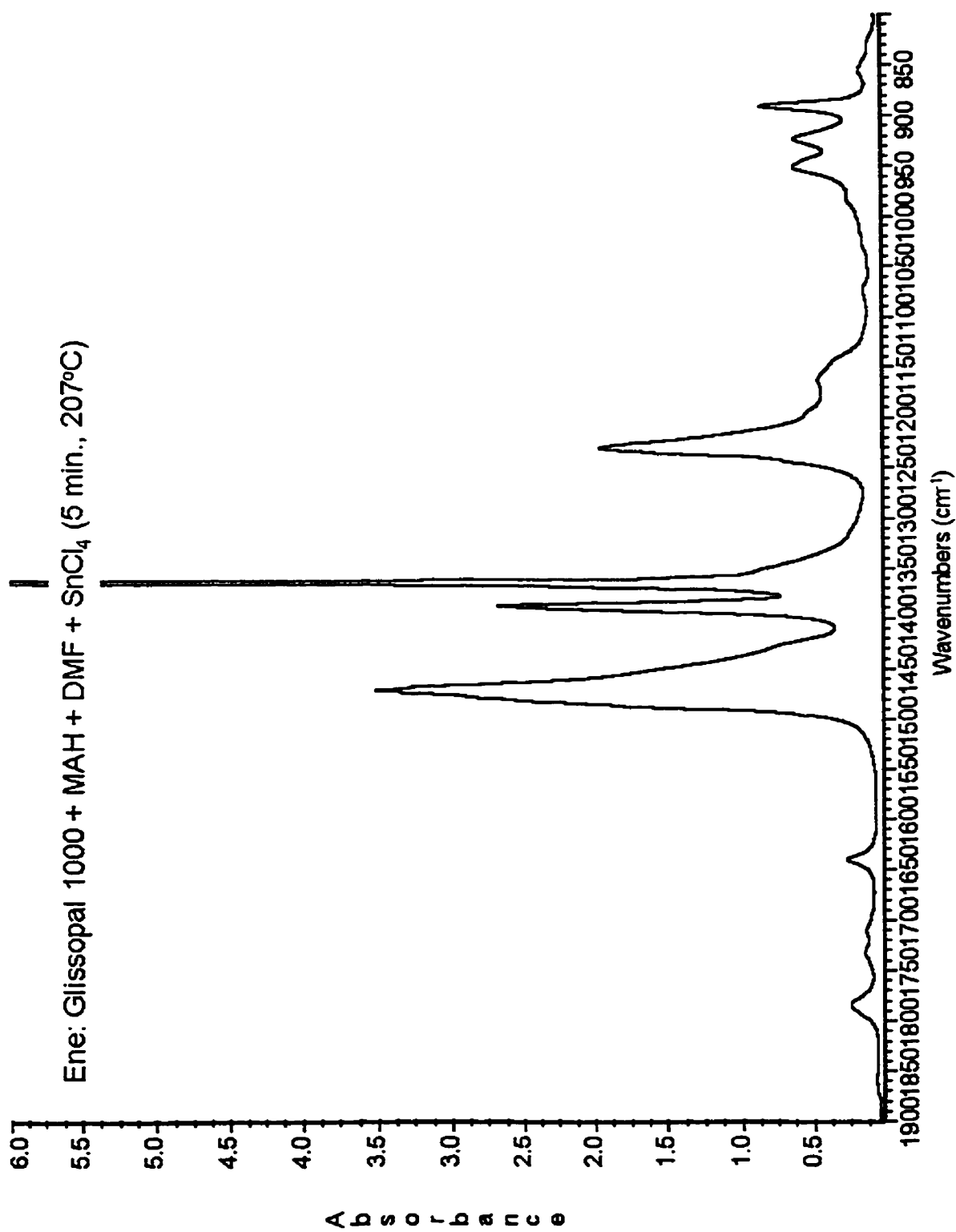












**APPENDIX II:
CONVERSION DATA FROM THE MALEATION OF POLYPOL-19**

Conversion Data for uncatalyzed Alder Ene samples

Time (min)	Temp (°C)	MAH Conc. (mol-eq.)	SnCl₂ Conc. (% mol-eq.)	Conversion (%)
1	220	2.7	0	0.15
2				0.53
3				1.16
4				1.46
5				1.84
1	220	2.7	0	0.37
2				0.62
3				0.89
4				1.30
5				1.78
1	230	2.7	0	0.25
2				0.85
3				1.35
4				1.90
5				2.55
1	240	2.7	0	1.52
2				2.40
3				3.72
4				4.14
5				4.82
1	220	8	0	1.48
2				2.16
3				3.08
4				3.04
5				3.95
1	220	8	0	1.44
2				1.80
3				2.46
4				3.05
5				5.17
1	220	8	0	2.56
2				3.27
3				3.61
4				4.43
5				5.04
1	230	8	0	0.77
2				2.60
3				4.12
4				5.81
5				7.78

Conversion Data for uncatalyzed Alder Ene samples

Time (min)	Temp (°C)	MAH Conc. (mol-eq.)	SnCl ₂ Conc. (% mol-eq.)	Conversion (%)
1	250	8	0	4.05
2				6.52
3				9.25
4				13.08
5				16.21
1	250	8	0	4.60
2				7.55
3				9.76
4				13.90
5				15.87

Conversion Data for heterogeneous Alder Ene system

Time (min)	Temp (°C)	MAH Conc. (mol-eq.)	SnCl ₂ Conc. (% mol-eq.)	Conversion (%)
1	220	4	0.5	1.07
2				1.64
3				1.56
4				2.17
5				2.35
1	220	8	0.5	0.72
2				1.16
3				1.23
4				1.88
5				2.31
1	220	12	0.5	1.90
2				2.72
3				2.88
4				3.86
5				4.69
1	240	4	0.5	2.64
2				2.98
3				2.63
4				4.16
5				5.23
1	240	8	0.5	4.26
2				5.09
3				6.23
4				7.13
5				9.27
1	240	12	0.5	4.28
2				5.16
3				6.30
4				7.93
5				11.22
1	210	8	0.5	0.49
2				0.70
3				0.56
4				1.01
5				1.08
1	220	8	0.5	0.72
2				1.16
3				1.23
4				1.88
5				2.31

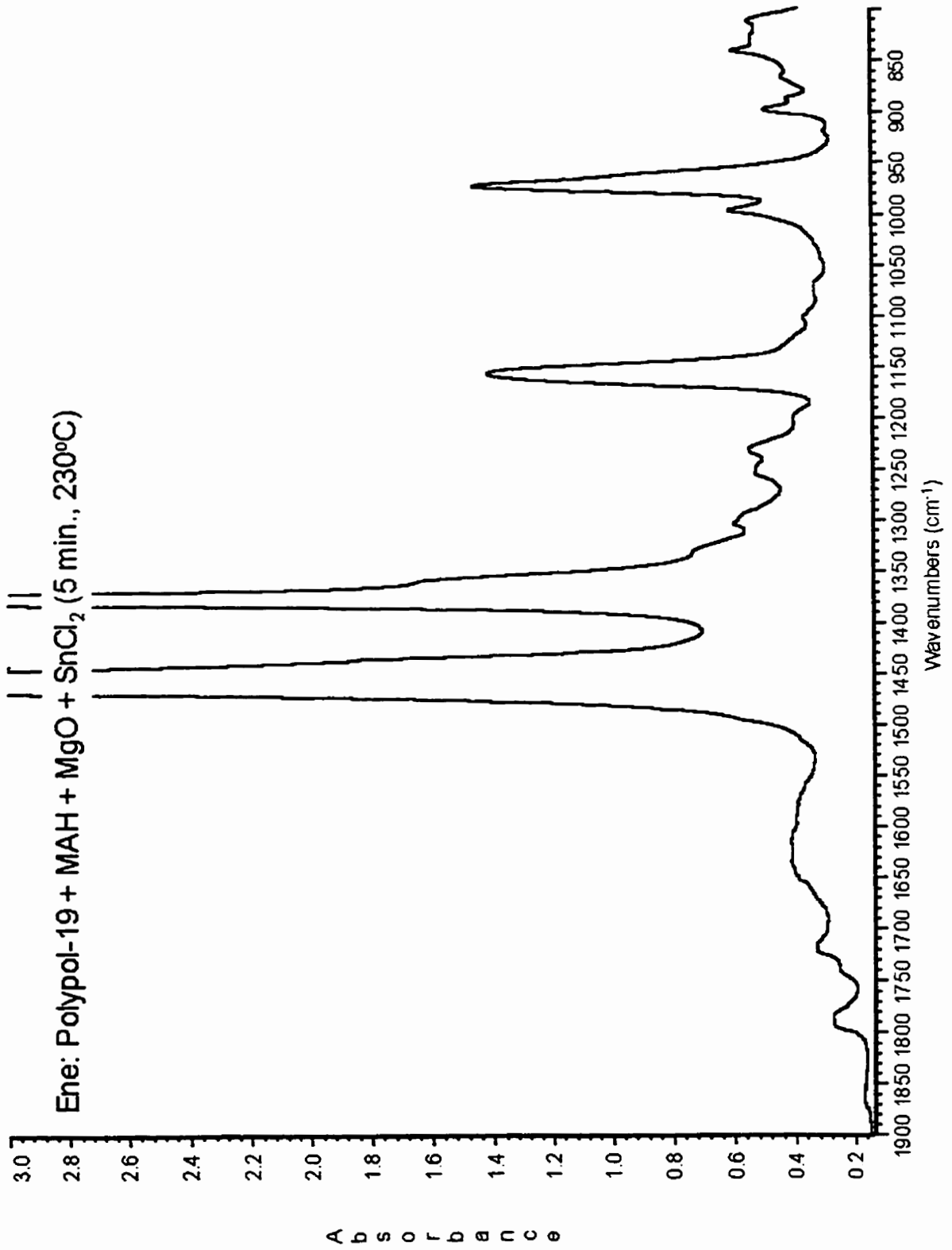
Conversion Data for heterogeneous Alder Ene system

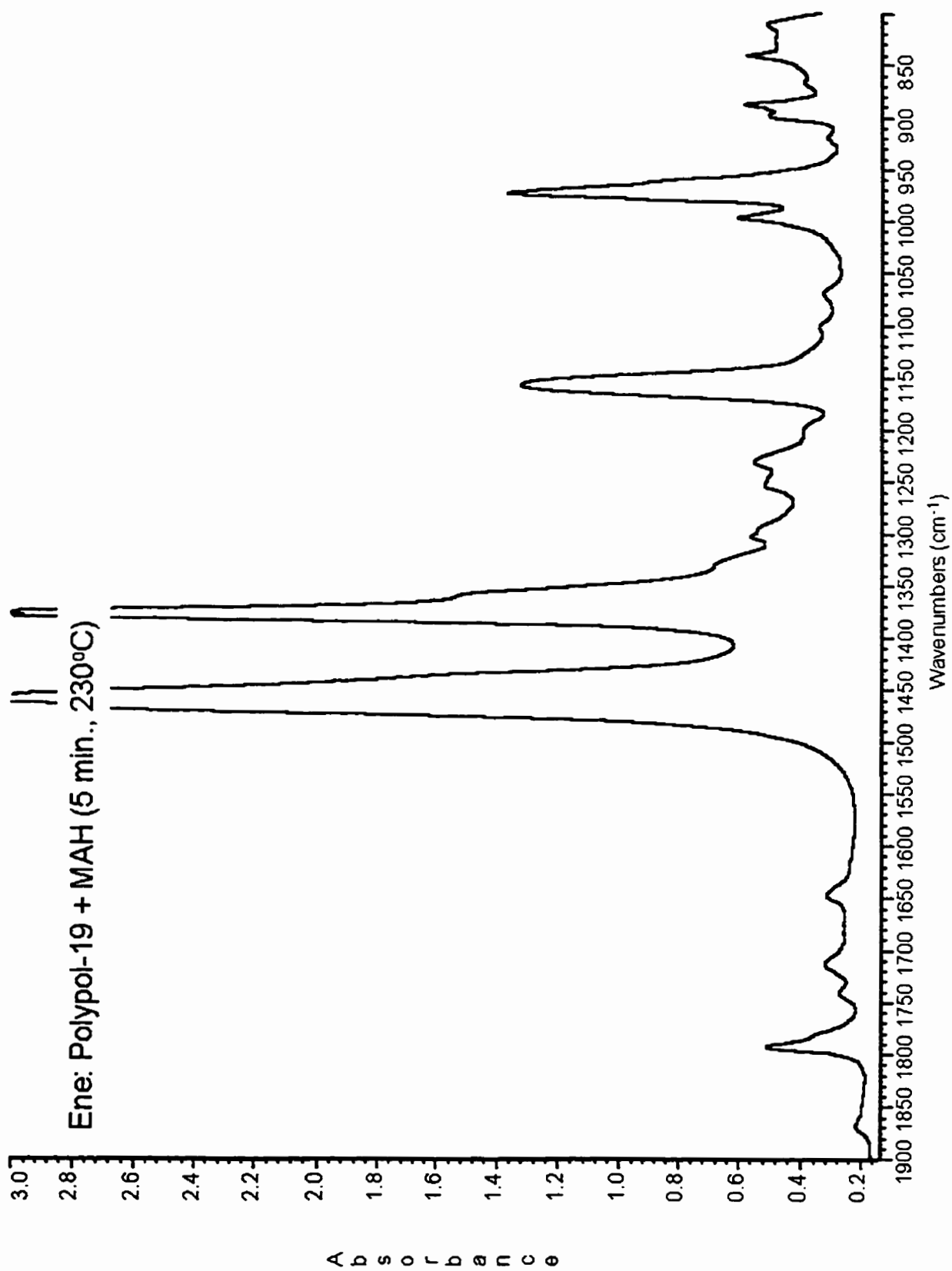
Time (min)	Temp (°C)	MAH Conc. (mol-eq.)	SnCl ₂ Conc. (% mol-eq.)	Conversion (%)
1	230	8	0.5	1.30
2				1.76
3				2.20
4				2.91
5				3.20
1	240	8	0.5	3.24
2				4.15
3				4.83
4				5.25
5				9.44
1	240	8	0.5	4.73
2				5.10
3				6.68
4				7.83
5				9.68
1	240	8	0.5	4.81
2				6.02
3				7.18
4				8.32
5				8.68
1	250	8	0.5	5.17
2				5.93
3				6.92
4				7.89
5				9.82

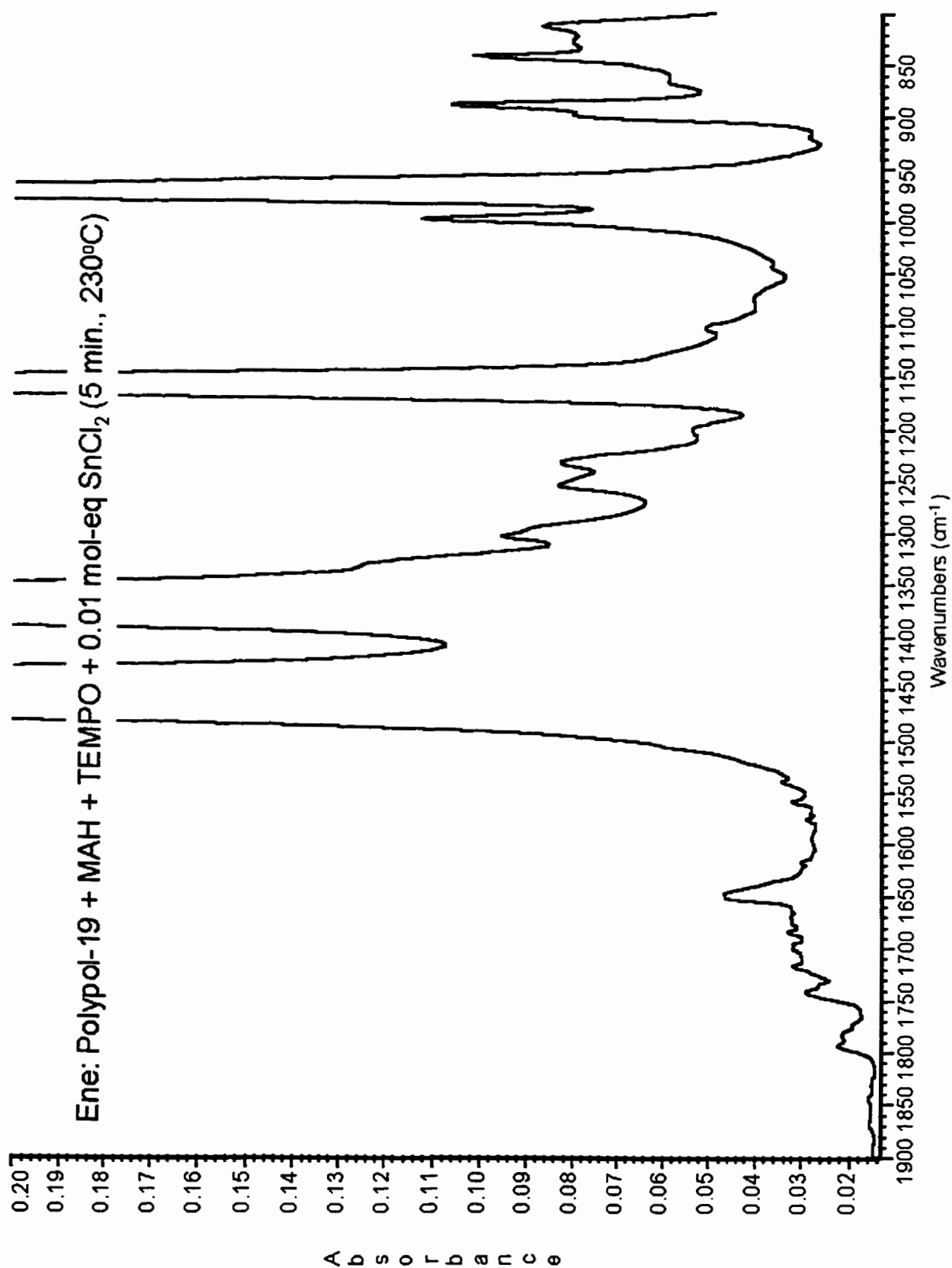
Conversion Data for homogeneous Alder Ene system

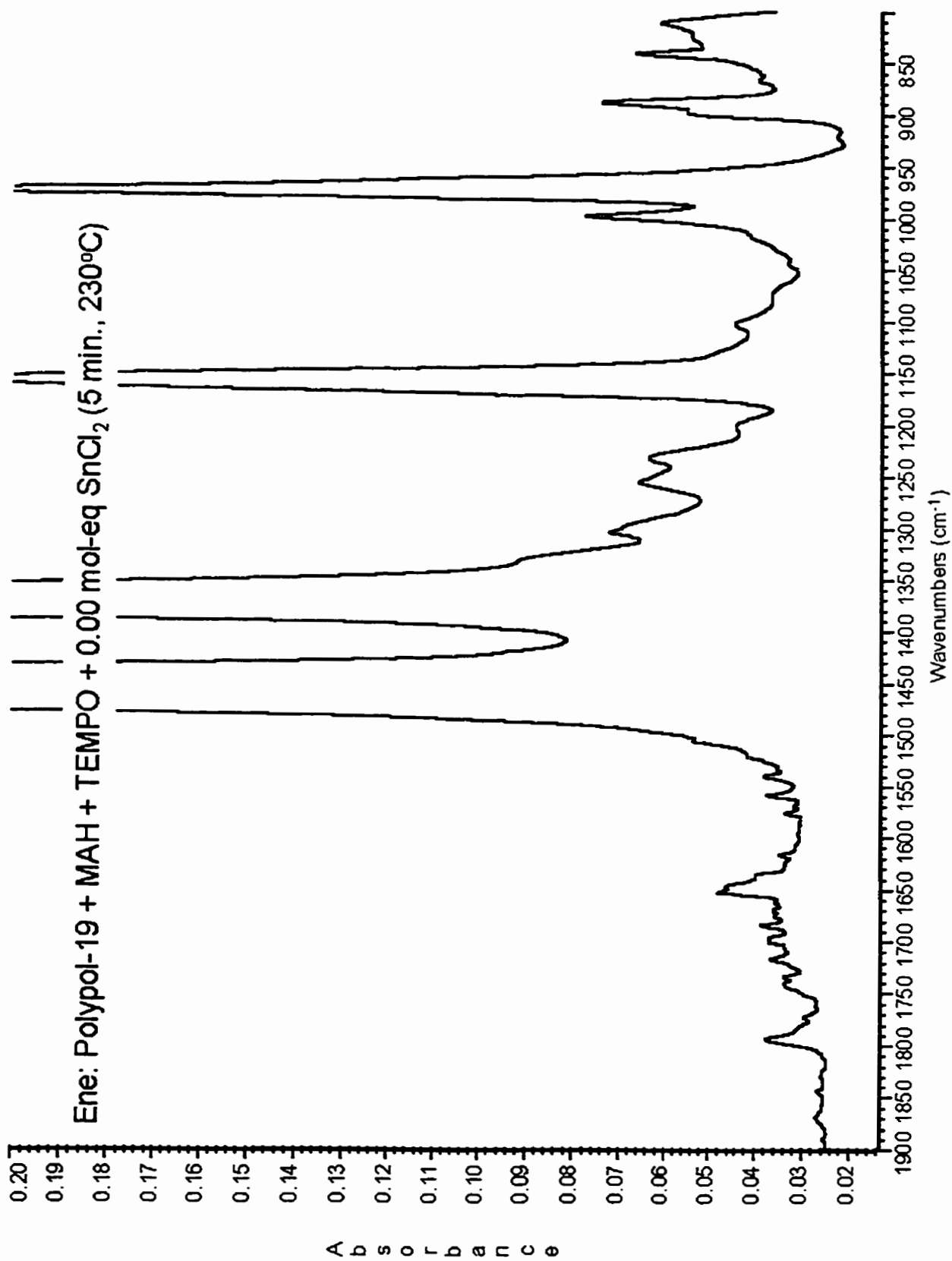
Time (min)	Temp (°C)	MAH Conc. (mol-eq.)	SnCl ₂ Conc. (% mol-eq.)	Conversion (%)
1	220	2.7	0.01	1.35
2				1.86
3				2.54
4				3.46
5				4.74
1	230	2.7	0.01	1.43
2				1.63
3				2.57
4				3.66
5				5.08
1	240	2.7	0.01	1.45
2				2.05
3				4.19
4				5.97
5				7.54
1	240	2.7	0.01	1.51
2				2.22
3				4.42
4				7.04
5				8.01
1	220	2.7	0.1	0.70
2				0.90
3				1.24
4				1.60
5				2.12
1	220	2.7	0.1	0.46
2				0.89
3				1.24
4				1.66
5				2.06
1	230	2.7	0.1	0.27
2				1.07
3				1.76
4				2.46
5				3.84
1	240	2.7	0.1	0.83
2				1.08
3				2.86
4				5.23
5				6.82

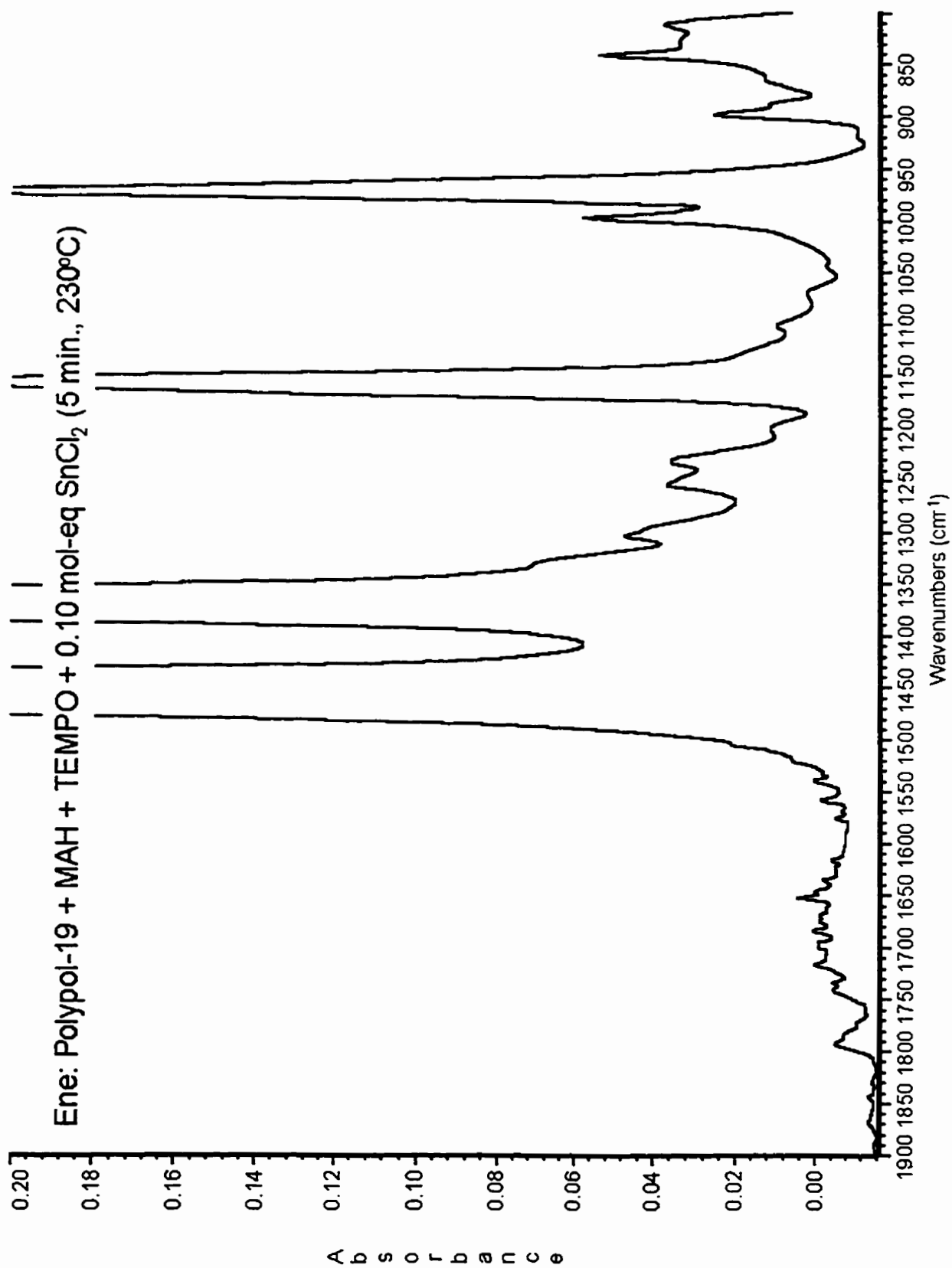
Appendix III:
Maleated Polypol-19

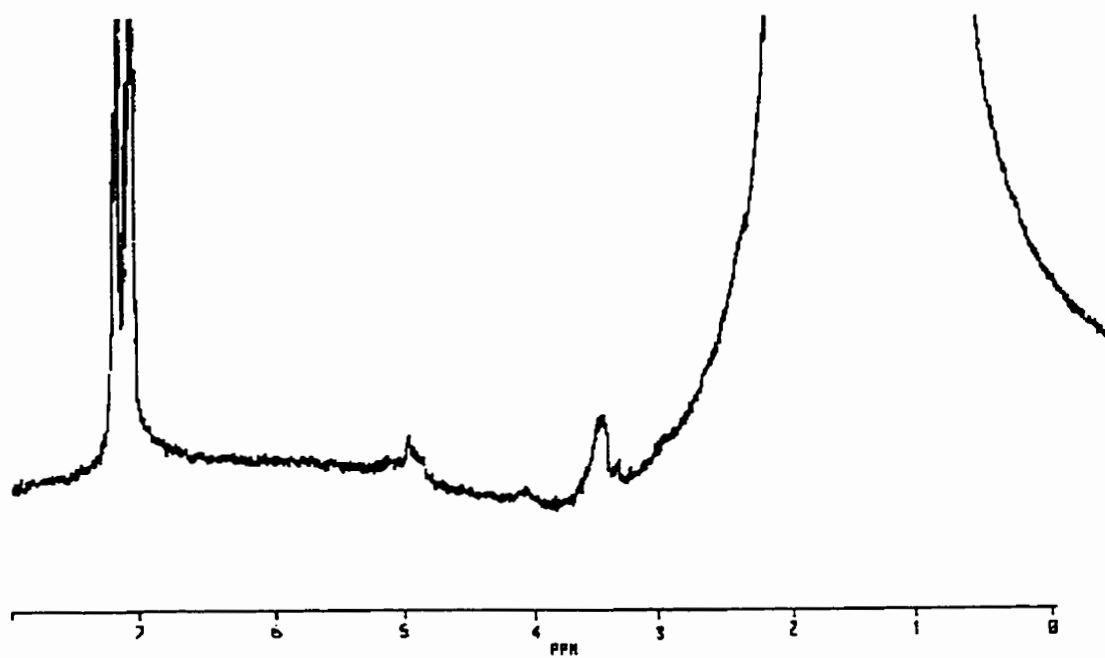




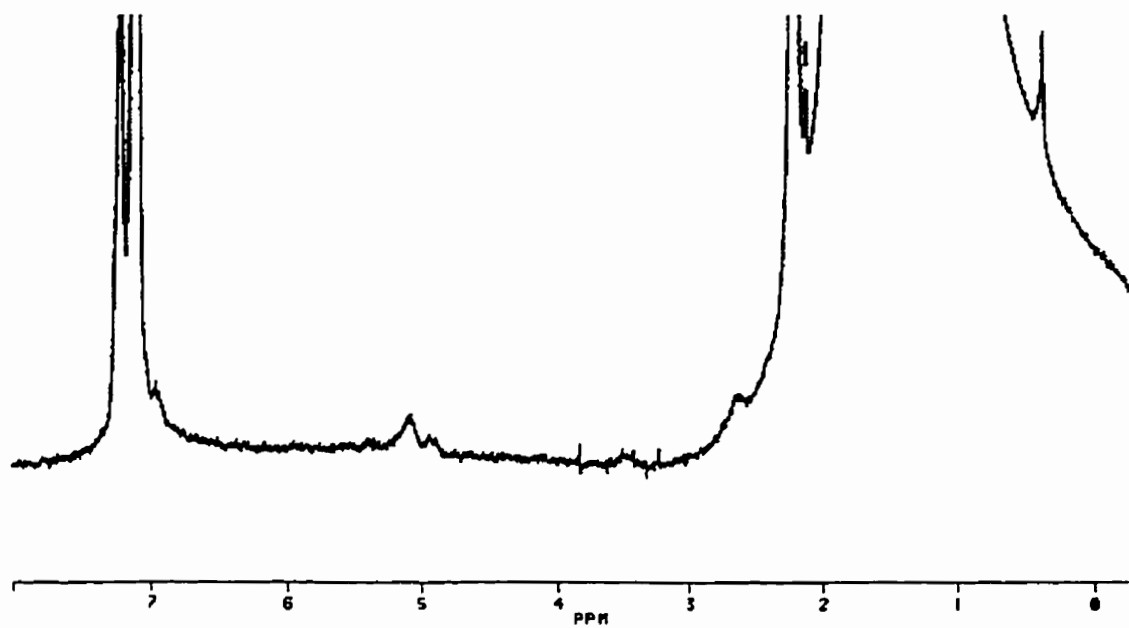




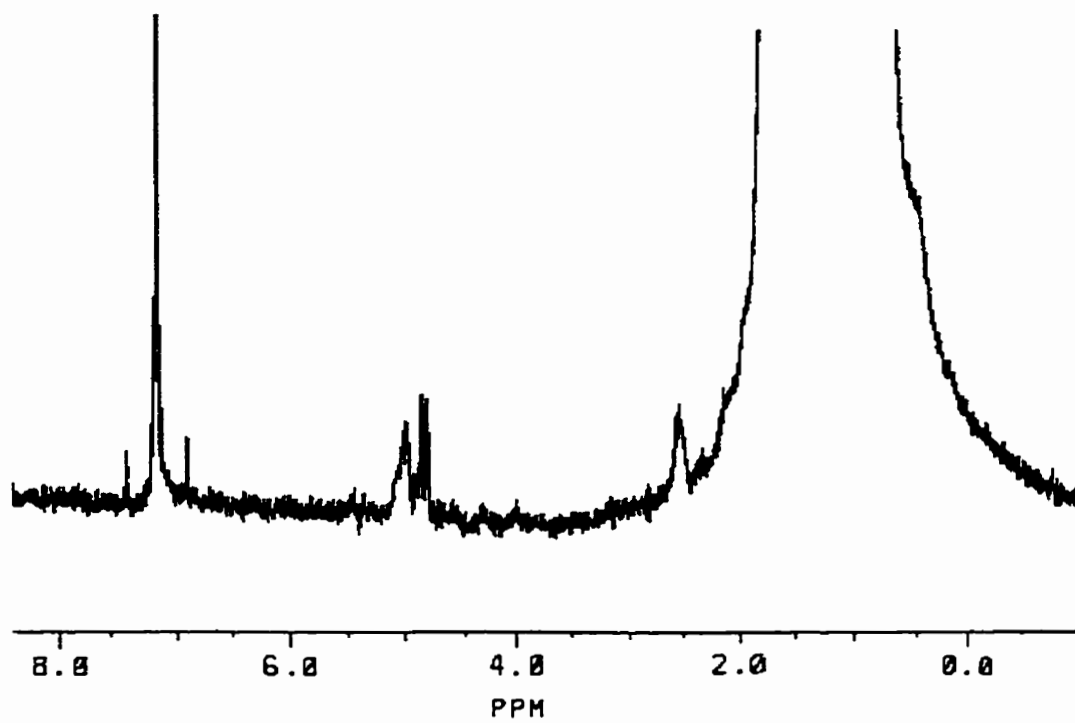




^1H NMR spectrum in benzene- d_6 of a peroxide-induced grafting of maleic anhydride-g-Polypol-19

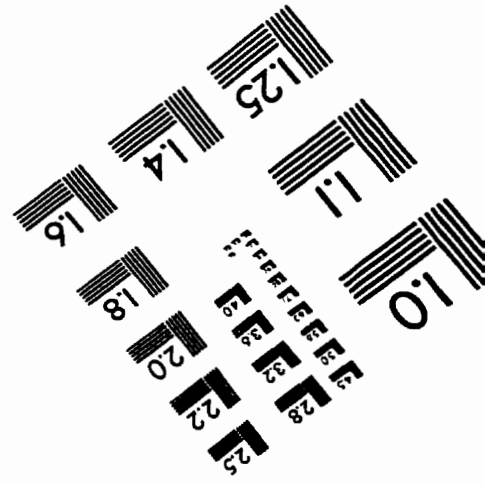
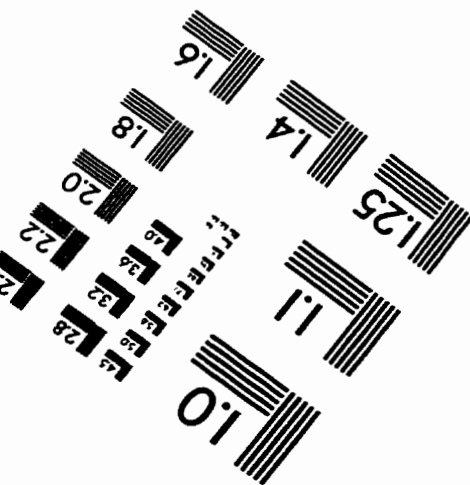
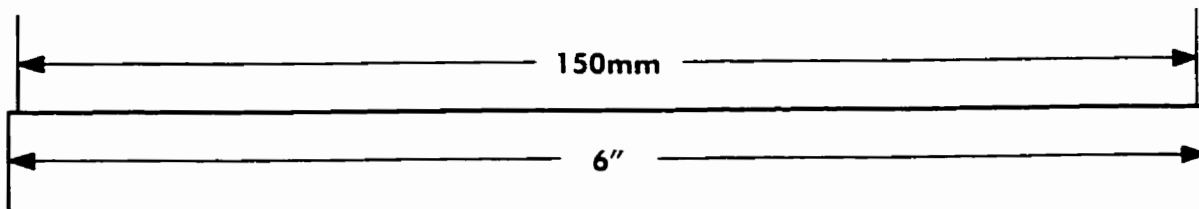
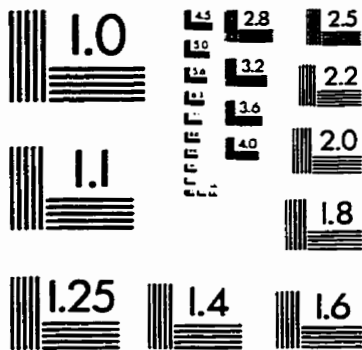
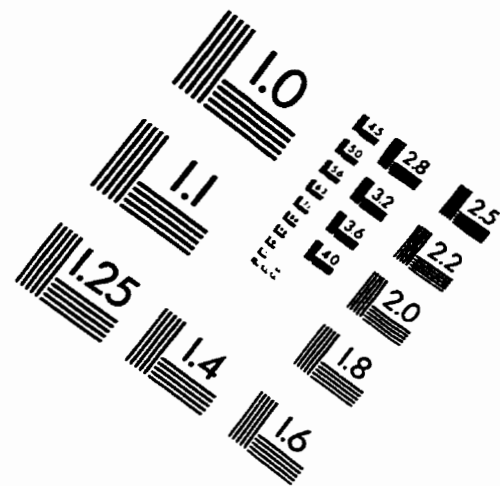
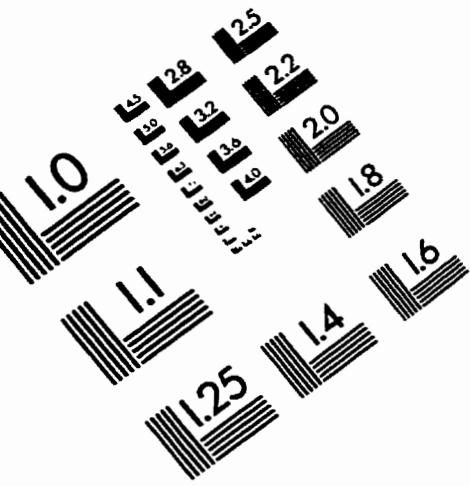


^1H NMR spectrum in toluene- d_6 of a maleated Polypol-19 via the catalyzed Alder Ene reaction in the absence of free radical inhibitor.



¹H NMR spectrum in benzene-*d*₆ of maleated Polypol-19 at 0.001 mole-eq SnCl₂ (heterogeneous) and 4 mole-eq. MAH reactant levels in the Parr reactor.

IMAGE EVALUATION TEST TARGET (QA-3)



APPLIED IMAGE, Inc
 1653 East Main Street
 Rochester, NY 14609 USA
 Phone: 716/482-0300
 Fax: 716/288-5989

© 1983, Applied Image, Inc., All Rights Reserved